FRACTURE TOUGHNESS AND CRACK PROPAGATION OF 300 M STEEL

TECHNICAL REPORT
No. DS-68-18

August 1968
by

S. L. Pendleberry
R. F. Simenz
E. K. Walker

LOCKHEED-CALIFORNIA COMPANY
Burbank, California 91503

Under Contract FA67-WA-1821

DEPARTMENT OF TRANSPORTATION
FEDERAL AVIATION ADMINISTRATION

Aircraft Development Service
Washington, D.C. 20590

TECHNICAL REPORT

Contract No. FA67-WA-1821

FRACTURE TOUGHNESS AND CRACK PROPAGATION OF 300 M STEEL

by

S. L. Pendleberry
R. F. Simenz
R. K. Walker

Prepared for

DEPARTMENT OF TRANSPORTATION
FEDERAL AVIATION ADMINISTRATION

Under Contract FA67-WA-1821

by

LOCKHEED-CALIFORNIA COMPANY
Burbank, California 91503

ABSTRACT

Fracture toughness and crack propagation behavior was investigated for 300 M steel in sheet, plate and forging products. The variables studied included material thickness of 1/8, 3/8, and 3/4 inch and material strength levels of 220 KSI, 270 KSI, and 290 KSI. Both surface-crack and through-crack specimens were evaluated in moist air and salt water spray environments for cyclic stress ratios of +0.1, +0.2, and +0.5.

For the above range of variables it was concluded that stress intensity methods show promise for correlating both fracture toughness and cracking rate behaviors. There appears to be an inverse relationship between fracture toughness and cracking rate although a quantitative mathematical relationship between the two was not found among available crack propagation equations. Among the data evaluated, variation in fracture toughness with heat chemistry was found to be relatively large with respect to that resulting from other metallurgical variables. Significant geometric variables included variations in fracture toughness with a/t ratio and variation of cracking rate with thickness. The influence of stress ratio on cracking rate was found to be accountable through available theory.

Based on the results of this program several approaches to MIL-HDBK-5 type presentation of crack growth data are discussed. A crack growth index based on a standard stress intensity is suggested for material selection or screening purposes. Log-log and log-linear forms of stress intensity vs. cracking rate are presented and discussed. Other techniques are curves of constant cracking rate plotted on stress vs. crack length coordinate and a modification of Goodman Diagrams to depict cracking rates in a presentation form which included the stress ratio variable.

SYMBOLS

a	=	Depth of surface crack or half length of through-crack (Inches)
c	=	One-half of crack length along surface for a surface-crack or one-half crack length for a through-the-thickness crack (Inches)
$\frac{d(2c)}{dN}$	=	Rate of crack propagation (surface measurement) (Inches/Cycle)
F_{tu}	=	Ultimate tensile strength (also UTS) (KSI)
F_{ty}	=	Yield strength (KSI)
K_{cr}	=	Stress intensity at which $d2c/dN \rightarrow \infty$ (KSI $\sqrt{\text{IN.}}$)
$K_{i(max)}$	=	Maximum stress intensity during cyclic loading (KSI$\sqrt{\text{IN.}}$)
K_{Ic}	=	Plane strain fracture toughness (KSI $\sqrt{\text{IN.}}$)
ΔK_i	=	Stress intensity range (maximum-minimum) (KSI $\sqrt{\text{IN.}}$)
$\Delta\overline{K}$	=	Effective intensity parameter adjusted for stress ratio influence (KSI $\sqrt{\text{IN.}}$)
l	=	Crack length of a surface crack (also 2c) (Inches)
N	=	Cycles of load or stress
Q	=	Parameter in surface crack stress intensity $f(a, 2c, \sigma, \sigma_y)$
R	=	Stress ratio $\sigma_{min}/\sigma_{max}$
r_p	=	Plastic zone size at tip of crack (Inches)
t	=	Thickness (Inches)
w	=	Width (Inches)
σ	=	Stress (KSI)
σ_{max}	=	Maximum cyclic stress (KSI)
σ_{min}	=	Minimum cyclic stress (KSI)

σ_y = Yield stress (also F_{ty}) (KSI)

ϕ = Angle denoting position on surface crack leading edge

Φ = Eliptical integral obtained during integration of strain energy for surface crack

γ_f = Front face correction factor for surface flaw

γ_b = Back face correction factor for surface flaw

C, M = Coefficients

a,b,n,m = Exponents

TABLE OF CONTENTS

TABLE OF CONTENTS (Continued)

LIST OF ILLUSTRATIONS

LIST OF ILLUSTRATIONS (Continued)

LIST OF ILLUSTRATIONS (Continued)

LIST OF ILLUSTRATIONS (Continued

LIST OF TABLES

LIST OF TABLES (Continued)

LIST OF TABLES (Continued)

Section I

INTRODUCTION

High strength steels are being used in aircraft landing gears, carry-through box structures, and various fittings and attachments. Service experience has demonstrated a need for more data on the properties of heat treated steels so that a better evaluation of the materials can be accomplished in the design stage and in the evaluation of operational and maintenance problems.

Material properties of major importance include fracture toughness, crack propagation, and their interrelationships. These properties are of interest because of their close relationship to the characteristic failure mode found in high-strength steel aircraft parts. In typical failed high-strength steel parts the fracture face usually indicates that a crack develops at a local defect, propagates by slow crack growth under cyclic loading to a critical crack size and then extends by rapid fracture. Thus, the resistance of a material to crack propagation under cyclic loading, the rate of crack growth and fracture toughness become important factors in material selection and design of high strength steel parts.

Fracture toughness of 300M has been studied in many previous programs however, very little has been done on crack propagation behavior of 300M. None of the programs reported in the literature provide the scope of data required to determine the interrelationship of fracture toughness and crack propagation or to confirm analytical techniques for crack propagation in 300M or any other high strength steel.

The subject program was conducted to better define these properties for 300M steel. The objectives of the program were as follows:

1. To study by experiment the interrelationships of fracture toughness and cyclic flaw growth in medium to very high strength 300M steel.

2. To evaluate analytically the interrelationships of the two behaviors for 300M steel for two environmental conditions (specific air relative humidity and salt spray).

3. To propose pertinent information and techniques of presentation for inclusion in MIL-HDBK-5.

To accomplish the above, fracture toughness and crack propagation data were obtained for 300 M steel in sheet, plate and forging products. Three thicknesses (0.125, 0.375, and 0.750) and three strength levels (220 KSI, 270 KSI, and 290 KSI were evaluated. Both surface-crack and through-crack test specimens were studied in air and salt spray environments. The effects of different minimum-to-maximum stress ratios were also evaluated in the crack propagation tests.

Appendix B presents comparable data from another program which studied several other high strength steel alloys.

Section II

DISCUSSION OF APPROACH

MATERIAL SELECTION

300M was chosen for this program because it is a high strength steel alloy being used in many current aircraft and being specified in new aircraft designs. The fracture toughness and crack propagation behavior of this alloy to be generally representative of these properties in other low alloy steels such as 4340 and D6AC which are also used in high strength steel aircraft structure. It is expected that the analysis methods and techniques of presentation found suitable for 300M will be applicable to other grades of high strength, low alloy steel. Several different product forms and thicknesses of 300M were evaluated to obtain data for typical product forms used in aircraft structure. These products included 1 1/2 inch hand forgings, 7/8 inch plate from different heats, 1/2 inch plate from different heats, and 3/16 inch sheet.

TEST METHODS

Axial tension-tension cyclic crack propagation and fracture toughness tests were conducted for the various product forms of 300M steel using surface-crack and through-crack test specimens. These two types of flaws most nearly represent the types of damage that occur in aircraft components. Surface-crack specimens were tested in thicknesses of 1/8, 3/8, and 3/4 inch and through-crack specimens were tested in thicknesses of 1/8 and 3/8 inch only. Through-crack specimens of 3/4 inch thickness were not tested because it would be very unlikely for a through-crack to exist undetected in an aircraft part of this thickness or for an undetected surface-flaw to propagate to a through-crack prior to catastrophic failure.

Figure 1 presents the surface-crack specimen geometries for 1/8 and 3/8 inch thicknesses and the 3/4 inch thick specimen is presented in Figure 2. These specimens have a minimum width-to-thickness ratio of six and generally conform to the geometry recommendations of ASTM Committee F-24 fracture testing of metallic materials. The through-crack specimen geometries for 1/8 and 3/8 inch thicknesses are presented in Figures 3 and 4.

The surface-crack and through-crack specimens and test methods used in this investigation were uniquely designed to produce both crack propagation and fracture toughness data with a single specimen. This was accomplished by cyclic propagation of pre-existing cracks to a different crack size in each of three test specimens for each combination of test and material variables. When the cracks were propagated to the specific sizes chosen, the cyclic tests were discontinued and the specimens were statically tested to failure to obtain fracture toughness data. This method permitted verification of cyclic crack propagation data for each set of test conditions and produced fracture toughness data for three different crack sizes in both surface-crack and through-crack specimens.

For the 3/8 and 3/4 inch thick surface-crack specimens, one of the final propagated crack sizes had a crack depth less than half the specimen thickness and the other two crack sizes had depths near or greater than half thickness. Half thickness has been an arbitrarily recommended maximum surface-crack depth for fracture mechanics considerations. To date, fracture toughness evaluations of high strength metals using surface-crack specimens have been primarily concerned with highly stressed pressure vessels such as rocket motor cases where operating stresses are so high that catastrophic failure would occur as a result of very small crack like defects which would not propagate beyond half thickness prior to failure. In aircraft applications of high strength metals, the operating stresses are sufficiently low to allow surface defects to propagate beyond half thickness and in some cases the defects could even propagate through the thickness prior to failure. Test data on the behavior of high strength metals containing large cracks are extremely limited and are required for fail safe analyses of aircraft components. If currently developed modifications of fracture mechanics equations can not predict behavior of high strenth metals contining large cracks which can and do exist in aircraft components, then additional modifications of fracture mechanics equations are required or other methods of evaluating behavior of damaged structure must be developed.

In order to obtain sufficient cyclic crack propagation data for surface-cracks in 1/8 inch thick specimens, it was necessary to propagate all the surface-cracks to depths beyond half-thickness. Of the three crack sizes obtained for 1/8 inch surface-crack specimens, one did not penetrate the thickness, one penetrated the thickness with unequal crack lengths on the two surfaces, and one was propagated to a through-crack of nearly equal crack lengths on the two surfaces.

For the 1/8 and 3/8 inch thick through-crack specimens, pre-existing through-cracks were propagated to three different crack lengths with the maximum length approximately equal to half the specimen width.

TEST VARIABLES

Cyclic crack propagation tests of surface-crack and through-crack specimens were conducted in both air and salt water spray environments to simulate environments encountered by aircraft. Two choices of air environment were considered. One was dry air (approximately 20% relative humidity) and the other was moist air (80 to 85% relative humidity). Preliminary cyclic crack propagation tests of 1/8 inch surface-crack and through-crack specimens were conducted in dry air and moist air environments to determine which was more damaging for selection of the "air" environment used in the test program.

Three ultimate strength levels (290, 270, and 220 KSI) of 300M steel were evaluated to represent the strength level range commonly used for high strength steels in aircraft applications.

Cyclic crack propagation tests were conducted by axial tension-tension loading. A constant mean stress was used for surface-crack specimens and a

different constant mean stress was used for through-crack specimens. Three minimum-to-maximum cyclic stress ratios (+0.1, +0.2, and +0.5) were evaluated for surface-crack specimens and two (+0.1, +0.5) were evaluated for through-crack specimens. Each minimum-to-maximum cyclic stress ratio (R) coupled with the constant mean stresses resulted in different maximum cyclic stress levels. The combinations of selected mean stresses, minimum-to-maximum cyclic stress ratios, initial crack sizes, and specimen geometries resulted in approximately the same initial calculated stress intensity (K_I) for both the surface-crack and through-crack specimens. By maintaining the same initial stress intensity, the effects of crack type (surface-crack and through-crack) and specimen thickness (relative to degree of plane-strain stress state) should become apparent.

Selection of cyclic rate for the crack propagation tests was of critical importance in this test program. Since a primary objective was to evaluate the effects of a salt water spray environment on cyclic crack propagation, a cyclic rate had to be selected which would insure that the environment be present at the crack tip and that sufficient time was permitted for development of crack propagation modes which would reflect the environment. A cyclic rate of 20 CPS was chosen for the crack propagation tests in this program. Selection of this rate was based on the results of similar Lockheed tests conducted where cyclic crack propagation in air and salt water environments were evaluated for several high strength steels including 300M forged billet.

A summary table of the test program is presented in Table 1. All variables of test environment, strength level, and stress conditions were evaluated with 3/8 inch thick surface-crack specimens. Other thicknesses, product forms, and specimen types were evaluated with respect to specific variables and compared with the results from the 3/8 inch surface-crack specimens.

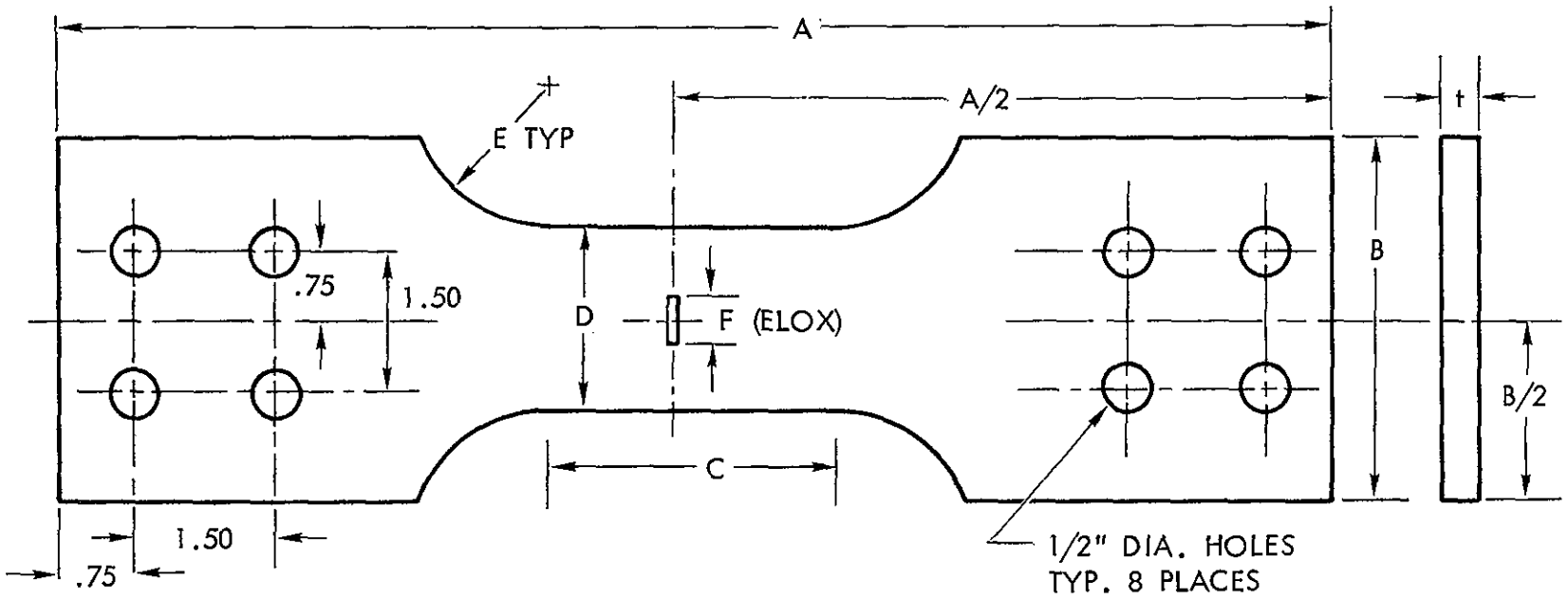

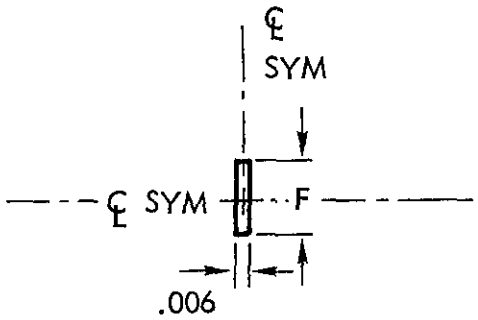

DETAIL OF ELOX SLOT
DEPTH TO BE 1/2 OF
"F" DIMENSION

t	A	B	C	D	E	F
.125	14	4	3.5	2.25	1.50	.08
.375	16	5	3.5	2.25	2.00	.08

Figure 1 Crack Propagation Specimen, Surface Crack for 1/8 and 3/8-Inch Material

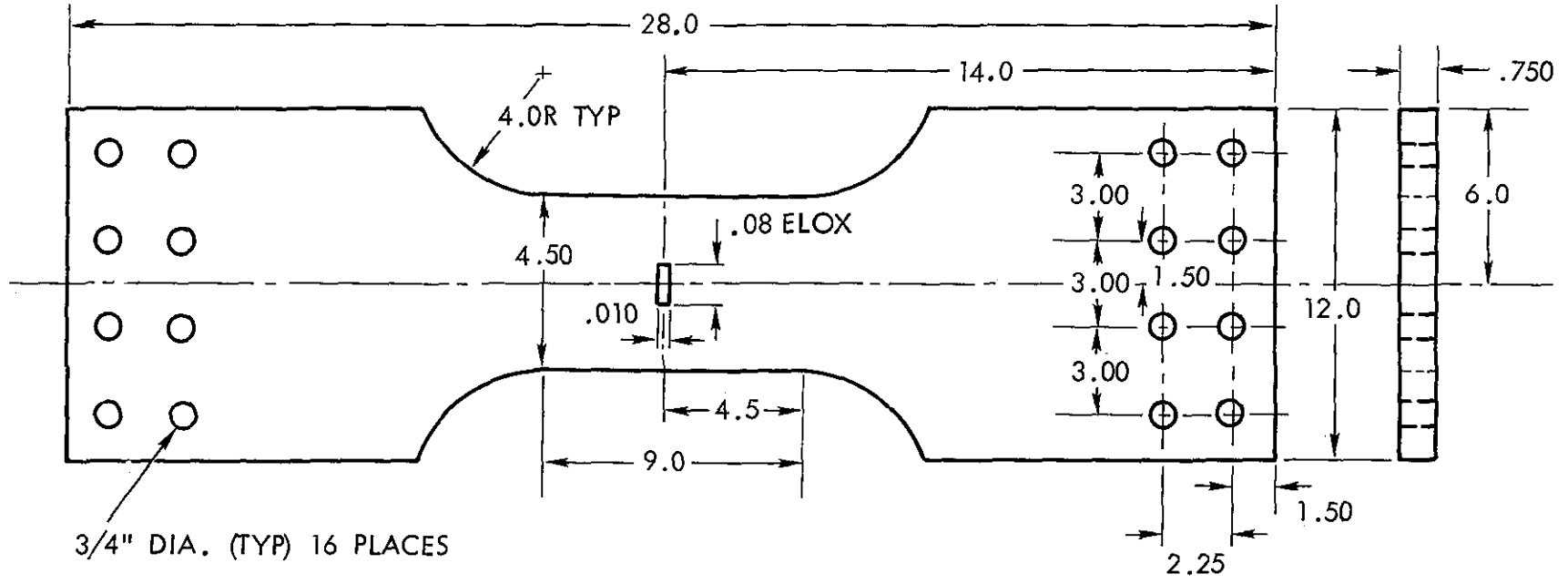

Figure 2 Crack Propagation Specimen Surface Crack for 3/4-Inch Material

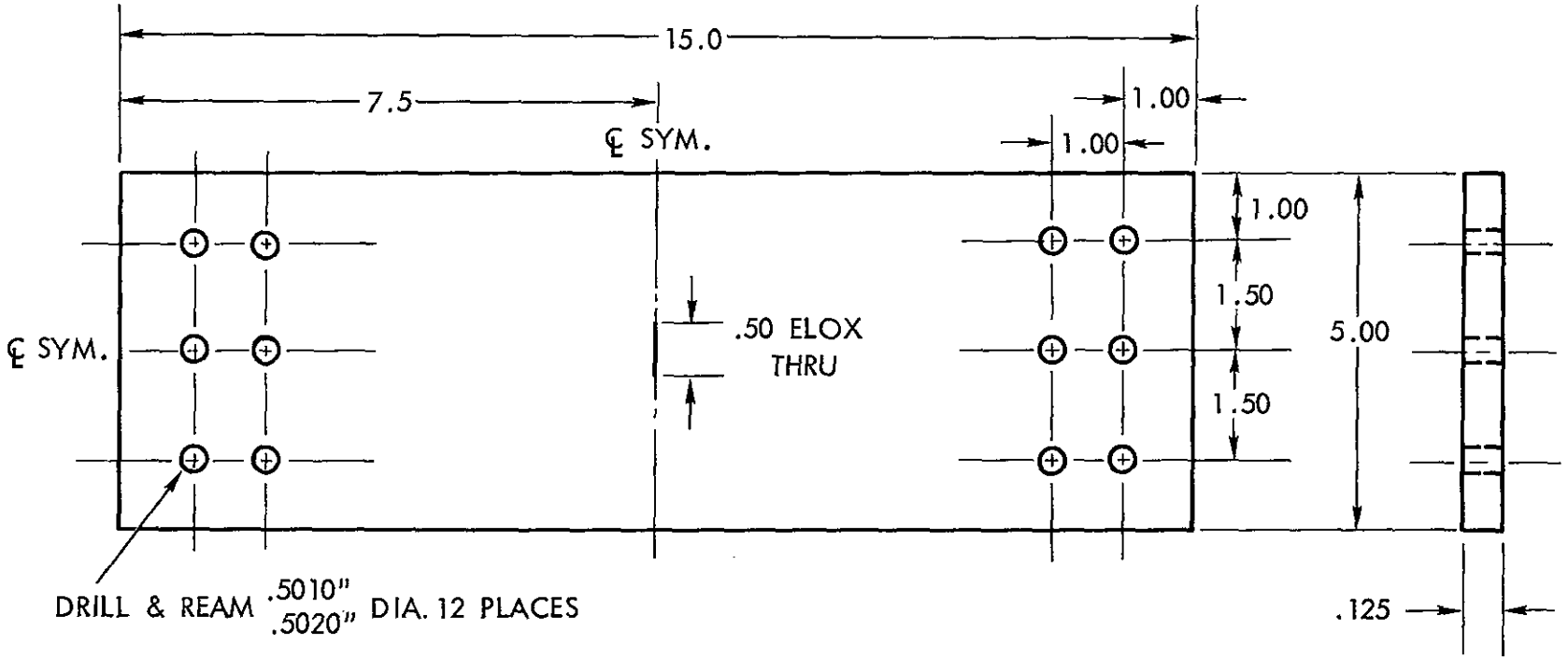

Figure 3 Crack Propagation Specimen Through-Crack for 1/8-Inch Material

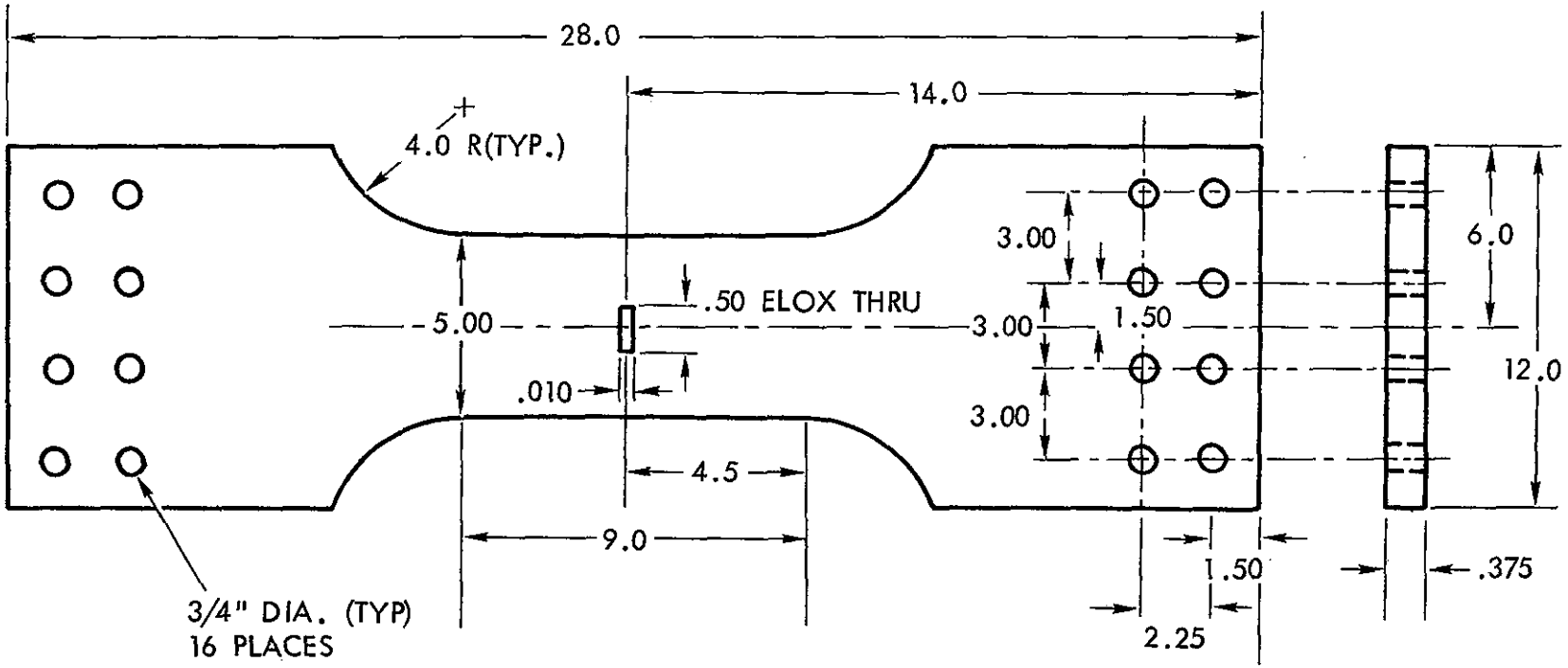

Figure 4 Crack Propagation Specimen Through Crack for 3/8-Inch Material

TABLE 1 SUMMARY OF 300M STEEL CRACK PROPAGATION AND FRACTURE TOUGHNESS TESTS

FINAL PRODUCT	GRAIN DR.	SPECIMEN TYPE	FINAL THICKNESS	TEST ENVIR.	NUMBER OF SPECIMEN TEST *						
					220 KSI		270 KSI		290 KSI		
					STRESS RATIO		STRESS RATIO		STRESS RATIO		
					.1	.5	.1	.5	.1	.2	.5
SHEET AND PLATE	L	Surface crack	.125	Air					3	3	3
				Salt Spray					3	3	3
			.375	Air	3	3	3	3	3	3	3
				Salt Spray	3	3	3	3	3	3	3
			.750	Air					3	3	3
				Salt Spray					3	3	3
	L	Through Crack	.125	Air					3		
				Salt Spray					3		
			.375	Air	3	3	3	3	3		
				Salt Spray	3	3	3	3	3		
FORGING	L	Surface Crack	.750	Air	3		3		3		
				Salt Spray	3		3		3		

* Crack propagation and fracture toughness data obtained on each specimen.

Section III

PROCEDURE AND RESULTS

MATERIAL

All 300M steel used in this program was produced by consumable electrode vacuum melting. The forgings were procured to MIL-S-8844B Class 2 and the plate material was procured to the requirements of AMS 6434 except for chemistry which was specified as MIL-S-8844B Class 2. Plate thicknesses of 3/16, 1/2 and 7/8 inch were ordered to provide for removal of decarburization in producing specimens of 1/8, 3/8, and 3/4 inch final thicknesses respectively. The forgings were initially 1" thick and machined to 3/4 inch final thickness for the same reason. Complete supplier test report information is reported in Appendix A.

During procurement it was necessary to accept material produced from several different heats, thus heat chemistry is a variable in the program. The phosphorus and sulphur contents showed little variation and were well below the levels known to significantly affect fracture toughness. Carbon content among the various heats did vary from .39 to .43. Some effects of this variation on fracture toughness and crack propagation were noted and are discussed later in this report.

SPECIMEN PREPARATION

Specimen Location and Machining.-The 1/8 inch thick surface-crack and through-crack specimens and tensile specimen blanks were cut from one sheet (3/16"X36"x96") of 300 M steel. Individual specimen locations within the sheet are shown in Figure 5.

The 3/8 inch thick surface-crack and through-crack specimens and tensile specimen blanks were cut from four plates (two plates 1/2"X36"X120" and two plates 1/2"X36"X96") of 300 M steel. Individual specimen locations within the plates are shown in Figures 6, 7, 8, and 9.

The 3/4 inch thick surface-crack specimens and tensile specimen blanks were cut from two plates (7/8"X36"X96") of 300 M steel. Individual specimen locations within the plates are shown in Figures 10 and 11.

The 300 M steel forgings were received cut to individual surface-crack specimen blank size (1 1/2"X13"X34"). Tensile specimen blanks were cut from each forging section. As-received 300 M steel forgings are shown in Figure 12.

All surface-crack and through-crack test specimens were machined to their final dimensions, except for thickness, in the as-received, normalized heat treat condition. The specimen thicknesses were 0.020 inch over size. The specimens were then heat treated to their appropriate strength levels. After heat treatment, the test section thickness of each specimen was machined to

the final thickness specified by removing a minimum of 0.010 inch from each surface to remove possible decarburized material. The final machining operation was accomplished by heavy coolant flow and with thickness of material removed per pass restricted to 0.001 inch.

Tensile specimens were heat treated as rough cut blanks and machined after heat treatment.

Heat Treatment.-A heat treat study was conducted to determine the appropriate tempering temperatures to achieve the target tensile values of 290 KSI, 270 KSI and 220 KSI. All specimens were normalized at 1700°F for 1 1/2 hours and air cooled and then austenitized at 1600°F for 1 1/2 hours and oil quenched. This treatment was followed by double tempering at various temperatures up to 1050°F. The minimum tempering temperature used was 500°F to be consistent with actual industry practice and Government and Industry specification requirements.

Tensile test results on the various products used in the heat treat study are reported in Table 2 and shown graphically in Figure 13. From these data tempering temperatures of 500, 675 and 975°F were selected to achieve 290, 270 and 220 KSI strengths levels respectively. All crack propagation specimens were then normalized at 1700°F for 1 1/2 hours air cooled, austenitized at 1600°F, 1 1/2 hours and oil quenched followed by double tempering for 2 hours each at the temperature selected for the desired strength level. Tensile control specimens were processed along with the crack propagation specimens. Results obtained on the control tensile specimens are reported in Table 3.

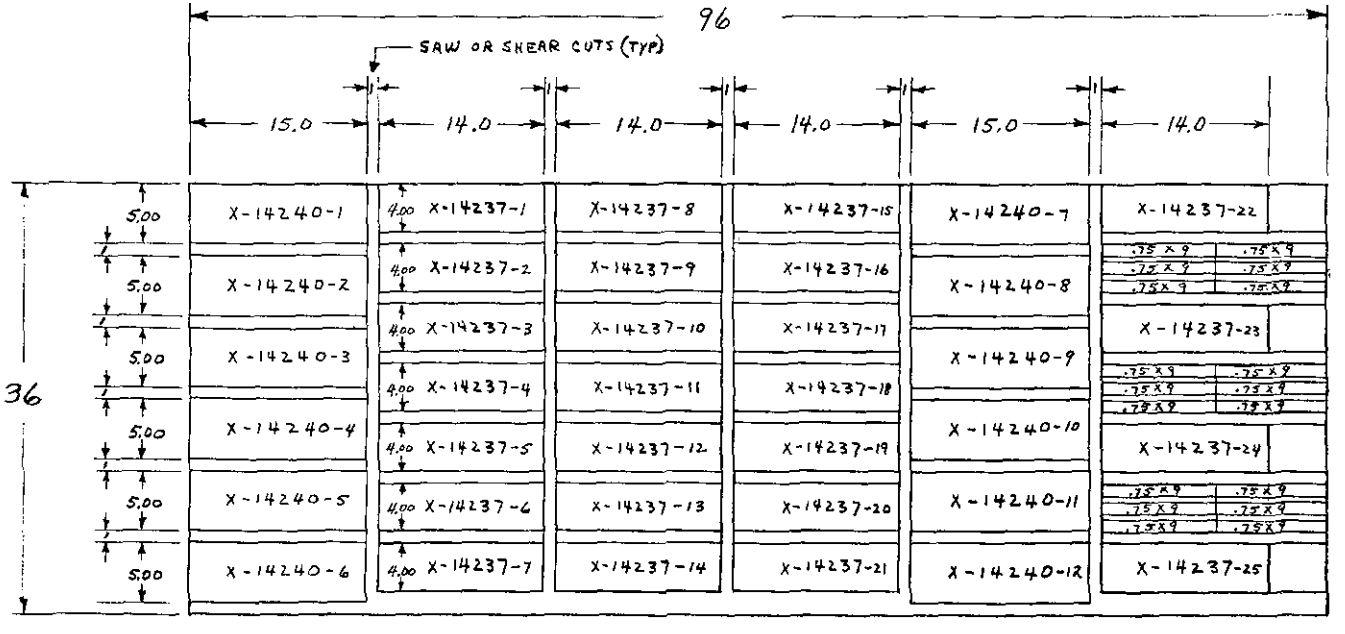

Original Thickness 3/16-Inch

Figure 5 Specimen Blank Lay-Out for 1/8-Inch Thick 300 M Steel, HT 3932022

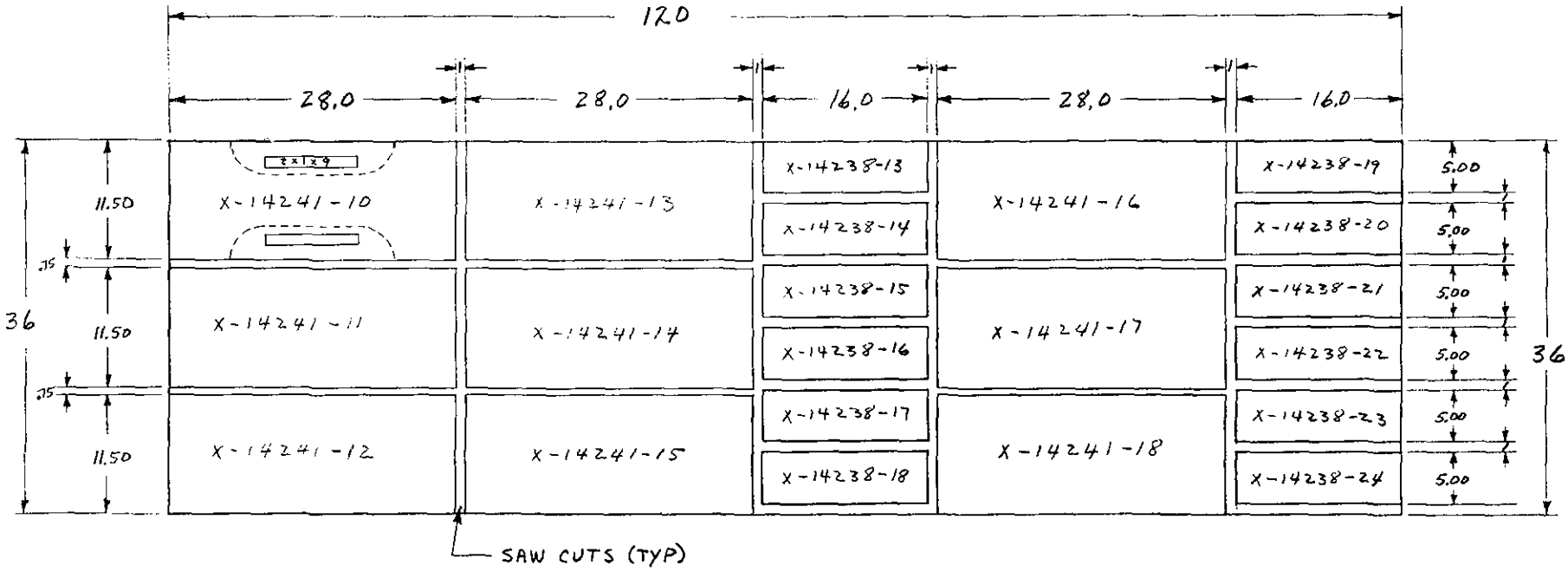

Original Thickness 1/2-Inch

Figure 6 Specimen Blank Lay-Out for 3/8-Inch Thick 300M Steel, HT 3961507

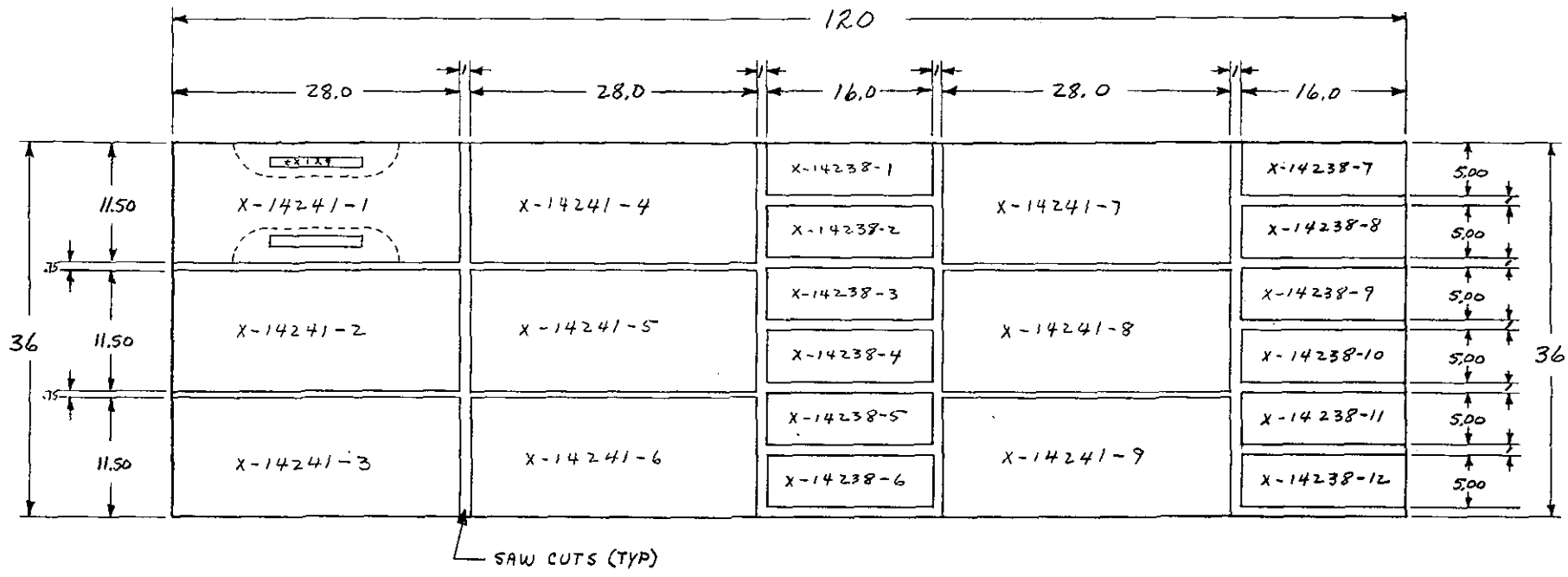

Original Thickness 1/2-Inch

Figure 7 Specimen Blank Lay-Out for 3/8-Inch Thick 300M Steel, HT 3932021

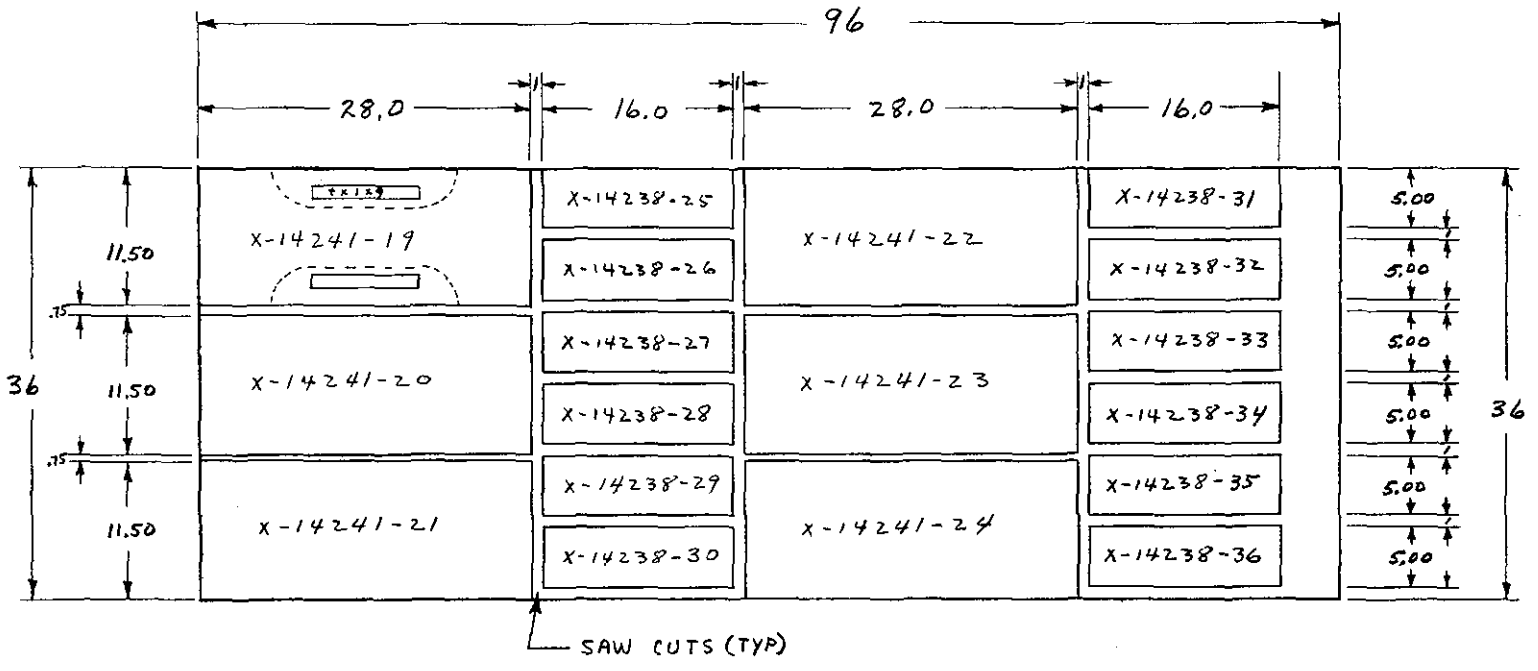

Original Thickness 1/2-Inch

Figure 8 Specimen Blank Lay-Out for 3/8-Inch Thick 300 M Steel, HT 3922452

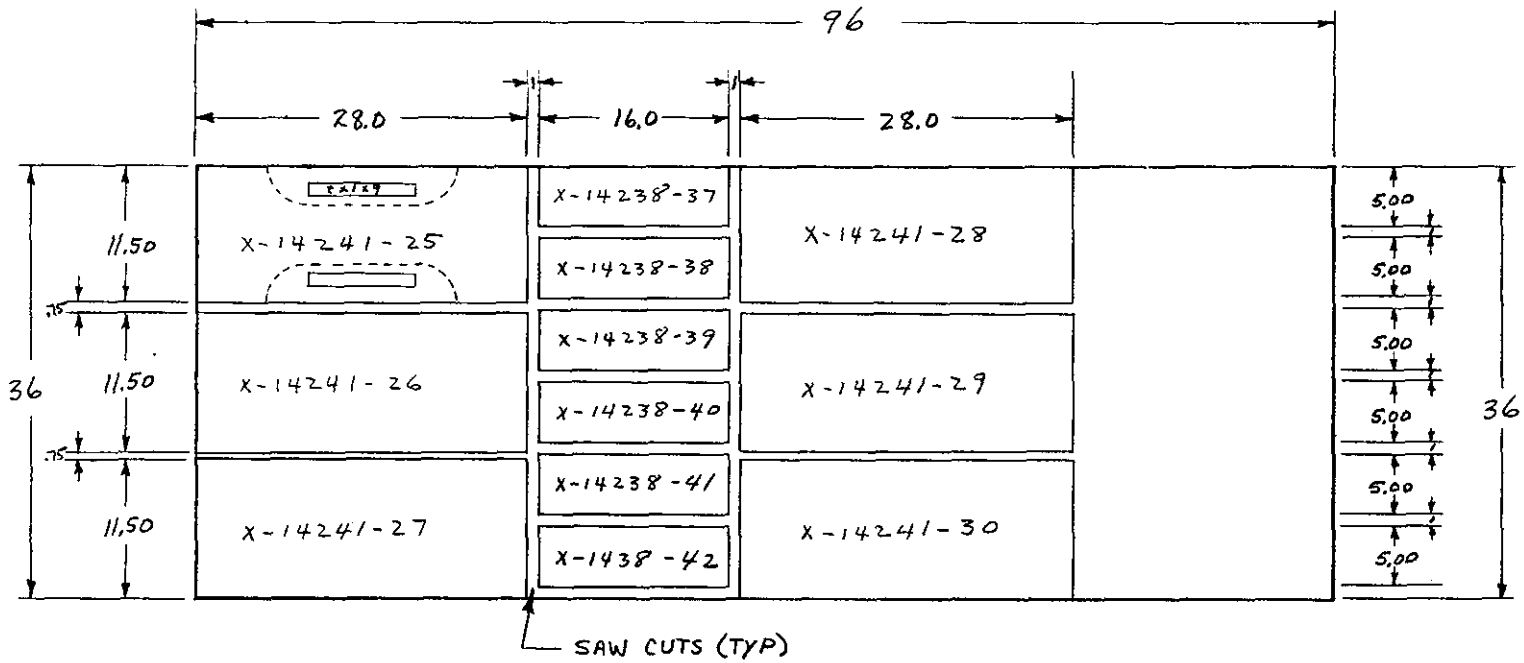

Original Thickness 1/2-Inch

Figure 9 Specimen Blank Lay-Out for 3/8-Inch Thick 300 M Steel, HT 3932021

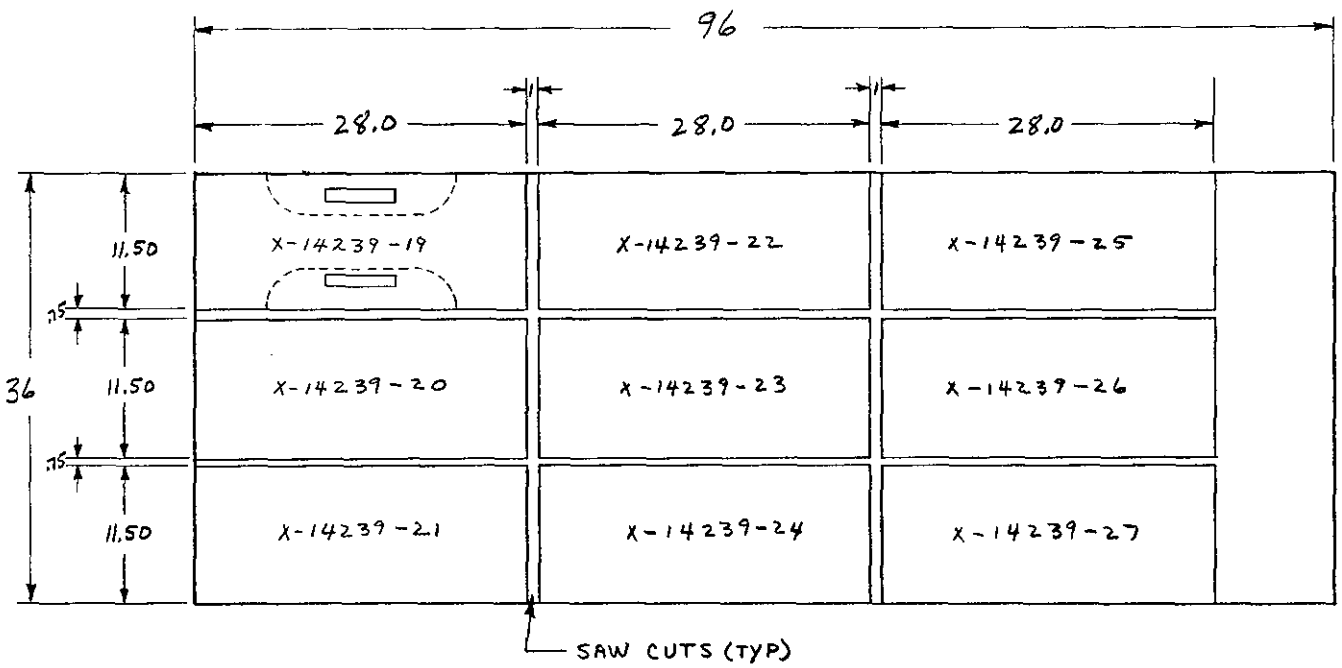

Original Thickness 7/8-Inch

Figure 10 Specimen Blank Lay-Out for 3/4-Inch Thick 300 M Steel, HT 3922452

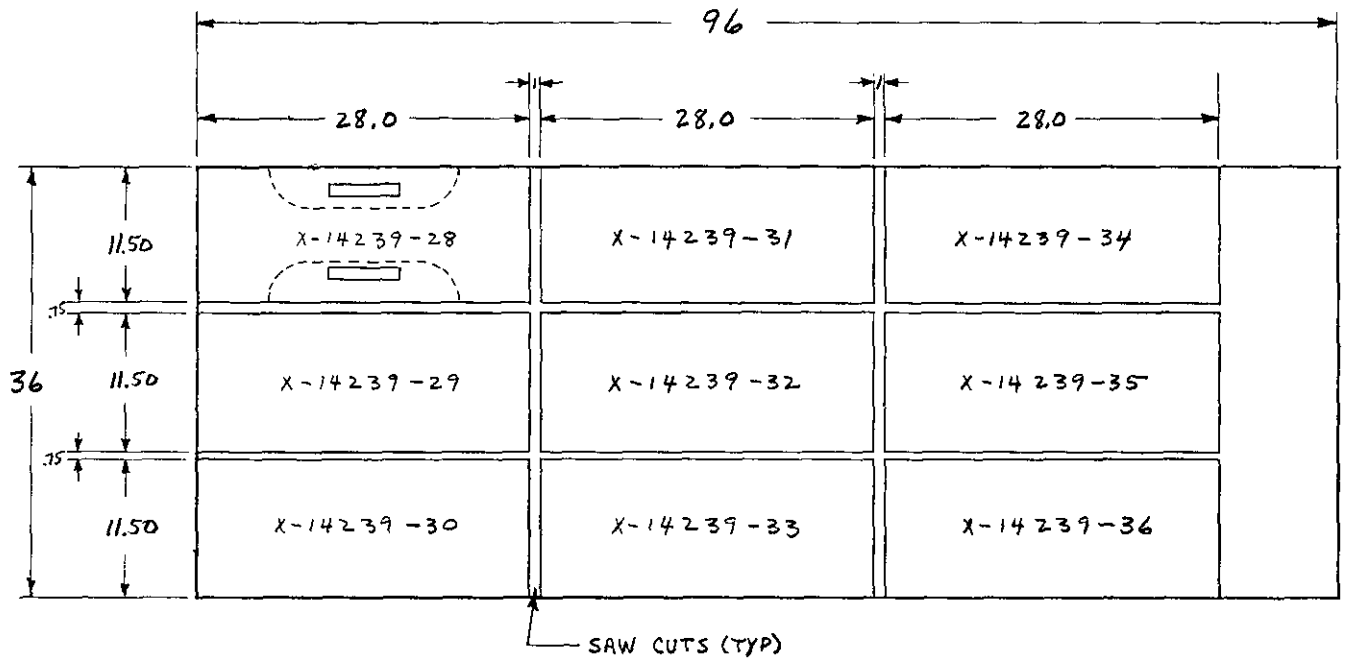

Original Thickness 7/8-Inch

Figure 11 Specimen Blank Lay-Out for 3/4-Inch Thick 300 M Steel, HT 3932021

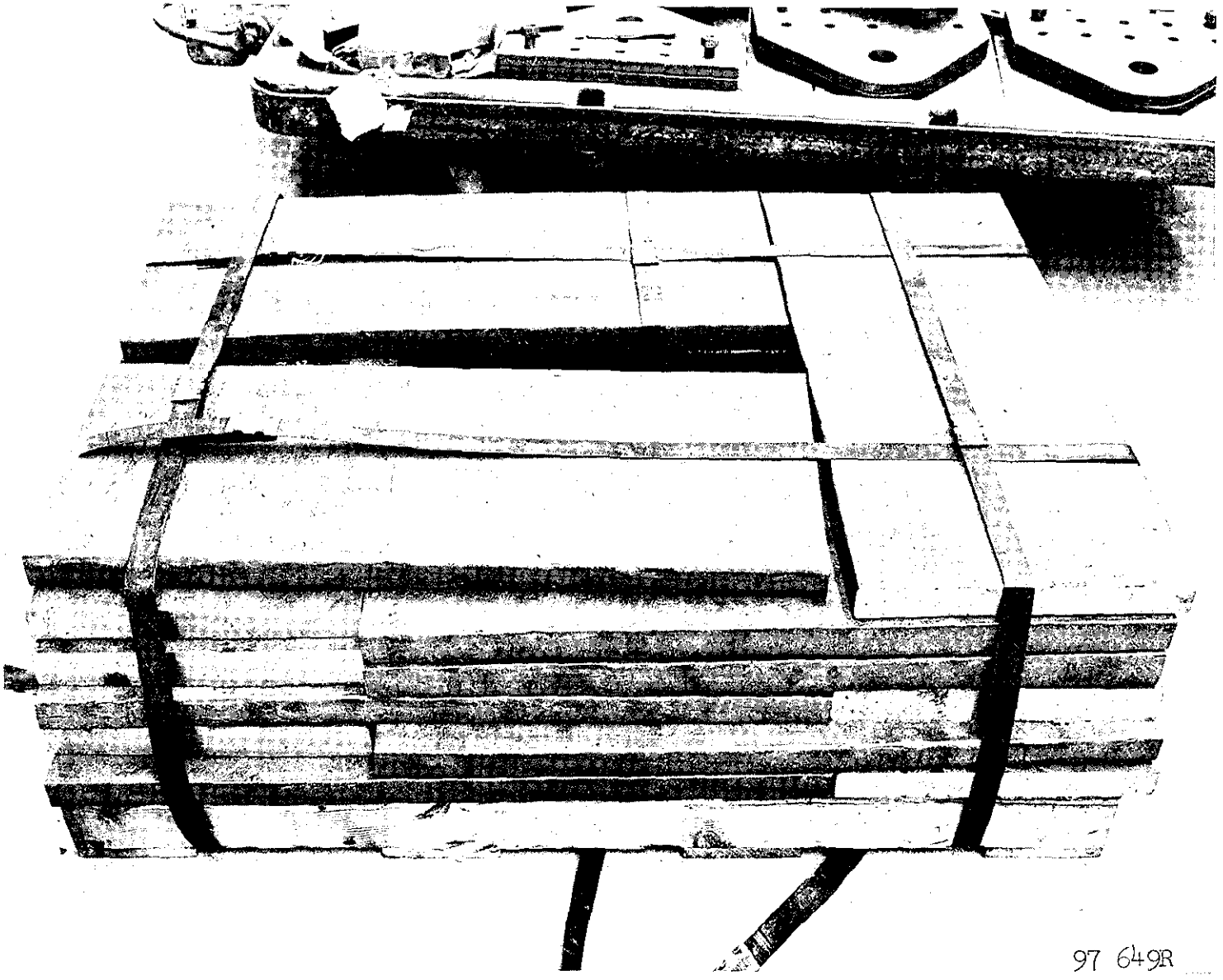

Figure 12 1-1/2 Inch Thick Rough Forgings 300 M Steel

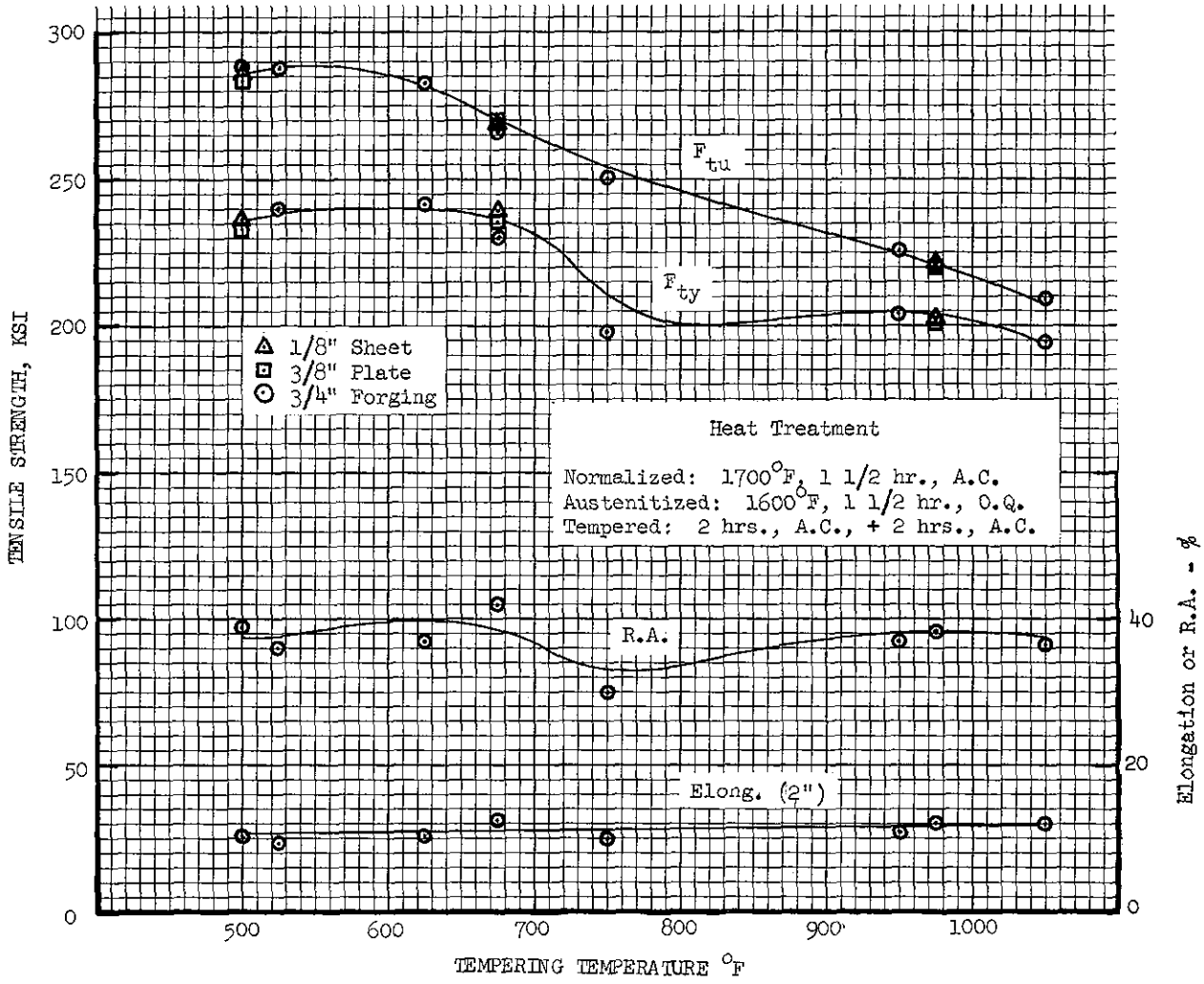

Figure 13 300 M Steel Heat Treat Study

TABLE 2 TENSILE PROPERTIES OF HEAT TREATMENT STUDY

Product Final Size	Heat Number	Specimen Number	Tempering Temperature 2 + 2 Hrs (1)	Ultimate Strength (KSI)	0.2% Yield Stress (KSI)	Elong. 2" G.L. (%)	R. A. (%)	Target F_{tu} (KSI)
3/4" forging	51782	F5-2	500°F	288	(2)	10	40	290
		F6-2	500°F	288	(2)	11	39	290
		F1-1	525°F	288	240	10	37	290
		F2-2	525°F	288	239	9	36	290
		F1-1	625°F	283	243	11	40	270
		F2-2	625°F	284	242	10	34	270
		F9-2	675°F	267	230	13	43	270
		F10-2	675°F	266	231	12	41	270
		F3-1	750°F	251	198	10	30	270
		F4-1	750°F	252	199	10	29	270
		F3-2	950°F	227	205	11	36	220
		F4-2	950°F	225	204	11	38	220
		F11-2	975°F	221	204	12	37	220
		F12-2	975°F	222	203	12	40	220
		F5-1	1050°F	210	194	12	35	220
		F6-1	1050°F	209	194	12	38	220
3/8" plate		P-1	500°F	284	237	9	-	290
		P1-1	500°F	282	230	9	-	290
		P1-3	675°F	270	243	10	-	270
		P1-4	675°F	270	230	10	-	270
		P1-5	975°F	220	200	12	-	220
		P1-6	975°F	221	202	12	-	220
1/8" sheet		S-3	500°F	285	234	8	-	290
		S-4	500°F	287	241	8	-	290
		S-5	675°F	270	243	8	-	270
		S-6	675°F	268	235	8	-	270
		S-7	975°F	222	202	9	-	220
		S-8	975°F	223	203	10	-	220

(1) Normalized - 1700°F - 1-1/2 hrs - A.C.; Austenitized - 1600°F - 1-1/2 hrs - O.Q.
(2) Yield not determinable from load-strain curve.

TABLE 3 TENSILE PROPERTIES OF HEAT TREATMENT CONTROL SPECIMENS

Product Final Size	Heat Number	Specimen Number	Tempering Temperature 2 + 2 Hrs (1)	Ultimate Strength (ksi)	0.2% Yield Stress (ksi)	Elong. 2" G.L. (%)	R. A. (%)	Target F_{tu} (ksi)
1/8" sheet	3932022	S-9	500°F	285	233	9	-	290
		S-10		284	245	8	-	
3/8" plate	3932021	P1-1	500°F	286	236	9	-	290
		P1-3		286	239	9	-	
	3932021	P1-7	675°F	272	233	9	-	270
		P1-9		274	236	9	-	
	3961507	P1-13	975°F	229	208	11	-	220
		P1-15		230	209	11	-	
3/4" plate	3922452	P2-19	500°F	297	239	10	38	290
		P2-25		297	240	11	32	
Forging	51782	F 11-1	500°F	287	237	10	37	290
		F 12-1		287	234	11	40	
		F 17-2	675°F	276	236	10	38	270
		F 18-1		276	238	11	41	
		F 10-1	975°F	230	202	12	36	220
		F 17-1		228	201	12	39	

(1) Normalized - 1700°F - 1 1/2 Hrs - A.C.; Austenitized - 1600°F - 1 1/2 Hrs - O.Q.

Pre-cracking of Test Specimens.-Pre-cracking of surface-crack and through-crack test specimens was accomplished by axial tension-tension fatigue at a minimum-to-maximum stress ratio (R) of +0.1 and a cyclic frequency of 20 cycles per second in a normal air environment (approximately 40 percent relative humidity) at room temperature (68 to 72°F).

For the surface-crack specimens, the pre-crack was generated from an EDM slot (0.006" wide X 0.040" deep X 0.080" long) located in the center of the test section. A maximum gross area stress of 45 ksi was used to propagate the 0.080 inch long EDM slot to a final pre-crack length of 0.18 inch. The corresponding pre-crack depth was 0.085 to 0.095 inch. Measurement of the pre-crack length was accomplished with a stainless steel scale graduated into 0.010 inch increments and a magnifying optical lens. The number of fatigue cycles required for pre-cracking was recorded for each specimen.

For through-crack specimens, the pre-crack was generated from an EDM slot (0.010" wide X 0.50" long X through-thickness) located in the center of the test section. A maximum gross area stress of 25 KSI was used to propagate the 0.50 inch long EDM slot to a final pre-crack length of 0.75 inch. Measurement of the pre-crack length was accomplished in the same manner as for the surface-crack specimens. The number of fatigue cycles required for pre-cracking was recorded for each specimen.

Pre-cracking of the test specimens was accomplished in the same test equipment and set-up as was used for the crack propagation tests. Each specimen was pre-cracked and then immediately crack propagation tested in the same test set-up without specimen removal and re-installation. The reason for this procedure was twofold. The specimen remained in the same position under the same load distribution for both pre-cracking and crack propagation testing. Also the time span between pre-cracking and crack propagation testing was minimized and essentially constant for all test specimens. Similar testing of high strength steel specimens in previous test programs indicated that the delay time between pre-cracking and crack propagation testing can increase the number of cycles required to incubate propagation of the pre-crack. It is suspected that the crack tip geometry and material condition is altered by strain relaxation and possible contamination of the crack surface material near the crack tip if the pre-cracked specimen is left unstressed for some time. The delay time between pre-cracking and crack propagation testing in this test program was 15 to 30 minutes.

TEST EQUIPMENT

Specimen pre-cracking and crack propagation testing of the 1/8 inch and 3/8 inch thick surface-crack and through-crack specimens were conducted with a Lockheed-designed 150,000 pound capacity closed-loop servohydraulic fatigue test machine (Figure 14).

Specimen pre-cracking and crack propagation testing of the 3/4 inch thick surface-crack specimens were conducted with a Lockheed-designed 250,000 pound capacity axial load resonant fatigue machine (Figure 15).

Cyclic load control, counting, and monitoring during specimen pre-cracking and crack propagation testing was accomplished with the following instruments:

(1) Function Generator (hp Model 200 CD wide range oscillator).

(2) REDCOR 391 Differential Amplifier and Dynamic Strain Indicator.

(3) MTS SERVAC Model 401.01.

(4) Hewlett-Packard Model 130C Oscilloscope.

(5) CMC Model 315A Electronic Counter.

(6) Honeywell Model 1108 Visicorder Oscillograph.

Static tensile and fracture toughness tests were conducted with Universal Hydraulic Testing Machines ranging in capacity from 60,000 pounds to 400,000 pounds (Figures 16) automatic recording systems which consist of ASTM Class B-2 extensometers and deflectometers coupled to drum-type load-strain recorders were used.

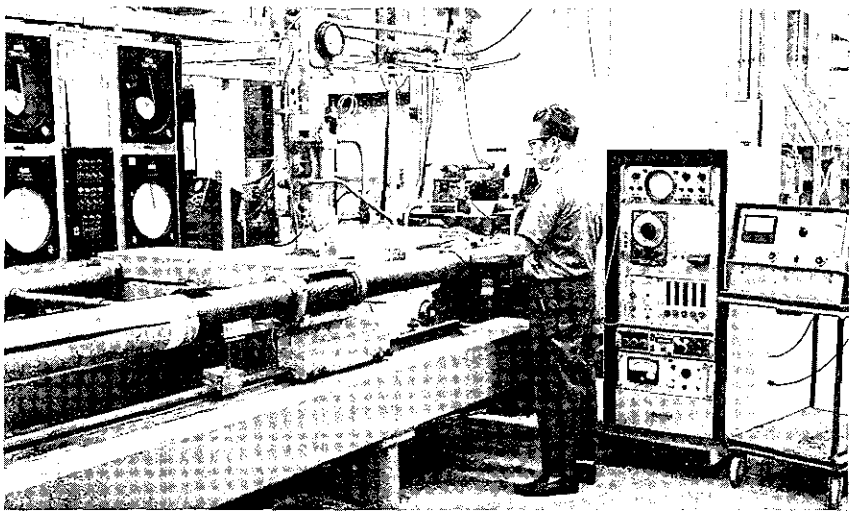

Figure 14 150,000 Pound Capacity Closed-Loop Servohydraulic Fatigue Test Machine

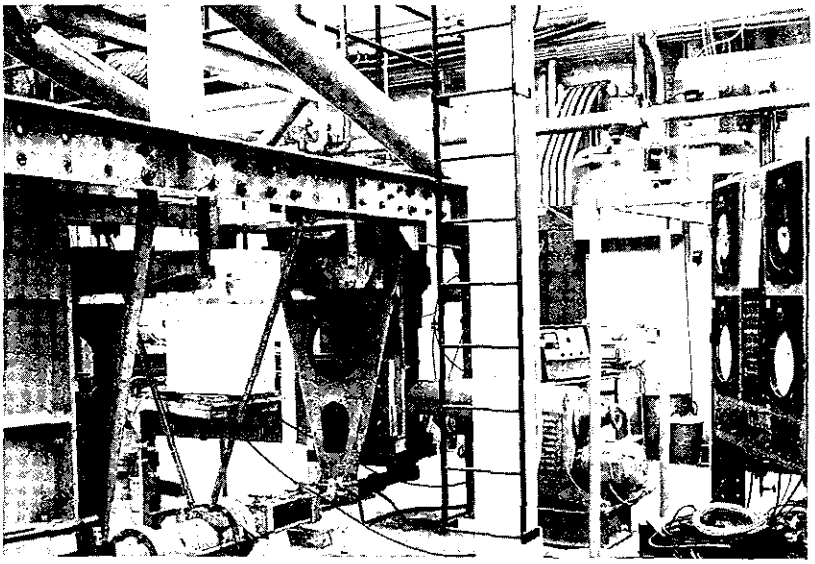

Figure 15 250,000 Pound Capacity Axial Load Resonant Fatigue Machine

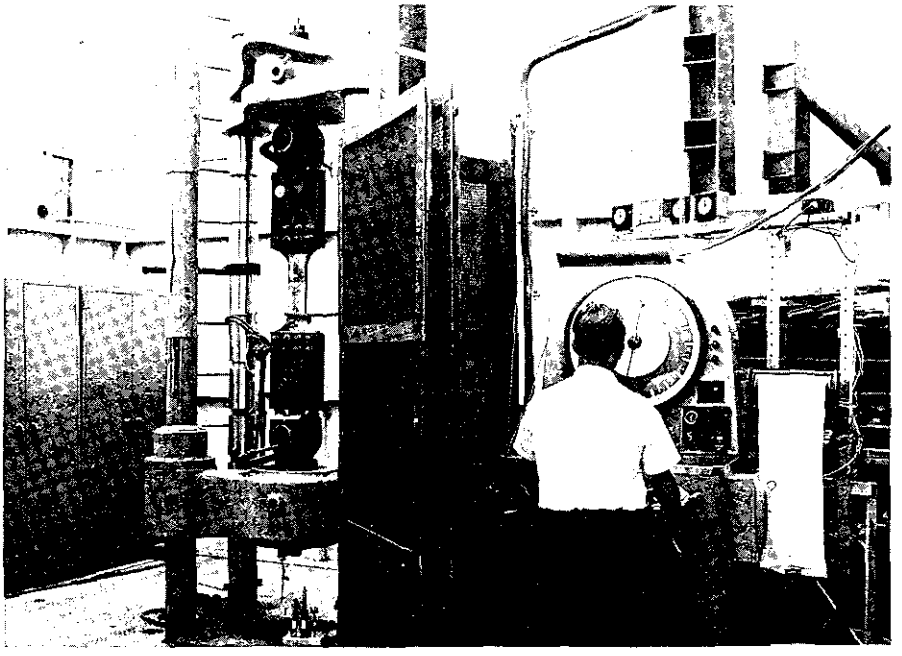

Figure 16 Fracture Toughness Test of 3/4-Inch Thick Surface-Crack Specimen

TEST ENVIRONMENT

The test program required conducting cyclic crack propagation tests for surface-crack and through-crack specimens in air and salt water spray environments. To accommodate the two environments, an environmental test chamber was constructed to enclose the test section of the specimens. The chamber consisted of a lower main polyethylene tank which housed a circulating fan, wet and dry bulb thermometers, and a fogger nozzle. Attached to the top of this tank, was a removable plexiglass chamber which enclosed the specimen test section. All internal parts of the environmental chamber were constructed from non-corrosive materials to prevent contamination of the test environments. Figures 17 and 18 present photographs of the environmental chamber in operating position.

The air environment was produced in the environmental test chamber by atomizing distilled water with compressed, dried, and filtered air through a fogger nozzle. The fogger nozzle was located, directed, and baffled so that it did not spray directly on the test specimen. The humidity level was controlled and recorded with standard wet and dry bulb controllers and recorders.

The salt water spray environment was produced by a continuous spray of atomized 5 percent NaCl salt water solution through the fogger nozzle. The salt water solution was prepared by dissolving 5 parts by weight of NaCl salt in 95 parts of distilled water. The compressed air supply to the nozzle was maintained at pressures between 10 and 25 psi.

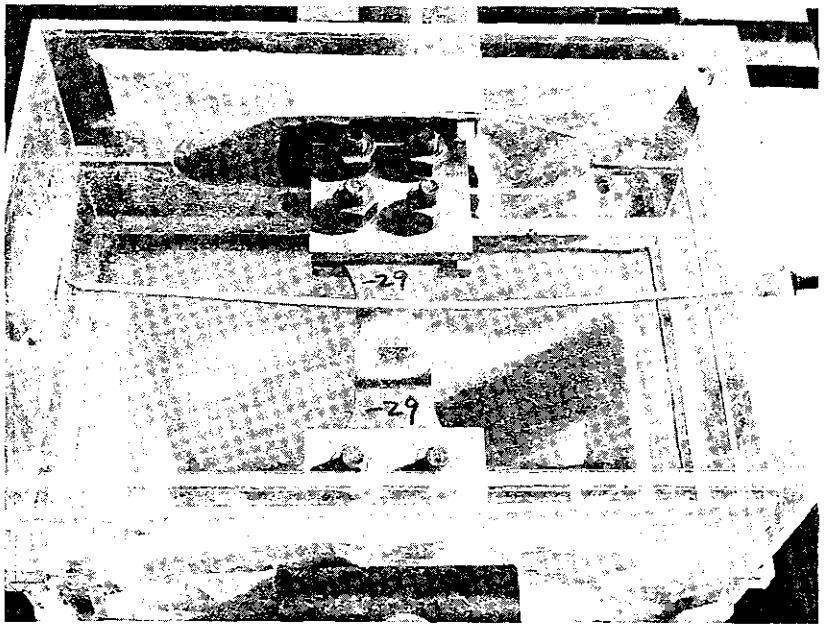

Figure 17 3/8 Surface-Crack Specimen Installed in Chamber Prior to Introducing Environment

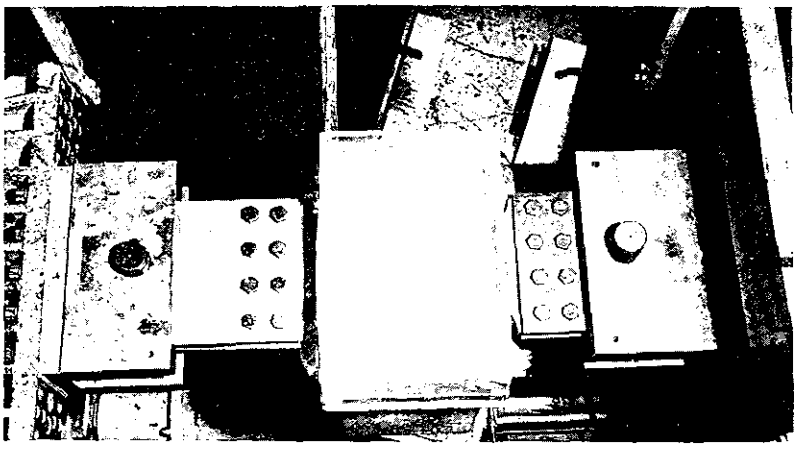

Figure 18 3/4 Surface-Crack Specimen Installed in Environmental Chamber with Salt Water Spray Operating

ENVIRONMENTAL SELECTION TEST

The relative severity of dry air versus moist air test environment was investigated early in the program in order to select a specific relative humidity for use in the balance of the program.

The environmental selection tests consisted of conducting cyclic tests on two through-crack specimens and two surface-crack specimens of 0.125 inch thickness in each of two air environments. One environment was dry air (22% relative humidity) and the other was moist air (83% relative humidity).

The relative humidity was controlled and maintained by conducting the tests in the environmental chamber described above. Desiccant or water vapor was used as required to maintain the specified humidity levels.

The test specimens and two control tensile specimens were tempered at 525°F. The test results of the tensile specimens were as follows:

Specimen Number	Tempering Temperature 2 + 2 Hrs (1)	Ultimate Strength (KSI)	0.2% Yield Stress (KSI)	Elong. 2" G.L. (%)
X-14291-1	525	278	235	7
X-14291-2		281	236	7

(1) Normalize: 1700°F, 1-1/2 hrs, air cool

Austenitize: 1600°F, 1-1/2 hrs, oil quench

The through-crack specimens were 5 inches wide and contained an 0.75 inch long center-through-crack which was generated from an 0.5 inch long EDM slot by tension-tension fatigue. The surface-crack specimens were 2.25 inches wide and contained a center surface crack 0.18 inch long and 0.05 inch deep which was generated from an EDM slot which was 0.08 inch long and 0.02 inch deep by tension-tension fatigue.

The tests were conducted with a minimum-to-maximum fatigue stress ratio (R) of +0.1 at a cyclic frequency of 20 cycles per second. The minimum fatigue stress (gross area) was 45 KSI for the surface-crack specimens and 15 KSI for the through-crack specimens. These maximum fatigue stress levels with their respective initial crack sizes and specimen geometries resulted in identical calculated initial stress intensities (K_I of 16 KSI$\sqrt{IN}$) for both the surface-crack and through-crack specimens. Selection of this initial stress intensity value was based on test results from Lockheed Independent Research work on similar materials in which cyclic crack propagation was produced in a practical number of fatigue cycles. This stress intensity level also reasonably simulates the combination of service stress levels and the degree of possible

material damage in aircraft applications. The results of these tests are graphically presented as plots of crack length vs. number of fatigue cycles in Figures 19 and 20.

The test results did not indicate a conclusive difference in behavior between the dry and moist air environments. A possible tendency for the moist air to be slightly conservative for both the surface-crack and through-crack specimens and result in less scatter for the through-crack specimens was observed. For these reasons, the moist air environment (80 to 85% relative humidity) was selected as the "air" environment for all the cyclic crack propagation tests in the program.

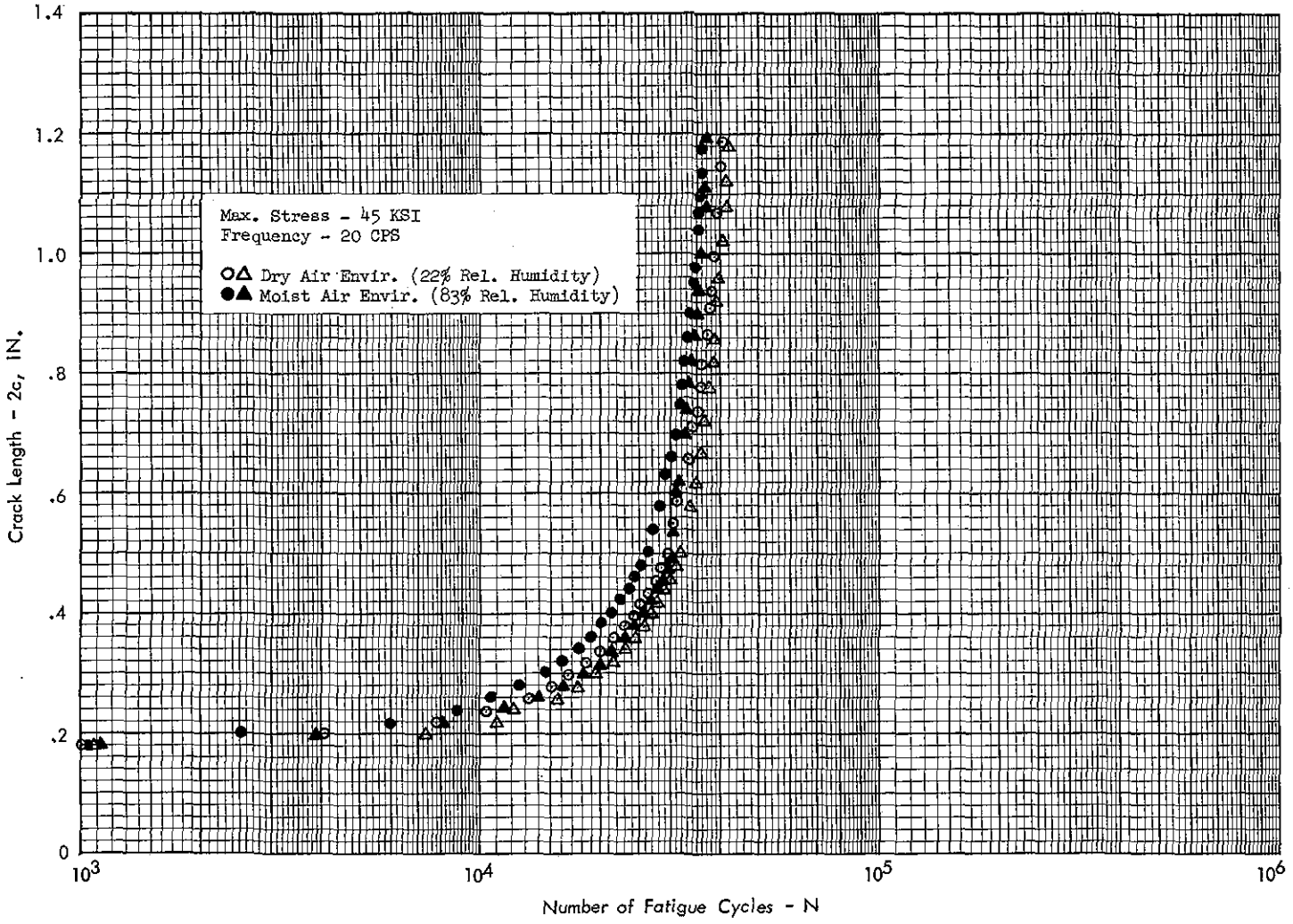

Figure 19 Cyclic Crack Propagation of 1/8-Inch Surface-Crack 300M Steel Sheet for Environment Selection at F_{tu} = 290 KSI, R = +0.1

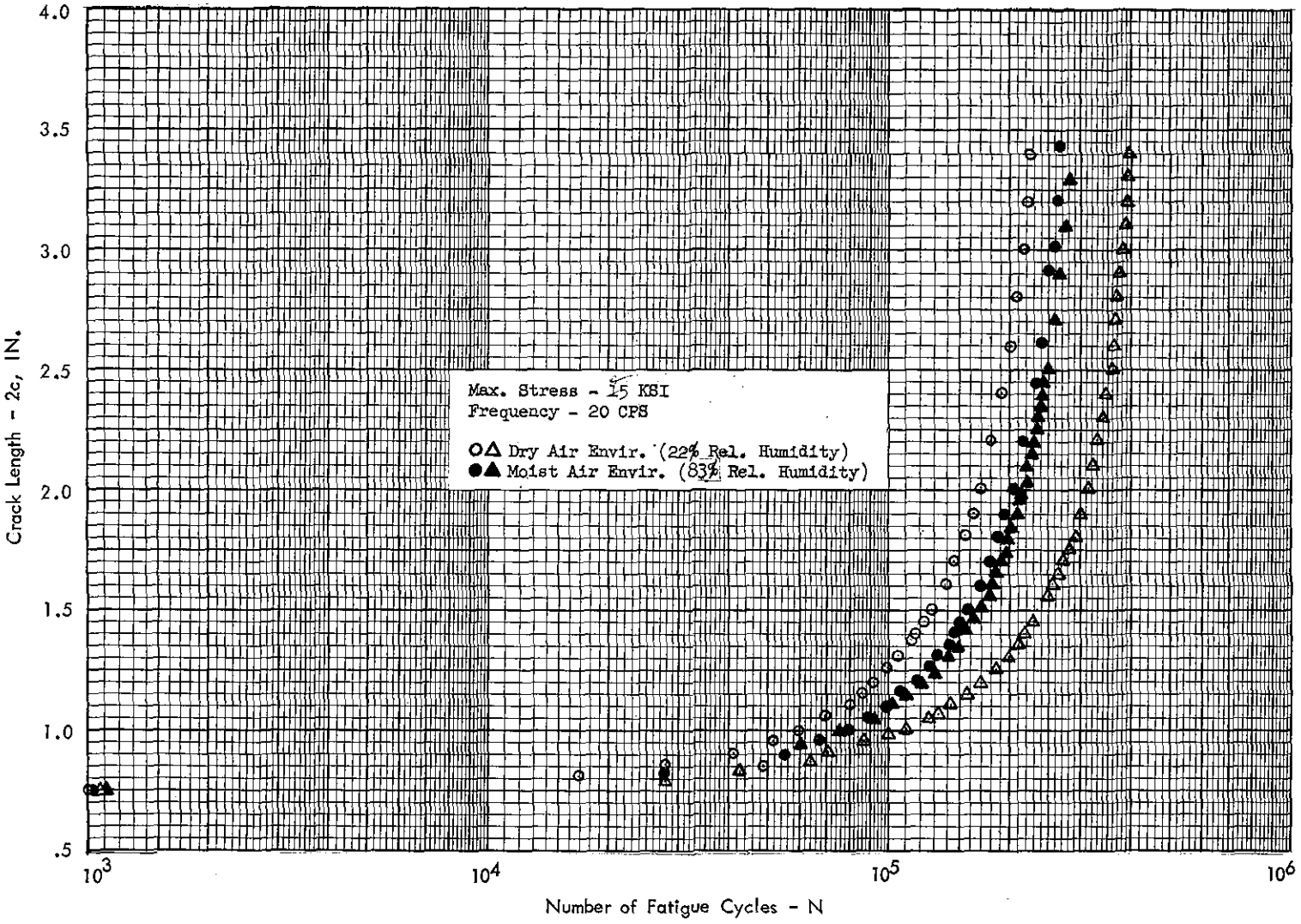

Figure 20 Cyclic Crack Propagation of 1/8-Inch Through-Crack 300M Steel Sheet for Environmental Selection at F_{tu} - 290 KSI, R = +0.1

SURFACE-CRACK PROPAGATION TESTS

Cyclic crack propagation tests were conducted for 1/8, 3/8, and 3/4 inch thick pre-cracked surface-crack specimens in moist air (80 to 85% relative humidity) and salt water spray environments. All the specimens contained an initial crack length of 0.18 inch and a crack depth of 0.085 to 0.095 inch. The initial crack was propagated by axial tension-tension cyclic loading at a cyclic frequency of 20 cycles per second. Three specimens were tested for each condition of product, environment, range ratio, and maximum fatigue stress. The initial crack was propagated to a different final crack size without failure for each of the three specimens. The three final crack lengths were approximately 0.26, 0.38, and 0.56 inch respectively for the 1/8 inch thick specimens; 0.38, 0.56, and 0.76 inch for the 3/8 inch thick specimens; and 0.60, 0.80, and 1.00 inch for the 3/4 inch thick specimens.

The crack propagation tests were conducted at a constant mean stress of 25 KSI and range ratios of +0.1, +0.2, and +0.5 which resulted in maximum cyclic stresses of 45 KSI, 42 KSI, and 33 KSI respectively.

Crack length measurements and corresponding number of fatigue cycles were recorded for crack length increments of approximately 0.02 inch up to a crack length of 0.60 inch followed by increments of 0.04 inch until the final crack length was obtained. The crack length measurements were accomplished by visual comparison of the crack and a transparent plastic scale attached to the specimen surface adjacent to the crack. A magnifying lens was used in making these measurements. Cycling of the specimen had to be stopped for a brief period while the crack lengths were measured. During these cycling interruptions, the mean load and test environment were maintained.

Upon completion of the crack propagation tests, the specimens were statically tested to failure to obtain fracture toughness properties. The unique feature of the procedure used was that both cyclic crack propagation test data and fracture toughness data were obtained from the same specimen. This procedure resulted in an obvious economical benefit and also permitted direct correlation between fracture toughness and a specific cyclic crack propagation history.

The test results are presented as graphical plots of crack length vs. number of fatigue cycles in Figures 21 through 36 inclusive and numerically in Tables 4 through 19.

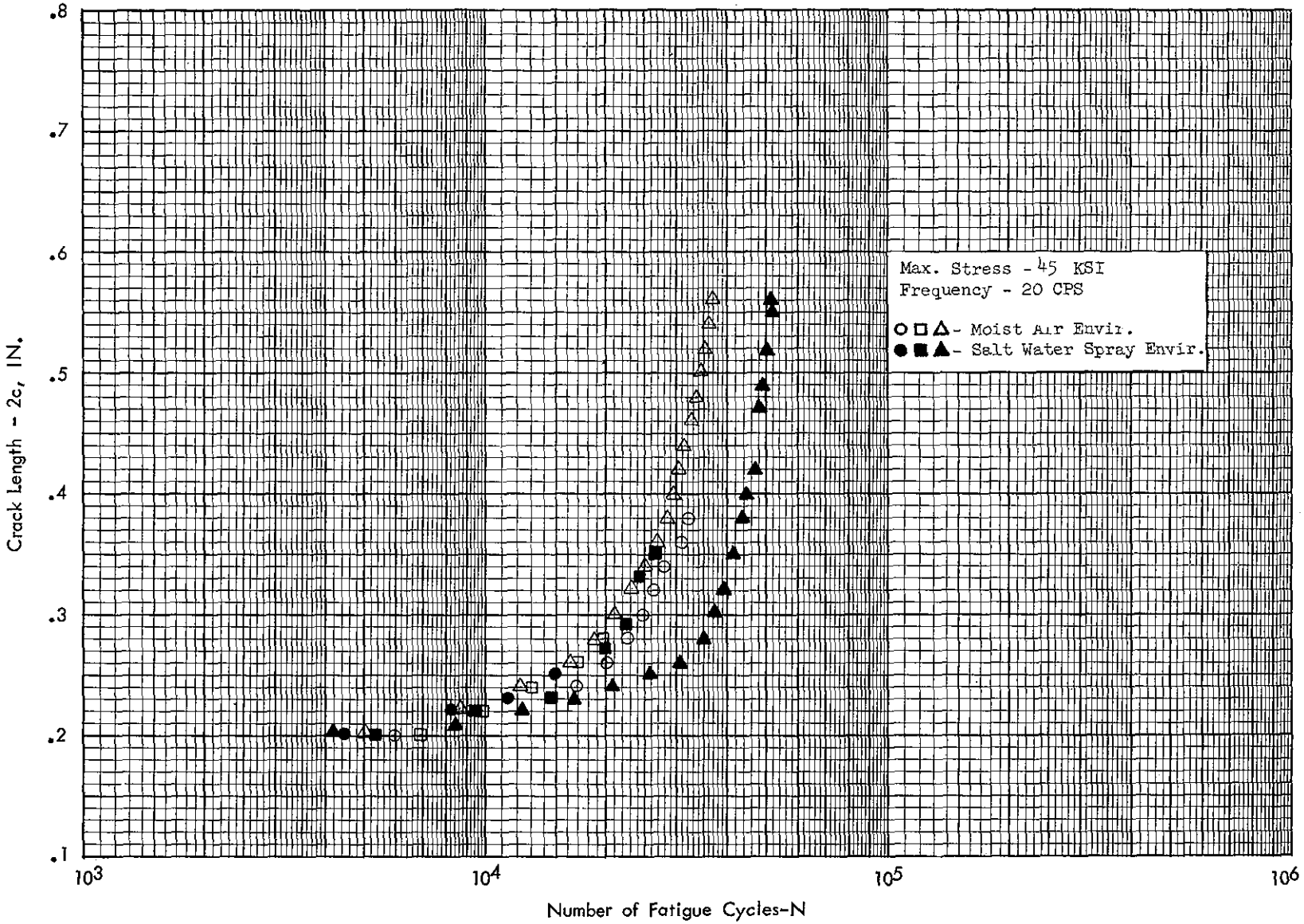

Figure 21 Cyclic Crack Propagation of 1/8-Inch Surface-Crack 300 M Steel Sheet at F_{tu} - 290 KSI, R = +0.1

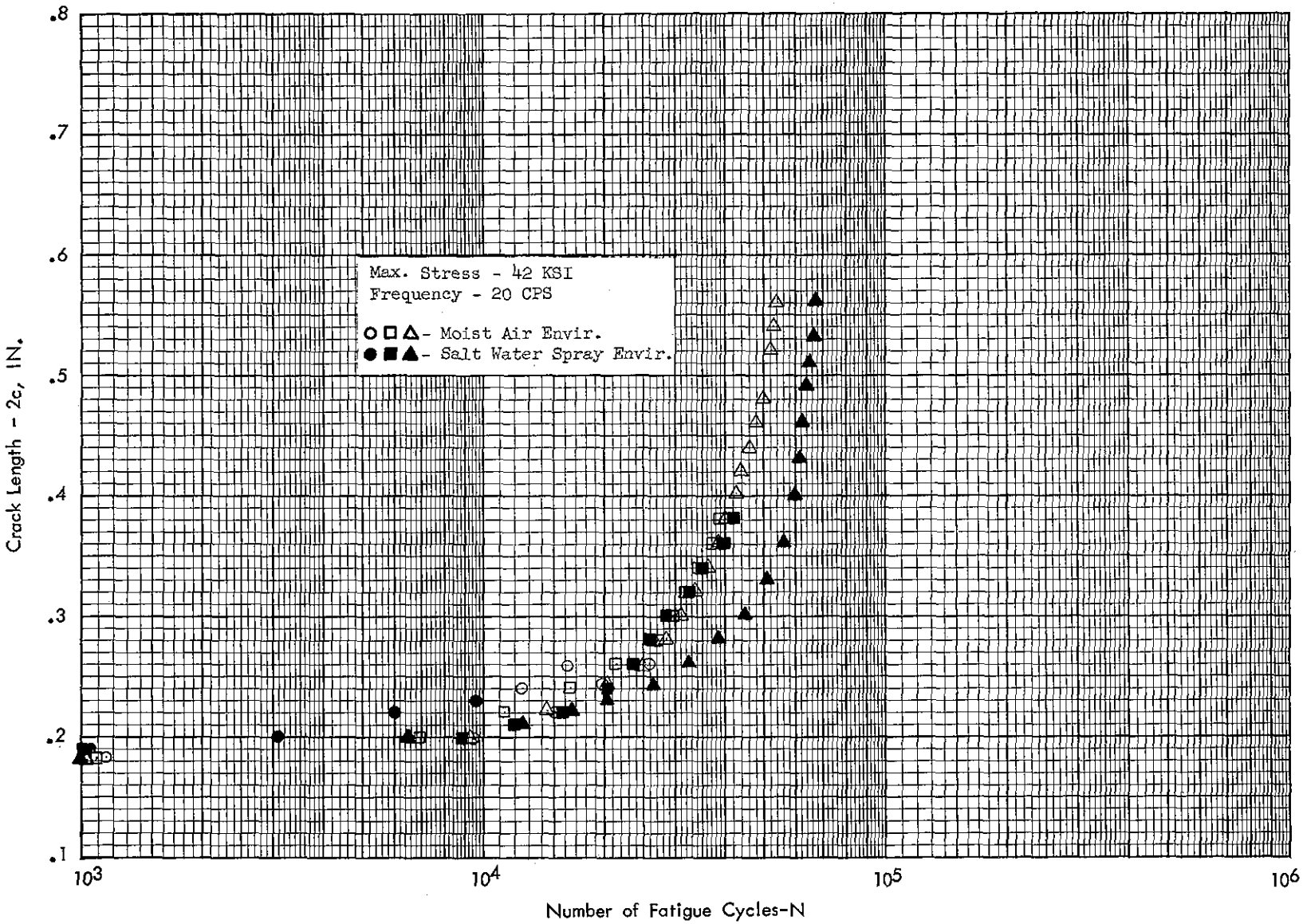

Figure 22 Cyclic Crack Propagation of 1/8-Inch Surface- Crack 300M Steel Sheet at F_{tu} - 290 KSI, R = +0.2

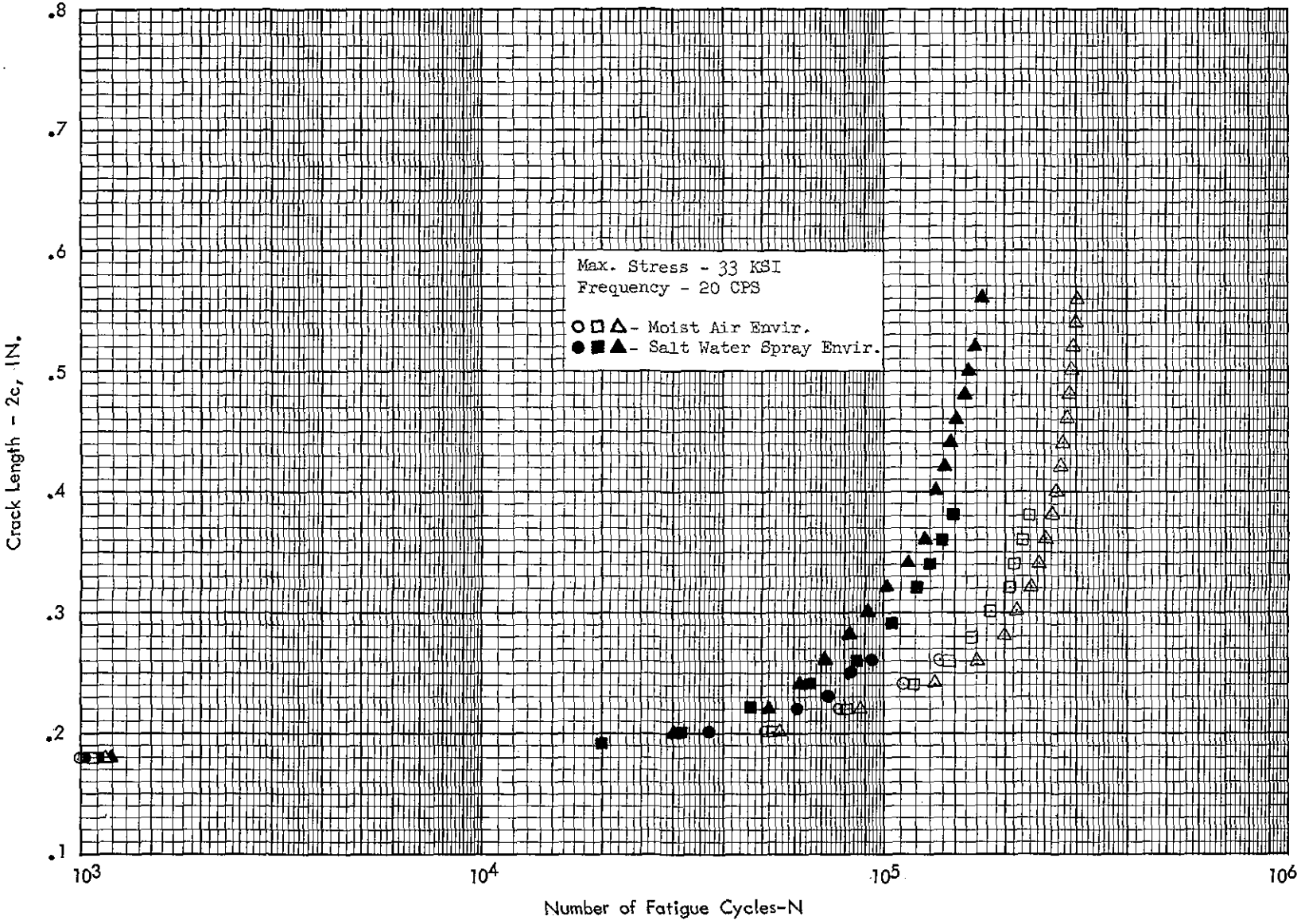

Figure 23 Cyclic Crack Propagation of 1/8-Inch Surface-Crack 300M Steel Sheet at F_{tu} - 290, R = +0.5

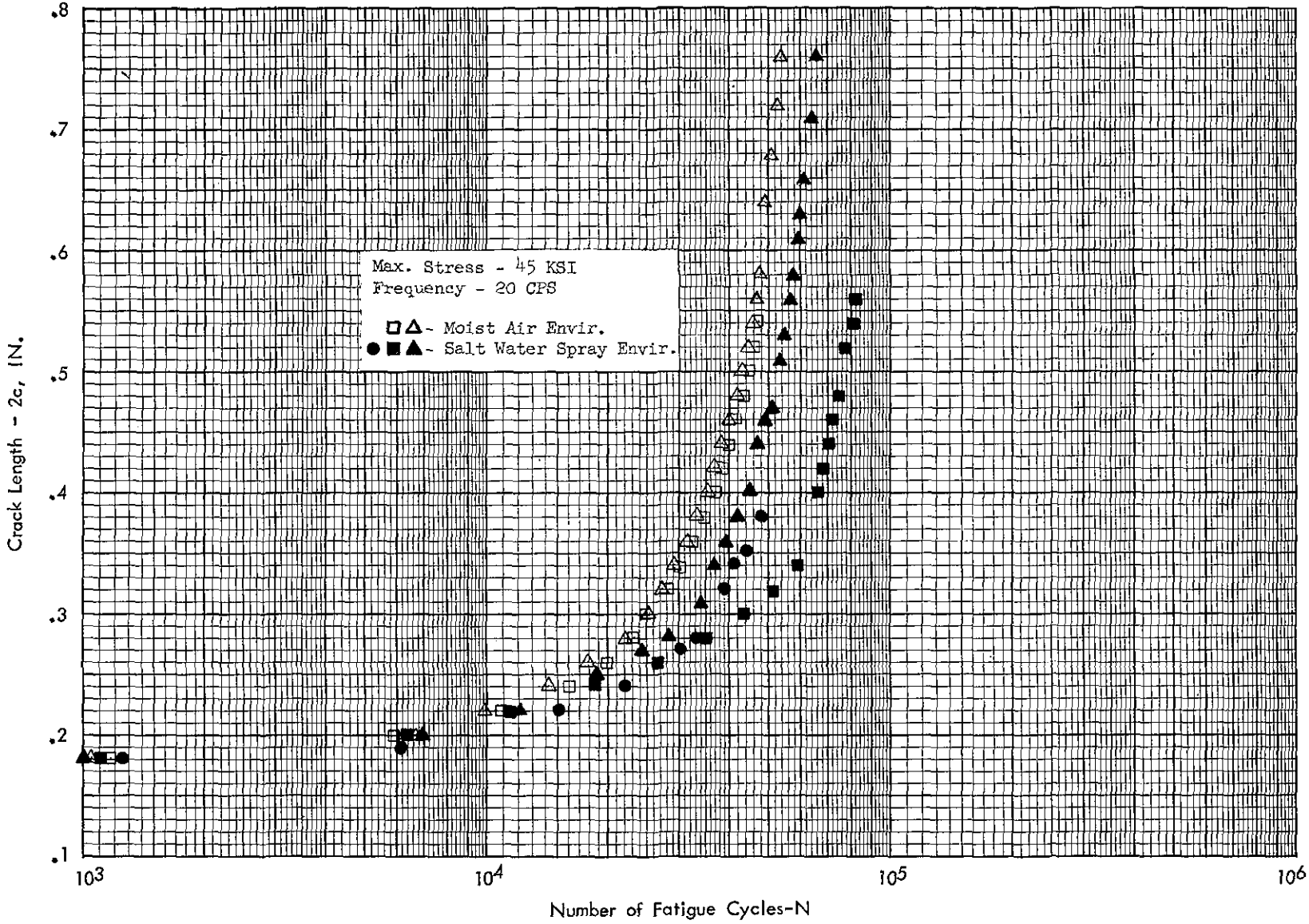

Figure 24 Cyclic Crack Propagation of 3/8-Inch Surface-Crack 300 M Steel Plate at F_{tu} - 290 KSI, R = +0.1

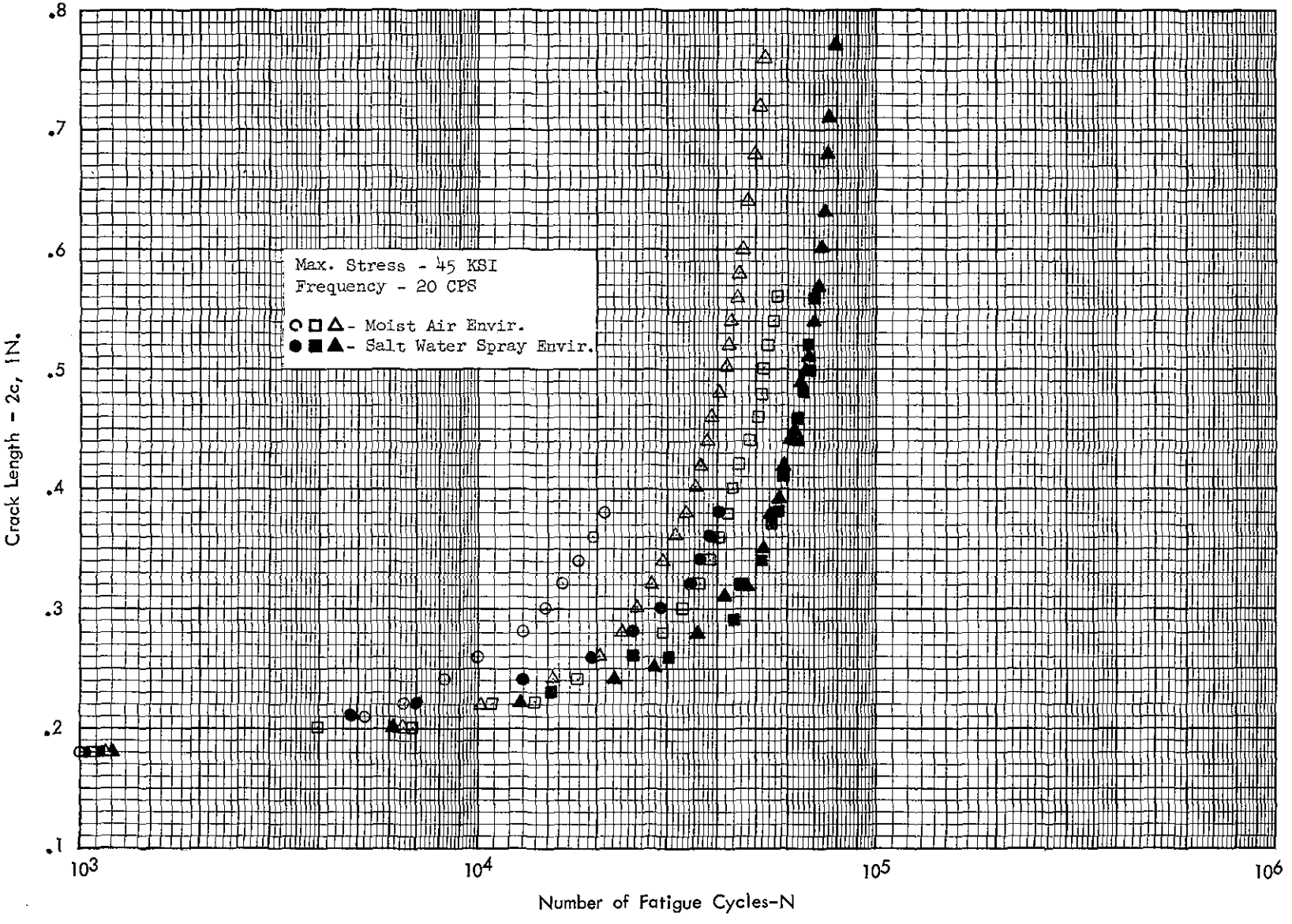

Figure 25 Cyclic Crack Propagation of 3/8-Inch Surface-Crack 300 M Steel Plate at F_{tu} - 270 KSI, R = +0.1

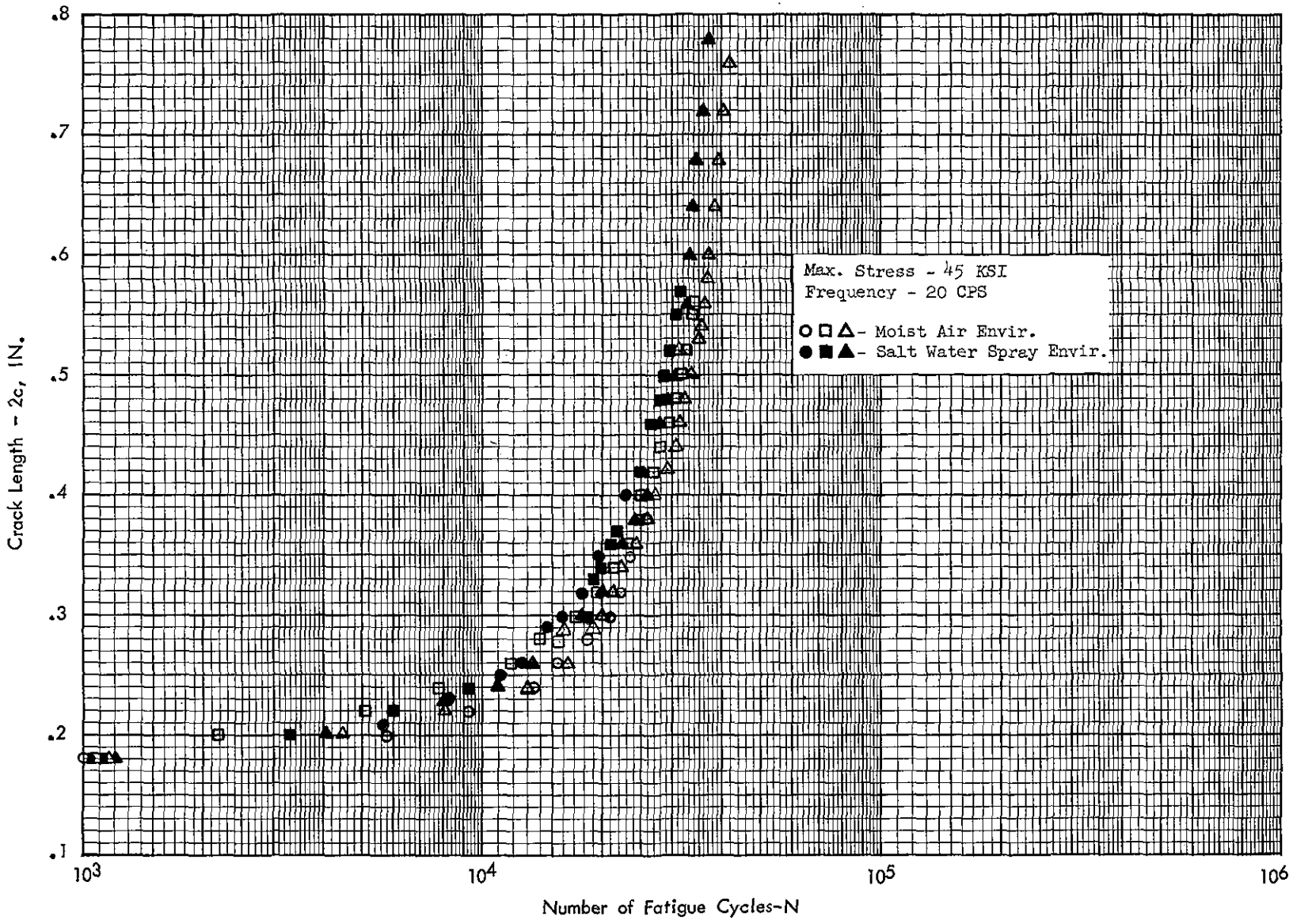

Figure 26 Cyclic Crack Propagation of 3/8-Inch Surface-Crack 300 M Steel Plate at F_{tu} - 220 KSI, R = +0.1

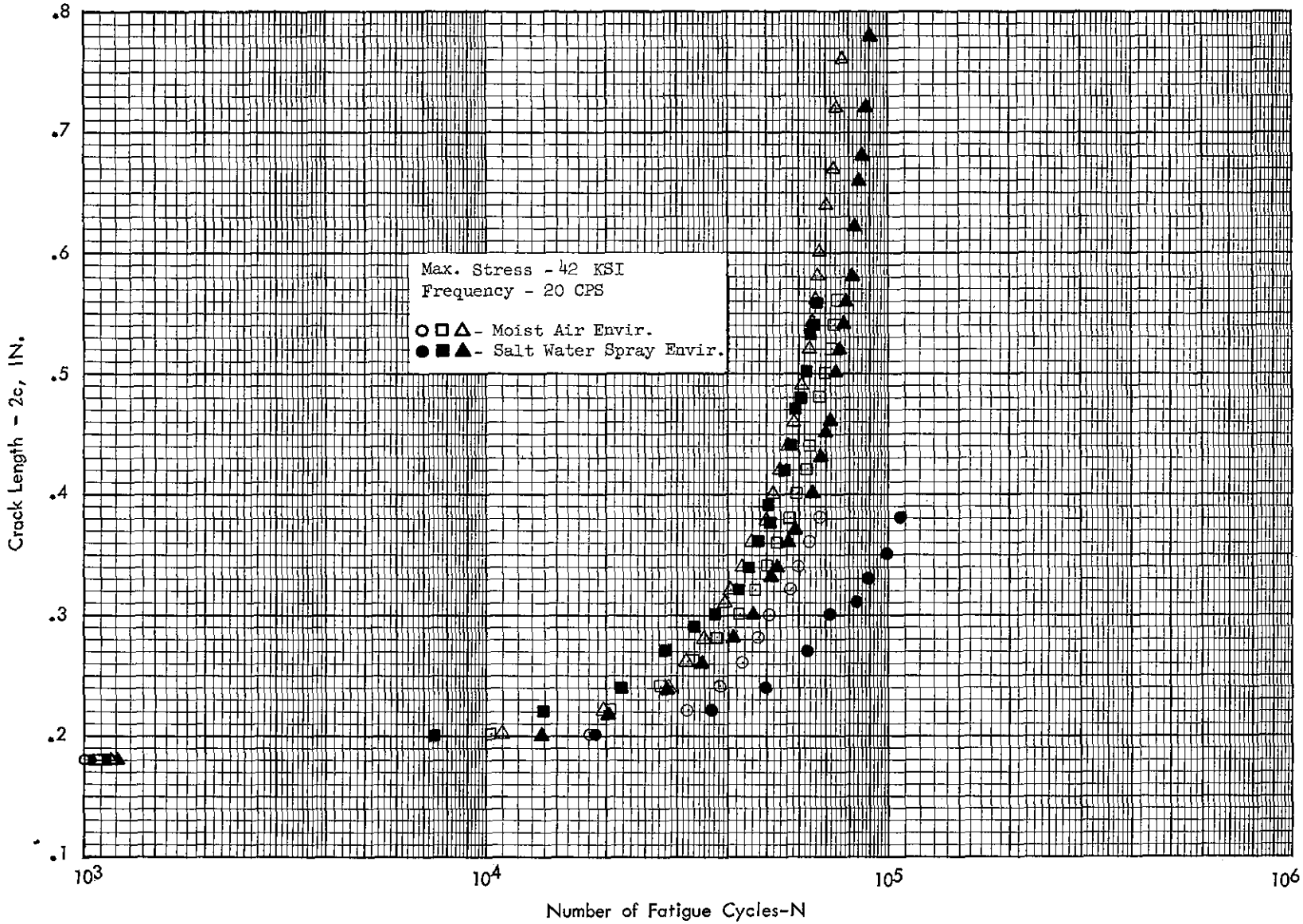

Figure 27 Cyclic Crack Propagation of 3/8-Inch Surface-Crack 300 M Steel Plate at F_{tu} - 290 KSI, R = +0.2

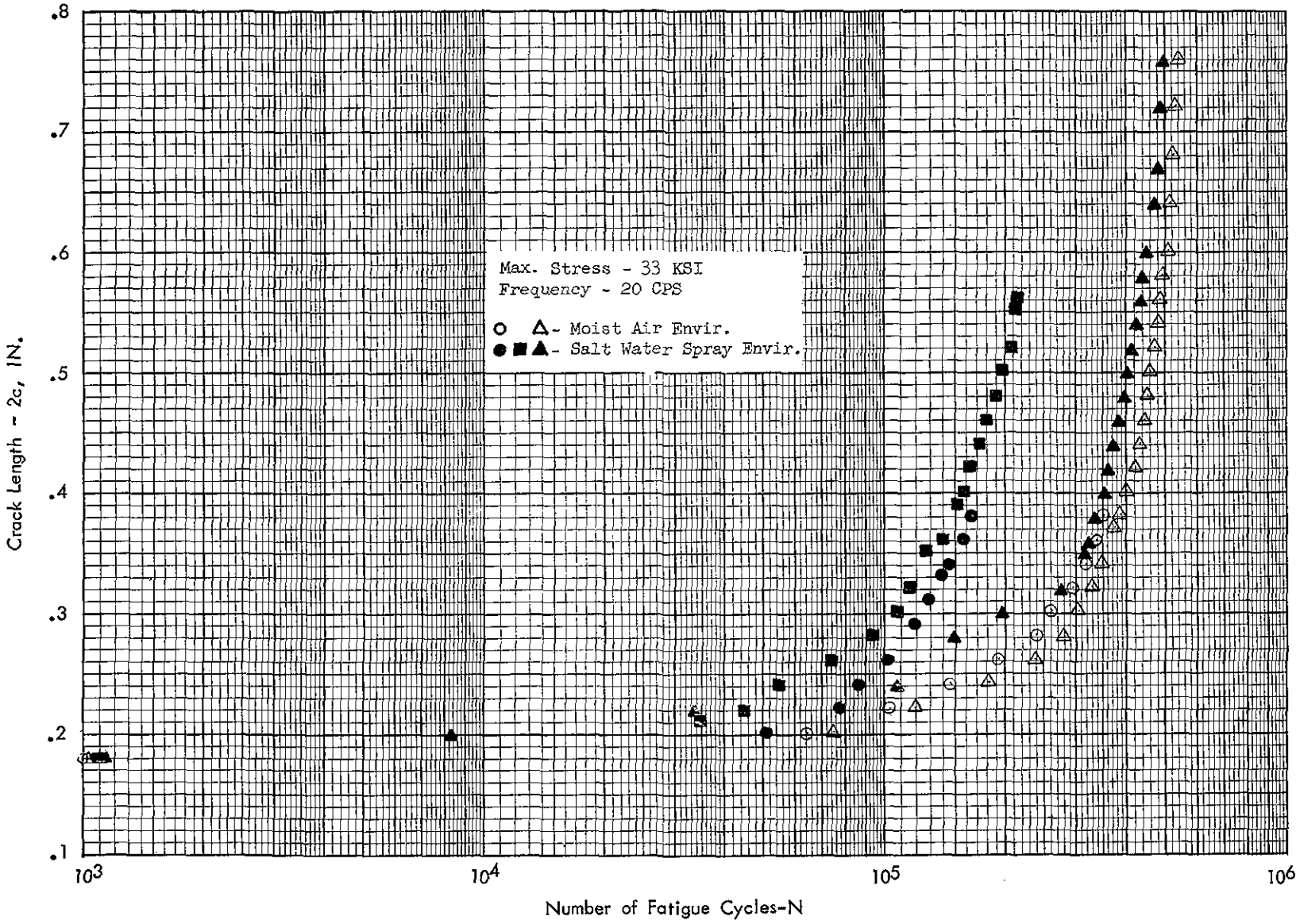

Figure 28 Cyclic Crack Propagation of 3/8-Inch Surface-Crack 300 M Steel Plate at F_{tu} - 290 KSI, R = +0.5

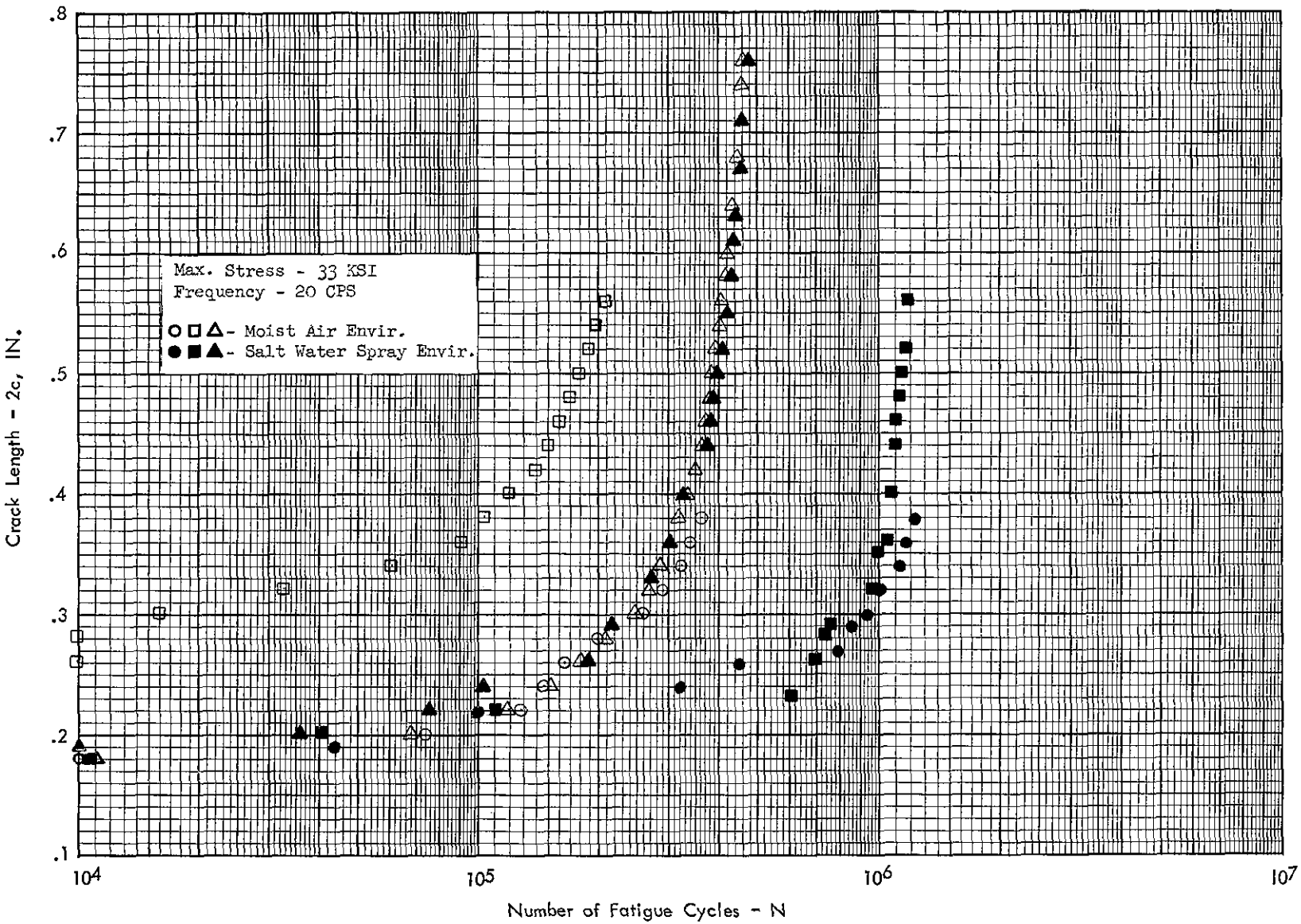

Figure 29 Cyclic Crack Propagation of 3/8-Inch Surface-Crack 300 M Steel Plate at F_{tu} - 270 KSI, R = +0.5

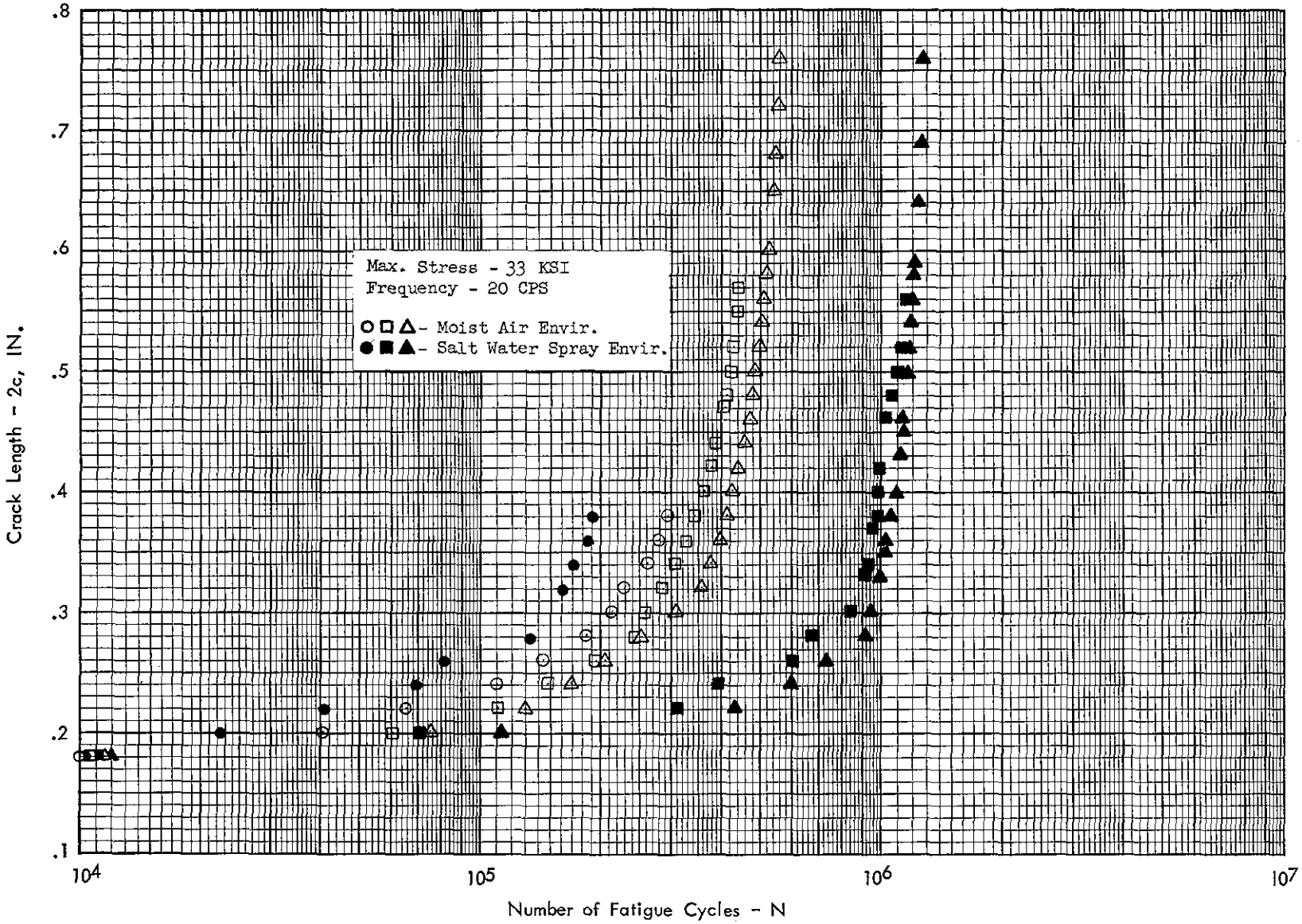

Figure 30 Cyclic Crack Propagation of 3/8-Inch Surface-Crack 300 M Steel Plate at F_{tu} - 220 KSI, R = +0.5

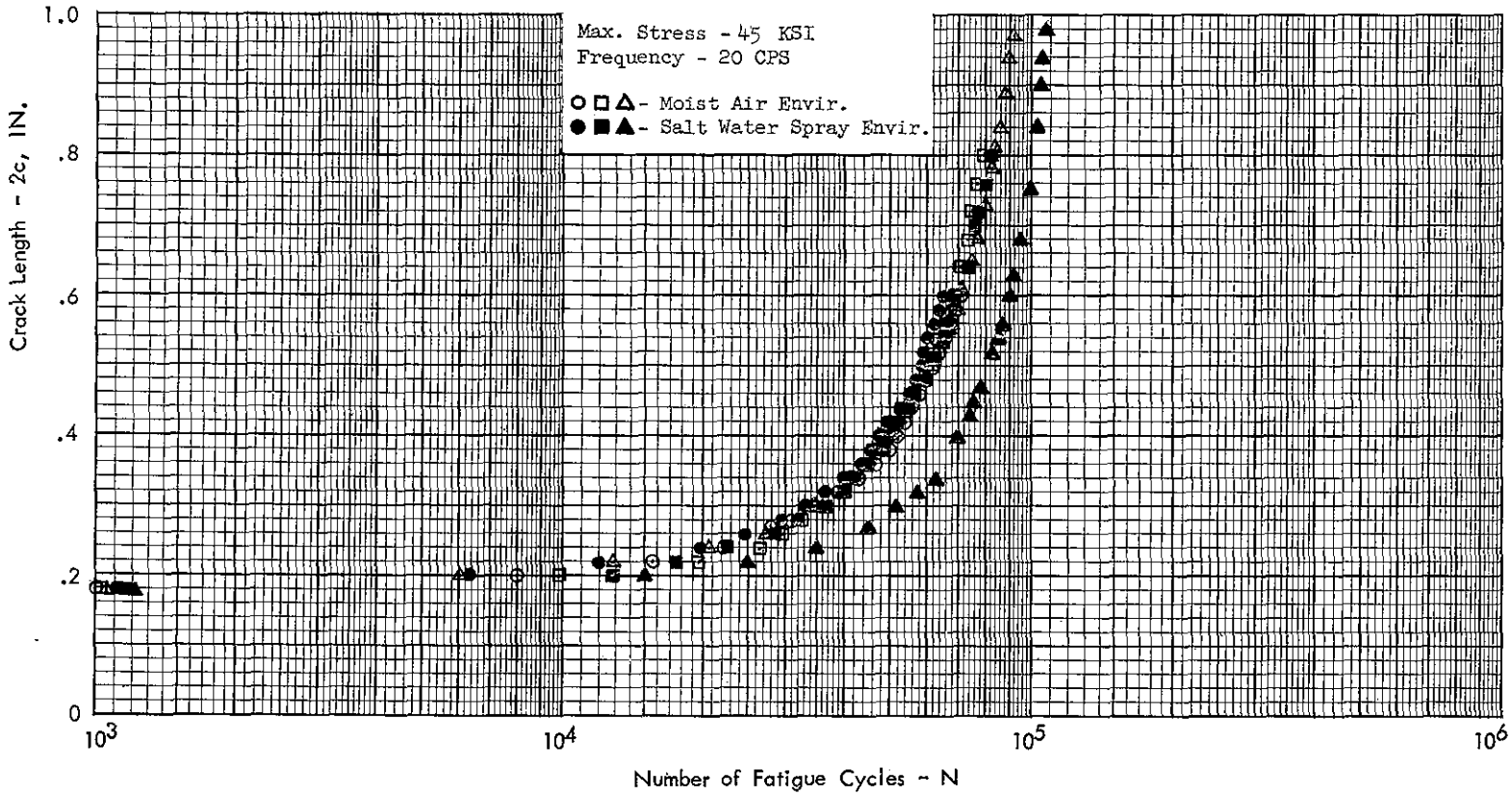

Figure 31 Cyclic Crack Propagation of 3/4-Inch Surface-Crack 300 M Steel Plate at F_{tu} - 290 KSI, R = +0.1

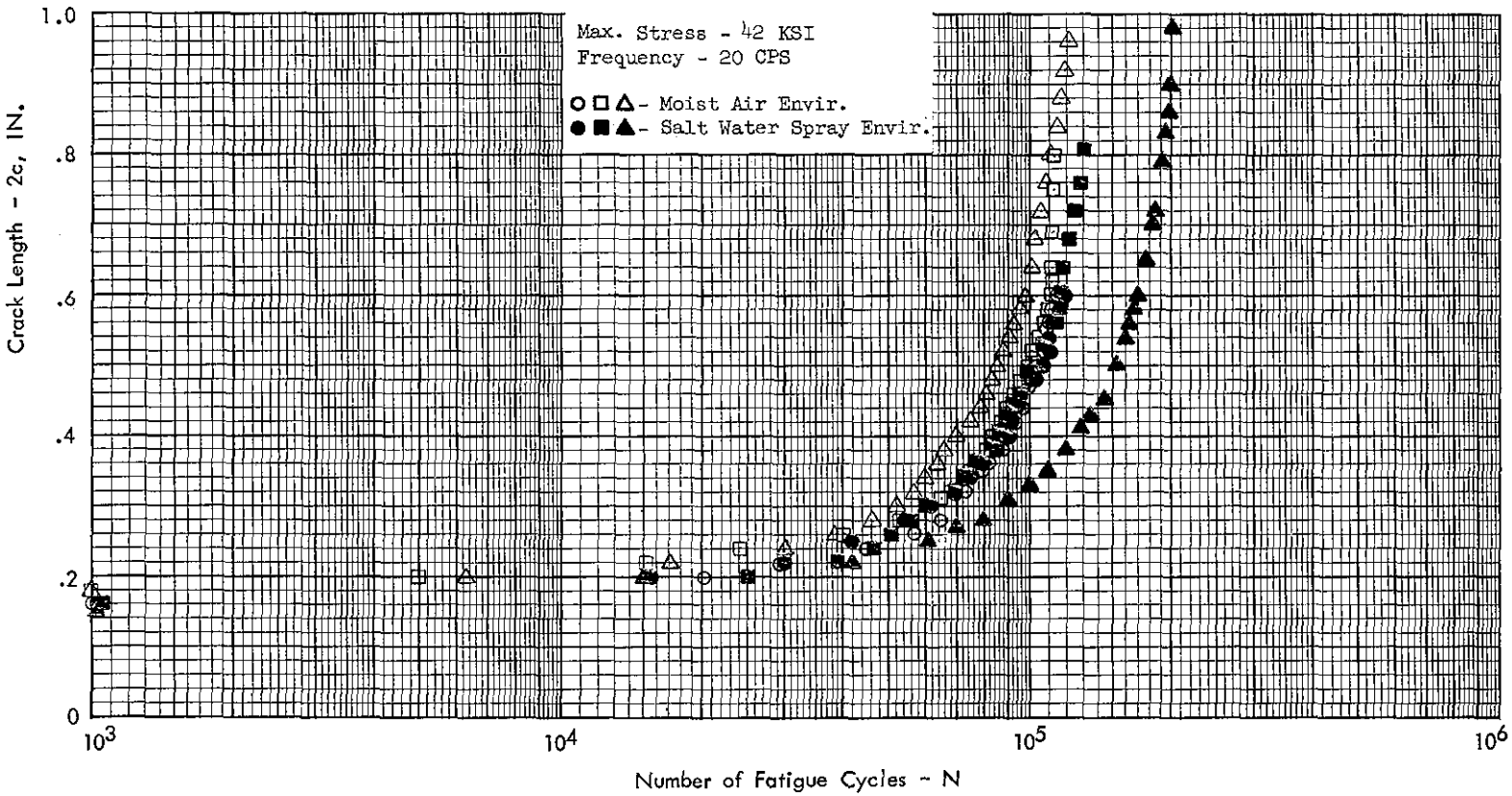

Figure 32 Cyclic Crack Propagation of 3/4-Inch Surface-Crack 300 M Steel Plate at F_{tu} - 290 KSI, R = +0.2

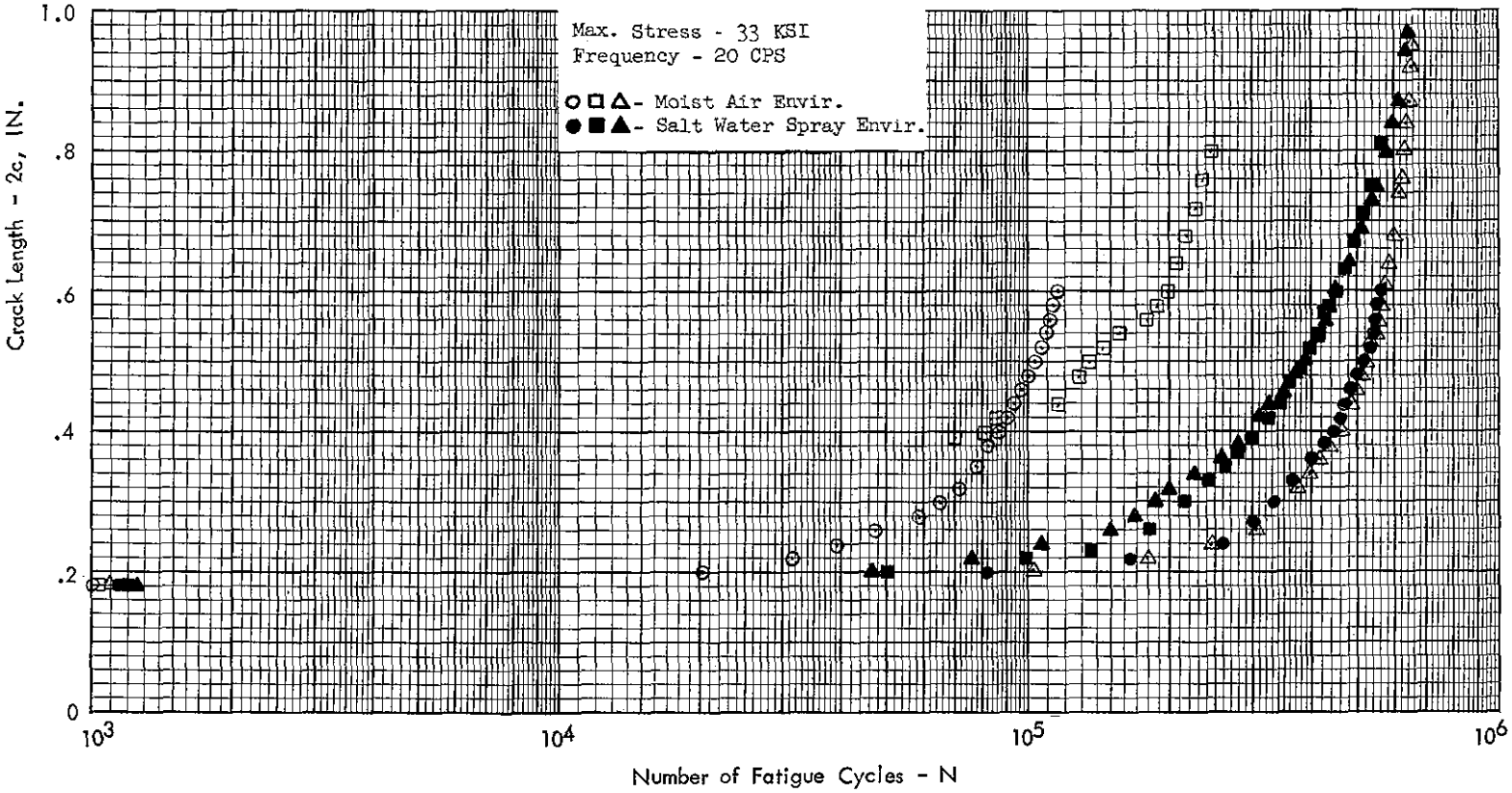

Figure 33 Cyclic Crack Propagation of 3/4-Inch Surface-Crack 300 M Steel Plate at F_{tu} - 290 KSI, R = +0.5

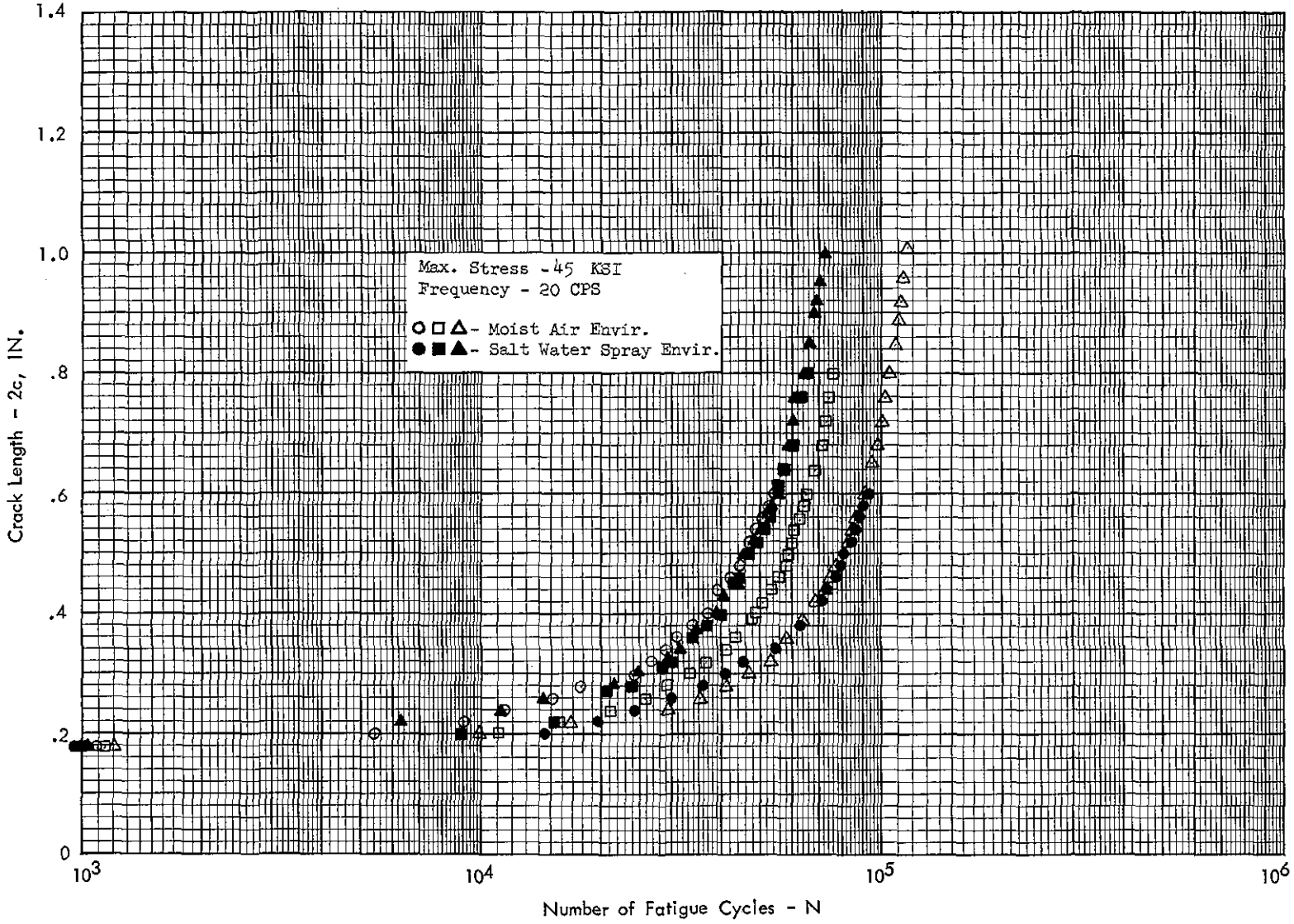

Figure 34 Cyclic Crack Propagation of 3/4-Inch Surface-Crack 300 M Steel Forging at F_{tu} - 290 KSI, R = +0.1

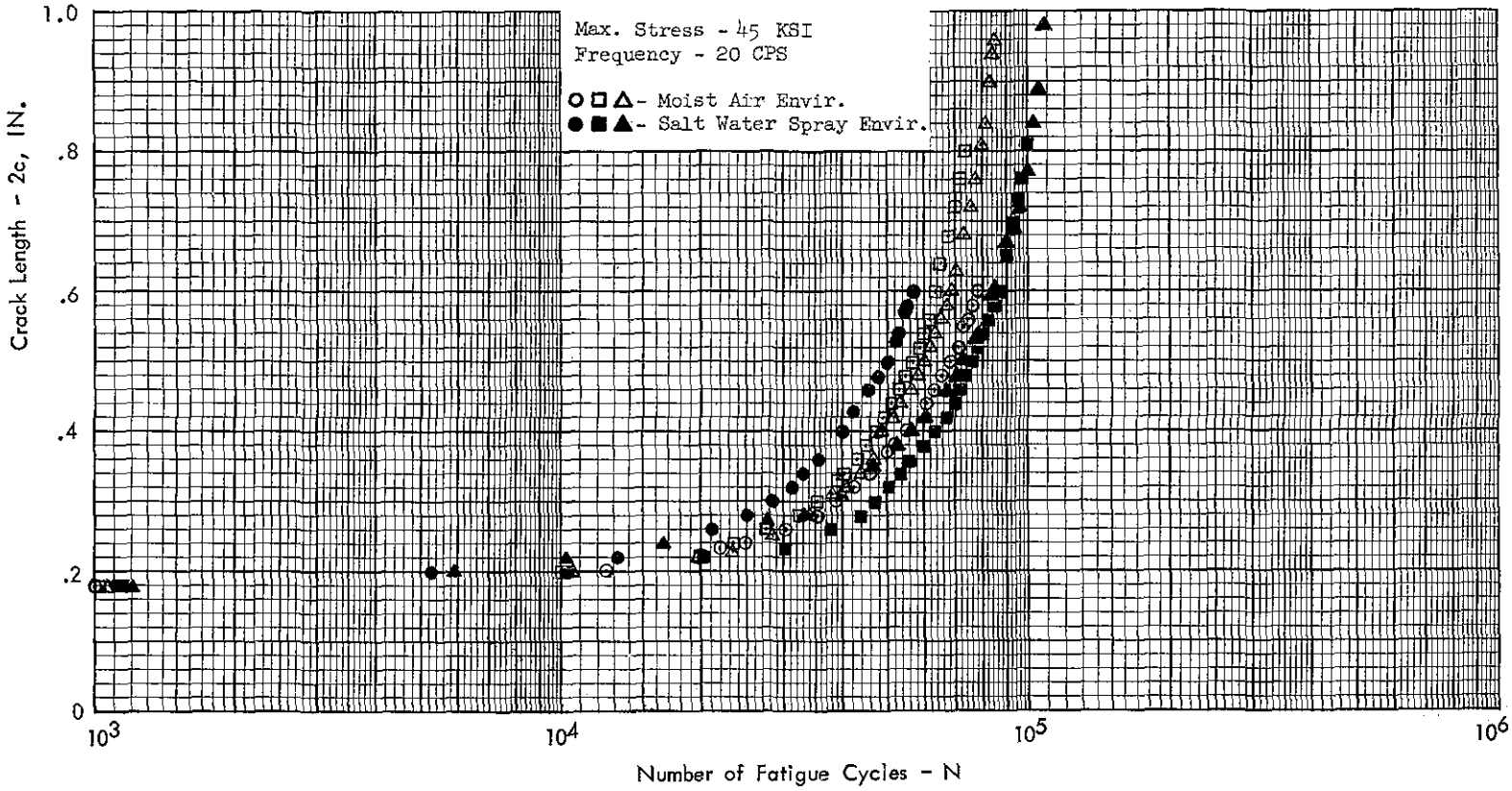

Figure 35 Cyclic Crack Propagation of 3/4-Inch Surface-Crack 300 M Steel Forging at F_{tu} - 270 KSI, R = +0.1

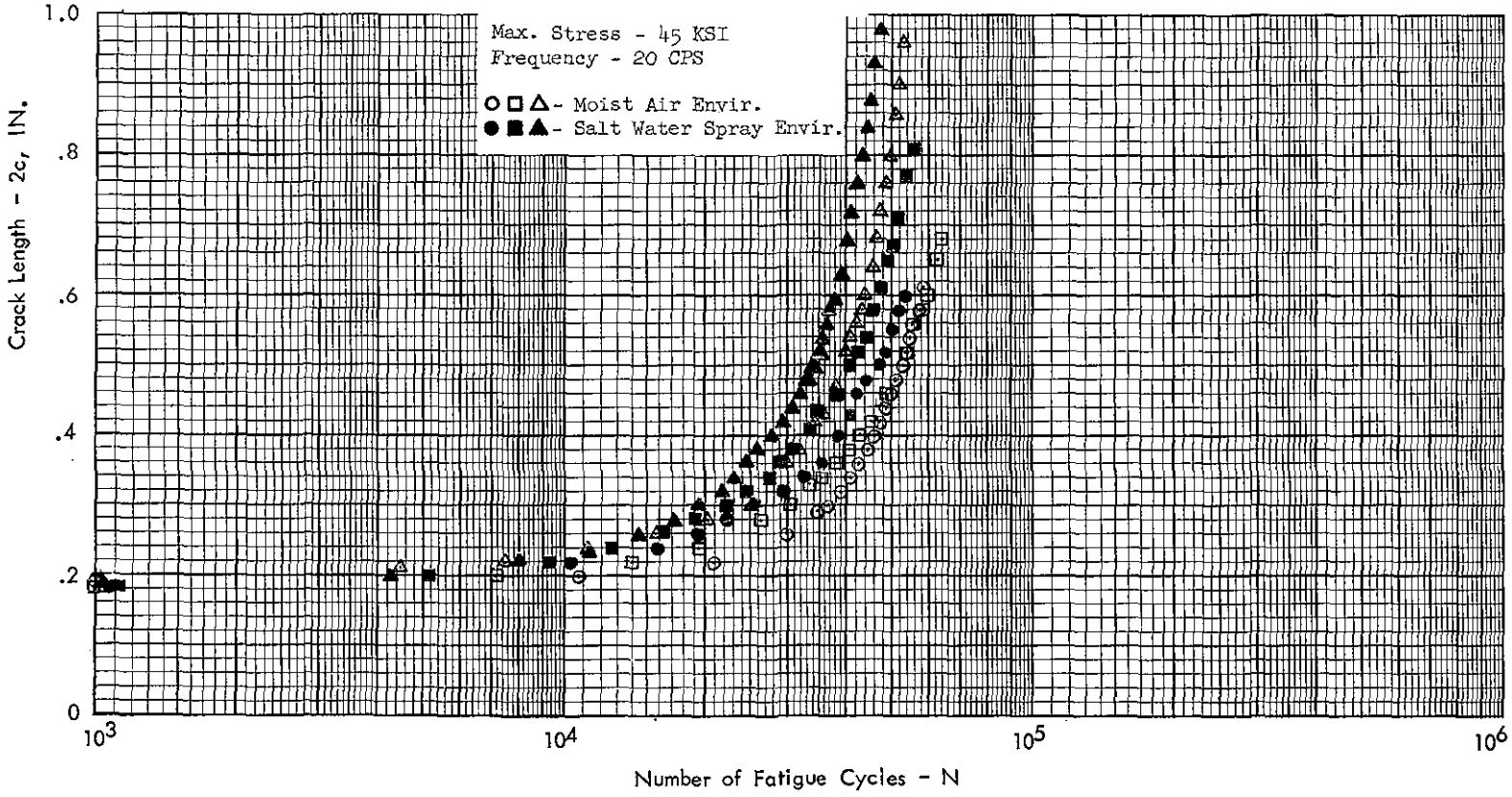

Figure 36 Cyclic Crack Propagation of 3/4-Inch Surface-Crack 300 M Steel Forging at F_{tu} - 220 KSI, R = +0.1

THROUGH-CRACK PROPAGATION TESTS

Cyclic crack propagation tests were conducted for 1/8 and 3/8 inch thick pre-cracked through-crack specimens in moist air (80 to 85% relative humidity) and salt water spray environments. All the specimens contained an initial crack length of 0.75 inch. The initial cracks were propagated in the same manner as the surface-crack specimens for three specimens for each set of conditions. The three final crack lengths for each set of conditions were approximately 1.30, 1.90, and 2.50 inches for both the 1/8 and 3/8 inch thick specimens.

It was originally scheduled to conduct the crack propagation tests at a constant mean stress of 8 KSI and range ratios of +0.1 and +0.5 which would have resulted in maximum cyclic stresses of 15 KSI and 11 KSI respectively. As previously mentioned in the "Environment Selection Tests", the maximum length of 0.75 inch and the maximum stress of 45 KSI with the surface-crack specimen geometry and initial crack length of 0.18 inch resulted in approximately the same initial stress intensities (K_I) of 16 KSI in. The +0.1 range ratio tests were conducted as scheduled but during initial testing of the +0.5 range ratio tests, it was found that the cracks could not be propagated within a reasonable number of fatigue cycles in either moist air or salt water spray environments. Two 270 KSI strength level specimens were tested in moist air and one in salt water spray at the maximum fatigue stress of 11 KSI. For the remainder of the +0.5 range ratio tests, the maximum cyclic stress was raised from 11 KSI to 22.5 KSI. The increased maximum cyclic stress was compatible with the balance of the test program and permitted cross comparisons which is discussed in the "Data Analysis" section.

After cyclic crack propagation testing, the specimens were statically tested to failure to obtain fracture toughness properties.

The test results are presented as graphical plots of crack length vs. number of fatigue cycles in Figures 37 through 43 and numerically in Tables 20 through 25.

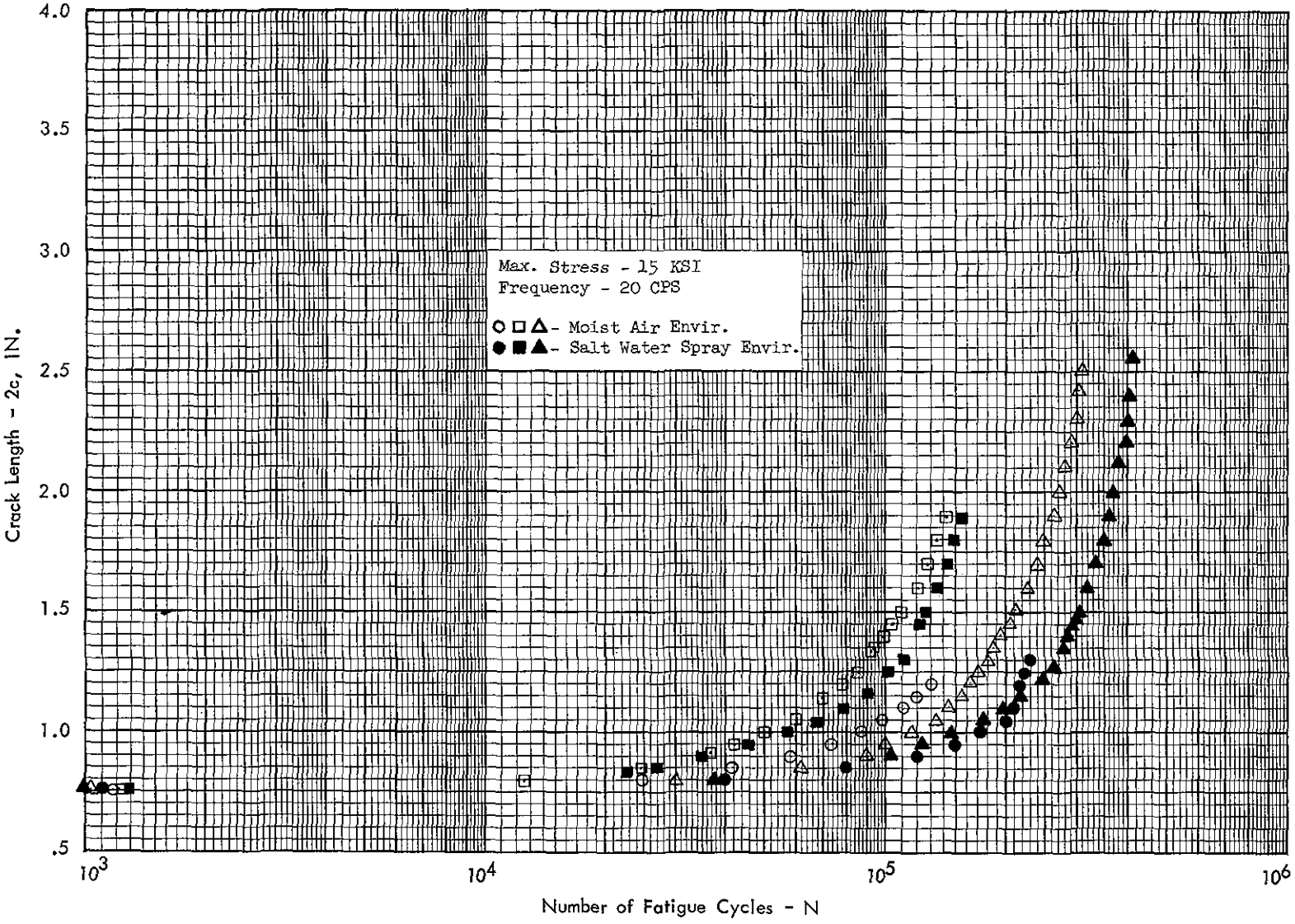

Figure 37 Cyclic Crack Propagation of 1/8-Inch Through-Crack 300 M Steel Sheet at F_{tu} - 290 KSI, R = +0.1

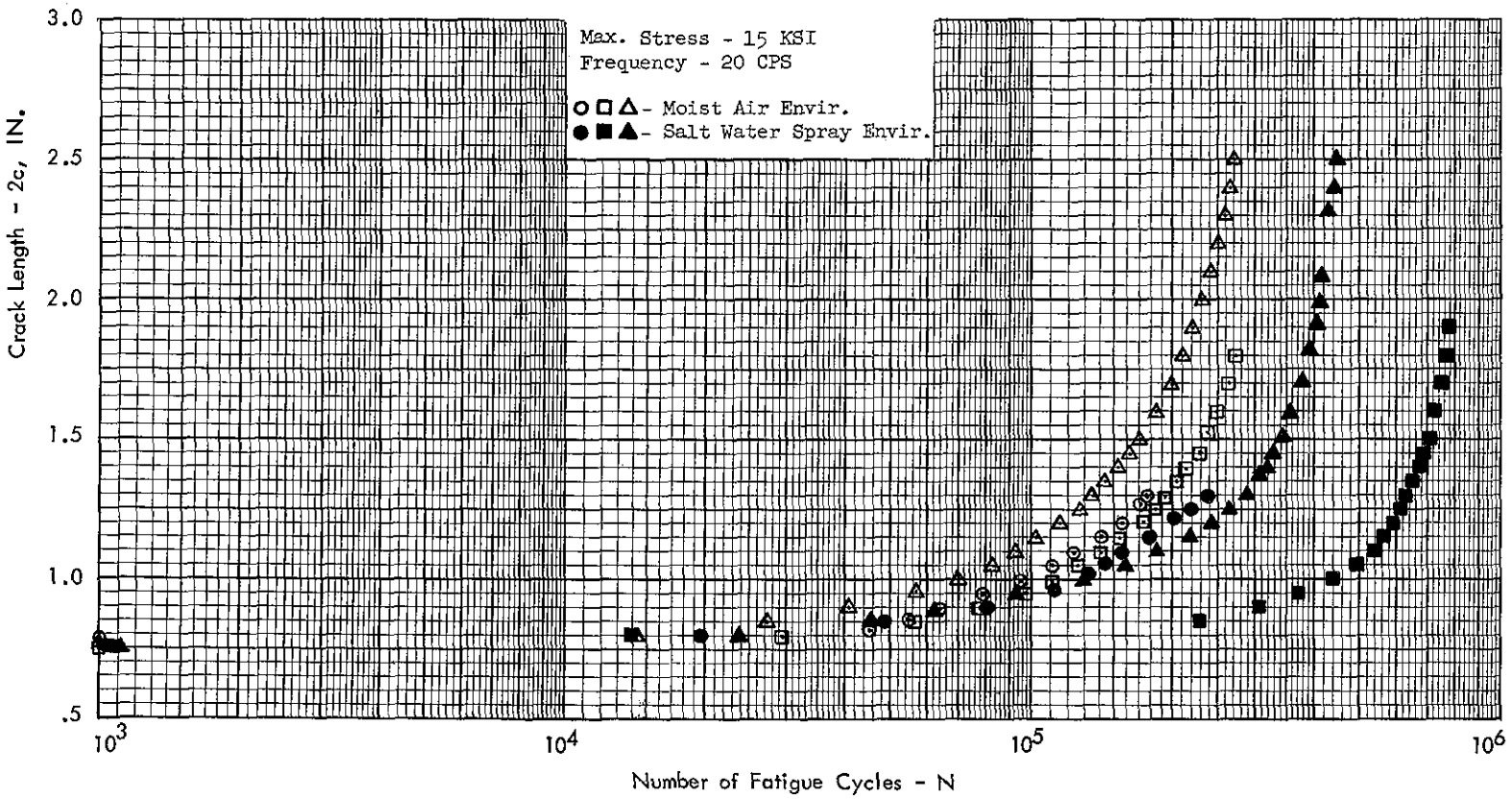

Figure 38 Cyclic Crack Propagation of 3/8-Inch Through-Crack 300 M Steel Plate at F_{tu} - 290 KSI, R = +0.1

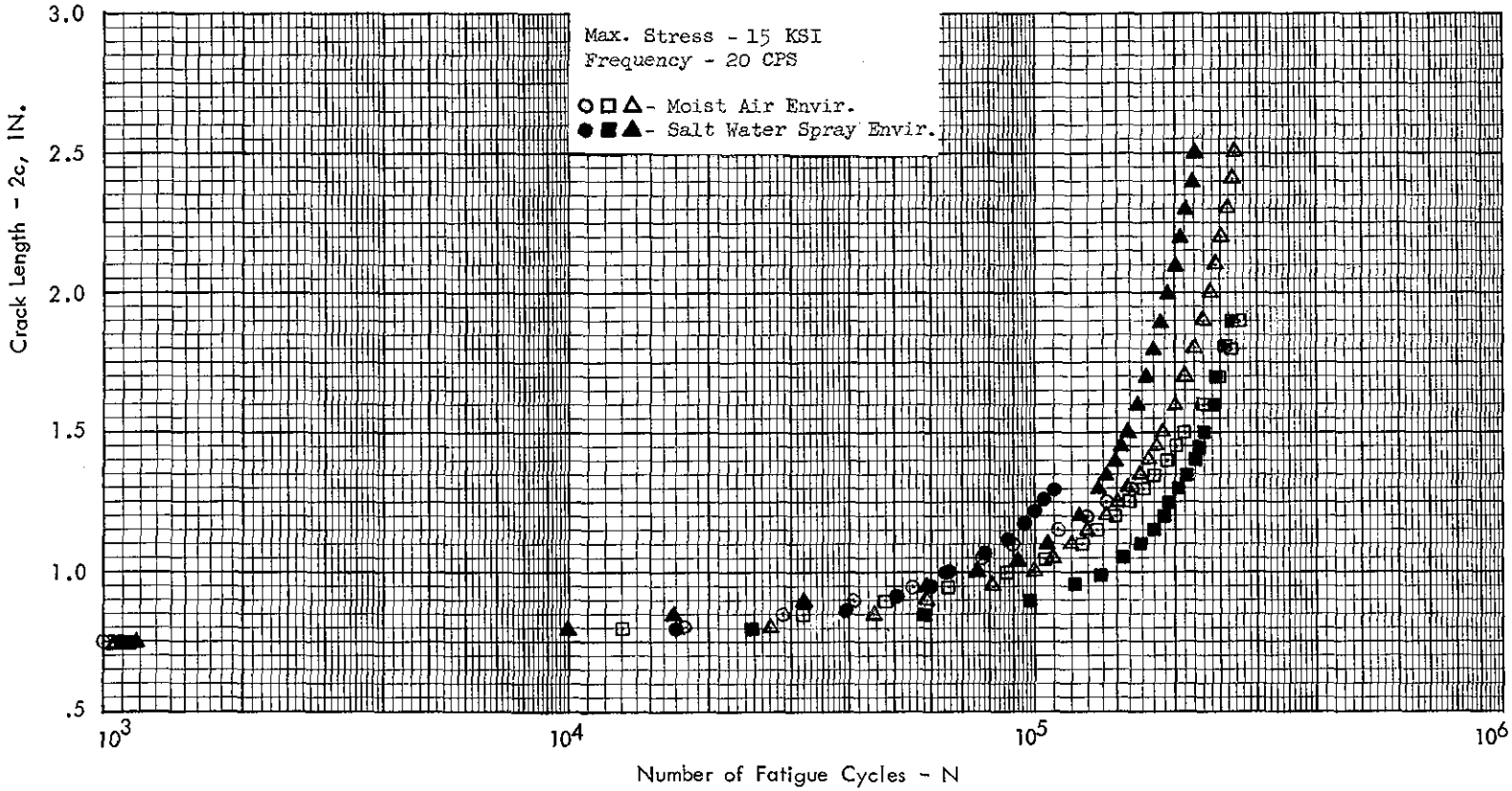

Figure 39 Cyclic Crack Propagation of 3/8-Inch Through-Crack 300 M Steel Plate at F_{tu} - 270 KSI, R = +0.1

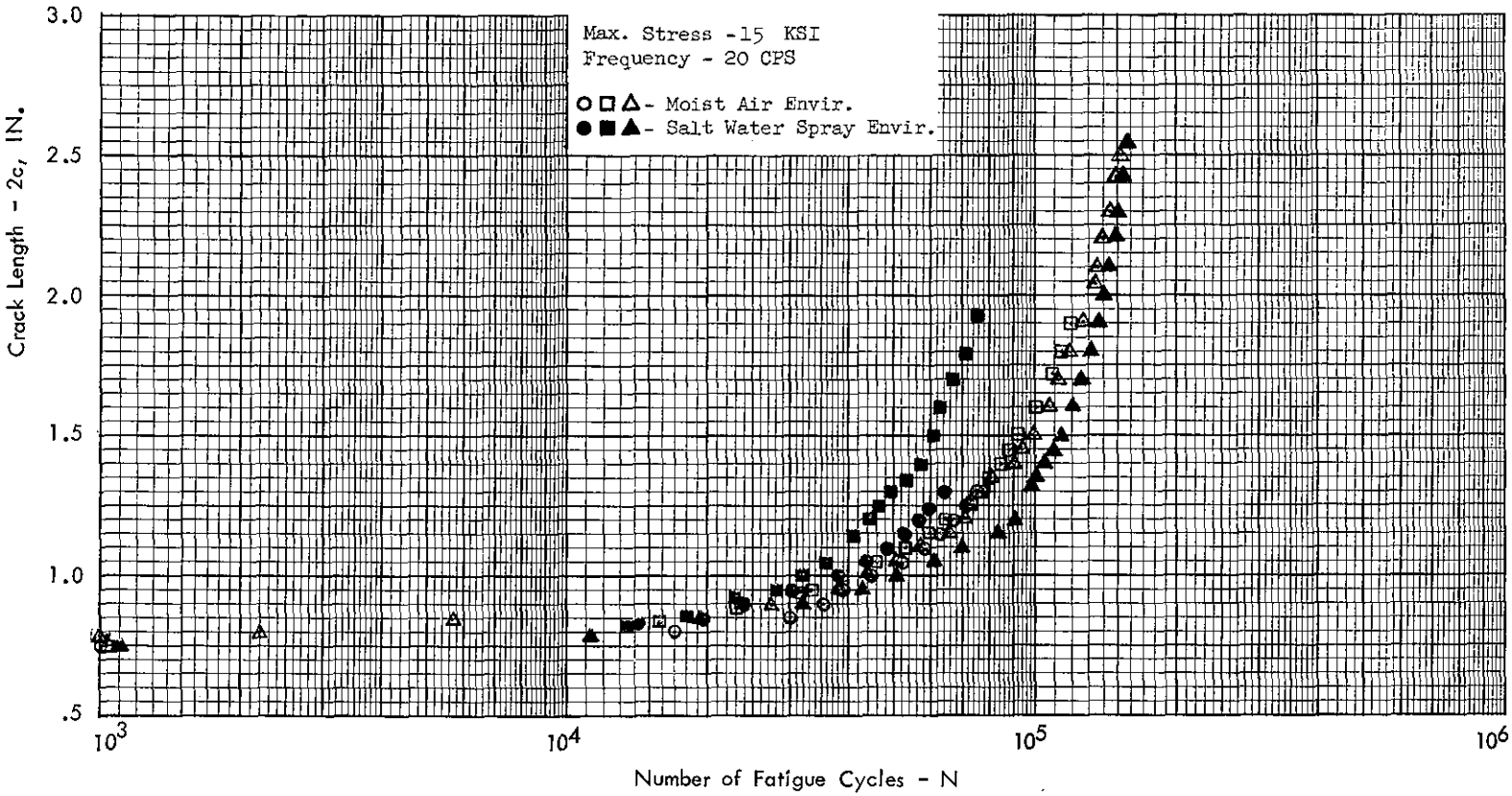

Figure 40 Cyclic Crack Propagation of 3/8-Inch Through-Crack 300 M Steel Plate at F_{tu} - 220 KSI, R = +0.1

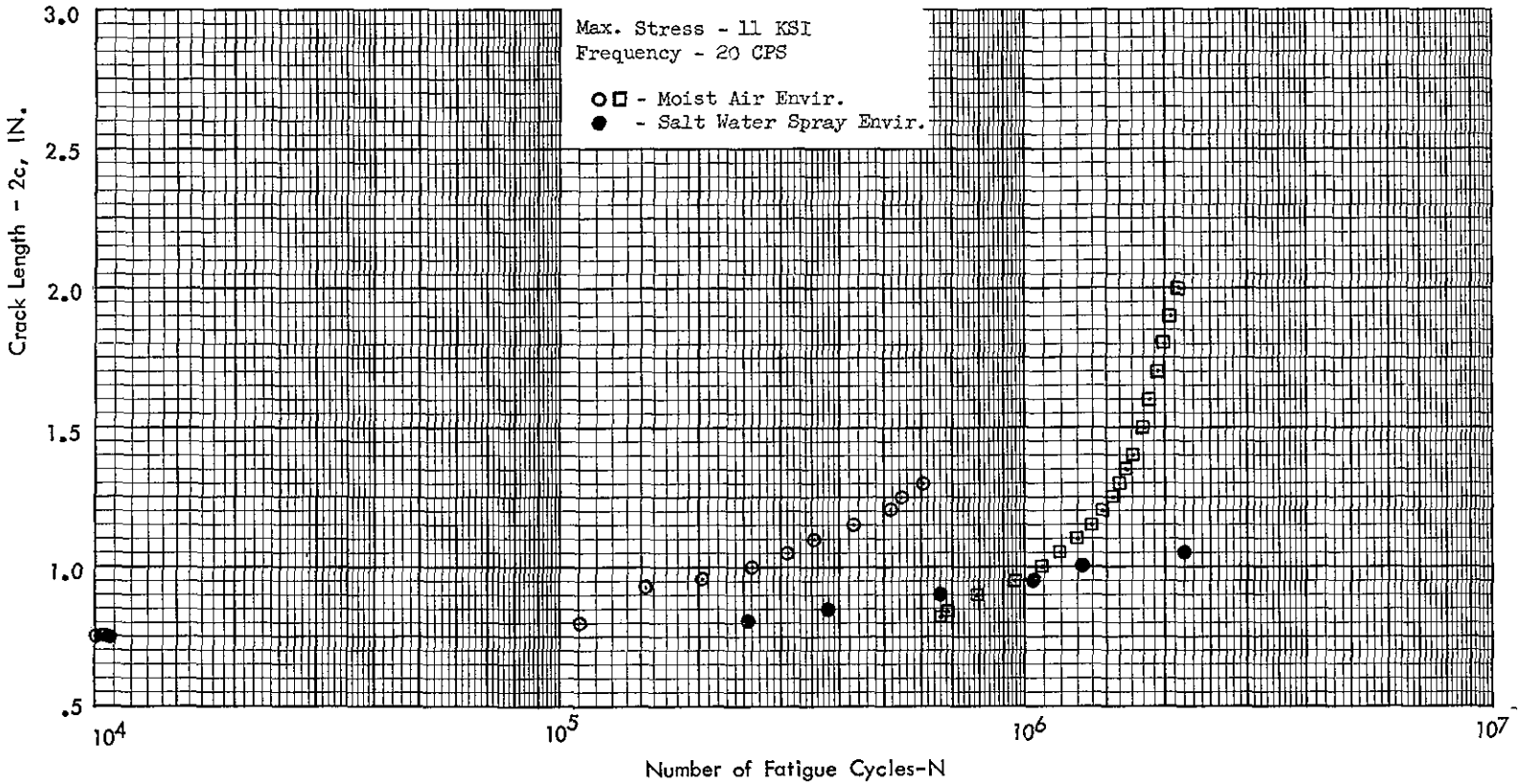

Figure 41 Cyclic Crack Propagation of 3/8-Inch Through-Crack 300 M Steel Plate at F_{tu} - 270 KSI, R = +0.5

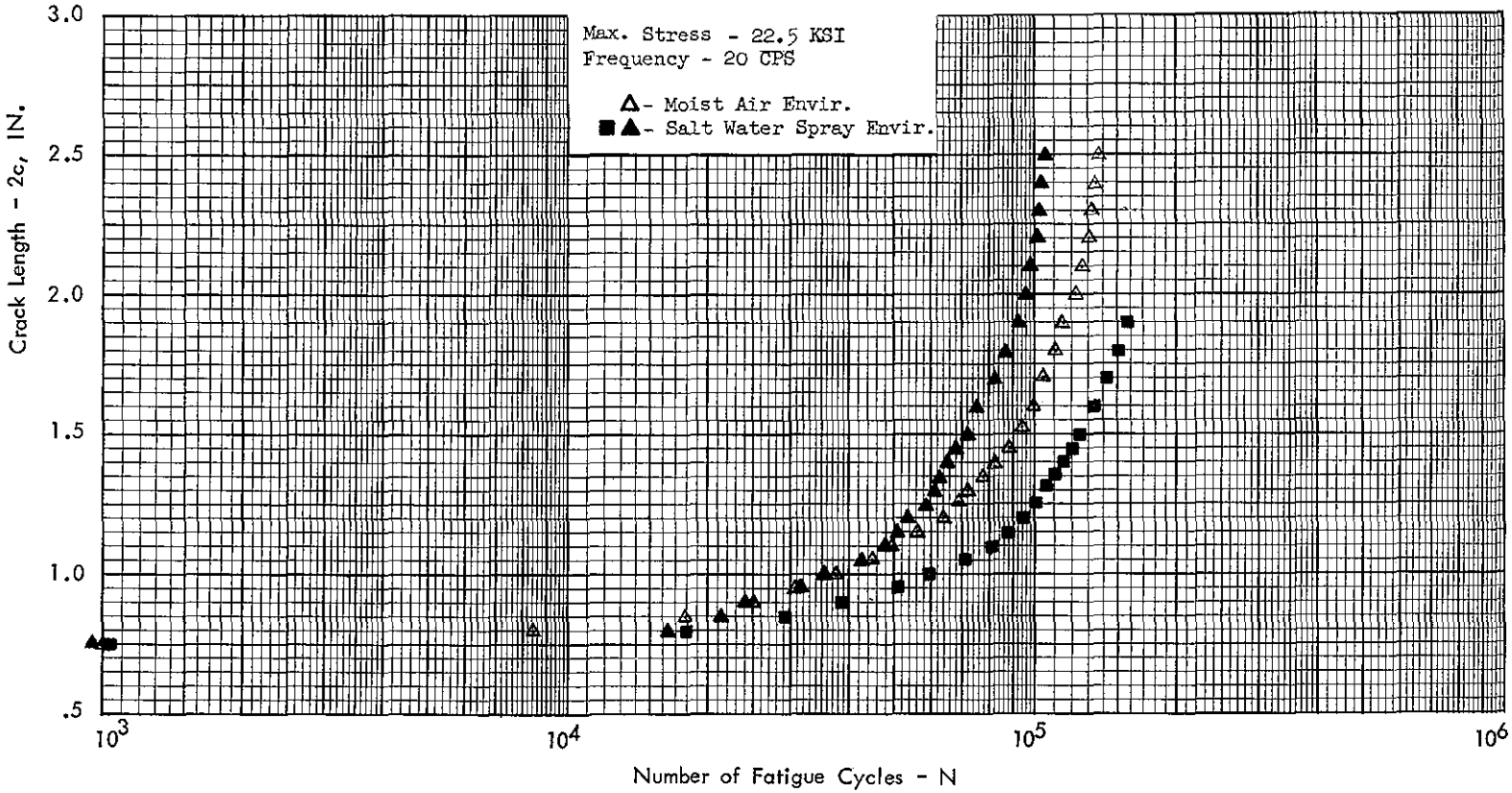

Figure 42 Cyclic Crack Propagation of 3/8-Inch Through-Crack 300 M Steel Plate at F_{tu} - 270 KSI, R = +0.5

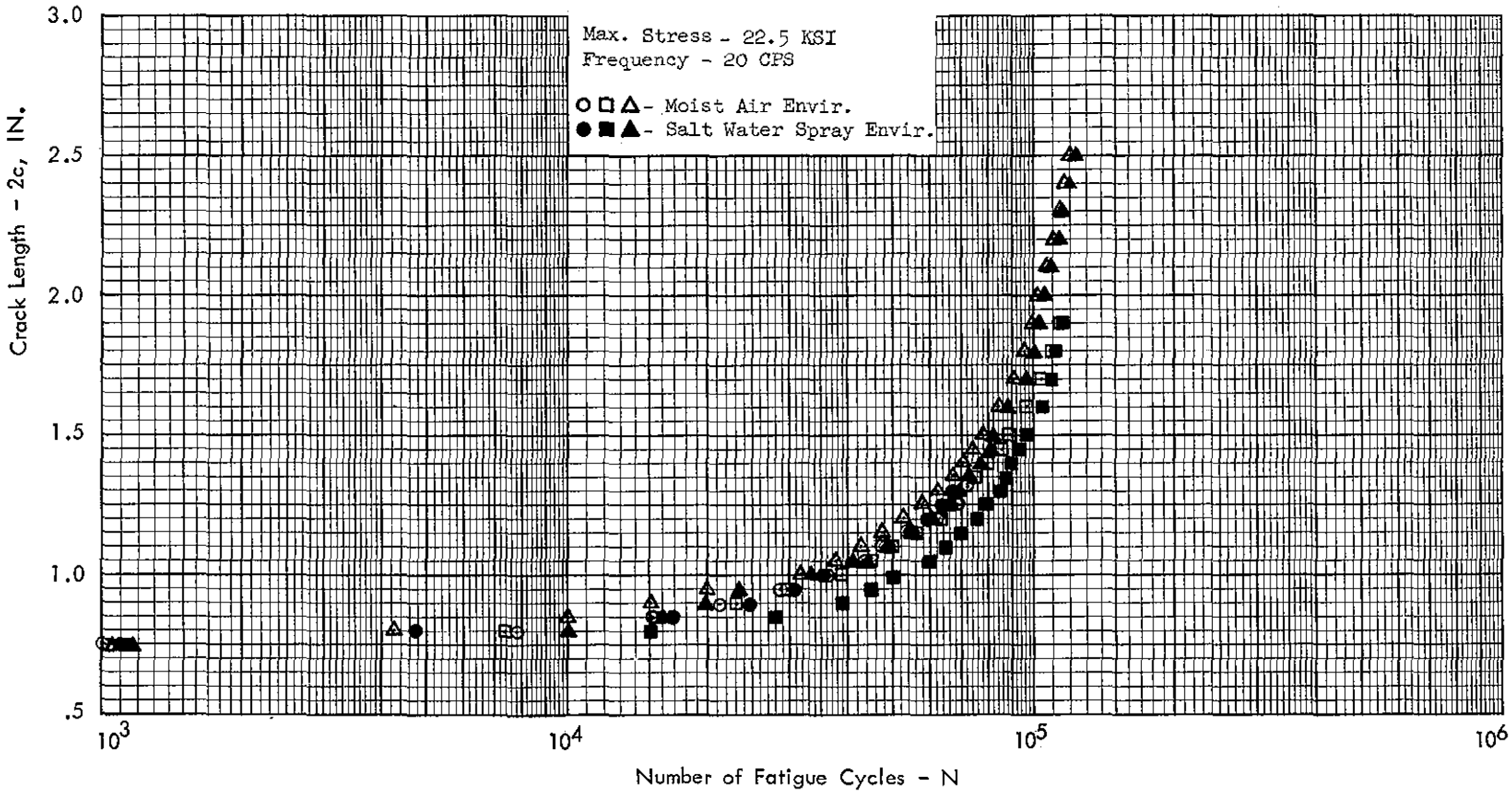

Figure 43 Cyclic Crack Propagation of 3/8-Inch Through-Crack 300 M Steel Plate at F_{tu} - 220 KSI, R = +0.5

TABLE 4 SURFACE-CRACK LENGTH VS NUMBER OF FATIGUE CYCLES FOR 1/8" THICK 300 M STEEL (F_{tu} 290 KSI) AT 45 KSI MAX. STRESS AND R OF +0.1

MOIST AIR ENVIRONMENT						SALT WATER SPRAY ENVIRONMENT					
SPECIMEN NO. X-14237-6		SPECIMEN NO. X-14237-5		SPECIMEN NO. X-14237-7		SPECIMEN NO. X-14237-8		SPECIMEN NO. X-14237-9		SPECIMEN NO. X-14237-10	
CRACK LENGTH (IN.)	NO. OF CYCLES (10^{-3})	CRACK LENGTH (IN.)	NO. OF CYCLES (10^{-3})	CRACK LENGTH (IN.)	NO. OF CYCLES (10^{-3})	CRACK LENGTH (IN.)	NO. OF CYCLES (10^{-3})	CRACK LENGTH (IN.)	NO. OF CYCLES (10^{-3})	CRACK LENGTH (IN.)	NO. OF CYCLES (10^{-3})
.18	0	.18	0	.18	0	.18	0	.18	0	.18	0
.20	7.0	.20	6.1	.20	5.1	.20	4.5	.20	5.3	.20	4.2
.22	9.9	.22	13.2	.22	8.8	.22	8.4	.22	9.8	.21	8.4
.24	13.2	.24	17.1	.24	12.6	.23	11.6	.23	14.7	.22	12.6
.26	17.1	.26	20.4	.26	16.5	.25	15.0	.27	20.1	.23	16.7
.28	19.8	.28	23.0	.28	19.3	.26	16.6	.29	22.5	.24	21.0
		.30	25.1	.30	21.4			.33	24.5	.25	26.2
		.32	26.6	.32	23.5			.35	26.6	.26	30.8
		.34	28.5	.34	25.3			.37	28.9	.28	35.1
		.36	31.1	.36	27.2					.30	37.3
		.38	32.5	.38	28.9					.32	39.4
				.40	30.2					.35	41.6
				.42	31.1					.38	43.7
				.44	32.2					.40	45.1
				.46	33.1					.42	46.9
				.48	34.0					.47	48.5
				.50	35.0					.49	49.6
				.52	36.0					.52	50.6
				.54	36.8					.55	51.7
				.56	37.8					.56	52.1

TABLE 5 SURFACE-CRACK LENGTH VS NUMBER OF FATIGUE CYCLES FOR 1/8" THICK 300 M STEEL (F_{tu} 290 KSI) AT 42 KSI MAX. STRESS AND R OF +.02

MOIST AIR ENVIRONMENT						SALT WATER SPRAY ENVIRONMENT					
SPECIMEN NO. 14237-11		SPECIMEN NO. 14237-23		SPECIMEN NO. 14237-13		SPECIMEN NO. 14237-14		SPECIMEN NO. 14237-15		SPECIMEN NO. 14237-16	
CRACK LENGTH (IN.)	NO. OF CYCLES (10^{-3})	CRACK LENGTH (IN.)	NO. OF CYCLES (10^{-3})	CRACK LENGTH (IN.)	NO. OF CYCLES (10^{-3})	CRACK LENGTH (IN.)	NO. OF CYCLES (10^{-3})	CRACK LENGTH (IN.)	NO. OF CYCLES (10^{-3})	CRACK LENGTH (IN.)	NO. OF CYCLES (10^{-3})
.18	0	.18	0	.18	0	.19	0	.19	0	.18	0
.20	9.3	.20	6.9	.20	9.2	.20	3.1	.20	9.1	.20	6.6
.22	15.0	.22	11.2	.22	14.5	.22	6.0	.21	12.6	.21	12.6
.24	20.1	.24	16.5	.24	20.5	.23	9.6	.22	16.1	.22	16.7
.26	25.3	.26	21.6	.26	25.1	.24	12.4	.24	20.7	.23	20.5
		.28	26.7	.28	28.4	.26	16.3	.26	23.7	.24	26.5
		.30	30.0	.30	31.0			.28	26.5	.26	32.6
		.32	32.5	.32	33.6			.30	29.5	.28	38.6
		.34	35.4	.34	36.1			.32	32.6	.30	44.7
		.36	38.6	.36	38.9			.34	35.7	.33	50.4
		.38	40.1	.38	40.2			.36	38.8	.36	56.6
				.40	42.5			.38	41.5	.40	59.6
				.42	44.1					.43	61.5
				.44	46.1					.46	63.0
				.46	47.9					.49	64.5
				.48	50.0					.51	65.5
				.52	52.1					.53	66.6
				.54	53.0					.55	67.8
				.56	53.8					.56	68.2

TABLE 6 SURFACE-CRACK LENGTH VS NUMBER OF FATIGUE CYCLES FOR 1/8" THICK 300 M STEEL (F_{tu} 290 KSI) AT 33 KSI MAX. STRESS AND R OF +0.5

MOIST AIR ENVIRONMENT						SALT WATER SPRAY ENVIRONMENT					
SPECIMEN NO. 14237-17		SPECIMEN NO. 14237-18		SPECIMEN NO. 14237-19		SPECIMEN NO. 14237-20		SPECIMEN NO. 14237-21		SPECIMEN NO. 14237-24	
CRACK LENGTH (IN.)	NO. OF CYCLES (10^{-3})	CRACK LENGTH (IN.)	NO. OF CYCLES (10^{-3})	CRACK LENGTH (IN.)	NO. OF CYCLES (10^{-3})	CRACK LENGTH (IN.)	NO. OF CYCLES (10^{-3})	CRACK LENGTH (IN.)	NO. OF CYCLES (10^{-3})	CRACK LENGTH (IN.)	NO. OF CYCLES (10^{-3})
.18	0	.18	0	.18	0	.18	0	.18	0	.18	0
.20	53.5	.20	54.1	.20	55.6	.20	37.2	.19	20.1	.20	29.9
.22	78.3	.22	81.8	.22	88.1	.22	61.0	.20	31.4	.22	52.4
.24	114.1	.24	119.6	.24	134.7	.23	73.2	.22	46.8	.24	61.9
.26	138.7	.26	144.8	.26	170.9	.25	83.4	.24	65.2	.26	72.3
		.28	168.0	.28	199.7	.26	93.2	.26	85.4	.28	83.1
		.30	187.0	.30	216.5			.29	105.5	.30	93.3
		.32	204.2	.32	232.4			.32	121.4	.32	103.5
		.34	211.3	.34	244.4			.34	130.2	.34	116.3
		.36	220.5	.36	254.0			.36	139.1	.36	126.5
		.38	230.9	.38	261.9			.38	148.1	.40	135.6
				.40	268.0					.42	142.1
				.42	272.7					.44	147.8
				.44	279.2					.46	153.2
				.46	284.5					.48	158.6
				.48	289.9					.50	163.3
				.50	293.4					.52	168.6
				.52	297.8					.56	175.8
				.54	301.4						
				.56	304.4						

TABLE 7 SURFACE-CRACK LENGTH VS NUMBER OF FATIGUE CYCLES FOR 3/8" THICK 300 M STEEL (F_{tu} 290KSI) AT 45 KSI MAX. STRESS AND R OF +0.1

MOIST AIR ENVIRONMENT						SALT WATER SPRAY ENVIRONMENT					
SPECIMEN NO. X-14238-1		SPECIMEN NO. X-14238-3		SPECIMEN NO. X-14238-2		SPECIMEN NO. X-14238-4		SPECIMEN NO. X-14238-5		SPECIMEN NO. X-14236-6	
CRACK LENGTH (IN.)	NO. OF CYCLES (10^{-3})	CRACK LENGTH (IN.)	NO. OF CYCLES (10^{-3})	CRACK LENGTH (IN.)	NO. OF CYCLES (10^{-3})	CRACK LENGTH (IN.)	NO. OF CYCLES (10^{-3})	CRACK LENGTH (IN.)	NO. OF CYCLES (10^{-3})	CRACK LENGTH (IN.)	NO. OF CYCLES (10^{-3})
		.18	0	.18	0	.18	0	.18	0	.18	0
		.20	5.9	.20	6.7	.19	6.2	.20	6.4	.20	6.9
		.22	11.0	.22	9.9	.22	15.2	.22	11.0	.22	12.1
		.24	16.2	.24	14.3	.24	22.2	.24	18.7	.25	18.9
		.26	20.0	.26	17.8	.27	30.4	.26	26.9	.27	24.6
		.28	23.0	.28	22.2	.28	33.9	.28	35.1	.28	28.5
		.30	24.9	.30	24.9	.32	39.1	.30	43.8	.31	34.5
		.32	27.8	.32	27.4	.34	41.5	.32	51.9	.34	36.8
		.34	29.8	.34	29.3	.35	44.2	.34	60.1	.36	39.5
		.36	32.3	.36	31.7	.38	48.1	.40	66.5	.38	42.3
		.38	34.4	.38	33.2			.42	68.6	.40	45.0
		.40	36.9	.40	35.2			.44	70.6	.44	47.6
		.42	38.2	.42	36.7			.46	72.7	.46	49.3
		.44	39.8	.44	38.5			.48	75.2	.47	51.1
		.46	41.2	.46	40.1			.52	78.0	.51	53.5
		.48	42.5	.48	41.9			.54	80.7	.53	55.0
		.50	43.6	.50	43.3			.56	82.5	.56	57.1
		.52	44.7	.52	44.7					.58	58.1
		.54	45.7	.54	45.8					.61	59.3
		.56		.56	46.8					.63	60.4
				.58	47.5					.66	61.3
				.64	49.6					.71	64.0
				.68	51.3					.76	65.6
				.72	52.5						
				.76	53.8						

TABLE 8 SURFACE-CRACK LENGTH VS NUMBER OF FATIGUE CYCLES FOR 3/8" THICK 300 M STEEL (F_{tu} 290 KSI) AT 42 KSI MAX. STRESS AND R OF +0.2

MOIST AIR ENVIRONMENT						SALT WATER SPRAY ENVIRONMENT					
SPECIMEN NO. X-14238-7		SPECIMEN NO. X-14238-8		SPECIMEN NO. X-14238-9		SPECIMEN NO. X-14238-10		SPECIMEN NO. X-14238-11		SPECIMEN NO. X-14238-12	
CRACK LENGTH (IN.)	NO. OF CYCLES (10^{-3})	CRACK LENGTH (IN.)	NO. OF CYCLES (10^{-3})	CRACK LENGTH (IN.)	NO. OF CYCLES (10^{-3})	CRACK LENGTH (IN.)	NO. OF CYCLES (10^{-3})	CRACK LENGTH (IN.)	NO. OF CYCLES (10^{-3})	CRACK LENGTH (IN.)	NO. OF CYCLES (10^{-3})
.18	0	.18	0	.18	0	.18	0	.18	0	.18	0
.20	18.6	.20	10.6	.20	11.2	.20	18.4	.20	7.6	.20	13.8
.22	32.4	.22	20.5	.22	19.9	.22	36.7	.22	14.0	.22	20.5
.24	38.8	.24	27.9	.24	28.4	.24	50.3	.24	22.2	.24	28.1
.26	43.9	.26	33.3	.26	22.3	.27	63.4	.27	28.6	.26	34.3
.28	48.3	.28	38.1	.28	32.3	.30	72.5	.29	34.2	.28	41.7
.30	51.6	.30	43.4	.31	35.6	.31	84.4	.30	38.0	.30	47.1
.32	58.0	.32	47.4	.32	39.9	.33	90.2	.32	43.0	.33	51.7
.34	60.6	.34	50.4	.34	41.2	.35	101.3	.34	45.2	.34	53.4
.36	64.5	.36	53.8			.38	108.4	.36	48.0	.36	56.3
.38	68.4	.38	57.4					.39	51.2	.37	59.7
		.40	59.7					.40	52.1	.40	65.8
		.42	62.4					.42	54.9	.43	68.4
		.48	65.2					.44	57.4	.45	70.0
		.50	68.3					.47	60.1	.46	72.2
		.52	70.5					.48	61.6	.50	74.5
		.54	72.8					.50	63.4	.52	76.2
		.56	74.6					.53	64.9	.54	77.8
			76.1					.54	65.8	.56	79.4
								.56	67.3	.58	81.7
										.62	83.6
										.66	85.4
										.68	86.9
										.72	88.5
										.78	90.6

TABLE 9 SURFACE-CRACK LENGTH VS NUMBER OF FATIGUE CYCLES FOR 3/8" THICK 300 M STEEL (F_{tu} 290 KSI) AT 33 KSI MAX. STRESS AND R OF +0.5

MOIST AIR ENVIRONMENT						SALT WATER SPRAY ENVIRONMENT					
SPECIMEN NO. X-14238-13		SPECIMEN NO. X-14238-14		SPECIMEN NO. X-14238-15		SPECIMEN NO. X-14238-16		SPECIMEN NO. X-14238-17		SPECIMEN NO. X-14238-18	
CRACK LENGTH (IN.)	NO. OF CYCLES (10^{-3})	CRACK LENGTH (IN.)	NO. OF CYCLES (10^{-3})	CRACK LENGTH (IN.)	NO. OF CYCLES (10^{-3})	CRACK LENGTH (IN.)	NO. OF CYCLES (10^{-3})	CRACK LENGTH (IN.)	NO. OF CYCLES (10^{-3})	CRACK LENGTH (IN.)	NO. OF CYCLES (10^{-3})
.18	0			.18	0	.18	0	.18	0	.18	0
.20	63.8			.20	74.4	.20	51.2	.21	35.0	.20	8.3
.22	103.3			.22	119.4	.22	77.6	.22	45.1	.22	33.5
.24	146.2			.24	182.1	.24	86.0	.24	55.0	.24	108.2
.26	191.8			.26	236.6	.26	103.1	.26	75.0	.28	149.6
.28	239.3			.28	279.8	.29	118.4	.28	94.2	.30	196.9
.30	262.1			.30	302.8	.31	130.2	.30	107.5	.32	274.5
.32	295.2			.32	327.8	.33	138.5	.32	117.3	.35	314.2
.34	318.2			.34	347.7	.34	147.4	.35	128.1	.36	324.8
.36	337.6			.37	373.5	.36	156.7	.36	139.8	.38	334.7
.38	351.3			.38	386.5	.38	163.6	.39	152.7	.40	356.4
				.40	403.2			.40	158.1	.42	362.3
				.42	419.7			.42	165.1	.44	372.0
				.44	433.9			.44	195.0	.46	385.9
				.46	446.9			.46	183.0	.48	397.8
				.48	454.8			.48	191.3	.50	405.0
				.50	462.6			.50	199.1	.52	413.3
				.52	474.5			.52	208.1	.54	424.9
				.54	482.4			.55	216.2	.56	433.8
				.56	488.8			.56	216.9	.58	440.2
				.58	496.4					.60	449.0
				.60	509.7					.64	470.3
				.64	516.9					.67	480.1
				.68	524.6					.72	487.2
				.72	533.1					.76	495.7
				.76	542.0						

TABLE 10 SURFACE-CRACK LENGTH VS NUMBER OF FATIGUE CYCLES FOR 3/8" THICK 300 M STEEL (F_{tu} 270 KSI) AT 45 KSI MAX. STRESS AND R OF +0.1

MOIST AIR ENVIRONMENT						SALT WATER SPRAY ENVIRONMENT					
SPECIMEN NO. X-14238-19		SPECIMEN NO. X-14238-20		SPECIMEN NO. X-14238-21		SPECIMEN NO. X-14238-22		SPECIMEN NO. X-14238-23		SPECIMEN NO. X-14238-24	
CRACK LENGTH (IN.)	NO. OF CYCLES (10^{-3})	CRACK LENGTH (IN.)	NO. OF CYCLES (10^{-3})	CRACK LENGTH (IN.)	NO. OF CYCLES (10^{-3})	CRACK LENGTH (IN.)	NO. OF CYCLES (10^{-3})	CRACK LENGTH (IN.)	NO. OF CYCLES (10^{-3})	CRACK LENGTH (IN.)	NO. OF CYCLES (10^{-3})
.18	70.9	.18	110.1	.18	0	.18	0	.18	0	.18	0
.21	5.2	.20	7.0	.20	6.5	.21	4.8	.20	4.0	.20	6.4
.22	6.6	.22	140.0	.22	10.3	.22	7.1	.22	10.8	.22	12.9
.24	8.3	.24	17.9	.24	15.6	.24	13.2	.23	15.4	.24	22.2
.26	10.1	.26	24.9	.26	20.5	.26	19.9	.26	30.8	.25	28.1
.28	13.1	.28	29.7	.28	23.3	.28	24.7	.28	35.0	.28	36.2
.30	14.9	.30	33.1	.30	25.5	.30	29.5	.29	40.5	.31	42.3
.32	16.4	.32	35.9	.32	27.7	.32	34.8	.32	46.7	.32	48.1
.34	17.9	.34	38.3	.34	29.4	.34	36.4	.34	52.5	.35	52.3
.36	19.4	.36	40.2	.36	31.6	.36	38.6	.37	55.1	.38	55.2
.38	20.9	.38	42.9	.38	33.5	.38	41.1	.38	57.3	.39	57.0
		.40	44.3	.40	35.3			.41	59.2	.42	59.2
		.42	46.2	.42	36.8			.42	60.6	.44	61.6
		.44	48.6	.44	38.0			.44	62.1	.45	63.2
		.46	50.6	.46	38.9			.46	65.0	.49	65.7
		.48	52.1	.48	41.3			.48	66.0	.50	66.8
		.50	53.0	.50	42.5			.50	67.1	.51	68.3
		.52	54.5	.52	43.2			.52	68.0	.54	70.1
		.54	55.8	.54	44.1			.54	69.1	.57	72.1
		.56	57.1	.56	44.9			.56	70.5	.60	73.3
				.58	45.6					.63	74.9
				.60	47.0					.68	76.4
				.64	48.5					.71	77.6
				.68	50.2					.77	79.6
				.72	51.7						
				.76	52.6						

TABLE 11 SURFACE-CRACK LENGTH VS NUMBER OF FATIGUE CYCLES FOR 3/8" THICK 300 M STEEL (F_{tu} 270 KSI) AT 33 KSI MAX. STRESS AND R OF +0.5

MOIST AIR ENVIRONMENT						SALT WATER SPRAY ENVIRONMENT					
SPECIMEN NO. X-14238-25		SPECIMEN NO. X-14238-26		SPECIMEN NO. X-14238-27		SPECIMEN NO. X-14238-28		SPECIMEN NO. X-14238-29		SPECIMEN NO. X-14238-30	
CRACK LENGTH (IN.)	NO. OF CYCLES (10^{-3})	CRACK LENGTH (IN.)	NO. OF CYCLES (10^{-3})	CRACK LENGTH (IN.)	NO. OF CYCLES (10^{-3})	CRACK LENGTH (IN.)	NO. OF CYCLES (10^{-3})	CRACK LENGTH (IN.)	NO. OF CYCLES (10^{-3})	CRACK LENGTH (IN.)	NO. OF CYCLES (10^{-3})
.18	0	.26	0	.18	0	.18	0	.18	0	.19	0
.20	73.9	.28	8.1	.20	67.7	.19	43.4	.20	41.2	.20	36.0
.22	127.9	.30	15.8	.22	117.8	.22	100.0	.22	110.0	.22	65.6
.24	146.6	.32	32.8	.24	152.3	.24	137.8	.23	612.2	.24	103.5
.26	165.7	.34	61.6	.26	181.0	.26	323.6	.26	690.5	.26	188.1
.28	202.0	.36	91.1	.28	210.4	.27	456.4	.28	743.1	.29	215.7
.30	258.5	.38	104.2	.30	248.7	.29	790.4	.29	763.1	.30	247.7
.32	290.6	.40	120.2	.32	269.6	.30	866.3	.32	972.2	.33	273.2
.34	326.5	.42	140.5	.34	287.0	.32	944.4	.35	1,000.5	.34	291.5
.36	341.6	.44	150.5	.36	300.9	.34	999.6	.36	1,055.5	.36	305.6
.38	365.4	.46	161.6	.38	318.4	.36	1,152.1	.40	1,074.6	.38	318.4
		.48	172.1	.40	335.8	.38	1,170.2	.44	1,100.5	.40	332.3
		.50	180.6	.42	350.9		1,242.0	.46	1,118.7	.42	352.4
		.52	188.8	.44	362.1			.48	1,136.8	.44	370.7
		.54	198.0	.46	372.3			.50	1,155.5	.46	382.1
		.56	208.0	.48	383.0			.52	1,170.9	.48	389.1
				.50	388.0			.56	1,181.5	.50	398.8
				.52	396.2					.52	409.8
				.54	404.7					.55	420.6
				.56	412.2					.58	429.9
				.58	418.6					.61	437.3
				.60	425.8					.63	445.4
				.64	435.7					.67	453.8
				.68	447.0					.71	462.5
				.74	458.0					.76	474.3
				.76	461.5						

TABLE 12 SURFACE-CRACK LENGTH VS NUMBER OF FATIGUE CYCLES FOR 3/8" THICK 300 M STEEL (F_{tu} 220 KSI) AT 45 KSI MAX. STRESS AND R OF +0.1

MOIST AIR ENVIRONMENT						SALT WATER SPRAY ENVIRONMENT					
SPECIMEN NO. X-14238-31		SPECIMEN NO. X-14238-32		SPECIMEN NO. X-14238-33		SPECIMEN NO. X-14238-34		SPECIMEN NO. X-14238-35		SPECIMEN NO. X-14238-36	
CRACK LENGTH (IN.)	NO. OF CYCLES (10^{-3})	CRACK LENGTH (IN.)	NO. OF CYCLES (10^{-3})	CRACK LENGTH (IN.)	NO. OF CYCLES (10^{-3})	CRACK LENGTH (IN.)	NO. OF CYCLES (10^{-3})	CRACK LENGTH (IN.)	NO. OF CYCLES (10^{-3})	CRACK LENGTH (IN.)	NO. OF CYCLES (10^{-3})
.18	0	.18	0	.18	0	.18	0	.18	0	.18	0
.20	5.9	.20	2.2	.20	4.5	.21	5.7	.20	3.3	.20	4.1
.22	9.3	.22	5.1	.22	8.1	.23	8.1	.22	6.0	.23	8.1
.24	13.2	.24	7.9	.24	13.0	.25	11.1	.24	9.3	.24	10.9
.26	15.7	.26	11.9	.26	16.5	.26	12.4	.26	12.7	.26	13.6
.28	18.5	.28	14.1	.29	19.2	.29	14.7	.28	15.7	.29	16.2
.30	20.8	.30	17.7	.30	20.2	.30	15.9	.30	18.0	.30	18.1
.32	22.6	.32	20.1	.32	21.5	.32	17.8	.33	19.3	.32	20.2
.35	23.6	.34	21.8	.34	22.3	.35	19.8	.34	20.0	.36	22.7
.36	24.6	.36	23.3	.36	24.7	.36	21.2	.36	21.1	.38	24.5
.38	25.8	.38	24.8	.38	26.1	.40	23.3	.37	22.0	.40	26.4
		.40	25.8	.40	27.5			.40	23.5	.46	28.1
		.42	27.0	.42	29.5			.42	25.2	.48	29.2
		.44	28.1	.44	30.5			.46	26.8	.50	30.4
		.46	29.6	.46	31.5			.48	28.0	.52	31.4
		.48	30.8	.48	32.3			.50	29.0	.56	32.4
		.50	31.8	.50	33.4			.56	30.0	.60	33.2
		.52	32.6	.53	34.8			.55	31.1	.64	33.8
		.55	33.8	.54	35.4			.57	31.5	.68	34.8
		.56	34.3	.56	36.1					.72	35.8
				.58	36.7					.78	37.0
				.60	37.3						
				.64	38.4						
				.68	39.6						
				.72	40.5						
				.76	41.7						

TABLE 13 SURFACE-CRACK LENGTH VS NUMBER OF FATIGUE CYCLES FOR 3/8" THICK 300 M STEEL (F_{tu} 220 KSI) AT 33 KSI MAX. STRESS AND R OF +0.5

MOIST AIR ENVIRONMENT						SALT WATER SPRAY ENVIRONMENT					
SPECIMEN NO. X-14238-37		SPECIMEN NO. X-14238-38		SPECIMEN NO. X-14238-39		SPECIMEN NO. X-14238-40		SPECIMEN NO. X-14238-41		SPECIMEN NO. X-14238-42	
CRACK LENGTH (IN.)	NO. OF CYCLES (10^{-3})	CRACK LENGTH (IN.)	NO. OF CYCLES (10^{-3})	CRACK LENGTH (IN.)	NO. OF CYCLES (10^{-3})	CRACK LENGTH (IN.)	NO. OF CYCLES (10^{-3})	CRACK LENGTH (IN.)	NO. OF CYCLES (10^{-3})	CRACK LENGTH (IN.)	NO. OF CYCLES (10^{-3})
.18	0	.18	0	.18	0	.18	0	.18	0	.18	0
.20	40.5	.20	61.3	.20	75.3	.20	22.4	.20	70.1	.20	114.5
.22	65.4	.22	111.5	.22	130.9	.22	40.7	.22	312.7	.22	436.3
.24	111.0	.24	147.8	.24	170.8	.24	58.8	.24	399.7	.24	600.2
.26	145.2	.26	197.4	.26	205.0	.26	81.1	.26	604.0	.26	736.9
.28	186.4	.28	246.5	.28	251.4	.28	133.4	.28	675.4	.28	928.0
.30	213.7	.30	261.4	.30	310.3	.32	160.8	.30	848.0	.30	955.1
.32	231.1	.32	286.5	.32	359.8	.34	170.5	.33	920.9	.33	1,009.0
.34	265.4	.34	311.3	.34	377.6	.36	184.7	.34	942.7	.35	1,027.0
.36	281.9	.36	328.2	.36	398.6	.38	190.4	.37	974.5	.36	1,037.1
.38	295.7	.38	345.6	.38	414.3			.38	988.1	.38	1,068.4
		.40	364.9	.40	430.5			.40	1,004.7	.40	1,100.6
		.42	381.0	.42	446.3			.42	1,010.3	.43	1,133.6
		.44	388.2	.44	462.7			.46	1,050.0	.45	1,141.4
		.47	408.8	.46	476.6			.48	1,079.4	.46	1,148.3
		.48	415.4	.48	481.8			.50	1,108.9	.50	1,170.1
		.50	424.9	.50	487.2			.52	1,142.5	.52	1,188.2
		.52	431.7	.52	500.6			.56	1,164.8	.54	1,197.6
		.55	439.5	.54	507.3					.56	1,210.5
		.56	442.7	.56	515.8					.58	1,221.1
				.58	522.1					.59	1,230.1
				.60	531.8					.64	1,251.7
				.65	543.3					.69	1,270.9
				.68	550.7					.76	1,284.6
				.72	556.7						
				.76	563.3						

TABLE 14 SURFACE-CRACK LENGTH VS NUMBER OF FATIGUE CYCLES FOR 3/4" THICK 300 M STEEL (F_{tu} 290 KSI) AT 45 KSI MAX. STRESS AND R OF +0.1

MOIST AIR ENVIRONMENT						SALT WATER SPRAY ENVIRONMENT					
SPECIMEN NO. X-14239-19		SPECIMEN NO. X-14239-20		SPECIMEN NO. X-14239-21		SPECIMEN NO. X-14239-22		SPECIMEN NO. X-14239-23		SPECIMEN NO. X-14239-24	
CRACK LENGTH (IN.)	NO. OF CYCLES (10^{-3})	CRACK LENGTH (IN.)	NO. OF CYCLES (10^{-3})	CRACK LENGTH (IN.)	NO. OF CYCLES (10^{-3})	CRACK LENGTH (IN.)	NO. OF CYCLES (10^{-3})	CRACK LENGTH (IN.)	NO. OF CYCLES (10^{-3})	CRACK LENGTH (IN.)	NO. OF CYCLES (10^{-3})
.18	0	.18	0	.18	0	.18	0	.18	0	.18	0
.20	8.0	.20	9.8	.20	6.1	.20	6.3	.20	12.9	.20	15.0
.22	15.7	.22	19.7	.22	12.8	.22	12.0	.22	17.6	.22	25.0
.24	22.3	.24	26.6	.24	20.7	.24	20.0	.24	22.3	.24	35.0
.27	27.9	.26	29.7	.26	27.3	.26	24.7	.26	27.6	.27	45.0
.28	31.0	.28	32.6	.30	34.3	.28	29.8	.28	32.3	.30	52.0
.30	34.5	.30	35.5	.32	38.9	.30	33.0	.30	36.9	.32	57.2
.32	39.1	.32	39.6	.34	42.6	.32	36.5	.32	40.2	.34	63.0
.34	42.9	.34	41.9	.38	46.7	.34	40.0	.34	42.3	.40	70.0
.36	46.8	.36	44.0	.40	50.4	.36	43.6	.36	44.8	.43	74.0
.38	50.2	.38	46.0	.43	53.8	.38	45.4	.38	48.0	.45	76.0
.40	52.2	.40	48.6	.44	55.8	.40	47.6	.40	49.7	.47	78.3
.42	54.0	.42	51.2	.48	59.4	.42	49.7	.42	51.9	.52	82.7
.44	55.9	.44	53.3	.50	61.9	.44	52.4	.44	55.0	.54	85.2
.46	57.9	.46	55.3	.53	64.7	.46	55.0	.46	57.2	.56	87.1
.48	59.8	.48	57.8	.55	66.9	.48	57.0	.48	59.9	.60	90.0
.50	61.9	.50	60.0	.56	68.2	.50	58.2	.51	62.3	.63	92.0
.52	64.2	.52	62.0	.58	70.1	.52	59.0	.54	64.9	.68	94.8
.54	66.1	.54	63.8	.61	72.1	.54	60.0	.56	66.0	.75	99.0
.56	67.8	.56	66.0	.65	74.8	.56	62.3	.58	68.2	.84	102.7
.58	69.1	.58	67.7	.68	77.2	.58	64.6	.60	69.7	.90	105.0
.60	71.6	.60	69.3	.73	80.1	.60	65.1	.64	72.8	.94	106.5
		.64	71.2	.78	82.7			.70	76.0	.98	108.0
		.68	73.7	.81	84.4			.72	76.5	1.00	108.7
		.72	75.2	.84	86.4			.76	79.0		
		.76	77.2	.89	88.4			.80	82.3		
		.80	79.7	.94	90.3						
				.97	91.9						
				1.00	93.1						

TABLE 15 SURFACE-CRACK LENGTH VS NUMBER OF FATIGUE CYCLES FOR 3/4" THICK 300 M STEEL (F_{tu} 290 KSI) AT 42 KSI MAX. STRESS AND R OF +0.2

MOIST AIR ENVIRONMENT						*SALT WATER SPRAY ENVIRONMENT*					
SPECIMEN NO. X-14239-25		SPECIMEN NO. X-14239-26		SPECIMEN NO. X-14239-27		SPECIMEN NO. X-14239-28		SPECIMEN NO. X-14239-29		SPECIMEN NO. X-14239-30	
CRACK LENGTH (IN.)	NO. OF CYCLES (10^{-3})	CRACK LENGTH (IN.)	NO. OF CYCLES (10^{-3})	CRACK LENGTH (IN.)	NO. OF CYCLES (10^{-3})	CRACK LENGTH (IN.)	NO. OF CYCLES (10^{-3})	CRACK LENGTH (IN.)	NO. OF CYCLES (10^{-3})	CRACK LENGTH (IN.)	NO. OF CYCLES (10^{-3})
.18	0	.19	0	.19	0	.18	0	.18	0	.18	0
.20	20.3	.20	5.0	.20	6.3	.20	15.6	.20	25.3	.20	15.0
.22	29.5	.22	15.4	.22	17.1	.22	30.1	.22	39.3	.22	41.8
.24	45.3	.24	24.2	.24	30.4	.25	42.2	.24	46.7	.25	60.5
.26	57.2	.26	40.0	.26	38.5	.28	54.3	.26	57.0	.27	70.0
.28	65.2	.28	53.0	.28	46.2	.30	62.3	.28	56.2	.28	80.0
.32	73.6	.31	65.0	.30	52.1	.32	69.2	.30	62.9	.31	90.4
.35	80.2	.32	68.4	.32	57.4	.34	75.4	.32	69.5	.33	100.0
.36	82.0	.35	75.1	.34	60.1	.36	80.5	.34	73.6	.35	110.0
.40	87.9	.38	80.6	.36	64.2	.38	85.3	.36	77.2	.38	120.0
.42	92.5	.40	84.2	.38	67.9	.40	89.2	.38	81.8	.41	128.0
.44	96.5	.42	87.2	.40	71.9	.42	93.3	.40	86.0	.43	135.0
.47	100.3	.44	90.0	.42	75.2	.45	96.8	.42	90.0	.45	144.0
.48	101.9	.46	93.2	.44	78.5	.48	102.1	.44	93.9	.50	153.1
.50	104.7	.48	96.3	.46	80.7	.50	105.2	.46	96.7	.54	160.0
.52	107.4	.50	99.3	.48	83.0	.52	108.2	.48	100.0	.56	163.1
.55	109.5	.52	102.3	.50	86.0	.54	110.9	.50	102.7	.58	166.5
.56	111.0	.54	105.3	.52	88.3	.56	113.2	.52	105.0	.60	170.0
.58	113.0	.56	108.4	.54	90.6	.58	116.0	.54	107.3	.65	176.0
.60	157.0	.58	111.3	.56	93.2	.60	118.3	.56	110.1	.70	182.0
		.62	114.4	.58	95.9			.58	112.8	.72	185.2
		.64	116.7	.60	98.3			.60	115.3	.79	191.0
		.69	122.1	.64	101.0			.64	118.7	.83	194.0
		.75	126.8	.68	103.8			.68	121.9	.86	197.0
		.80	130.2	.72	106.1			.72	125.0	.90	200.0
				.76	109.2			.76	128.5	.98	204.0
				.80	112.5			.81	131.0	1.00	205.4
				.84	115.2						
				.88	117.2						
				.92	119.0						
				.96	121.3						
				1.00	123.2						

TABLE 16 SURFACE-CRACK LENGTH VS NUMBER OF FATIGUE CYCLES FOR 3/4" THICK 300 M STEEL (F_{tu} 290 KSI) AT 33 KSI MAX. STRESS AND R OF +0.5

MOIST AIR ENVIRONMENT						SALT WATER SPRAY ENVIRONMENT					
SPECIMEN NO. X-14239-31		SPECIMEN NO. X-14239-32		SPECIMEN NO. X-14239-33		SPECIMEN NO. X-14239-34		SPECIMEN NO. X-14239-35		SPECIMEN NO. X-14239-36	
CRACK LENGTH (IN.)	NO. OF CYCLES (10^{-3})	CRACK LENGTH (IN.)	NO. OF CYCLES (10^{-3})	CRACK LENGTH (IN.)	NO. OF CYCLES (10^{-3})	CRACK LENGTH (IN.)	NO. OF CYCLES (10^{-3})	CRACK LENGTH (IN.)	NO. OF CYCLES (10^{-3})	CRACK LENGTH (IN.)	NO. OF CYCLES (10^{-3})
.18	0	.18	0	.18	0	.18	0	.18	0	.18	0
.20	20.2	.39	70.2	.20	102.5	.20	82.1	.20	51.0	.20	44.2
.22	31.7	.40	81.4	.22	179.8	.22	160.3	.22	98.4	.22	75.8
.24	39.2	.42	86.4	.24	244.9	.24	260.1	.23	135.7	.24	106.5
.26	47.5	.44	116.0	.26	300.4	.27	302.1	.26	180.2	.26	149.1
.28	58.9	.48	129.2	.32	374.2	.30	335.9	.30	217.9	.28	168.1
.30	65.5	.50	137.0	.34	395.8	.33	367.1	.33	240.4	.30	185.3
.32	71.7	.52	142.7	.36	415.4	.36	405.1	.35	261.5	.32	200.0
.35	77.8	.54	154.8	.38	438.6	.38	430.2	.37	281.0	.34	227.6
.38	82.4	.56	180.1	.40	461.5	.40	449.1	.39	300.0	.36	256.6
.40	87.1	.58	189.2	.44	484.0	.42	463.6	.42	320.7	.38	279.9
.42	90.6	.60	199.3	.46	498.9	.44	477.0	.44	340.6	.42	310.5
.44	93.5	.64	207.2	.48	512.8	.46	490.0	.47	360.0	.44	324.5
.46	97.0	.68	219.2	.50	525.9	.48	505.5	.49	380.0	.45	350.0
.48	100.9	.72	228.0	.53	537.3	.50	521.1	.52	400.0	.48	371.9
.50	103.6	.76	235.7	.54	547.4	.52	537.6	.54	415.0	.50	385.3
.52	106.9	.80	247.4	.56	555.2	.54	547.3	.57	430.0	.53	410.0
.54	109.8			.58	563.2	.56	555.3	.58	440.0	.56	429.1
.56	111.8			.61	571.3	.58	561.9	.60	455.0	.60	450.0
.58	113.7			.64	582.3	.60	568.6	.63	475.0	.64	481.0
.60	116.9			.68	599.0			.67	495.0	.69	511.7
				.74	614.9			.71	514.0	.73	535.0
				.76	620.2			.75	541.3	.75	551.2
				.80	629.3			.81	565.3	.80	576.4
				.84	638.2					.84	597.4
				.87	645.7					.87	617.0
				.92	653.7					.94	637.5
				.95	656.0					.97	649.8
				1.00	667.7					1.00	655.1

TABLE 17 SURFACE-CRACK LENGTH VS NUMBER OF FATIGUE CYCLES FOR 3/4" THICK 300 M STEEL (F_{tu} 290 KSI) AT 45 KSI MAX. STRESS AND R OF +0.1

MOIST AIR ENVIRONMENT						SALT WATER SPRAY ENVIRONMENT					
SPECIMEN NO. F-1		SPECIMEN NO. F-2		SPECIMEN NO. F-3		SPECIMEN NO. F-4		SPECIMEN NO. F-5		SPECIMEN NO. F-6	
CRACK LENGTH (IN.)	NO. OF CYCLES (10^{-3})	CRACK LENGTH (IN.)	NO. OF CYCLES (10^{-3})	CRACK LENGTH (IN.)	NO. OF CYCLES (10^{-3})	CRACK LENGTH (IN.)	NO. OF CYCLES (10^{-3})	CRACK LENGTH (IN.)	NO. OF CYCLES (10^{-3})	CRACK LENGTH (IN.)	NO. OF CYCLES (10^{-3})
.18	0	.18	0	.18	0	.18	0	.18	0	.18	0
.20	5.5	.20	11.3	.20	10.0	.20	14.5	.20	8.9	.22	6.3
.22	9.3	.22	15.8	.22	17.0	.22	19.7	.22	15.6	.24	11.4
.24	11.7	.24	21.2	.24	29.6	.24	24.3	.27	20.8	.26	14.4
.26	15.5	.26	26.0	.26	35.7	.26	30.1	.28	24.0	.28	21.4
.28	84.1	.28	29.3	.28	41.1	.28	36.1	.31	28.4	.30	24.3
.30	24.7	.30	33.1	.30	47.2	.30	40.9	.32	30.2	.32	28.4
.32	27.2	.32	36.7	.32	53.5	.32	45.9	.36	34.0	.34	31.4
.34	29.6	.34	40.7	.36	59.4	.34	54.6	.38	37.1	.37	34.6
.36	31.6	.36	43.9	.39	64.2	.38	63.5	.40	40.0	.40	37.5
.38	34.2	.39	47.6	.40	66.3	.43	71.5	.45	43.0	.43	40.4
.40	37.7	.40	48.8	.42	69.2	.44	72.9	.46	44.5	.45	43.7
.44	40.0	.42	50.8	.44	73.3	.46	76.9	.50	47.0	.50	45.4
.46	42.8	.44	53.8	.46	75.4	.49	79.3	.52	49.2	.52	47.6
.48	45.1	.46	55.9	.48	77.8	.50	80.8	.54	51.3	.54	49.8
.52	47.6	.48	58.5	.50	80.3	.52	83.8	.56	53.3	.57	51.8
.54	49.0	.50	59.0	.52	83.1	.54	86.1	.61	55.3	.58	52.6
.56	50.6	.52	60.3	.54	85.1	.56	88.2	.64	57.5	.60	54.7
.58	52.7	.54	61.3	.56	87.2	.58	90.2	.68	60.3	.68	58.5
.60	54.4	.56	62.8	.58	89.3	.60	92.6	.76	63.6	.72	60.4
		.58	64.4	.60	91.5			.80	66.0	.76	62.5
		.60	66.2	.65	95.1					.80	64.5
		.64	68.7	.68	98.1					.85	66.4
		.68	71.6	.72	100.7					.90	67.9
		.72	72.8	.76	102.9					.92	68.9
		.76	74.3	.80	106.1						70.4
		.80	76.1	.85	109.1						72.3
				.89	111.2						
				.92	112.8						
				.96	114.9						
				1.01	117.0						

TABLE 18 SURFACE-CRACK LENGTH VS NUMBER OF FATIGUE CYCLES FOR 3/4" THICK 300 M STEEL (F_{tu} 270 KSI) AT 45 KSI MAX. STRESS AND R OF +0.1

MOIST AIR ENVIRONMENT						SALT WATER SPRAY ENVIRONMENT					
SPECIMEN NO. F-7		SPECIMEN NO. F-8		SPECIMEN NO. F-9		SPECIMEN NO. F-10		SPECIMEN NO. F-11		SPECIMEN NO. F-12	
CRACK LENGTH (IN.)	NO. OF CYCLES (10^{-3})	CRACK LENGTH (IN.)	NO. OF CYCLES (10^{-3})	CRACK LENGTH (IN.)	NO. OF CYCLES (10^{-3})	CRACK LENGTH (IN.)	NO. OF CYCLES (10^{-3})	CRACK LENGTH (IN.)	NO. OF CYCLES (10^{-3})	CRACK LENGTH (IN.)	NO. OF CYCLES (10^{-3})
.18	0	.18	0	.18	0	.18	0	.18	0	.18	0
.20	12.6	.20	10.3	.20	10.4	.20	5.3	.20	10.4	.20	5.9
.23	22.0	.22	19.8	.22	19.8	.22	13.3	.22	20.3	.22	10.3
.24	24.8	.24	23.5	.23	23.5	.26	21.2	.23	30.4	.24	16.5
.26	30.3	.26	27.6	.25	28.5	.28	25.1	.26	38.0	.27	27.6
.28	35.4	.28	35.5	.28	34.1	.30	28.5	.28	43.9	.28	32.7
.30	38.9	.30	39.0	.31	38.2	.32	31.6	.30	47.1	.31	40.0
.32	42.4	.33	40.4	.32	40.9	.34	33.2	.32	50.5	.35	46.8
.34	46.2	.34	43.3	.34	43.8	.36	35.9	.34	53.6	.38	52.0
.37	49.9	.36	45.5	.36	46.5	.40	40.2	.36	56.0	.40	55.7
.38	52.2	.38	47.7	.40	49.3	.43	42.7	.38	60.1	.42	60.6
.40	55.6	.40	49.3	.42	51.7	.45	44.4	.40	63.3	.46	67.8
.44	60.6	.42	51.1	.44	53.6	.46	45.3	.42	67.1	.48	71.1
.46	63.3	.44	53.3	.46	56.3	.48	48.1	.44	69.6	.50	73.8
.48	65.6	.46	55.3	.48	58.6	.50	50.2	.46	71.3	.53	77.6
.50	68.5	.48	57.0	.50	60.2	.53	52.3	.48	73.2	.54	79.6
.52	70.7	.50	58.8	.52	61.8	.54	53.1	.50	76.1	.59	83.6
.55	73.0	.52	60.1	.54	63.1	.57	55.2	.52	78.2	.60	85.0
.56	74.8	.54	61.8	.56	65.0	.58	55.8	.54	80.3	.67	90.0
.58	76.6	.56	63.7	.58	67.1	.60	57.1	.56	82.5	.69	92.8
.60	78.4	.60	65.6	.60	68.7			.58	85.0	.72	96.0
		.64	68.0	.63	70.0			.60	87.6	.77	99.7
		.68	70.1	.68	73.3			.65	90.1	.84	103.1
		.72	72.0	.72	75.4			.70	93.1	.89	106.0
		.76	73.5	.76	77.5			.73	95.7	.98	109.3
		.80		.81	79.6			.76	97.4	1.00	110.5
				.84	81.2			.81	100.0		
				.90	83.1						
				.94	84.5						
				.96	85.3						
				1.00	87.7						

TABLE 19 SURFACE-CRACK LENGTH VS NUMBER OF FATIGUE CYCLES FOR 3/4" THICK 300 M STEEL (F_{tu} 220 KSI) AT 45 KSI MAX. STRESS AND R OF +0.1

MOIST AIR ENVIRONMENT						SALT WATER SPRAY ENVIRONMENT					
SPECIMEN NO. F-13		SPECIMEN NO. F-14		SPECIMEN NO. F-15		SPECIMEN NO. F-16		SPECIMEN NO. F-17		SPECIMEN NO. F-18	
CRACK LENGTH (IN.)	NO. OF CYCLES (10^{-3})	CRACK LENGTH (IN.)	NO. OF CYCLES (10^{-3})	CRACK LENGTH (IN.)	NO. OF CYCLES (10^{-3})	CRACK LENGTH (IN.)	NO. OF CYCLES (10^{-3})	CRACK LENGTH (IN.)	NO. OF CYCLES (10^{-3})	CRACK LENGTH (IN.)	NO. OF CYCLES (10^{-3})
.19	0	.18	0	.18	0	.18	0	.18	0	.18	0
.20	10.7	.20	7.2	.21	4.5	.22	10.3	.20	5.2	.20	4.3
.22	20.8	.22	13.9	.22	7.5	.24	15.9	.22	9.3	.22	8.0
.26	29.9	.24	19.4	.24	11.3	.26	19.4	.24	12.7	.24	11.3
.29	34.7	.28	26.4	.26	15.7	.28	22.3	.26	16.2	.26	14.4
.30	36.8	.30	30.4	.28	20.3	.30	25.7	.28	19.2	.28	17.0
.32	39.1	.33	33.5	.30	25.1	.32	29.4	.30	22.2	.30	19.4
.34	40.9	.34	35.4	.36	30.0	.34	32.7	.32	24.5	.32	21.6
.36	43.0	.36	38.3	.38	32.2	.36	35.6	.34	27.4	.34	23.0
.38	45.1	.38	40.9	.42	34.3	.40	38.5	.36	29.6	.36	24.6
.40	46.4	.40	43.2	.43	36.0	.43	40.5	.38	31.9	.38	26.0
.42	47.5	.42	45.6	.47	38.5	.46	42.6	.41	33.8	.40	27.9
.44	49.0	.45	47.9	.52	40.1	.48	44.6	.43	35.3	.42	29.5
.46	50.3	.46	49.0	.54	41.3	.50	47.3	.46	38.5	.44	30.8
.48	57.6	.48	51.1	.56	42.4	.52	49.2	.50	40.8	.46	32.0
.50	52.8	.52	53.9	.58	43.4	.55	50.8	.52	42.4	.48	33.1
.52	53.9	.56	56.3	.60	44.2	.58	52.5	.54	44.2	.50	34.0
.54	54.8	.58	58.5	.64	46.0	.60	54.0	.58	45.8	.52	35.1
.56	55.6	.60	60.3	.68	46.3			.61	47.3	.54	35.9
.58	57.6	.65	62.6	.72	47.5			.65	49.2	.56	36.3
.61	58.6	.68	64.3	.76	49.0			.67	50.3	.58	37.0
				.80	49.8			.71	51.7	.59	38.0
				.86	51.4			.77	53.3	.63	39.0
				.90	52.2			.81	55.9	.68	40.0
				.96	53.1					.72	41.0
				1.01	54.3					.76	42.1
										.80	43.4
										.84	44.3
										.88	45.2
										.93	46.1
										.98	47.2

TABLE 20 THROUGH-CRACK LENGTH VS NUMBER OF FATIGUE CYCLES FOR 1/8" THICK 300 M STEEL (F_{tu} 290 KSI) AT 15 KSI MAX. STRESS AND R OF +0.1

MOIST AIR ENVIRONMENT						SALT WATER SPRAY ENVIRONMENT					
SPECIMEN NO. X-14240-6		SPECIMEN NO. X-14240-12		SPECIMEN NO. X-14240-7		SPECIMEN NO. X-14240-8		SPECIMEN NO. X-14240-11		SPECIMEN NO. X-14240-10	
CRACK LENGTH (IN.)	NO. OF CYCLES (10^{-3})	CRACK LENGTH (IN.)	NO. OF CYCLES (10^{-3})	CRACK LENGTH (IN.)	NO. OF CYCLES (10^{-3})	CRACK LENGTH (IN.)	NO. OF CYCLES (10^{-3})	CRACK LENGTH (IN.)	NO. OF CYCLES (10^{-3})	CRACK LENGTH (IN.)	NO. OF CYCLES (10^{-3})
.75	0	.75	0	.75	0	.75	0	.75	0	.75	38.0
.80	24.7	.80	12.7	.80	30.0	.79	39.8	.83	22.5	.80	80.1
.85	41.5	.85	24.5	.85	61.5	.84	80.1	.85	26.8	.85	103.5
.90	57.8	.92	36.5	.90	88.9	.90	120.1	.90	34.8	.90	124.4
.95	73.5	.95	42.0	.95	100.9	.95	150.9	.95	45.9	.95	147.0
1.00	86.2	1.00	50.0	1.00	116.4	1.00	174.0	1.00	57.0	1.00	177.3
1.05	97.7	1.05	60.2	1.05	134.2	1.05	200.2	1.04	67.2	1.05	197.1
1.10	111.7	1.14	70.1	1.10	144.1	1.10	212.2	1.10	78.3	1.09	215.4
1.15	121.4	1.20	78.0	1.15	153.7	1.15	217.4	1.16	90.0	1.15	240.3
1.20	129.8	1.25	85.7	1.20	162.0	1.20	221.0	1.25	101.5	1.22	248.3
		1.33	92.5	1.25	170.6	1.25	225.1	1.30	111.5	1.27	263.6
		1.35	94.1	1.30	180.2	1.30	230.8	1.40	121.5	1.35	278.6
		1.40	99.8	1.35	186.1			1.50	127.0	1.40	286.1
		1.45	104.9	1.40	195.1			1.60	136.0	1.45	294.1
		1.50	110.1	1.45	205.1			1.70	143.0	1.48	302.2
		1.60	120.3	1.50	212.2			1.80	149.0	1.50	305.1
		1.70	128.2	1.60	224.9			1.89	155.9	1.60	322.1
		1.80	135.0	1.70	241.2					1.70	337.2
		1.90	141.3	1.80	248.0					1.80	349.1
				1.90	262.0					1.90	361.5
				2.00	270.0					2.00	373.0
				2.11	280.0					2.13	387.1
				2.20	289.0					2.21	397.0
				2.30	296.5					2.31	401.0
				2.42	303.0					2.40	409.0
				2.51	309.0					2.55	414.0

TABLE 21 THROUGH-CRACK LENGTH VS NUMBER OF FATIGUE CYCLES FOR 3/8" THICK 300 M STEEL (F_{tu} 290 KSI) AT 15 KSI MAX. STRESS AND R OF +0.1

MOIST AIR ENVIRONMENT						SALT WATER SPRAY ENVIRONMENT					
SPECIMEN NO. X-14241-1		SPECIMEN NO. X-14241-2		SPECIMEN NO. X-14241-3		SPECIMEN NO. X-14241-4		SPECIMEN NO. X-14241-5		SPECIMEN NO. X-14241-6	
CRACK LENGTH (IN.)	NO. OF CYCLES (10^{-3})	CRACK LENGTH (IN.)	NO. OF CYCLES (10^{-3})	CRACK LENGTH (IN.)	NO. OF CYCLES (10^{-3})	CRACK LENGTH (IN.)	NO. OF CYCLES (10^{-3})	CRACK LENGTH (IN.)	NO. OF CYCLES (10^{-3})	CRACK LENGTH (IN.)	NO. OF CYCLES (10^{-3})
.78	0	.75	0	.76	0	.75	0	.77	0	.75	0
.82	45.6	.80	29.4	.80	14.3	.80	19.9	.80	14.1	.80	23.8
.86	54.9	.85	56.0	.85	27.3	.85	48.7	.85	230.0	.85	45.9
.89	64.1	.91	77.9	.90	40.8	.90	81.0	.90	307.4	.89	63.1
.95	79.3	.95	97.6	.96	57.3	.97	112.9	.95	372.9	.95	92.8
.99	94.8	.99	111.1	1.00	70.2	1.02	132.8	1.00	438.5	1.00	128.8
1.05	112.1	1.05	126.6	1.05	83.4	1.06	146.3	1.05	497.2	1.05	160.3
1.09	124.0	1.09	142.2	1.10	93.1	1.09	157.1	1.10	542.2	1.10	187.3
1.15	141.4	1.14	156.0	1.15	103.3	1.15	179.5	1.15	567.9	1.15	217.6
1.20	157.0	1.21	173.4	1.20	116.0	1.22	202.1	1.20	595.3	1.20	243.7
1.27	170.7	1.25	184.0	1.25	126.8	1.25	220.2	1.25	614.8	1.25	266.4
1.30	177.4	1.29	194.2	1.30	136.5	1.30	237.7	1.30	635.8	1.31	290.4
		1.35	205.1	1.35	144.5			1.35	654.1	1.38	308.7
		1.39	214.0	1.40	153.4			1.40	675.7	1.40	318.6
		1.46	230.3	1.45	162.9			1.45	693.1	1.45	328.2
		1.52	238.4	1.50	170.4			1.50	708.3	1.51	342.8
		1.60	249.7	1.60	186.4			1.60	729.0	1.59	358.0
		1.70	263.5	1.70	200.1			1.70	748.6	1.71	377.5
		1.80	273.8	1.80	211.5			1.80	767.9	1.82	394.4
		1.90	285.5	1.90	222.0			1.90	776.9	1.92	405.1
				2.00	231.7					1.99	413.7
				2.10	242.7					2.08	420.1
				2.20	250.2					2.32	432.8
				2.30	258.3					2.40	445.2
				2.40	265.4					2.50	453.4
				2.50	271.1						

TABLE 22 THROUGH-CRACK LENGTH VS NUMBER OF FATIGUE CYCLES FOR 3/8" THICK 300 M STEEL (F_{tu} 270 KSI) AT 15 KSI MAX. STRESS AND R OF +0.1

MOIST AIR ENVIRONMENT						SALT WATER SPRAY ENVIRONMENT					
SPECIMEN NO. X-14241-7		SPECIMEN NO. X-14241-8		SPECIMEN NO. X-14271-9		SPECIMEN NO. X-14241-10		SPECIMEN NO. X-14241-11		SPECIMEN NO. X-14241-12	
CRACK LENGTH (IN.)	NO. OF CYCLES (10^{-3})	CRACK LENGTH (IN.)	NO. OF CYCLES (10^{-3})	CRACK LENGTH (IN.)	NO. OF CYCLES (10^{-3})	CRACK LENGTH (IN.)	NO. OF CYCLES (10^{-3})	CRACK LENGTH (IN.)	NO. OF CYCLES (10^{-3})	CRACK LENGTH (IN.)	NO. OF CYCLES (10^{-3})
.75	0	.75	0	.75	0	.75	0	.76	0	.75	0
.80	17.8	.80	13.2	.80	27.3	.80	17.1	.80	24.8	.80	10.0
.85	28.9	.85	32.0	.85	45.4	.87	39.4	.85	58.4	.85	16.8
.90	41.2	.90	47.9	.90	58.7	.92	50.5	.90	98.0	.90	32.1
.95	54.9	.95	65.4	.95	81.1	.96	59.9	.96	123.2	.95	59.8
1.00	65.4	1.00	86.9	1.00	100.3	1.00	64.6	.99	138.1	1.00	75.9
1.05	77.2	1.05	105.7	1.05	109.4	1.07	77.7	1.05	155.1	1.04	91.9
1.10	89.8	1.10	126.5	1.10	119.7	1.12	88.3	1.10	168.4	1.10	107.5
1.15	112.9	1.15	136.4	1.15	129.4	1.18	95.4	1.15	181.0	1.20	125.7
1.20	129.5	1.20	148.2	1.20	142.9	1.22	100.3	1.20	190.2	1.29	137.2
1.25	143.0	1.26	160.1	1.25	152.1	1.26	105.4	1.25	196.1	1.35	143.2
1.30	163.0	1.30	171.9	1.30	160.4	1.29	110.2	1.30	204.0	1.40	147.7
		1.35	180.4	1.35	167.9			1.35	212.7	1.45	152.4
		1.40	192.8	1.40	175.4			1.40	222.0	1.50	157.7
		1.45	202.1	1.45	183.1			1.45	226.1	1.60	167.5
		1.50	210.2	1.50	189.2			1.50	230.0	1.70	174.8
		1.60	230.4	1.60	201.9			1.60	243.6	1.80	181.2
		1.70	250.0	1.70	212.0			1.70	250.9	1.90	187.1
		1.80	265.0	1.80	221.7			1.81	258.8	2.00	193.8
		1.90	275.2	1.90	230.1			1.90	268.3	2.10	201.6
				2.00	237.6					2.20	207.2
				2.10	245.7					2.30	212.5
				2.20	252.4					2.40	218.2
				2.30	257.9					2.50	221.7
				2.41	263.9						
				2.50	268.3						

TABLE 23 THROUGH-CRACK LENGTH VS NUMBER OF FATIGUE CYCLES FOR 3/8" THICK 300 M STEEL (F_{tu} 270 KSI) AT 11 KSI MAX. STRESS AND R OF +0.5

MOIST AIR ENVIRONMENT						SALT WATER SPRAY ENVIRONMENT					
SPECIMEN NO. X-14241-13		SPECIMEN NO. X-14241-15		SPECIMEN NO. X-14241-14*		SPECIMEN NO. X-14241-16		SPECIMEN NO. X-14241-17*		SPECIMEN NO. X-14241-18*	
CRACK LENGTH (IN.)	NO. OF CYCLES (10^{-3})	CRACK LENGTH (IN.)	NO. OF CYCLES (10^{-3})	CRACK LENGTH (IN.)	NO. OF CYCLES (10^{-3})	CRACK LENGTH (IN.)	NO. OF CYCLES (10^{-3})	CRACK LENGTH (IN.)	NO. OF CYCLES (10^{-3})	CRACK LENGTH (IN.)	NO. OF CYCLES (10^{-3})
.75	0	.75	0	.75	0	.75	0	.75	0	.75	0
.80	111.1	.82	663.5	.80	8.4	.81	254.6	.80	17.9	.83	16.4
.81	135.8	.84	682.1	.85	17.8	.85	379.3	.85	29.4	.88	21.4
.93	153.6	.90	796.5	.90	25.0	.90	660.2	.90	38.7	.90	24.3
.96	203.8	.95	955.7	.95	30.8	.95	1,045.6	.96	50.7	.98	31.1
1.00	260.6	1.00	1,086.4	1.00	37.5	1.00	1,334.5	1.00	59.4	1.01	35.3
1.05	311.8	1.05	1,196.3	1.05	44.8	1.05	2,205.8	1.05	71.0	1.07	42.8
1.10	354.7	1.10	1,300.6	1.10	49.5			1.10	81.2	1.13	48.0
1.15	433.4	1.15	1,391.1	1.15	56.3			1.15	88.0	1.15	50.6
1.20	517.6	1.20	1,478.2	1.20	63.6			1.20	94.9	1.20	53.8
1.25	546.8	1.25	1,547.9	1.26	68.6			1.26	101.5	1.26	58.3
1.30	603.7	1.30	1,599.4	1.30	72.3			1.32	106.6	1.30	61.2
		1.35	1,664.6	1.35	77.5			1.36	111.5	1.35	62.7
		1.40	1,707.5	1.40	82.4			1.40	115.8	1.40	64.9
		1.50	1,801.0	1.45	89.2			1.45	120.7	1.45	67.3
		1.60	1,866.1	1.52	94.1			1.50	124.8	1.52	71.5
		1.70	1,941.4	1.60	99.9			1.60	134.6	1.60	75.3
		1.80	2,003.8	1.70	104.5			1.70	143.0	1.70	82.0
		1.90	2,068.4	1.80	110.8			1.80	150.7	1.83	87.4
		2.00	2,151.0	1.90	116.1			1.90	157.3	1.95	92.2
				2.00	120.2					2.03	95.5
				2.10	126.7					2.10	97.2
				2.20	130.5					2.20	100.8
				2.30	133.9					2.30	101.9
				2.40	136.7					2.42	103.8
				2.50	138.5					2.52	106.0

*22.5 KSI Max. Stress

TABLE 24 THROUGH-CRACK LENGTH VS NUMBER OF FATIGUE CYCLES FOR 3/8" THICK 300 M STEEL (F_{tu} 220 KSI) AT 15 KSI MAX. STRESS AND R OF +0.1

MOIST AIR ENVIRONMENT						SALT WATER SPRAY ENVIRONMENT					
SPECIMEN NO. X-14241-19		SPECIMEN NO. X-14241-20		SPECIMEN NO. X-14241-21		SPECIMEN NO. X-14241-22		SPECIMEN NO. X-14241-23		SPECIMEN NO. X-14241-24	
CRACK LENGTH (IN.)	NO. OF CYCLES (10^{-3})	CRACK LENGTH (IN.)	NO. OF CYCLES (10^{-3})	CRACK LENGTH (IN.)	NO. OF CYCLES (10^{-3})	CRACK LENGTH (IN.)	NO. OF CYCLES (10^{-3})	CRACK LENGTH (IN.)	NO. OF CYCLES (10^{-3})	CRACK LENGTH (IN.)	NO. OF CYCLES (10^{-3})
.75	0	.75	0	.78	0	.75	0	.76	0	.75	0
.80	17.0	.83	15.6	.80	2.2	.83	14.3	.82	13.4	.83	11.7
.85	30.2	.88	23.2	.85	5.7	.85	19.7	.86	18.1	.85	19.4
.90	35.6	.94	31.7	.90	28.7	.90	24.2	.92	22.8	.90	32.0
.95	39.3	.95	33.5	.96	38.3	.95	30.4	.95	28.4	.95	42.8
1.00	44.8	1.00	38.7	1.01	44.2	1.00	38.4	1.00	32.2	1.00	50.8
1.05	52.5	1.05	46.2	1.05	51.0	1.05	44.3	1.05	36.3	1.05	61.3
1.10	57.9	1.10	53.3	1.10	57.6	1.10	48.5	1.14	41.2	1.10	70.3
1.15	62.7	1.15	59.4	1.15	66.1	1.15	53.1	1.20	44.6	1.15	83.7
1.20	67.6	1.20	64.8	1.21	71.1	1.20	57.1	1.25	46.4	1.20	91.1
1.25	71.7	1.26	73.3	1.25	74.5	1.24	59.8	1.30	49.6	1.32	99.2
1.30	75.6	1.30	76.1	1.30	76.9	1.30	64.5	1.34	53.6	1.35	101.8
		1.35	80.1	1.35	80.6			1.40	57.6	1.40	106.3
		1.40	84.5	1.40	90.1			1.50	60.7	1.45	109.8
		1.45	88.8	1.45	95.2			1.60	63.2	1.50	113.7
		1.50	92.5	1.50	99.7			1.70	66.8	1.60	120.7
		1.60	101.0	1.60	106.8			1.80	71.6	1.70	126.5
		1.72	109.6	1.70	113.1			1.93	76.1	1.80	131.5
		1.80	114.2	1.80	119.6					1.90	137.1
		1.90	119.4	1.91	126.5					2.00	141.6
				2.04	133.8					2.10	145.1
				2.10	136.4					2.21	148.8
				2.20	140.4					2.30	151.8
				2.30	145.0					2.42	155.9
				2.42	149.3					2.54	158.6
				2.50	152.6						

TABLE 25 THROUGH-CRACK LENGTH VS NUMBER OF FATIGUE CYCLES FOR 3/8" THICK 300 M STEEL (F_{tu} 220 KSI) AT 22.5 KSI MAX. STRESS AND R OF +0.5

MOIST AIR ENVIRONMENT						*SALT WATER SPRAY ENVIRONMENT*					
SPECIMEN NO. X-14241-25		SPECIMEN NO. X-14241-27		SPECIMEN NO. X-14241-26		SPECIMEN NO. X-14241-28		SPECIMEN NO. X-14241-29		SPECIMEN NO. X-14241-30	
CRACK LENGTH (IN.)	NO. OF CYCLES (10^{-3})	CRACK LENGTH (IN.)	NO. OF CYCLES (10^{-3})	CRACK LENGTH (IN.)	NO. OF CYCLES (10^{-3})	CRACK LENGTH (IN.)	NO. OF CYCLES (10^{-3})	CRACK LENGTH (IN.)	NO. OF CYCLES (10^{-3})	CRACK LENGTH (IN.)	NO. OF CYCLES (10^{-3})
.75	0	.75	0	.75	0	.75	0	.75	0	.75	0
.80	7.8	.80	7.3	.80	4.2	.80	4.7	.80	15.2	.80	10.1
.85	15.3	.85	15.6	.85	10.0	.85	16.8	.85	28.0	.85	16.2
.90	21.2	.90	23.0	.90	15.3	.90	24.7	.90	37.8	.90	19.9
.95	28.7	.95	29.8	.95	20.3	.95	30.9	.95	44.7	.95	23.5
1.00	36.2	1.00	39.0	1.00	31.5	1.00	35.9	.99	49.8	1.00	33.7
1.05	43.4	1.05	44.9	1.05	37.7	1.05	43.3	1.05	60.0	1.05	41.2
1.10	48.2	1.10	49.8	1.10	42.5	1.10	48.8	1.10	65.1	1.10	49.6
1.15	54.4	1.15	55.8	1.15	47.5	1.15	54.5	1.15	70.2	1.15	55.5
1.20	62.0	1.20	62.7	1.20	52.7	1.20	59.0	1.20	75.5	1.20	60.1
1.25	69.2	1.25	67.1	1.25	57.8	1.25	63.7	1.25	79.3	1.25	64.2
1.32	72.6	1.35	75.0	1.30	62.6	1.30	67.2	1.30	84.7	1.30	68.8
		1.40	80.0	1.36	67.6			1.35	87.8	1.35	72.9
				1.40	70.5			1.40	89.9	1.40	77.6
				1.45	74.4			1.45	93.8	1.45	80.8
				1.50	77.8			1.50	96.4	1.50	82.3
				1.60	84.3			1.60	105.1	1.60	88.3
				1.70	91.3			1.70	108.5	1.70	97.6
				1.80	95.5			1.80	112.1	1.80	100.9
				1.90	98.9			1.90	115.4	1.90	103.1
				2.00	103.4					2.00	107.1
				2.10	108.1					2.10	110.2
				2.20	111.5					2.20	114.1
				2.30	114.3					2.30	116.7
				2.40	117.5					2.40	121.0
				2.50	120.0					2.50	123.3

FRACTURE TOUGHNESS TESTS

Fracture toughness tests were conducted for the 1/8, 3/8, and 3/4 inch thick surface-crack specimens and the 1/8 and 3/8 inch thick through-crack specimens after they were cyclic crack propagation tested. The specimens were statically loaded to failure with universal hydraulic test machines at a load-rate equivalent to an elastic stress-rate of 100 KSI per minute.

Autographic load-extension curves were obtained for each specimen using Class B-2 extensometer or deflectometer set-ups. A modified extensometer set-up using extension rods and a microformer was attached to the center of the test section 1/4 inch above and below the crack in the 1/8 inch thick surface-crack and through-crack specimens. With this set-up linear load-extension curves to complete failure were obtained with no indication of crack "pop-in" or slow growth behavior. However, when the specimens failed with the extensometer attached, the microformer became damaged as a result of the sudden impact on the microformer plunger. The extensometers had to be repaired and re-calibrated after one or two tests. Several specimens were tested in this manner to confirm that no deviation from linearity occurred in the load-extension curves. To avoid additional microformer damage, a Class B-2 deflectometer set-up was used on 1/8 inch surface-crack and through-crack specimens to measure load-head travel. A linear load-head travel curve to complete failure also occurred with this set-up. A comparison of the load-extension curves obtained for 1/8 inch through-crack specimens with the extensometer set-up attached to the specimen and with the deflectometer set-up attached to the test machine movable head is presented in Figure 44 . The characteristics of the two curves were similar except for the extension scale. As a result, the deflectometer set-up was used to measure and record head travel for the remainder of the specimens. Since crack "pop-in" or evidence of slow crack growth was not observed with the 1/8 inch thick specimens, it was not expected that they would occur with the 3/8 and 3/4 inch thick specimens. To verify this, one 3/8 inch through-crack specimen was tested with the extensometer set-up attached to the specimen. A linear load-extension curve to failure was obtained.

The initial and final fatigue crack lengths and depths were measured from the fractured surfaces of each specimen.

The results of the fracture toughness tests for 1/8, 3/8, and 3/4 inch thick surface-crack specimens are tabulated in Tables 26 through 33. Results for 1/8 and 3/8 inch thick through-crack specimens are tabulated in Tables 34 through 37.

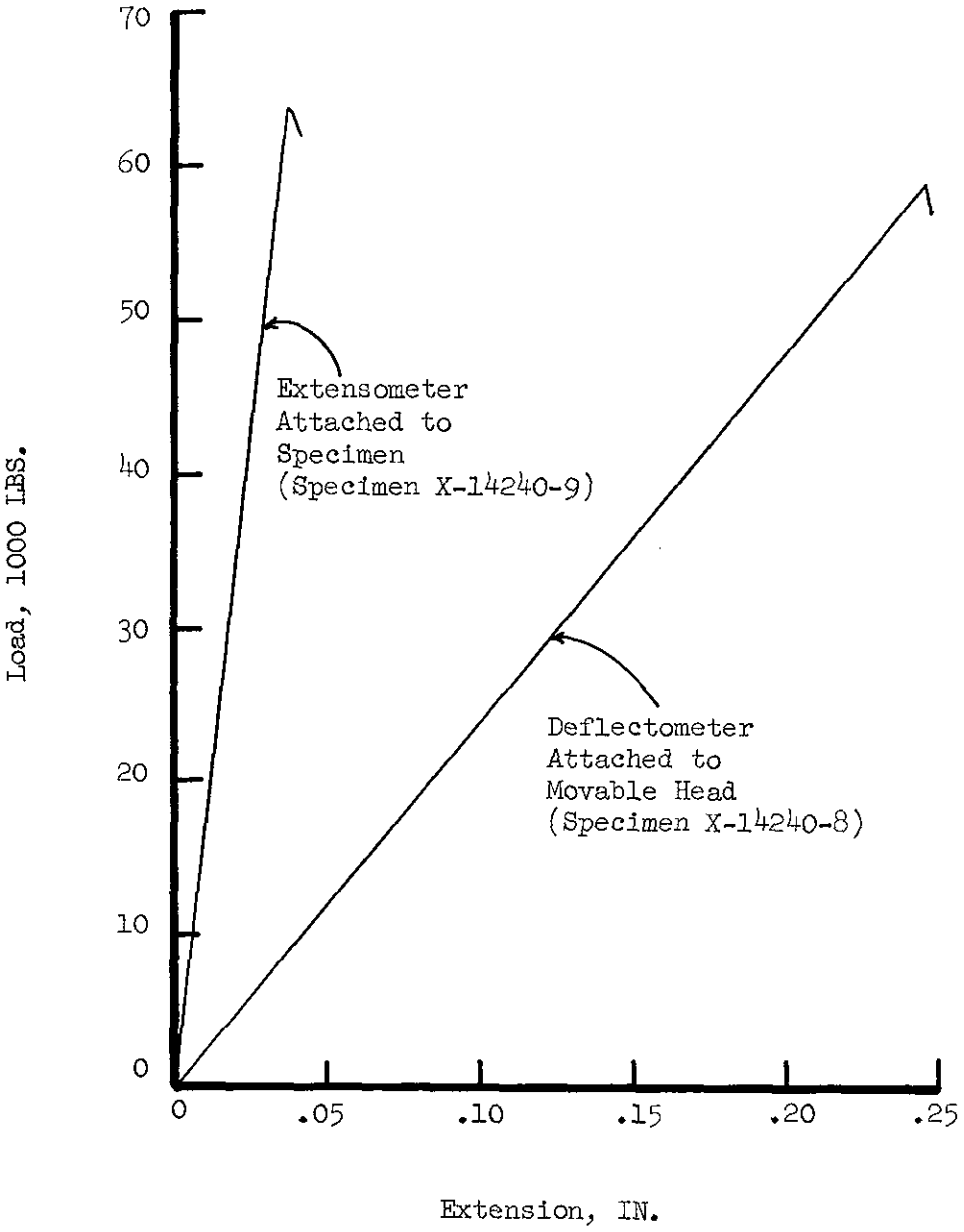

Figure 44 Comparison of Typical Load-Extension Curves Obtained From Extensometer and Deflectomer Set-Ups for Fracture Toughness Tests of 1/8-Inch Through-Crack Specimens

TABLE 26 FRACTURE TOUGHNESS TEST RESULTS FOR 300M STEEL SURFACE-CRACK SPECIMENS (UTS 290 KSI)

FATIGUE CRACKING CONDITIONS											
ENVIRONMENT	MAX. GROSS STRESS (KSI)	RANGE RATIO (R)	CYCLIC FREQUENCY (CPS)	SPECIMEN NUMBER	SPEC. THICK. (IN.)	CRACK LENGTH 2C (IN.)	CRACK DEPTH a (IN.)	$\frac{a}{2C}$	MAX. GROSS STRESS (KSI)	APPARENT K_{Ic} (KSI $\sqrt{IN.}$)	
Moist Air	45	+0.±	20	X-14237-5	.122	.380	.122	-	152	-	(1)
				-6	.124	.285	.100	.351	171	81.5	
				-7	.123	.560	.123	-	113	111	(2)
Salt Water Spray	45	+0.1	20	-8	.125	.250	.095	.380	175	79.0	
				-9	.122	.390	.122	-	138	-	(1)
				-10	.118	.600	.118	-	113	115	(2)
Moist Air	42	+0.2	20	-11	.123	.255	.095	.372	175	79.8	
				-23	.122	.360	.122	-	147	-	(1)
				-13	.126	.570	.126	-	105	104	(2)
Salt Water Spray	42	+0.2	20	-14	.121	.250	.090	.360	182	82.0	
				-15	.116	.380	.116	-	145	-	(1)
				-16	.125	.580	.125	-	112	112	(2)
Moist Air	33	+0.5	20	-17	.121	.260	.100	.385	169	77.6	
				-18	.123	.380	.123	-	138	-	(1)
				-19	.123	.570	.123	-	107	106	(2)
Salt Water Spray	33	+0.5	20	-20	.124	.260	.090	.346	157	70.9	
				-21	.123	.380	.123	-	131	-	(1)
				-24	.122	.560	.122	-	104	102	(2)

(1) Surface-crack propagated through the thickness resulting with a through-crack with large differences in crack length at the two surfaces. Since neither surface-crack nor through-crack stress intensity equations can adequately handle this shape of crack, no stress intensity value is reported.

(2) Surface-crack propagated through the thickness resulting with a through-crack with approximately equal crack lengths at the two surfaces. The stress intensity (K_{Ic}) values reported were calculated using the through-crack equation.

TABLE 27 FRACTURE TOUGHNESS TEST RESULTS FOR 300 M STEEL SURFACE-CRACK SPECIMENS (UTS 290 KSI)

FATIGUE CRACKING CONDITIONS				SPECIMEN NUMBER	SPEC. THICK. (IN.)	CRACK LENGTH 2C (IN.)	CRACK DEPTH a (IN.)	$\frac{a}{2C}$	MAX. GROSS STRESS (KSI)	APPARENT K_{Ic} (KSI $\sqrt{IN.}$)
ENVIRONMENT	MAX. GROSS STRESS (KSI)	RANGE RATIO (R)	CYCLIC FREQUENCY (CPS)							
Moist Air	45	+0.1	20	X-14238-1	-	-	-	-	-	- (1)
				-2	.374	.750	.290	.387	96.9	75.6
				-3	.376	.560	.220	.393	117	77.2
Salt Water Spray	45	+0.1	20	-4	.374	.380	.160	.421	152	84.4
				-5	.376	.560	.220	.393	118	78.1
				-6	.375	.760	.290	.382	88.3	67.6
Moist Air	42	+0.2	20	-7	.376	.380	.160	.421	135	74.3
				-8	.378	.560	.230	.411	112	74.3
				-9	.380	.760	.300	.395	73.3	56.0
Salt Water Spray	42	+0.2	20	-10	.374	.370	.140	.379	160	86.9
				-11	.375	.560	.230	.411	109	72.2
				-12	.376	.760	.300	.395	81.6	62.7
Moist Air	33	+0.5	20	-13	.372	.380	.150	3.95	136	74.3
				-14	.377	.220	.090	.409	178	76.0
				-15	.374	.760	.310	.408	77.9	59.6
Salt Water Spray	33	+0.5	20	-16	.376	.365	.155	.425	120	64.4
				-17	.371	.550	.220	.400	100	65.4
				-18	.376	.760	.290	.382	79.1	60.4

(1) Specimen X-14238 was overloaded beyond yield due to a hydraulic system malfunction.

TABLE 28 FRACTURE TOUGHNESS TEST RESULTS FOR 300M STEEL SURFACE-CRACK SPECIMENS (UTS 270 KSI)

FATIGUE CRACKING CONDITIONS										
ENVIRONMENT	MAX. GROSS STRESS (KSI)	RANGE RATIO (R)	CYCLIC FREQUENCY (CPS)	SPECIMEN NUMBER	SPEC. THICK. (IN.)	CRACK LENGTH 2C (IN.)	CRACK DEPTH a (IN.)	$\frac{a}{2C}$	MAX. GROSS STRESS (KSI)	APPARENT K_{Ic} (KSI $\sqrt{IN.}$)
Moist Air	45	+0.1	20	X-14238-19	.373	.370	.170	.459	107	57.9
				-20	.381	.550	.240	.437	91.9	60.4
				-21	.376	.760	.300	.394	72.1	55.2
Salt Water Spray	45	+0.1	20	-22	.376	.380	.160	.421	135	74.3
				-23	.374	.550	.220	.400	99.8	65.3
				-24	.374	.770	.300	.390	77.1	59.4
Moist Air	33	+0.5	20	-25	.376	.380	.160	.421	134	73.8
				-26	.376	.560	.240	.429	99.7	66.2
				-27	.381	.750	.300	.400	80.0	61.2
Salt Water Spray	33	+0.5	20	-28	.376	.370	.140	.379	145	78.5
				-29	.374	.560	.250	.447	106	70.4
				-30	.374	.760	.290	.382	92.1	70.6

TABLE 29 FRACTURE TOUGHNESS TEST RESULTS FOR 300M STEEL SURFACE-CRACK SPECIMENS (UTS 220 KSI)

FATIGUE CRACKING CONDITIONS				SPECIMEN NUMBER	SPEC. THICK. (IN.)	CRACK LENGTH 2C (IN.)	CRACK DEPTH a (IN.)	$\frac{a}{2C}$	MAX. GROSS STRESS (KSI)	APPARENT K_{Ic} (KSI $\sqrt{IN.}$)
ENVIRONMENT	MAX. GROSS STRESS (KSI)	RANGE RATIO (R)	CYCLIC FREQUENCY (CPS)							
Moist Air	45	+0.1	20	X-14238-31	.375	.380	.170	.447	124	68.6
				-32	.376	.560	.250	.447	90.3	60.0
				-33	.378	.760	.310	.408	73.5	56.6
Salt Water Spray	45	+0.1	20	-34	.379	.400	.180	.450	105	59.3
				-35	.378	.560	.240	.429	95.1	63.1
				-36	.374	.800	.310	.388	68.3	53.5
Moist Air	33	+0.5	20	-37	.376	.390	.160	.411	130	72.9
				-38	.376	.560	.230	.411	105	69.9
				-39	.376	.760	.310	.408	94.4	72.9
Salt Water Spray	33	+0.5		-40	.377	.370	.160	.433	147	81.4
				-41	.377	.560	.220	.393	115	76.2
				-42	.374	.760	.280	.369	90.9	69.3

TABLE 30 FRACTURE TOUGHNESS TEST RESULTS FOR 300 M STEEL SURFACE-CRACK SPECIMENS (UTS 290 KSI)

FATIGUE CRACKING CONDITIONS										
ENVIRONMENT	MAX. GROSS STRESS (KSI)	RANGE RATIO (R)	CYCLIC FREQUENCY (CPS)	SPECIMEN NUMBER	SPEC. THICK. (IN.)	CRACK LENGTH 2C (IN.)	CRACK DEPTH a (IN.)	$\frac{a}{2C}$	MAX. GROSS STRESS (KSI)	APPARENT K_{Ic} (KSI $\sqrt{IN.}$)
Moist Air	45	+0.1	20	X-14239-19	.751	.600	.280	.467	88.8	60.9
				-20	.749	.800	.340	.425	78.8	62.1
				-21	.751	1.00	.440	.440	67.5	59.4
Salt Water Spray	45	+0.1	20	-22	.751	.600	.250	.417	84.8	58.0
				-23	.750	.800	.350	.438	74.6	58.8
				-24	.749	1.00	.450	.450	63.6	55.9
Moist Air	42	+0.2	20	-25	.746	.600	.260	.433	85.4	58.3
				-26	.750	.800	.350	.438	91.5	72.1
				-27	.749	1.02	.450	.441	63.7	56.7
Salt Water Spray	42	+0.2	20	-28	.750	.600	.250	.417	108	73.9
				-29	.750	.850	.360	.424	87.3	70.8
				-30	.751	1.02	.450	.441	66.2	59.0
Moist Air	33	+0.5	20	-31	.761	.600	.280	.467	115	79.5
				-32	.751	.800	.340	.425	94.7	74.9
				-33	.752	1.03	.430	.417	77.8	69.3
Salt Water Spray	33	+0.5	20	-34	.749	.600	.260	.434	115	79.0
				-35	.745	.800	.370	.463	87.3	69.0
				-36	.749	1.00	.460	.460	76.3	67.1

TABLE 31 FRACTURE TOUGHNESS TEST RESULTS FOR 300 M STEEL SURFACE-CRACK SPECIMENS (UTS 290 KSI)

FATIGUE CRACKING CONDITIONS										
ENVIRONMENT	MAX. GROSS STRESS (KSI)	RANGE RATIO (R)	CYCLIC FREQUENCY (CPS)	SPECIMEN NUMBER	SPEC. THICK. (IN.)	CRACK LENGTH 2C (IN.)	CRACK DEPTH a (IN.)	$\frac{a}{2C}$	MAX. GROSS STRESS (KSI)	APPARENT K_{Ic} (KSI $\sqrt{IN.}$)
Moist Air	45	+0.1	20	F-1	.745	.615	.265	.431	86.7	60.0
				F-2	.746	.805	.345	.429	87.0	69.0
				F-3	.748	1.00	.420	.420	73.3	64.5
Salt Water Spray	45	+0.1	20	F-4	.748	.600	.200	.333	97.8	65.9
				F-5	.748	.800	.340	.426	83.9	66.0
				F-6	.749	1.00	.390	.390	72.3	63.4

TABLE 32 FRACTURE TOUGHNESS TEST RESULTS FOR 300 M STEEL SURFACE-CRACK SPECIMENS (UTS 270 KSI)

FATIGUE CRACKING CONDITIONS										
ENVIRONMENT	MAX. GROSS STRESS (KSI)	RANGE RATIO (R)	CYCLIC FREQUENCY (CPS)	SPECIMEN NUMBER	SPEC. THICK. (IN.)	CRACK LENGTH 2C (IN.)	CRACK DEPTH a (IN.)	$\frac{a}{2C}$	MAX. GROSS STRESS (KSI)	APPARENT K_{Ic} (KSI $\sqrt{IN.}$)
Moist Air	45	+0.1	20	F-7	.753	.600	.250	.417	95.9	65.4
				F-8	.750	.800	.350	.438	83.2	65.7
				F-9	.749	1.00	.420	.420	69.4	61.2
Salt Water Spray	45	+0.1	20	F-10	.749	.600	.260	.433	102	70.2
				F-11	.749	.800	.340	.426	89.8	71.1
				F-12	.751	1.00	.450	.450	70.7	62.4

TABLE 33 FRACTURE TOUGHNESS TEST RESULTS FOR 300 M STEEL SURFACE-CRACK SPECIMENS (UTS 220 KSI)

FATIGUE CRACKING CONDITIONS										
ENVIRONMENT	MAX. GROSS STRESS (KSI)	RANGE RATIO (R)	CYCLIC FREQUENCY (CPS)	SPECIMEN NUMBER	SPEC. THICK. (IN.)	CRACK LENGTH 2C (IN.)	CRACK DEPTH a (IN.)	$\frac{a}{2C}$	MAX. GROSS STRESS (KSI)	APPARENT K_{Ic} (KSI $\sqrt{IN.}$)
Moist Air	45	+0.1	20	F-13	.750	.600	.280	.467	91.0	62.8
				F-14	.750	.680	.310	.456	84.5	61.9
				F-15	.750	1.00	.420	.420	61.4	53.7
Salt Water Spray	45	+0.1	20	F-16	.749	.600	.280	.467	95.6	65.0
				F-17	.750	.820	.370	.451	67.5	54.1
				F-18	.749	1.00	.430	.430	67.6	59.6

TABLE 34 FRACTURE TOUGHNESS TEST RESULTS FOR 300 M STEEL THROUGH-CRACK SPECIMENS (UTS 290 KSI)

FATIGUE CRACKING CONDITIONS										
ENVIRONMENT	MAX. GROSS STRESS (KSI)	RANGE RATIO (R)	CYCLIC FREQUENCY (CPS)	SPECIMEN NUMBER	SPEC. THICK. (IN.)	CRACK LENGTH (IN.) SIDE A	CRACK LENGTH (IN.) SIDE B	MAX. GROSS STRESS (KSI)	APPARENT K_{Ic} (KSI $\sqrt{IN.}$) (1)	APPARENT K_{Ic} (KSI $\sqrt{IN.}$) (2)
Moist Air	15	+0.1	20	X-14240-6	.130	1.17	1.16	98.6	139	139
				-12	.119	1.89	1.87	71.1	134	134
				-7	.123	2.56	2.49	63.3	153	150
Salt Water Spray	15	+0.1	20	-8	.129	1.45	1.26	91.5	146	140
				-11	.120	1.95	1.90	79.8	154	153
				-10	.130	2.57	2.55	57.4	139	138

(1) Based on maximum crack length.
(2) Based on average crack length.

TABLE 35 FRACTURE TOUGHNESS TEST RESULTS FOR 300 M STEEL THROUGH-CRACK SPECIMENS (UTS 290 KSI)

FATIGUE CRACKING CONDITIONS										
ENVIRONMENT	MAX. GROSS STRESS (KSI)	RANGE RATIO (R)	CYCLIC FREQUENCY (CPS)	SPECIMEN NUMBER	SPEC. THICK. (IN.)	CRACK LENGTH (IN.) SIDE A	CRACK LENGTH (IN.) SIDE B	MAX. GROSS STRESS (KSI)	APPARENT K_{Ic} (KSI $\sqrt{IN.}$) (1)	APPARENT K_{Ic} (KSI $\sqrt{IN.}$) (2)
Moist Air	15	+0.1	20	X-14241-1	.372	1.30	.790	61.2	91.5	81.1
				-2	.372	1.90	1.90	46.4	88.0	88.0
				-3	.372	2.40	2.15	38.3	87.6	83.7
Salt Water Spray	15	+0.1	20	-4	.370	1.52	1.28	54.2	89.0	84.6
				-5	.370	1.93	1.87	46.5	89.3	88.3
				-6	.371	2.50	2.30	38.2	90.2	87.3

(1) Based on maximum crack length.
(2) Based on average crack length.

TABLE 36 FRACTURE TOUGHNESS TEST RESULTS FOR 300 M STEEL THROUGH-CRACK SPECIMENS (UTS 270 KSI)

FATIGUE CRACKING CONDITIONS				SPECIMEN NUMBER	SPEC. THICK. (IN.)	CRACK LENGTH (IN.)		MAX. GROSS STRESS (KSI)	APPARENT K_{Ic} (KSI $\sqrt{IN.}$)	
ENVIRONMENT	MAX. GROSS STRESS (KSI)	RANGE RATIO (R)	CYCLIC FREQUENCY (CPS)			SIDE A	SIDE B		(1)	(2)
Moist Air	15	+0.1	20	X-14241-7	.370	1.30	1.18	52.4	78.4	76.3
				-8	.368	1.89	1.53	44.3	83.9	78.3
				-9	.374	2.58	2.50	32.8	80.0	78.8
Salt Water Spray	15	+0.1	20	-10	.371	1.55	1.28	38.2	63.4	60.2
				-11	.371	2.06	1.90	32.4	65.1	63.4
				-12	.376	2.55	2.48	38.2	68.4	66.3
Moist Air	11	+0.5	20	-13	.372	1.45	1.30	41.9	66.9	64.9
	22.5	+0.5	20	-14	.371	2.50	2.50	27.0	63.8	63.8
	11	+0.5	20	-15	.369	2.10	2.05	33.0	67.3	66.9
Salt Water Spray	11	+0.5	20	-16	.372	1.03	.950	48.0	62.8	61.5
	22.5	+0.5	20	-17	.367	1.90	1.60	34.9	66.4	62.6
	11	+0.5	20	-18	.373	2.60	2.50	27.3	66.9	65.7

(1) Based on maximum crack length.
(2) Based on average crack length.

TABLE 37 FRACTURE TOUGHNESS TEST RESULTS FOR 300 M STEEL THROUGH-CRACK SPECIMENS (UTS 220 KSI)

FATIGUE CRACKING CONDITIONS				SPECIMEN NUMBER	SPEC. THICK. (IN.)	CRACK LENGTH (IN.)		MAX. GROSS STRESS (KSI)	APPARENT K_{Ic} (KSI $\sqrt{IN.}$)	
ENVIRONMENT	MAX. GROSS STRESS (KSI)	RANGE RATIO (R)	CYCLIC FREQUENCY (CPS)			SIDE A	SIDE B		(1)	(2)
Moist Air	15	+0.1	20	X-14241-19	.374	1.31	1.29	50.4	75.7	75.4
				-20	.370	1.90	1.60	36.1	68.6	64.8
				-21	.374	2.50	2.37	36.1	85.3	82.7
Salt Water Spray	15	+0.1	20	-22	.372	1.45	1.30	41.8	66.6	64.6
				-23	.373	2.25	1.95	30.9	66.5	63.4
				-24	.373	2.50	2.35	30.8	72.8	70.7
Moist Air	22.5	+0.5	20	-25	.371	1.35	1.28	43.2	66.1	65.2
				-26	.372	2.50	2.50	30.3	71.5	71.5
				-27	.370	1.90	1.80	35.9	68.1	66.9
Salt Water Spray	22.5	+0.5	20	-28	.373	1.35	1.30	41.5	63.5	62.8
				-29	.373	1.90	1.90	39.9	75.7	75.7
				-30	.375	2.50	2.50	30.8	72.7	72.7

(1) Based on maximum crack length.
(2) Based on average crack length.

FRACTURE CHARACTERISTICS

Photographs showing the fracture faces of 1/8 inch surface-crack and through-crack specimens used in the air environment selection tests are presented in Figure 45. The pre-cracks were propagated to specimen failure under cyclic loading. The amount of flat fracture was considerably less for the surface-crack specimens than for the through-crack specimens. In fact, much cyclic crack propagation occurred in a slant (shear mode) fracture for the surface-crack specimens.

Figure 46 presents photographs of fracture faces for 1/8 inch surface-crack specimens with pre-crack cyclic propagated to three specific sizes in moist air and salt water spray environments followed by static loading to failure. The smallest cyclic propagated cracks did not penetrate the specimen thickness whereas the two larger cracks did. The crack shapes were similar for cracks propagated in both moist air and salt water spray environments. Flat wing tipped flat fracture of increasing length with increasing crack size is evident followed by slant fracture.

Fracture faces of statically failed 3/8 inch surface-crack specimens with pre-cracks cyclic propagated to three specific sizes in moist air and salt water spray environments are shown in Figures 47 to 49. With the 3/8 inch thick specimens, none of the cyclic propagated cracks penetrate the thickness. The semi-elliptically shaped cracks propagated with a near constant depth to length ratio (a/2c) for both environments. The static failure portion of the fractures were predominantly flat fracture with a small shear lip around the specimen periphery except for fatigue cracked surface. The static fracture texture was very coarse and fibrous in appearance for the 220 KSI strength specimens (Figure 49) as compared with the fracture texture for the 290 and 270 KSI strength specimens (Figures 47, and 48).

Figures 50 through 52 present photographs showing fracture faces of statically failed 3/4 inch plate and forging surface-crack specimens cyclic tested in moist air and salt water spray environments. The fracture characteristics were similar to those for the 3/8 inch surface crack specimens.

Fracture faces of 1/8 and 3/8 inch through-crack specimens tested in a similar manner as the surface-crack specimens are shown in Figures 53 through 55. The fracture textures, flat fracture, and shear fracture characteristics were similar to those for surface-cracks. With many specimens, the through-cracks did not cyclic propagate with equal lengths on both sides of the specimens. There was a tendency for through-cracks to have equal lengths on both sides of the specimens as the cracks became longer. Some possible reasons for uneven crack propagation are (1) initial propagation probably occurred at one surface-pre-crack intersection and did not propagate to equal length for the shorter cracks and (2) minor warpage may have occurred during the heat treatment quench which could cause a small bending load component in the axial tension loaded test. Surprisingly, no tunneling effect was noted with the cyclic propagated through-cracks in either 1/8 and 3/8 inch thick specimens. That is, longer crack propagation in the center of the thickness than at the surfaces.

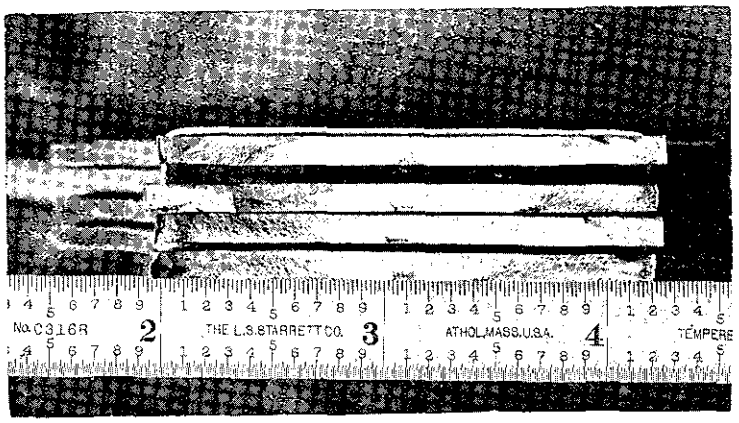

FROM BOTTOM X-14237-1, -4 (DRY AIR) -2, -3 (MOIST AIR)

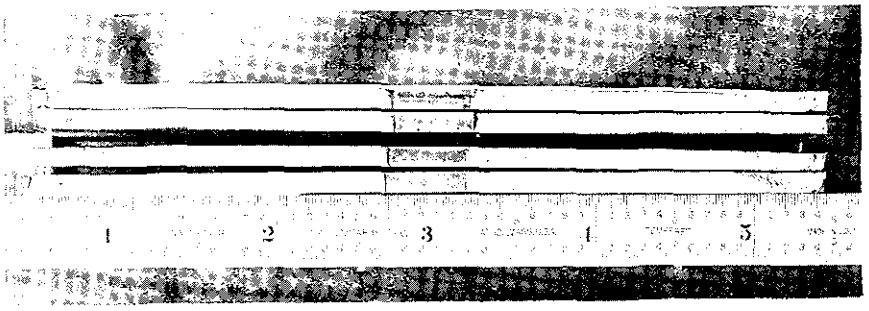

FROM BOTTOM X-14240-2, -4 (DRY AIR) -1, -3 (MOIST AIR)

FIGURE 45 - Fracture Faces 1/8" 300M Surface-Crack (Top) and Through-Crack (Bottom) Specimens, F_{tu} 290 KSI

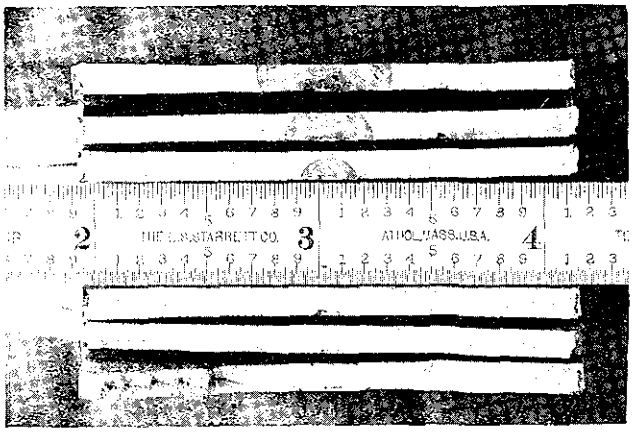

FROM BOTTOM, X-14237-6, -5, -7 (AIR) -8, -9, -10 (SALT SPRAY)

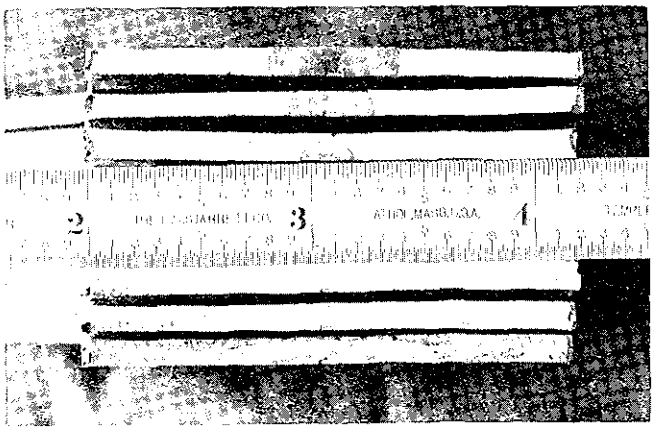

FROM BOTTOM, X-14237-11, -23, -13, (AIR) -14, -15, -16 (SALT SPRAY)

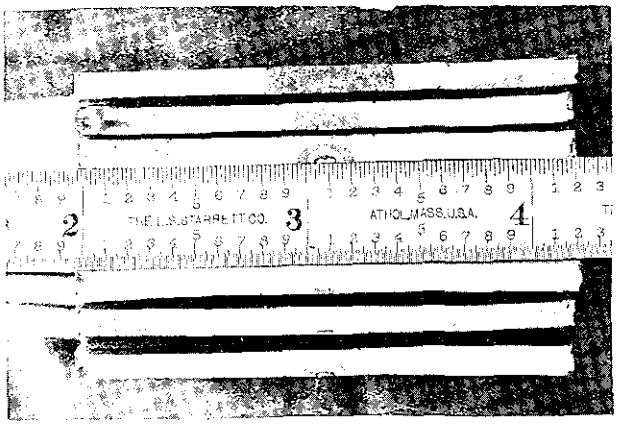

FROM BOTTOM, X-14237-17, -18, -19 (AIR) -20, -21, -24 (SALT SPRAY)

FIGURE 46 - Fracture Faces 1/8" 300 M Surface-Crack Specimens, F_{tu} 290 KSI

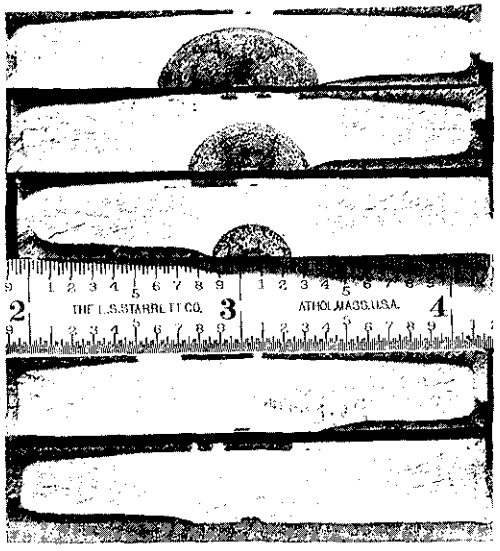

FROM BOTTOM
X-14238-3, -2 (AIR)
-4, -5, -6 (SALT SPRAY)

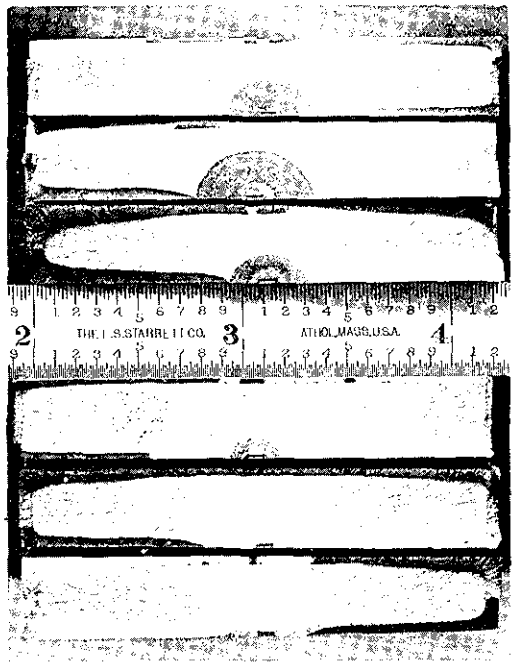

FROM BOTTOM
X-14238-7, -8, -9 (AIR)
-10, -11, -12 (SALT SPRAY)

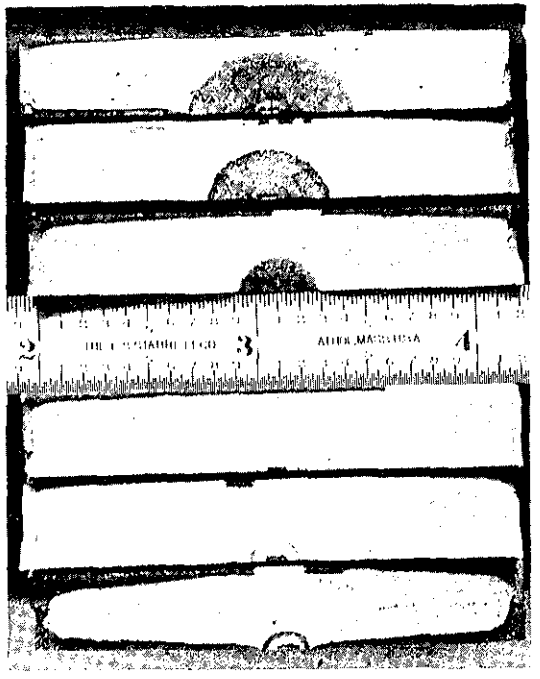

FROM BOTTOM
X-14238-14, -13, -15 (AIR)
-16, -17, -18 (SALT SPRAY)

FIGURE 47 - Fracture Faces 3/8" 300 M Surface-Crack Specimens, F_{tu} 290 KSI

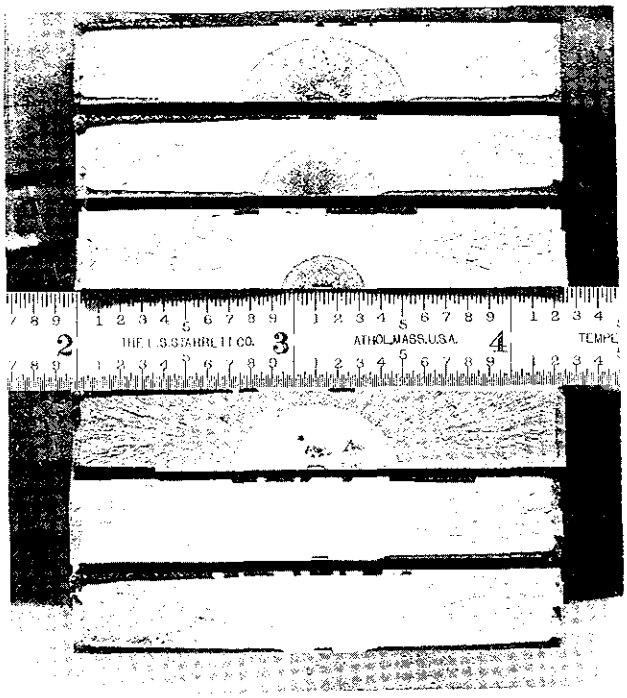

FROM BOTTOM X-14238-19, -20, -21 (AIR) -22, -23, -24 (SALT SPRAY)

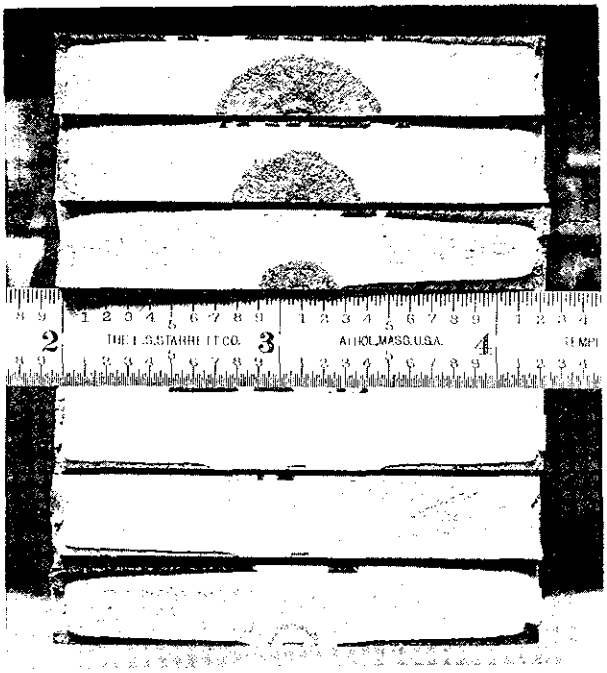

FROM BOTTOM X-14238-25, -26, -27 (AIR) -28, -29, -30 (SALT SPRAY)

FIGURE 48 - Fracture Faces 3/8" 300 M Surface-Crack Specimens, F_{tu} 270 KSI

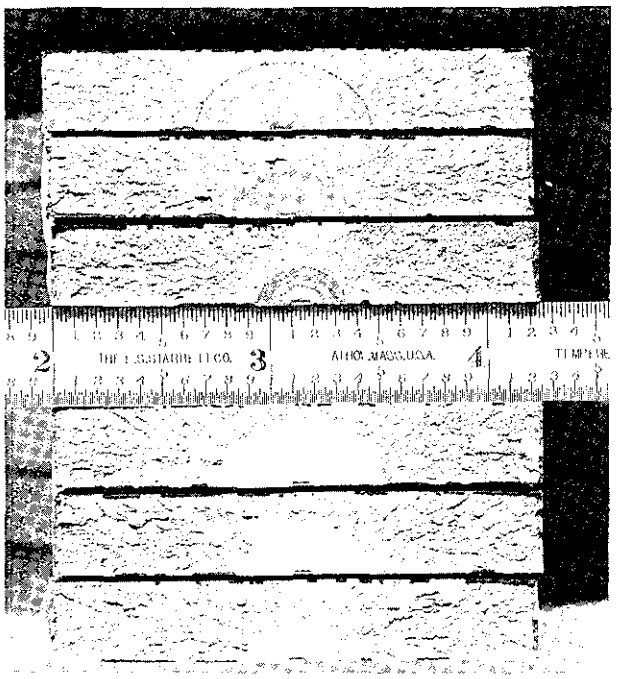

FROM BOTTOM X-14238-31, -32, -33 (AIR) -34, -35, -36 (SALT SPRAY)

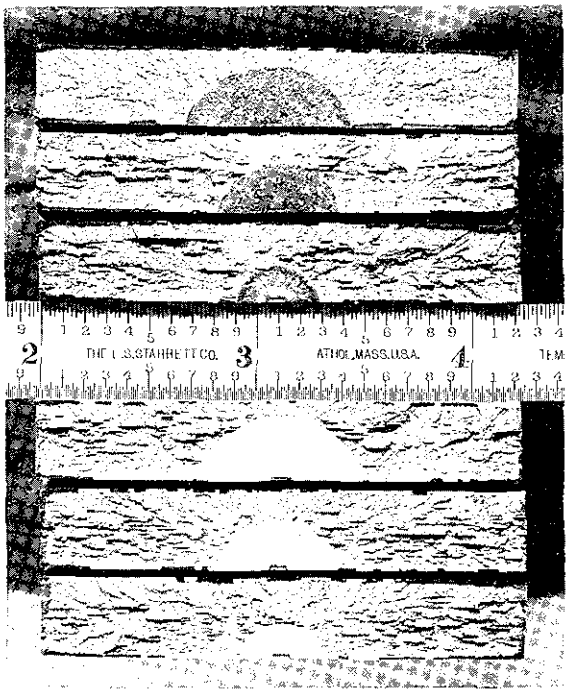

FROM BOTTOM X-14238-37, -38, -39 (AIR) -40, -41, -42 (SALT SPRAY)

FIGURE 49 - Fracture Faces 3/8" 300 M Surface-Crack Specimens, F_{tu} 220 KSI

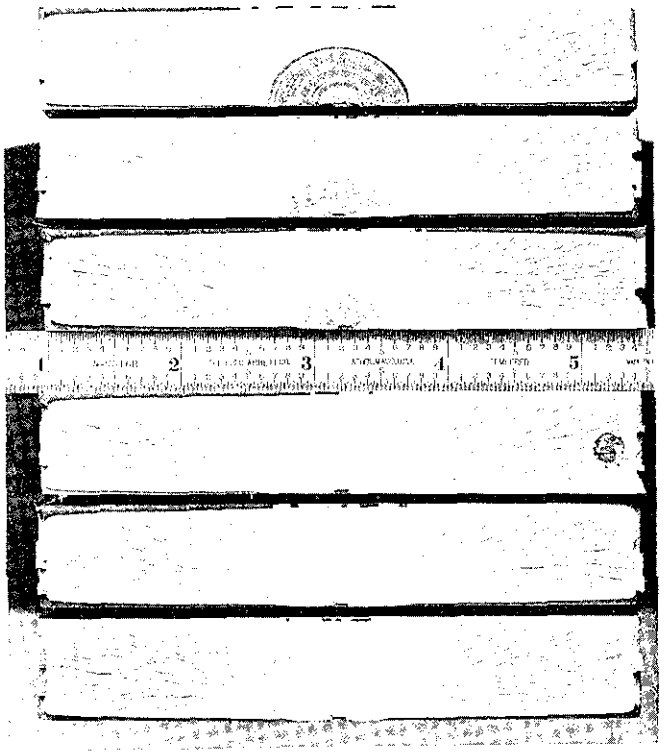

FROM BOTTOM X-14239-19, -20, -21 (AIR)
-22, -23, -24 (SALT SPRAY)

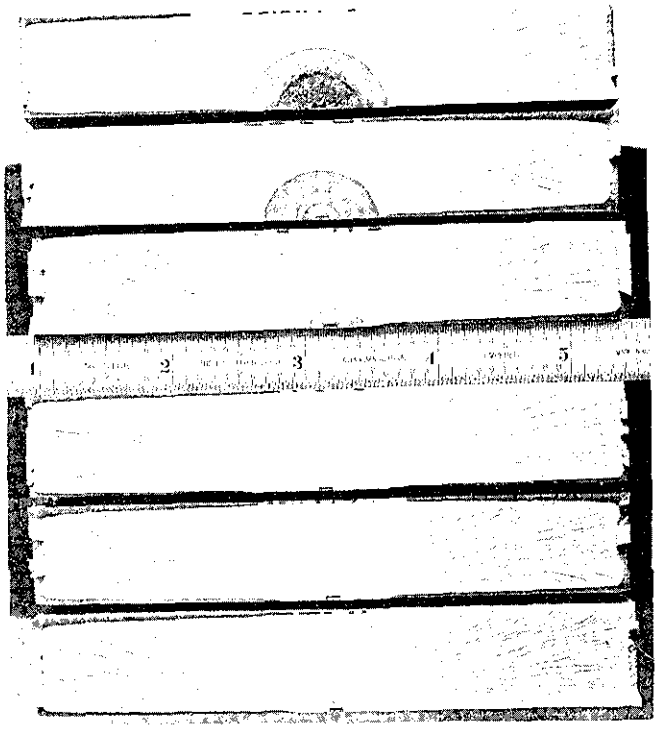

FROM BOTTOM X-14239-25, -26, -27 (AIR)
-28, -29, -30 (SALT SPRAY)

FIGURE 50 - Fracture Faces 3/4" 300 M Plate Surface-Crack Specimens, F_{tu} 290 KSI

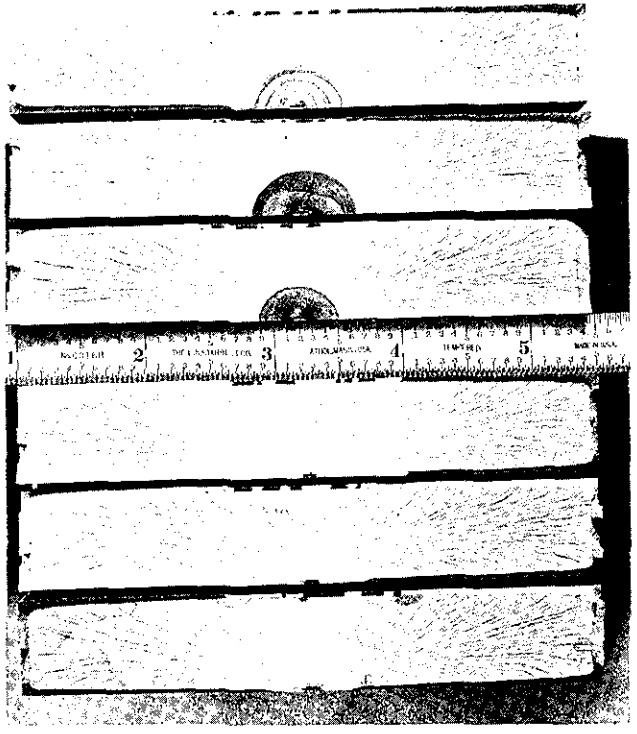

FORGING

FROM BOTTOM F-1, -2, -3 (AIR)
-4, -5, -6 (SALT SPRAY)

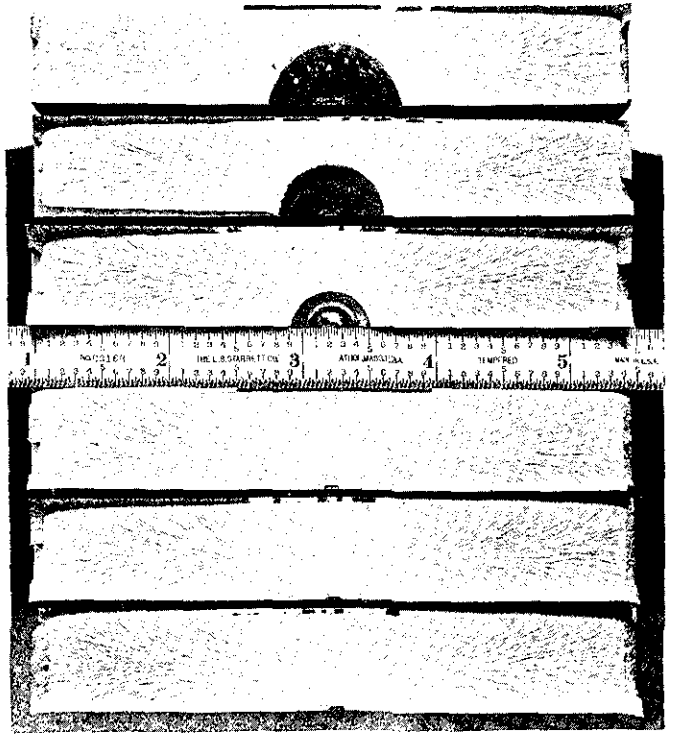

PLATE

FROM BOTTOM X-14239-31, -32, -33 (AIR)
-34, -35, -36 (SALT SPRAY)

FIGURE 51 - Fracture Faces 3/4" 300 M Forging and Plate Surface-Crack Specimens, F_{tu} 290 KSI

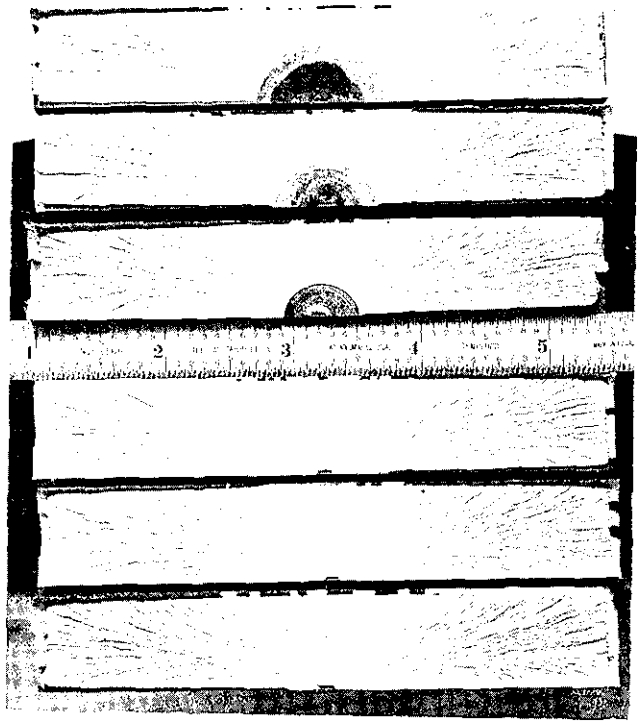

270 KSI
FROM BOTTOM F-7, -8, -9 (AIR) -10, -11,
-12 (SALT SPRAY)

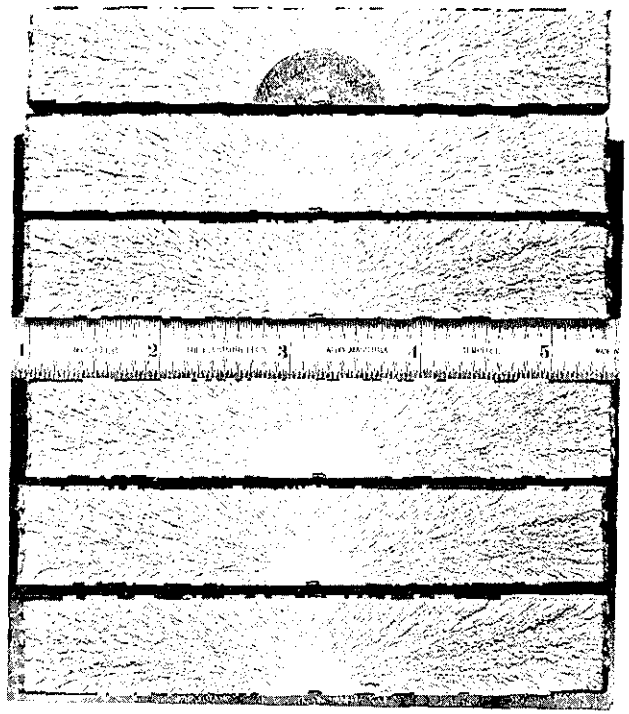

220 KSI
FROM BOTTOM F-13, -14, -15 (AIR) -16,
-17, -18 (SALT SPRAY)

FIGURE 52 - Fracture Faces 3/4" 300 M Forging Surface-Crack Specimens, F_{tu} 270 KSI and 220 KSI

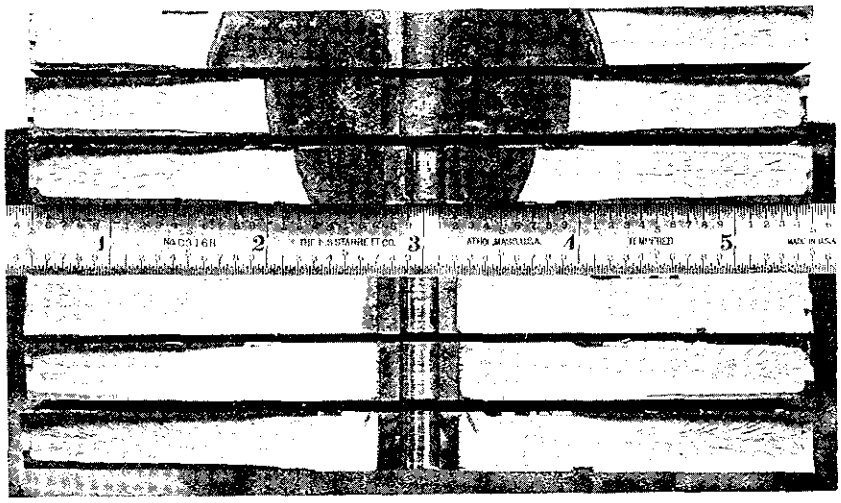

FROM BOTTOM X-14241-1, -2, -3 (AIR) -4, -5, -6
(SALT SPRAY)

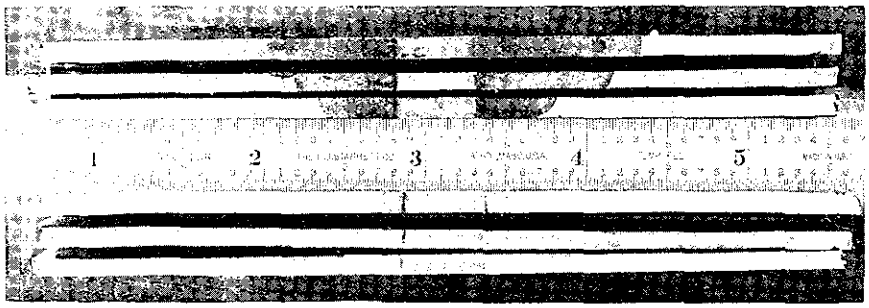

FROM BOTTOM X-14240-6, -12, -7 (AIR) -8, -11-, -10
(SALT SPRAY)

FIGURE 53- Fracture Faces 1/8" and 3/8" 300 M Through-Crack Specimens, F_{tu} 290 KSI

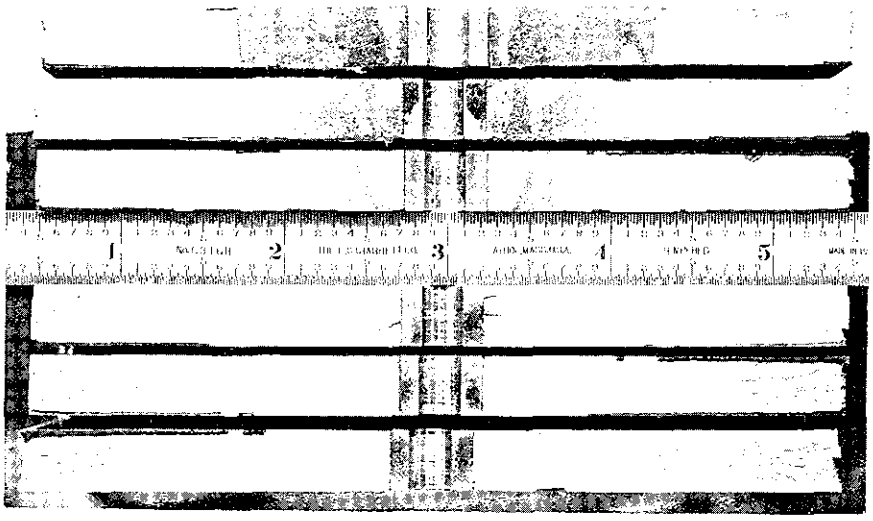

FROM BOTTOM X-14241-7, -8, -9 (AIR) -10, -11, -12
(SALT SPRAY)

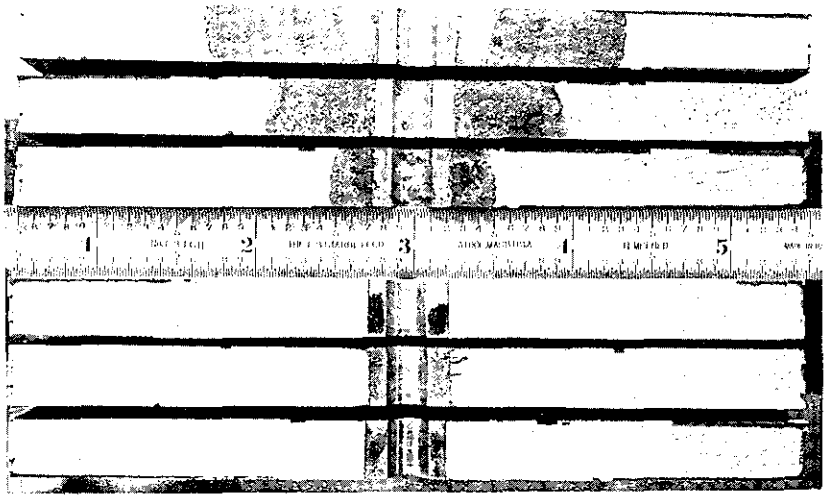

FROM BOTTOM X-14241-13, -15, -14 (AIR) -16, -17, -18
(SALT SPRAY)

FIGURE 54 - Fracture Faces 3/8" 300 M Through-Crack Specimens, F_{tu} 270 KSI

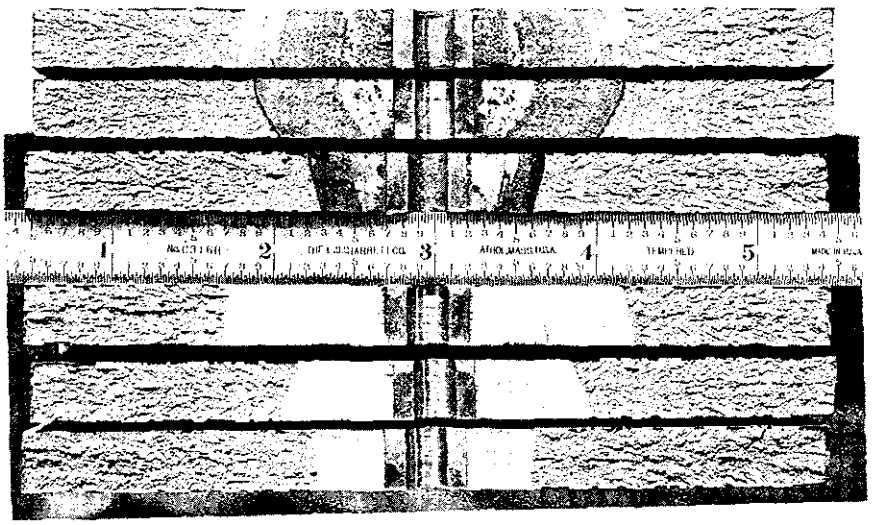

FROM BOTTOM X-14241-19, -20, -21 (AIR) -22, -23, -24
(SALT SPRAY)

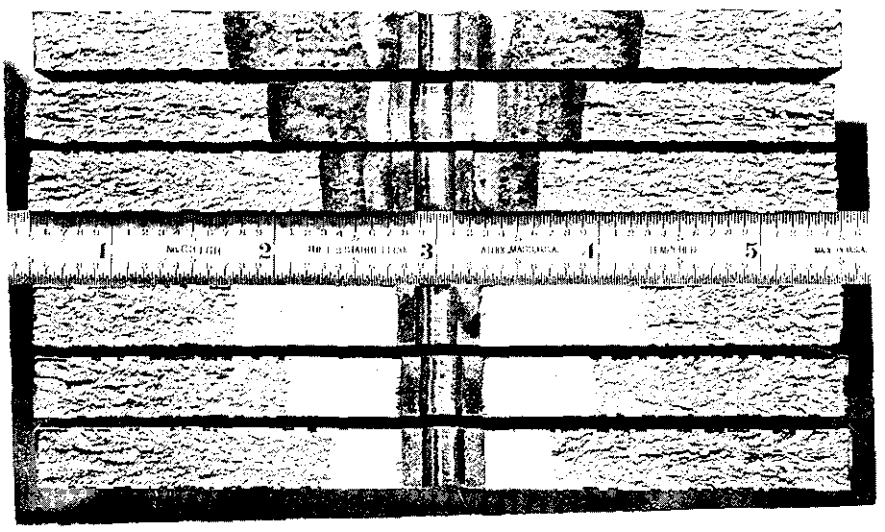

FROM BOTTOM x-14241-25, -27, -26 (AIR) -28, -29, -30
(SALT SPRAY)

FIGURE 55 - Fracture Faces 3/8" 300 M Through-Crack Specimens, F_{tu} 220 KSI

MICROSTRUCTURES

Representative microstructures are shown in Figures 56 through 60 for each products heat chemistry and strength level of 300 M steel used in the program.

The appearance of the tempered martensite is similar among all the products. Some banding is apparant in most of the material but this is not considered unusual for the 300 M composition.

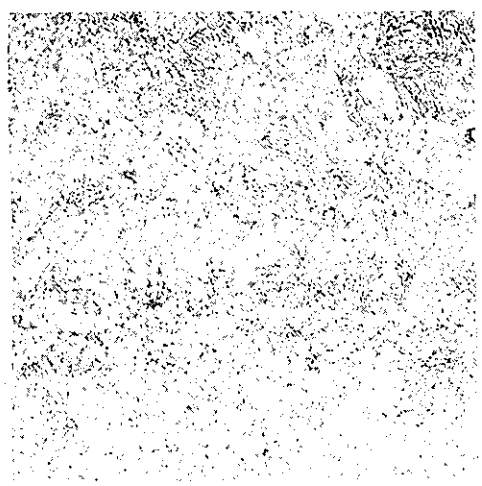

220 KSI

270 KSI

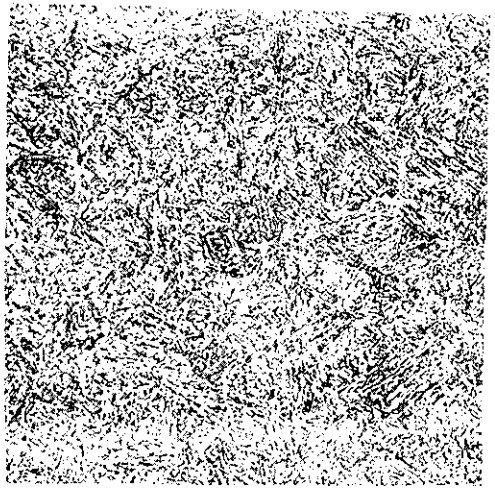

290 KSI

FIGURE 56 - Microstructures of 300 M 3/8" Plate Longitudinal Cross Section Ht. 3932021 (200X, - Etch)

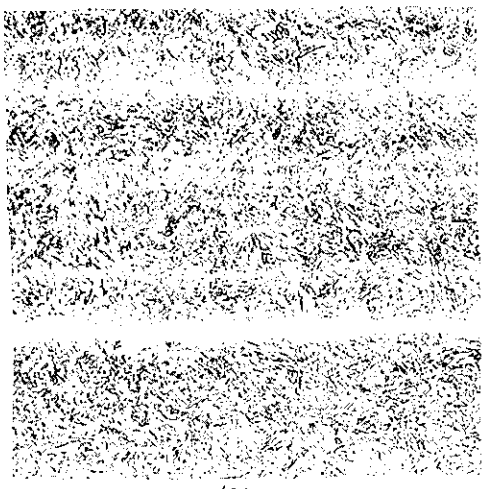

290 KSI - 1/8" Ht. 3932022

290 KSI - 3/8" Ht. 3961507

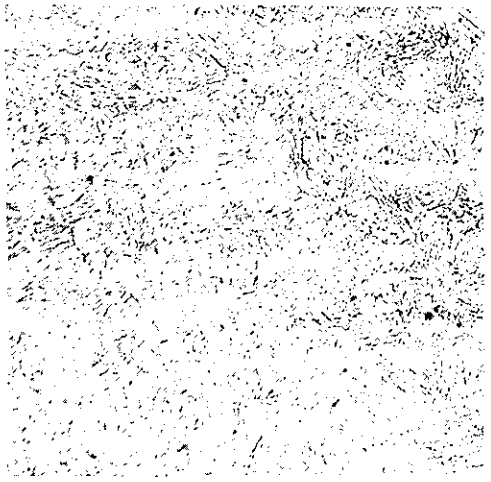

270 KSI - 3/8" Ht. 3961507

FIGURE 57 - Microstructures of 300M 1/8" and 3/8" Plate, Longitudinal Cross Section (200X – Etch)

270 KSI

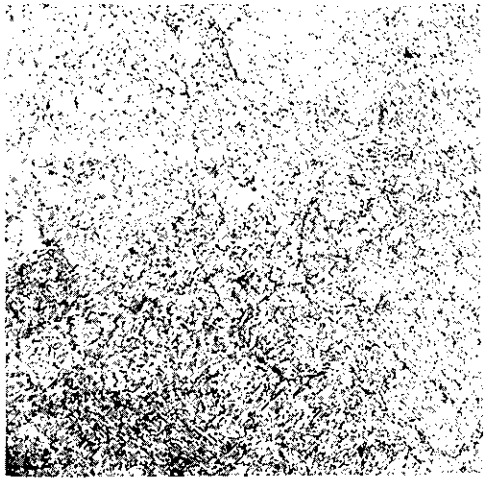

220 KSI

FIGURE 58 - Microstructures of 300 M 3/8" Plate, Longitudinal Cross Section, Ht. 3922452 (200X – Etch)

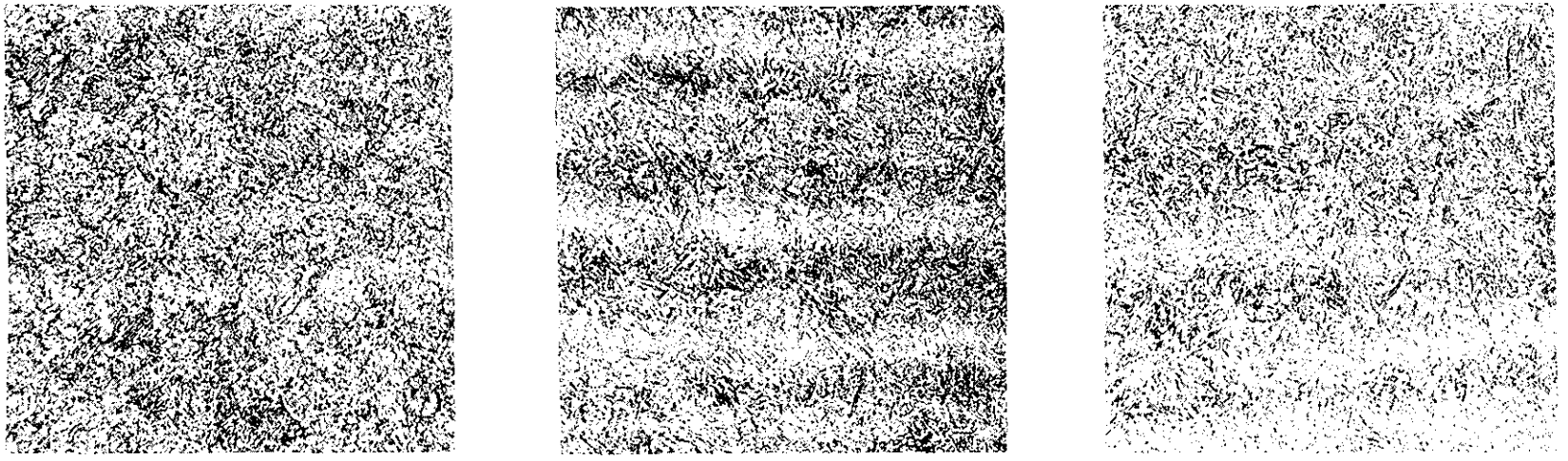

220 KSI 270 KSI 290 KSI

FIGURE 59 - Microstructures of 300M 3/4" Forgings, Longitudinal Cross Section Ht. 51782 (200X, - Etch)

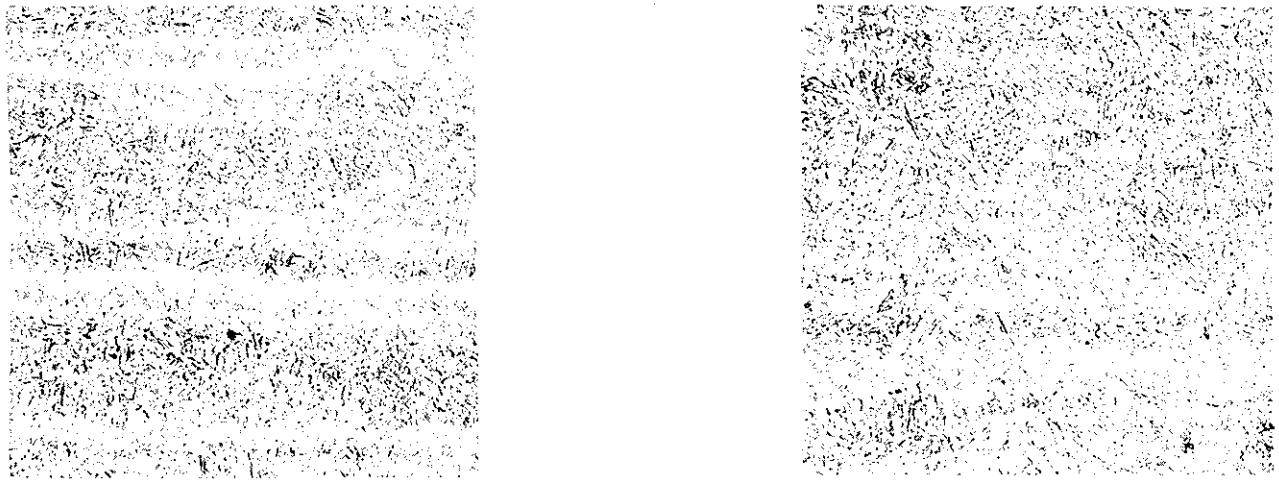

290 KSI - Ht. 3932021 290 KSI - Ht. 3922452

FIGURE 60 - Microstructures of 300 M 3/4" Plate, 200X, - E Longitudinal Cross Section

Section IV

DATA ANALYSIS

GENERAL

Structural failures under repeated external loads are generally thought of as consisting of three phases:

1) The nucleation of microcracks often early in the repeated load history. (In some instances the nucleation phase is greatly reduced or eliminated by pre-existing flaws.)

2) The growth of a dominant crack towards a size critical for catastrophic (unstable) propagation.

3) The catastrophic propagation of the critical size crack under some peak load condition.

Through proper selection of materials, processes, design stress level and details, the possibility of such a failure during the design life of the structure is made extremely remote. This design process is usually approached by: 1) making the occurrence of a macro size flaw during the design life unlikely (fatigue design), and 2) when possible, ensuring that if for unforeseen reasons, a macro crack did develop, that its propagation rate and size will ensure detection prior to reaching critical size (fail-safe design).

For very high strength materials, and for such applications as rocket motor casings where the cyclic stresses are high and critical flaw sizes are small, design practice has in some cases, been to assume the pre-existence of flaws of some size not detectable by inspection and/or proof testing and to base the estimate of service life on the growth of these flaws to critical size.

The question of whether to base primary estimates of design life on crack nucleation or crack growth depends to a large extent on the toughness and crack growth resistance of the material and on the expected loading and environmental history. For most aircraft where long life structures are designed using relatively tough materials, fatigue design (nucleation), supported by fail-safe design (growth and fracture) have proven effective.

Within the scope of the test program, the growth of dominant cracks towards critical size and the residual strengths of cracked coupons have been determined for 300 M steel. It is the purpose of the analysis section to analyze these data and with the aid of available crack growth rate and fracture theory, systemetize these data into forms easily understood and used by designers.

FRACTURE TOUGHNESS EQUATIONS

Fracture toughness of high strength materials can be expressed in terms of a plane strain fracture toughness parameter (K_{Ic}). Basic development and discussions of this parameter are given in References 1 through 4.

While most often derived from considerations of a critical energy release rate as the crack extends some finite increment, K_{Ic} can also be developed from static considerations of crack tip stress using the linear theory of elasticity (Ref. 3).

For test coupons containing part-through flaws, or through flaws, having the fracture substantially in the tensile mode (90° to the surface of the coupon), the plane strain K_{Ic} designation is normally used. For predominantly shear mode (45° to the surface of the coupon), the plane stress designation Kc is used. By these definitions, the test results showed primarily plane strain fracture (K_{Ic}).

Through-Cracks.-For through-cracks of sufficient width so that boundary influences are negligible; the plane strain fracture toughness can be determined from test data using the equation:

$$K_{Ic} = \sigma \sqrt{\pi a} \qquad (1)$$

For center through-cracked coupons of moderate width, a finite width correction is required. General practice is to use Westergard's stress function (Ref. 5 , 6) so that

$$K_{Ic} = \sigma \sqrt{\pi a} \cdot \sqrt{\frac{w}{\pi a} \cdot \tan \frac{\pi a}{w}}$$

$$K_{Ic} = \sigma \sqrt{w \tan \frac{\pi a}{w}} \qquad (2)$$

Recently an improved width correction has been proposed of the form (Ref. 7)

$$K_{Ic} = \sqrt{\pi a} \cdot \sqrt{\sec \frac{\pi a}{w}} \qquad (3)$$

For small flaws, it is customary to adjust the 1/2 crack length by the radius of the plastic zone to account for plasticity effects so that the "a" of equations (2) and (3) is increased to "a + r_p" where r_p is an estimate of the radius of plastic zone at the tip of the crack. For plane strain conditions (Ref. 2) r_p is given by:

$$r_p = \frac{K_{Ic}^2}{4\pi\sqrt{2}\,\sigma_y^2} \qquad (4)$$

or (Ref. 1):

$$r_p = \frac{K_{Ic}^2}{6\pi\sigma_y^2} \qquad (5)$$

Making "plastic zone" corrections to equations (2) and (3) gives:

$$K_{Ic} = \sigma\sqrt{w \tan\frac{a + r_p}{w}} \qquad (6)$$

$$K_{Ic} = \sigma\sqrt{\pi(a + r_p)} \cdot \sqrt{\sec\frac{\pi(a + r_p)}{w}} \qquad (7)$$

Equation (6) has been used in reducing most of the crack growth rate data in this report due to availability of computer data reduction programs. Equation (7) is recommended for future MIL HDBK-5 presentations of data. The differences between (6) and (7) are less than 3% for the bulk of the data tested. At the longest crack lengths, the difference is less than 5-1/2%.

Part-Through Cracks.-For part-through cracks, the plane strain fracture toughness for wide specimens can be computed using elastic solutions for stresses adjacent to a completely embedded elliptical crack (Ref. 2)

$$K_{Ic} = \frac{\sigma\sqrt{\pi a}}{\Phi}\left(\frac{a^2}{c^2}\cos^2\phi + \sin^2\phi\right)^{1/4} \qquad (8)$$

where

$$\Phi = \int_0^{\frac{\pi}{2}} \left[\sin^2\phi + \left(\frac{a}{c}\right)^2 \cos^2\phi \right]^{1/2} d\phi$$

In equation (8), the quantity Φ is an elliptical integral obtained during the integration of the incremental elastic strain energy around the periphery of the assumed elliptical crack. The term to the fourth power determines the variation of K_{Ic} around the ellipse. The stress intensity factor is maximum at the minor diameter of the ellipse ($\phi = 90°$) and minimum at the major axis ($\phi = 0°$). Thus at the end of the minor diameter

$$K_{Ic} = \frac{\sigma \sqrt{\pi a}}{\Phi} \qquad (9)$$

and at the major diameter;

$$K_{Ic} = \frac{\sigma \sqrt{\pi a}}{\Phi} \cdot \sqrt{\frac{a}{c}} \qquad (10)$$

For a surface crack, Irwin (Ref. 2) estimated that at the minor diameter of a semi-ellipse with a free surface along the major axis, the stress intensity factor would be about 1.1 x K_{Ic} given by equation (9). Adding the correction for plastic zone size (equation (4)) and the free surface correction allows the maximum stress intensity which occurs at the depth of the surface-crack to be expressed as

$$K_{Ic} = \frac{1.1\sigma\sqrt{\pi(a + r_p)}}{\Phi} \qquad (11)$$

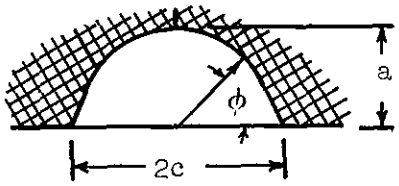

Substituting r_p as defined by equation (4) into (11) and combining terms:

$$K_{Ic} = \frac{1.1\sigma\sqrt{\pi a}}{\sqrt{\Phi - 0.212\sigma^2/\sigma_y^2}} \qquad (12)$$

by letting

$$Q = \left[\Phi^2 - 0.212\left(\frac{\sigma}{\sigma_y}\right)^2\right]$$

$$K_{Ic} = 1.1\sigma\sqrt{\frac{\pi a}{Q}} \qquad (13)$$

where Q is a function of a, c, r_p.

The front surface correction factor in equation (12) (i.e., 1.1) is considered valid for flaws of small a/c ratio where the boundaries of width and thickness are still remote. The effect of the front face diminishes as a/c approaches 1. The factor of 1.1 is kept constant in equation (12) on the premise that as a/c approaches 1, the crack will normally have grown well into the thickness of typical geometries so that the nearness of the back face would cause the correction to remain about 1.1. These free surface approximations of equation (13) are considered adequate for $a/c \leq 0.5t$.

As an alternative to (13), Paris and Sih (Ref. 3) recommend an equation that corrects for both surfaces:

$$K_{Ic} = \gamma_F \gamma_B \sigma \sqrt{\pi \frac{a}{Q}} \qquad (14)$$

where:

the front face correction $\gamma_F = 1 + 0.12 \left(1 - \frac{a}{c}\right)$

the back face correction $\gamma_B = \frac{2t}{\pi a} \tan \frac{\pi a}{2t}$

The front-face correction γ_F approaches 1.0 as a/c approaches 1, and the back face correction approaches 1.0 as a/t approaches zero. The accuracy of equation (14) is expected to be within 10 percent for $a/t < .75$ (provided $a/c \geq 0.2$). For greater flaw depths, however, the term γ_B approaches infinity, and equation (14) is not recommended. Equations (13) and (14) will be considered for determining plane strain fracture toughness of part-through flaws in this report.

The reasons for elaboration on the above derivations is to emphasize that the mathematical model is based on the elastic solution for a fully embedded elliptical crack and that the corrections applied are estimates of very complex effects of a free surface and plasticity. K_{Ic} as computed by either equations (6), (13) or (14) should be approximately the same for a given material. If they are not, there is reason to suspect that the differences are due to an error in the plasticity corrections or the free surface corrections.

CRACK PROPAGATION EQUATIONS

The propagation of fatigue cracks under cyclic loading has been shown to be amenable to stress intensity analysis (Ref. 8 through 13). This is to say that the same relationships used for fracture toughness parameters can form a basis for estimating crack growth under cyclic loading. There are, however, some differences between static loading to failure (fracture toughness) and cyclic loading (fatigue crack growth). These are:

1. Under cyclic conditions each cycle consists of a stress range ($\sigma_{max} - \sigma_{min}$) and a peak stress σ_{max}. The relationship between stress range and maximum stress varies with stress ratio, $\sigma_{min}/\sigma_{max} = R$. Generally, two stress quantities are needed for crack growth whereas one is sufficient for fracture under monotonic loading.

2. Under cyclic conditions, plasticity aspects estimated from static stress properties are generally not applicable. For instance, cracks will rotate from the tensile to the shear mode of cracking (presumably plane strain to plane stress) at stress intensities considerably below the like transition under monotonic loadings.

3. Environmental factors such as corrosive effects can play a significant part in cyclic crack propagation. Under normal loading rates for K_{Ic} determinations these factors are small, although they are known to be important for sustained static loadings (delayed failures).

The above differences between fracture and crack propagation have resulted in several equations being available for comparison to the program data. The state of art for crack growth analysis is not as far advanced as that of fracture analysis for high strength materials so that some judicious selection among available equations is necessary prior to proposing methods of data presentation suitable for design use.

The equation of Paris has perhaps been used more widely than any other to date:

$$\frac{d\ell}{dN} = \frac{(\Delta K_i)^n}{M} \tag{15}$$

The K_i is used here to denote subcritical values of crack tip stress intensity. These values are computed by replacing K_{Ic} by K_i in equations 13 and 14. Plasticity corrections are usually not made.

Equation (15) fits data from a single stress ratio ($R = \sigma_{min}/\sigma_{max}$) reasonably well and when the restriction of a log-log straight line data fit is removed, can be used for the majority of data, but will still show banding in terms of stress ratio.

$$\frac{d\ell}{dN} = f(\Delta K_i) \tag{16}$$

To correct for the observed banding, a modified equation was proposed (Ref. 12) in which the cracking rate is assumed to approach infinity as $K_{i_{max}}$ approaches the stress intensity level for fracture under cyclic loading K_{cr}.

$$\frac{d\ell}{dN} = \frac{C(\Delta K_i)^n}{(1 - R)K_{c_r} - \Delta K_i} \tag{17}$$

Equation (17) like equation (15) is based on the assumption that a straight line log-log relationship exists. Equation (17), however, tends to eliminate the banding in terms of stress ratio and shows considerable promise as a working equation for crack growth rate prediction. For purposes of comparing methods, equation (17) can be rewritten

$$\frac{d\ell}{dN} = f\left\{\frac{\Delta K_i}{\left[(1 - R)K_{cr} - K_i\right]^{1/n}}\right\} \tag{18}$$

In an extensive study of stress ratio influence on fatigue crack propagation in aluminum alloys (Ref. 11) another modification of equation (15) was shown to approximately fit the test data.

$$\frac{d\ell}{dN} = CK_{i_{max}}^2 \Delta K_i \tag{19}$$

Equation (19) indicates that the general form of crack growth equation may be:

$$\frac{d\ell}{dN} = C(K_{i_{max}})^a (\Delta K_i)^b$$

which may be rewritten

$$\frac{d\ell}{dN} = C(K_{i_{max}}^m \Delta K_i^{1-m})^n \tag{20}$$

or more generally,

$$\frac{d\ell}{dN} = f(K_{i_{max}}^m \Delta K_i^{1-m}) \tag{21}$$

Equation (21) has been shown to be useful for computing the influence of stress ratio for both steel and aluminum alloys (Ref. 14).

Equations (15), (18), and (21) have been selected for evaluation as to their applicability to test data generated during this program.

DATA INTERPRETATION METHODS

The crack growth data obtained during the test program consists for the most part of sequential observations of crack length and cumulative cycles. The crack front, however, moves forward in a series of jumps so that the growth between two consecutive observations may not represent the average growth rate. The larger the increments of length at which observations are made, however, the more "average" the computed rate, $\Delta \ell / \Delta N$, will be.

When plotting curves of length vs cycles small inconsistencies in slope ($d\ell/dN$) are usually smoothed out so that the irregular growth rate is not apparent. When plotting the derivatives $d\ell/dN$ of the curve, as approximated by $\Delta \ell / \Delta N$ computed directly from differences between observed data, the irregular growth rate appears as scatter about some mean rate for the specimen. This is illustrated on Figure 61 which shows how typical scatter in rate data for an individual specimens varies about the mean rate. When data for several similar specimens are plotted together, the average growth rate for individual specimens tends to correspond to the average for the group. The width of the scatter band does not represent the scatter of mean rates; the latter is relatively small.

Since most crack growth prediction equations and theories involve rates, it is expedient to convert the length vs cycles data to rate data for comparisons with theory. To accomplish this, incremental $\Delta \ell / \Delta N$ values were computed directly from the basic data. For general data presentation Figures 62 through 83, crack length increments were taken directly as those recorded on laboratory data sheets. These increments were 0.02 inch for surface crack lengths below 0.6 inch and 0.04 inch above 0.6 inch. For comparisons between theory and data, cracking rates were averaged over 3 increments (0.06 inch and 0.12 inch) etc. so as to obtain more average behavior for comparative purposes and to allow more specimens to be shown on a single plot. Log-linear plots have been selected as this type of plot tends to display irregularities in data better than a log-log plot.

The quantity of the ordinate for part-through cracks was selected as $d(2c)/dN$ rather than da/dN or $d(a/Q)/dN$ for two reasons. First, from a practical standpoint it is the directly observable quantity either from a test standpoint or from a flaw inspection standpoint. Secondly, as far as could be determined from inspection of the cracked surface after specimen failure, the $a/2c$ ratio was close enough to being constant so as to make it practical to assume a constant relationship between 2c, a, a/Q (Figure 84). From Figure 84, a value of $a/2c = 0.41$ has been selected for purposes of comparing data.

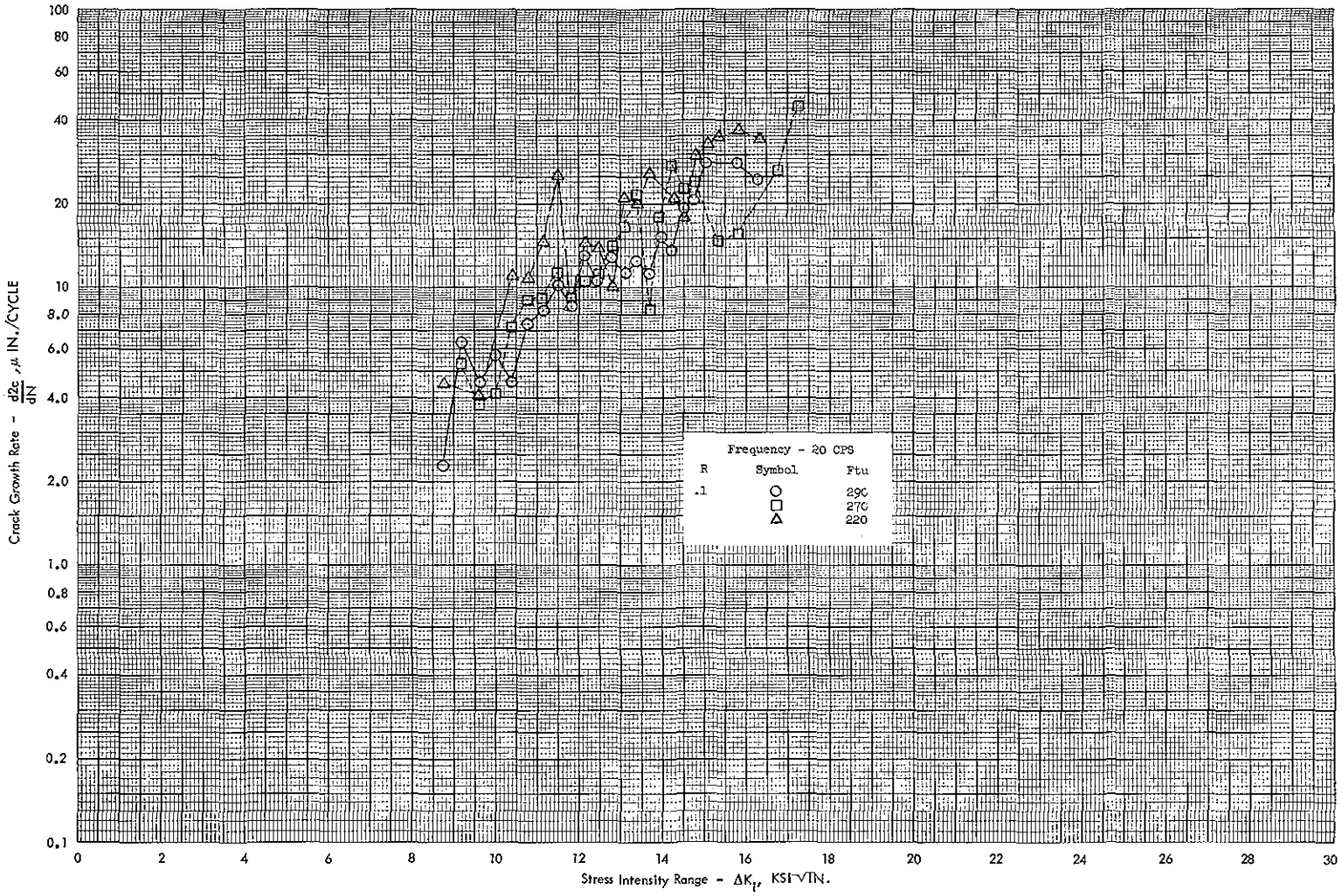

Figure 61 Variation of Cyclic Cracking Rate About Some Mean Rate for an Individual 300 M Surface-Crack Specimen

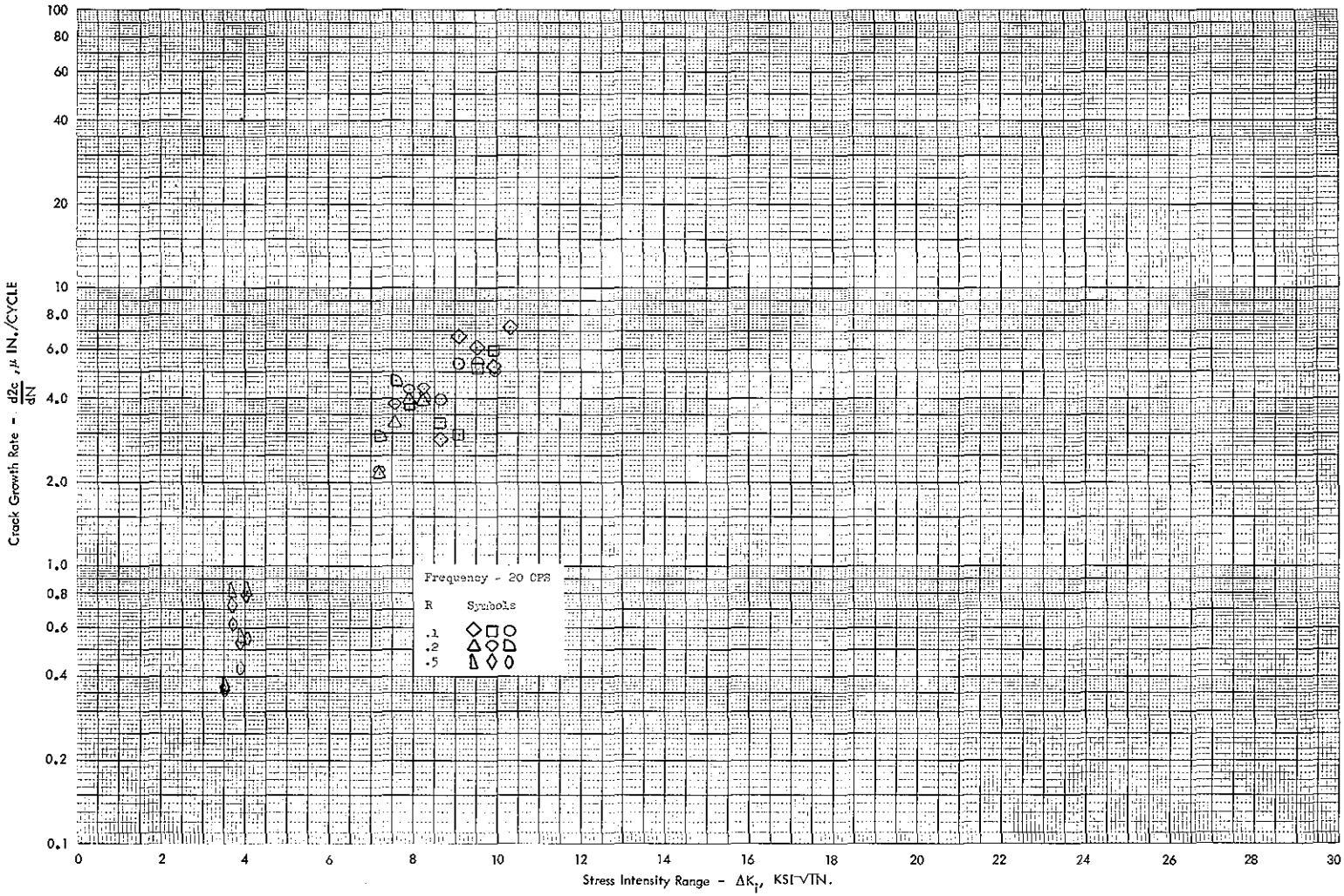

Figure 62 Cyclic Cracking Rate vs Stress Intensity Range for 1/8 Inch Thick 300 M Steel (F_{tu} 290 KSI) Surface-Crack Specimens In Moist Air Environment

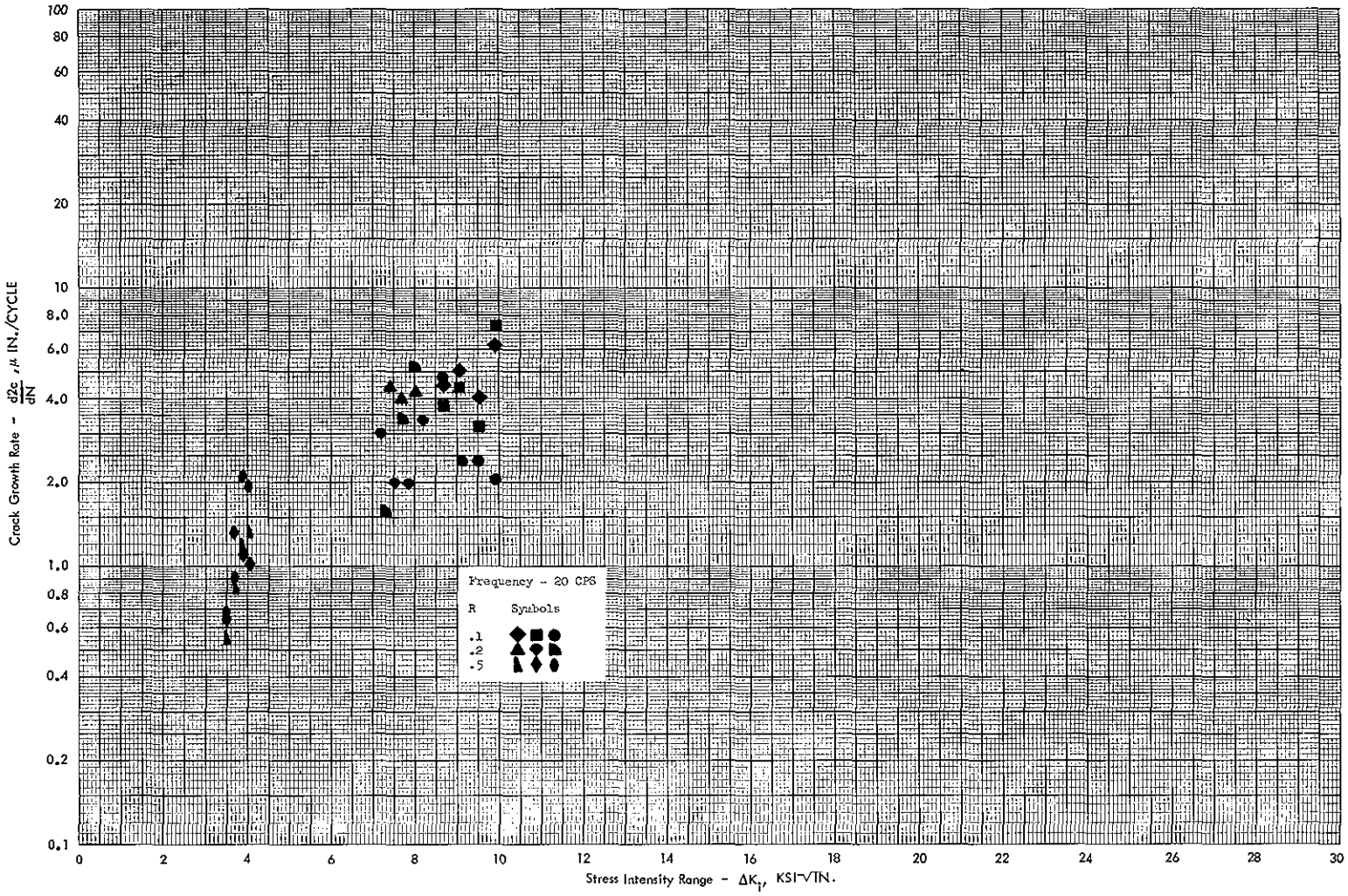

Figure 63 Cyclic Cracking Rate vs Stress Intensity Range for 1/8 Inch Thick 300 M Steel (F_{tu} 290 KSI) Surface-Crack Specimens in Salt Water Spray Environment

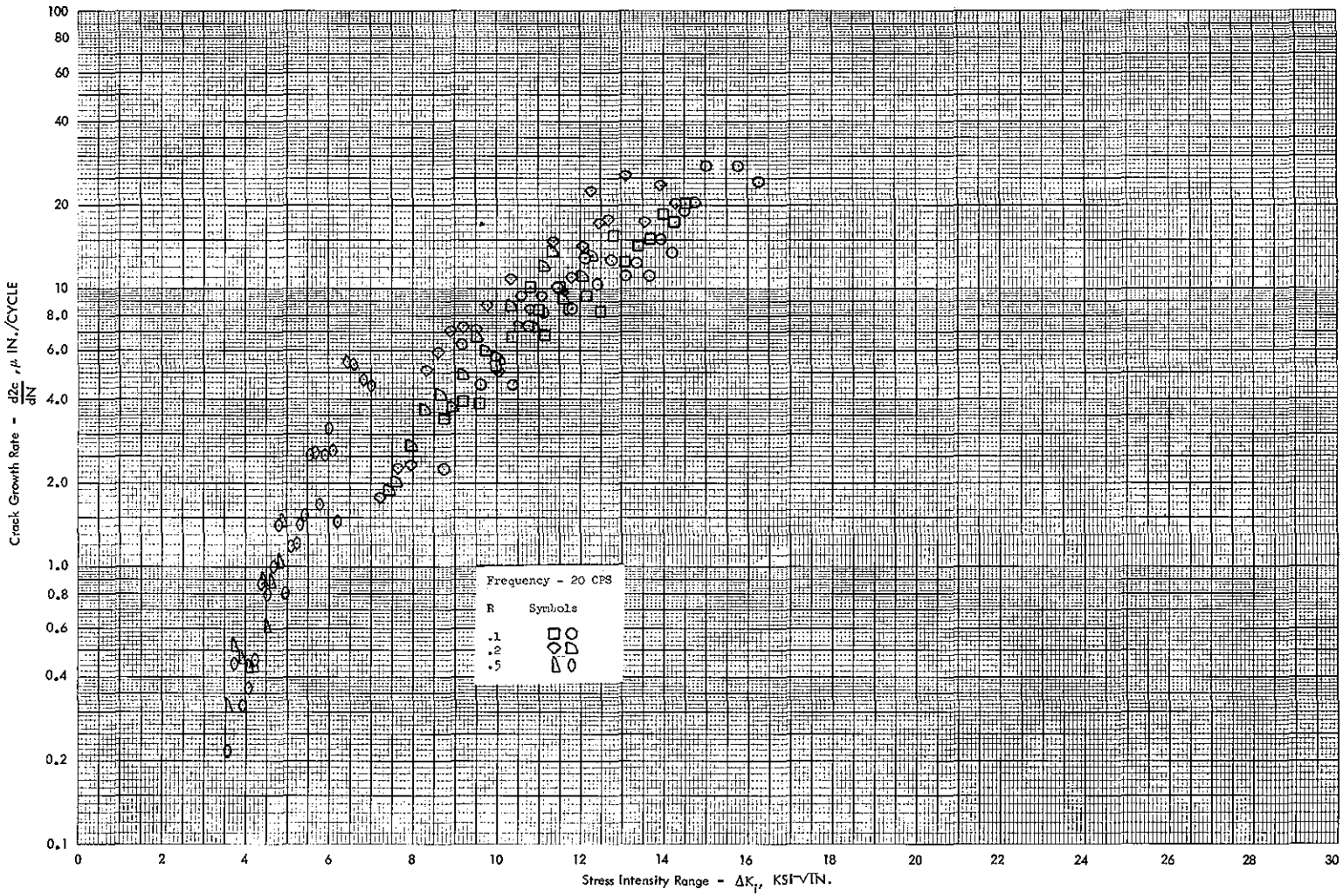

Figure 64 Cyclic Cracking Rate vs Stress Intensity Range for 3/8 Inch Thick 300 M Steel (F_{tu} 290 KSI) Surface-Crack Specimens in Moist Air Environment

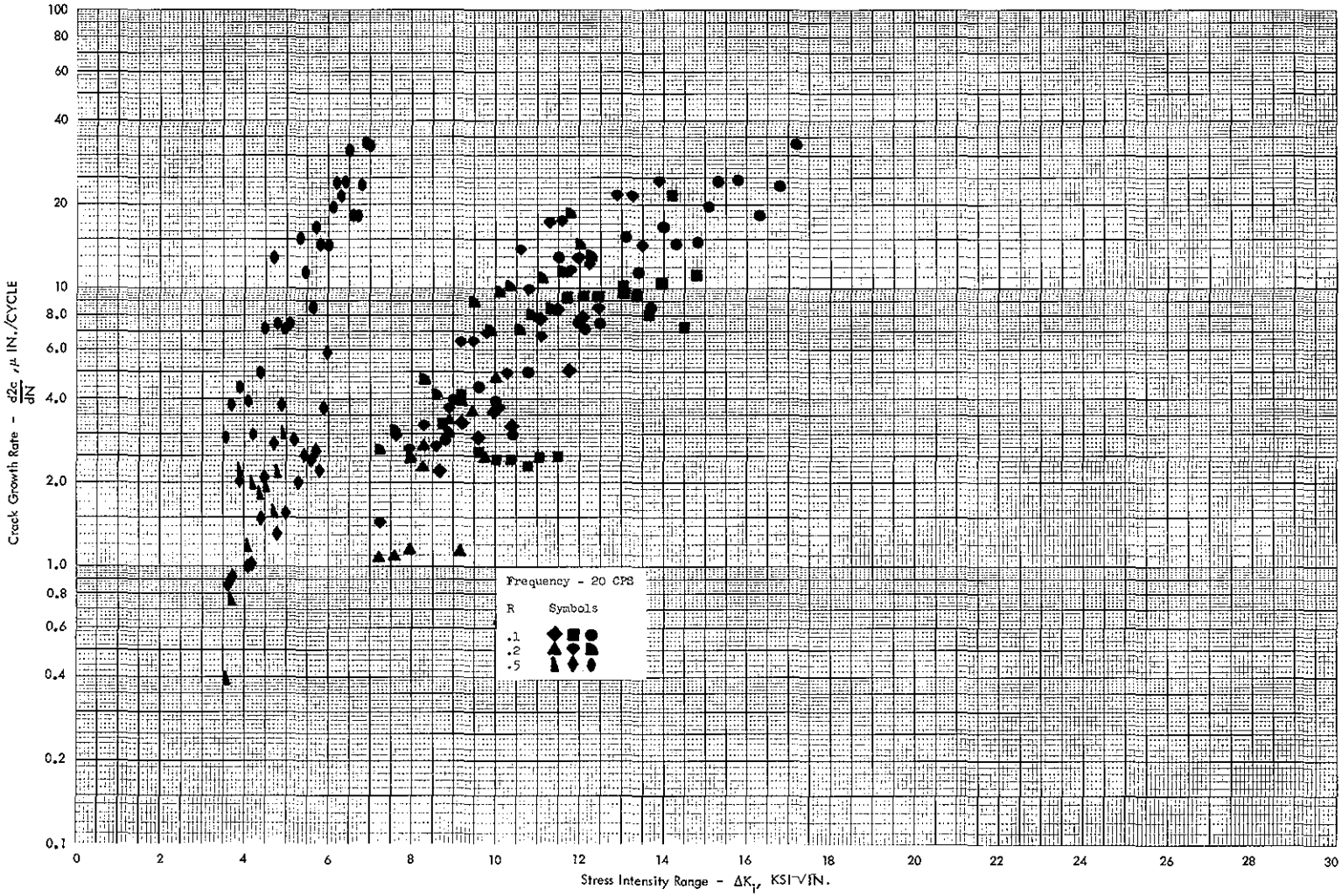

Figure 65 Cyclic Cracking Rate vs Stress Intensity Range for 3/8 Inch Thick 300 M Steel (F_{tu} 290 KSI) Surface-Crack Specimens in Salt Water Spray Environment

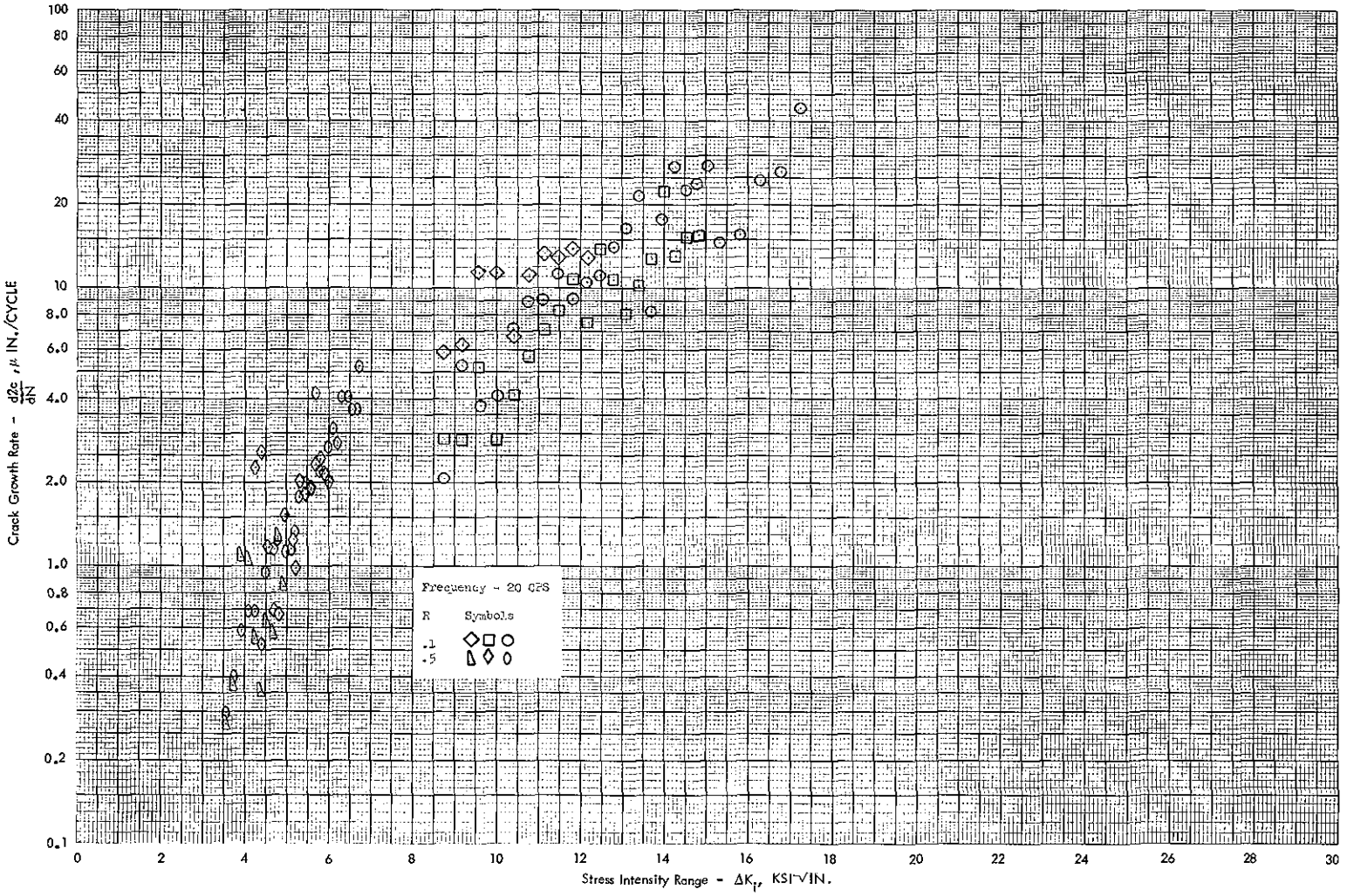

Figure 66 Cyclic Cracking Rate vs Stress Intensity Range for 3/8 Inch Thick 300 M Steel (F_{tu} 270 KSI) Surface-Crack Specimens in Moist Air Environment

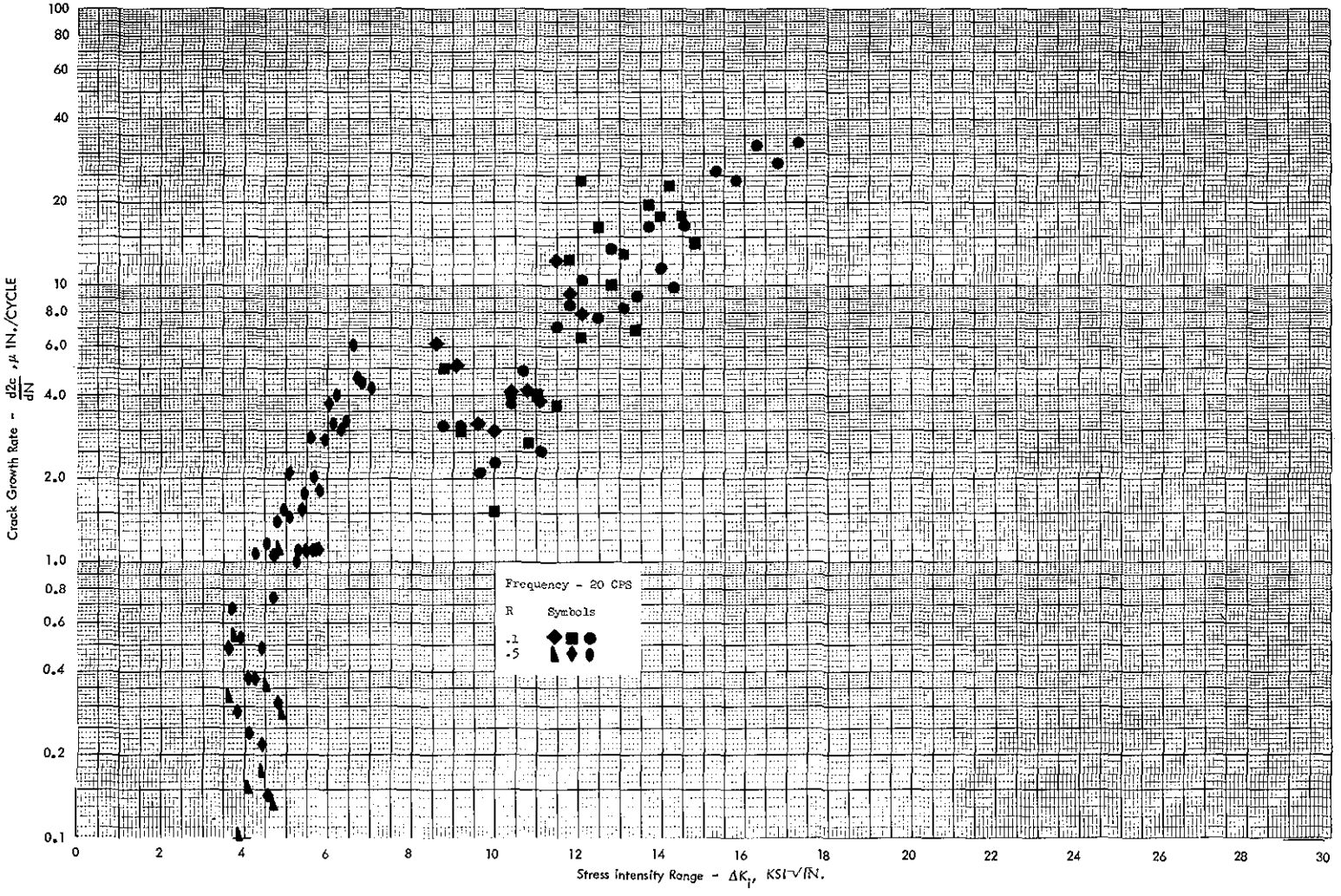

Figure 67 Cyclic Cracking Rate vs Stress Intensity Range for 3/8 Inch Thick 300 M Steel (F_{tu} 270 KSI) Surface-Crack Specimens in Salt Water Spray Environment

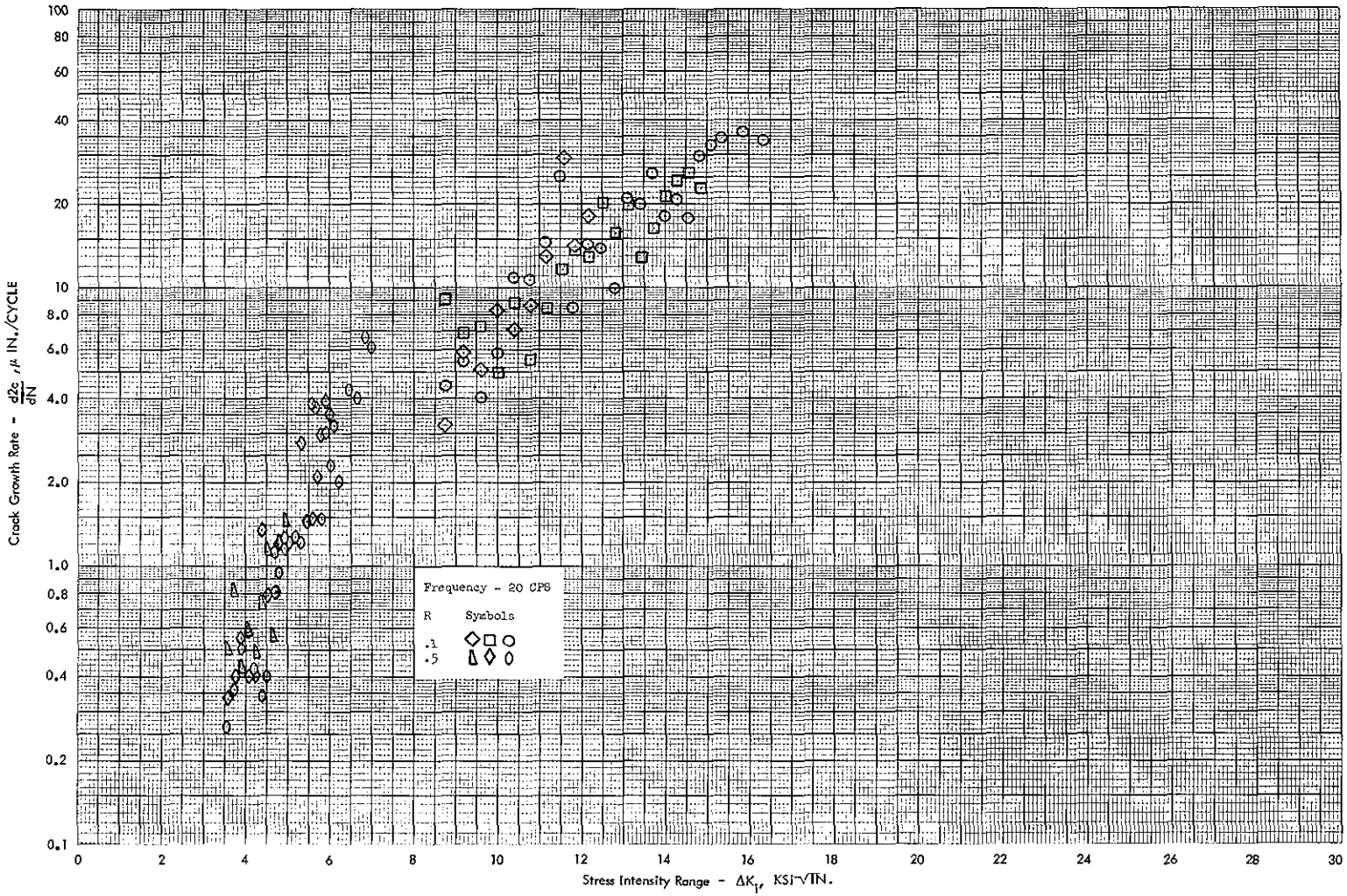

Figure 68 Cyclic Cracking Rate vs Stress Intensity Range for 3/8 Inch Thick 300 M Steel (F_{tu} 220 KSI) Surface-Crack Specimens in Moist Air Environment

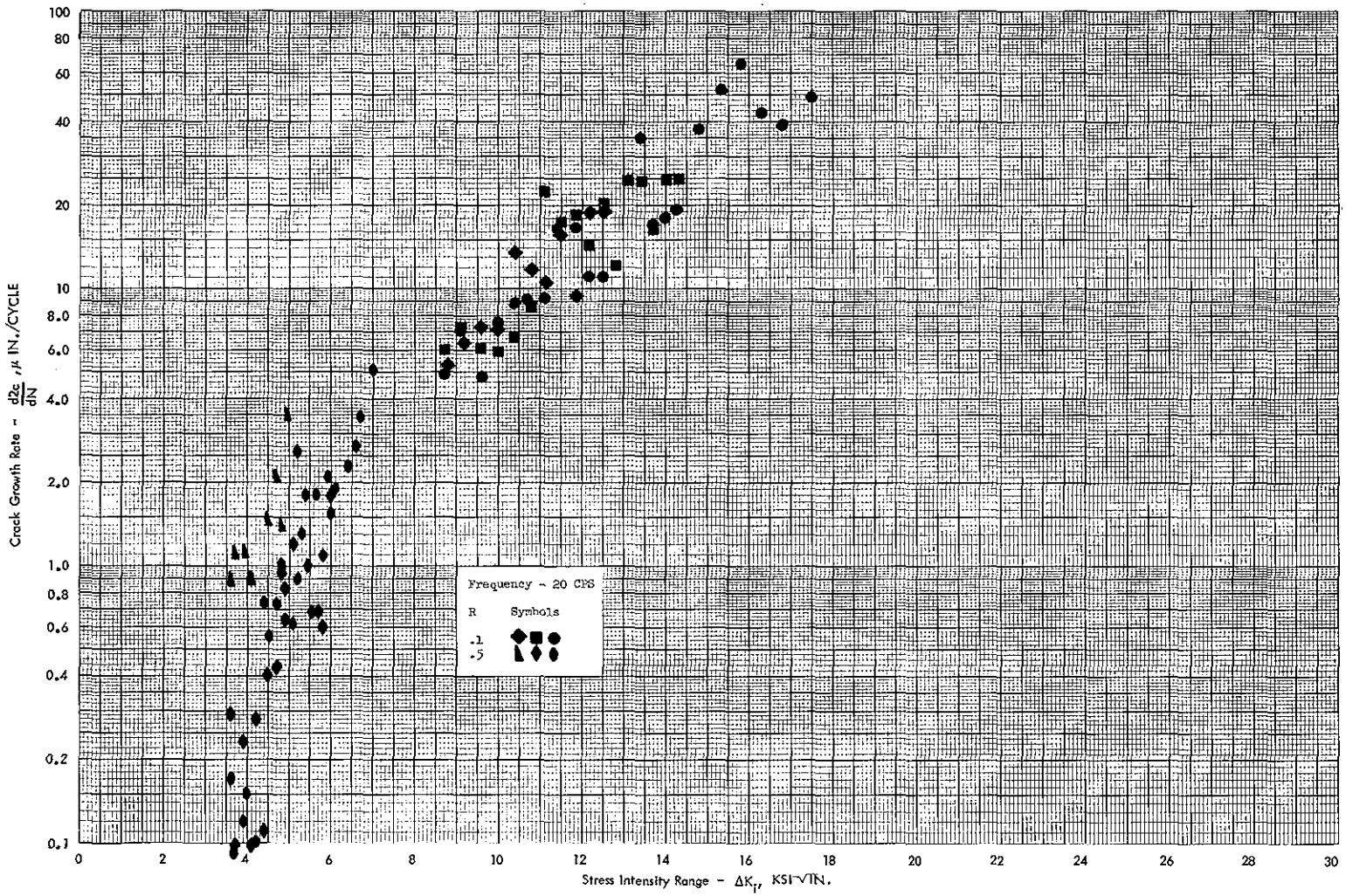

Figure 69 Cyclic Cracking Rate vs Stress Intensity Range for 3/8 Inch Thick 300 M Steel (F_{tu} 220 KSI) Surface-Crack Specimens in Salt Water Spray Environment

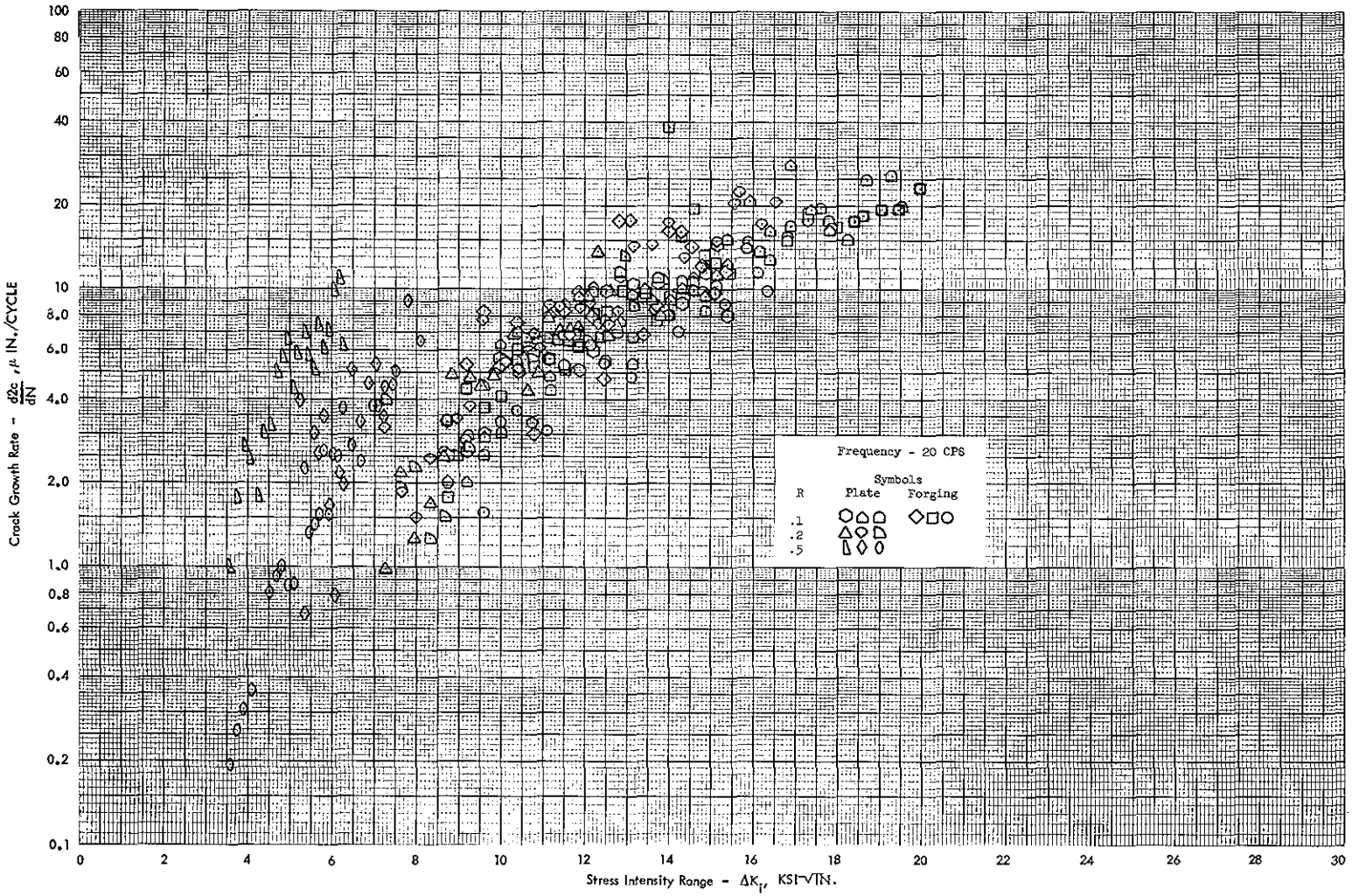

Figure 70 Cyclic Cracking Rate vs Stress Intensity Range For 3/4" Thick 300 M Steel Plate and Forging (F_{tu} 290 KSI) Surface-Crack Specimens in Moist Air Environment.

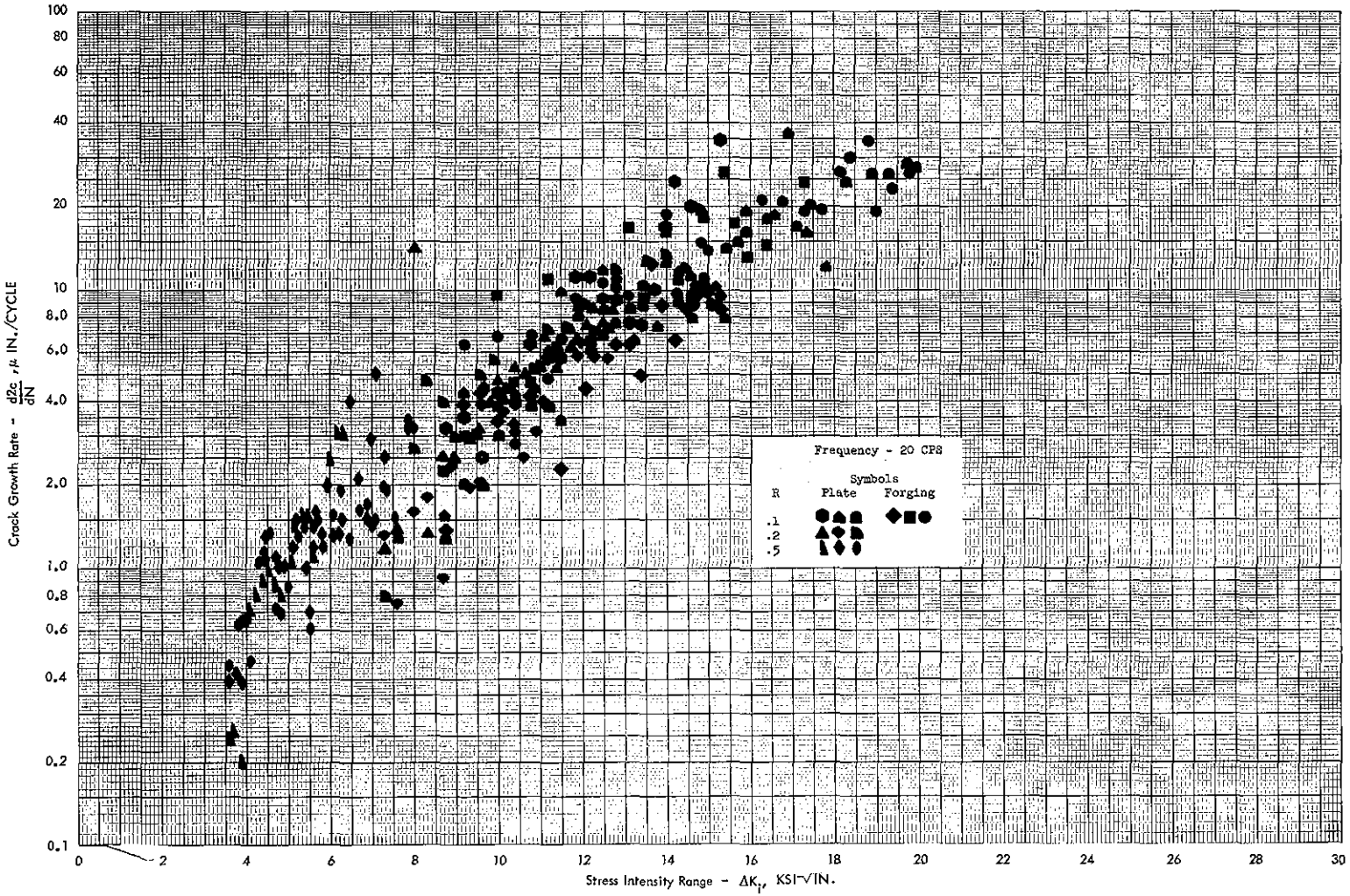

Figure 71 Cyclic Cracking Rate vs Stress Intensity Range For 3/4" Thick 300 M Steel Plate and Forging (F_{tu} 290 KSI) Surface-Crack Specimens in Salt Water Spray Environment.

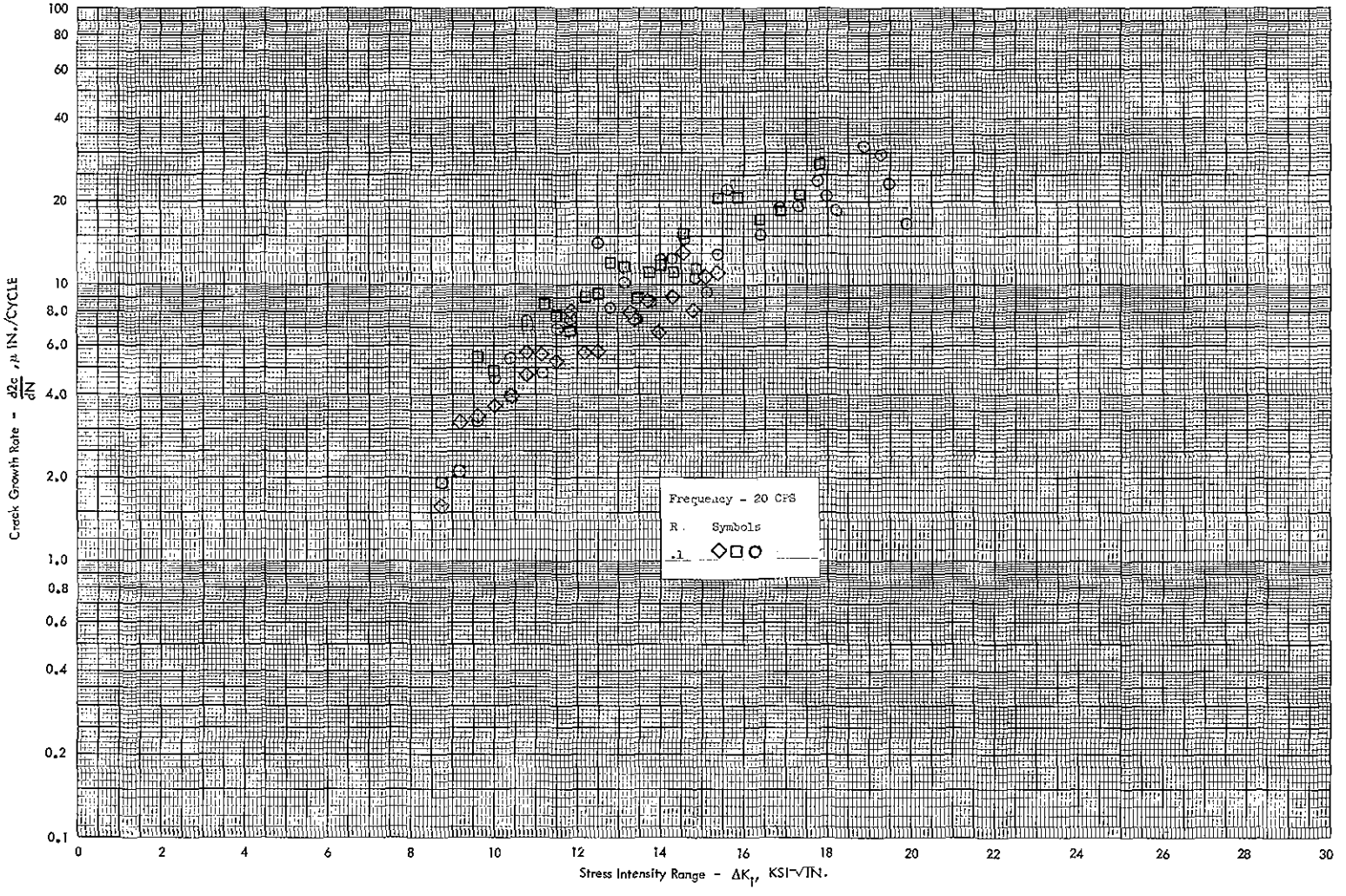

Figure 72 Cyclic Cracking Rate vs Stress Intensity Range For 3/4" Thick 300 M Steel Forging (F_{tu} 270 KSI) Surface-Crack Specimens in Moist Air Environment.

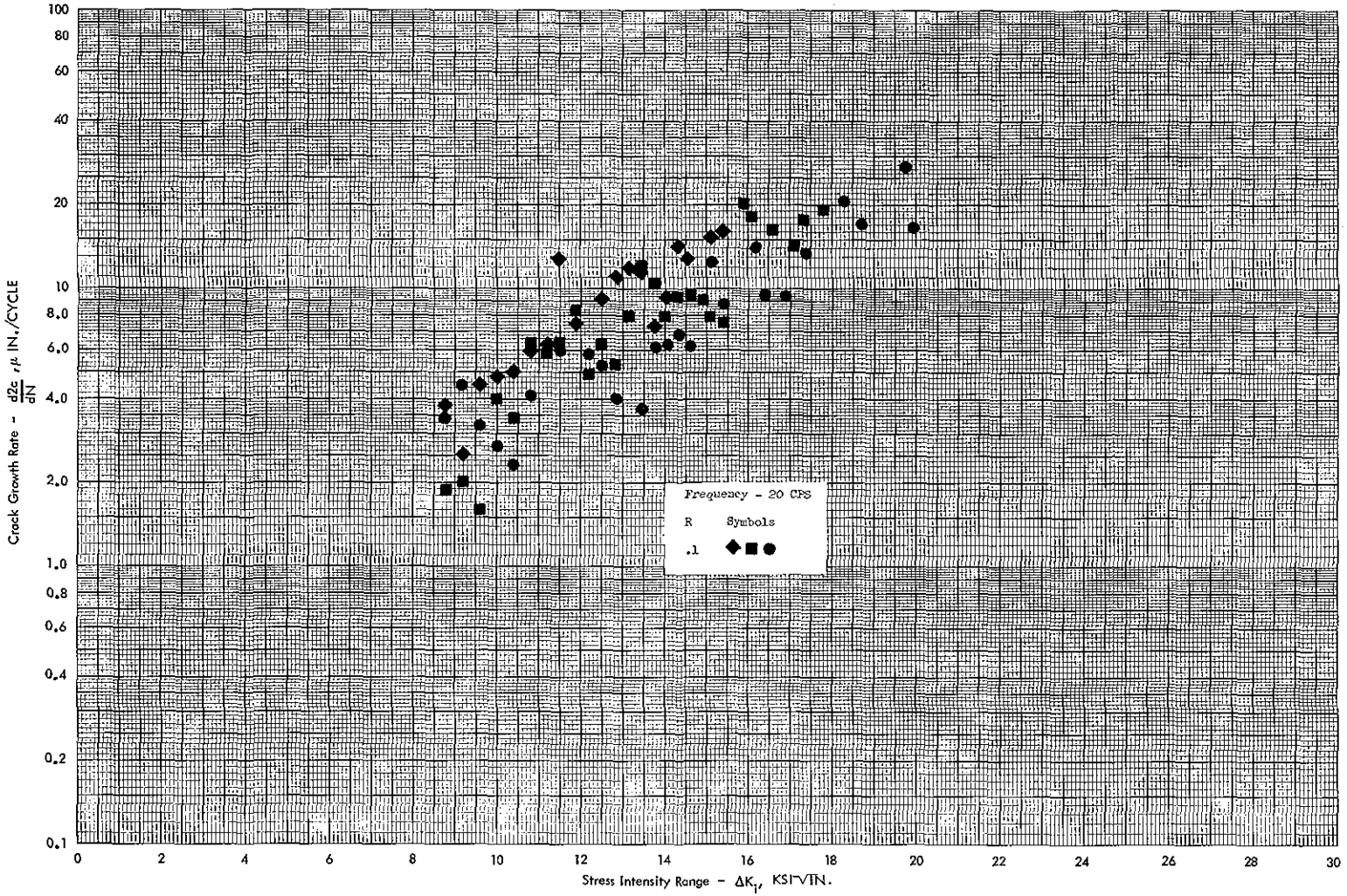

Figure 73 Cyclic Cracking Rate vs Stress Intensity Range For 3/4" Thick 300 M Steel Forging (F_{tu} 270 KSI) Surface-Crack Specimens in Salt Water Spray Environment.

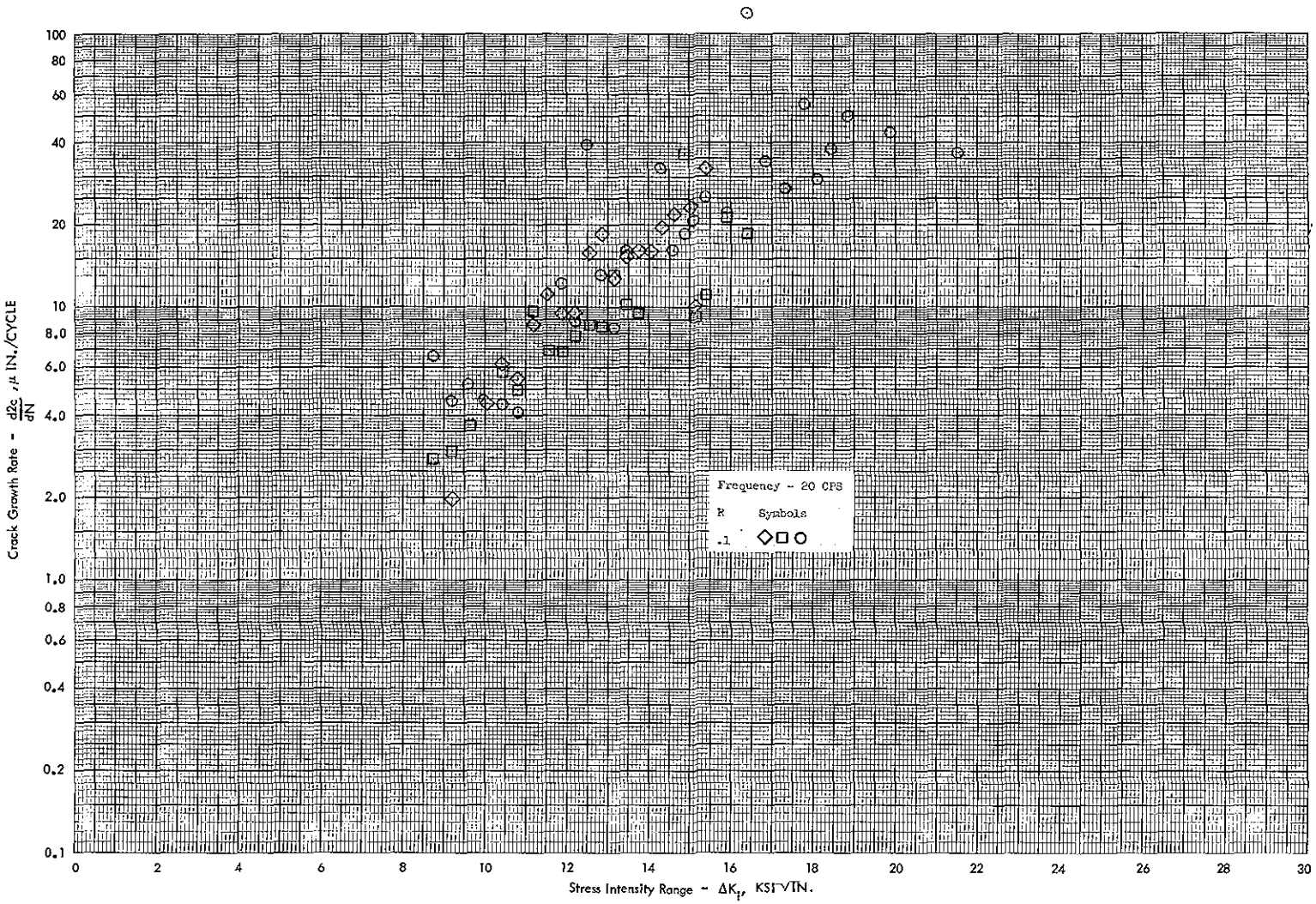

Figure 74 Cyclic Cracking Rate vs Stress Intensity Range For 3/4" Thick 300 M Steel Forging (F_{tu} 220 KSI) Surface-Crack Specimens in Moist Air Environment.

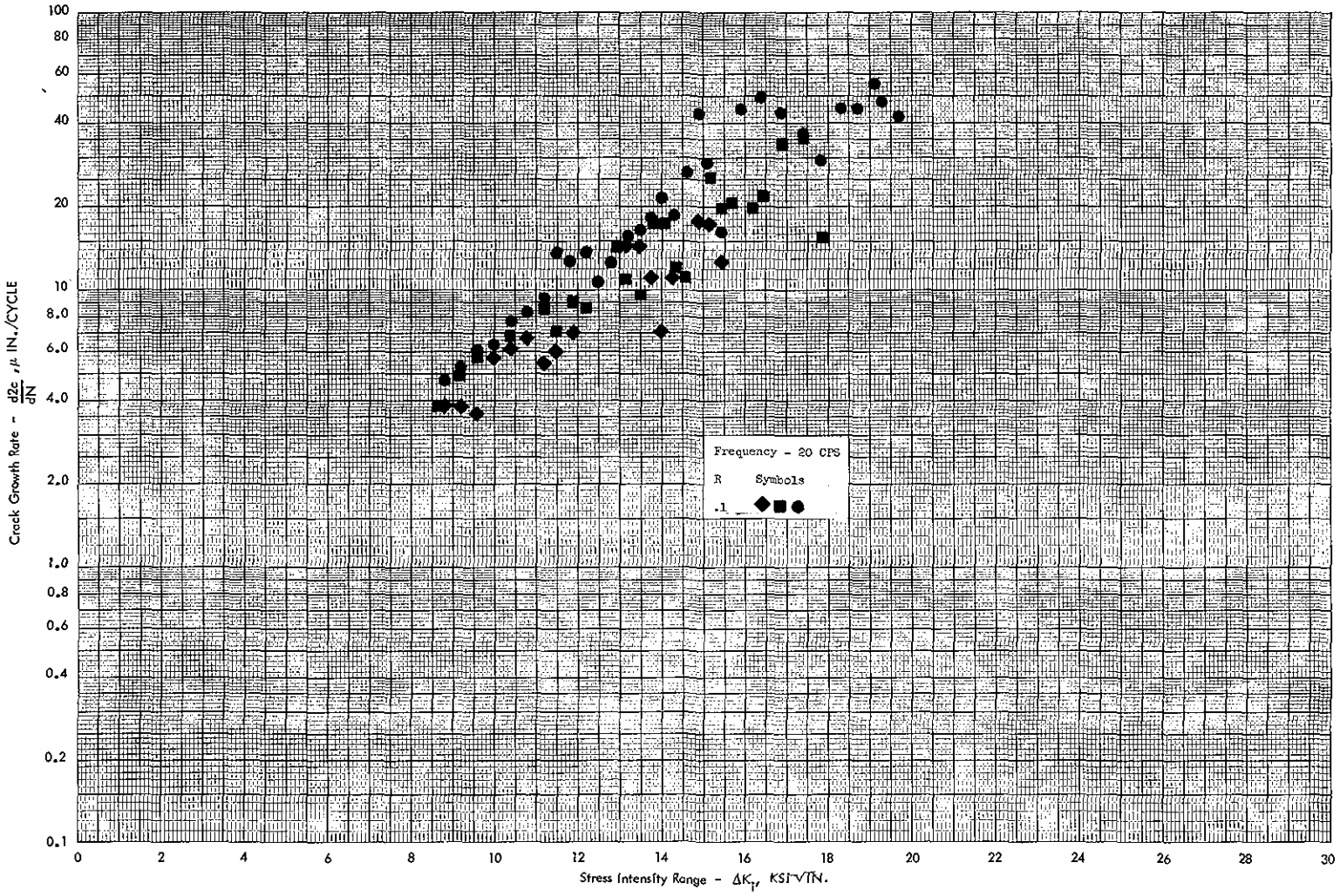

Figure 75 Cyclic Cracking Rate vs Stress Intensity Range For 3/4" Thick 300 M Steel Forging (F_{tu} 220 KSI) Surface-Crack Specimens in Salt Water Spray Environment.

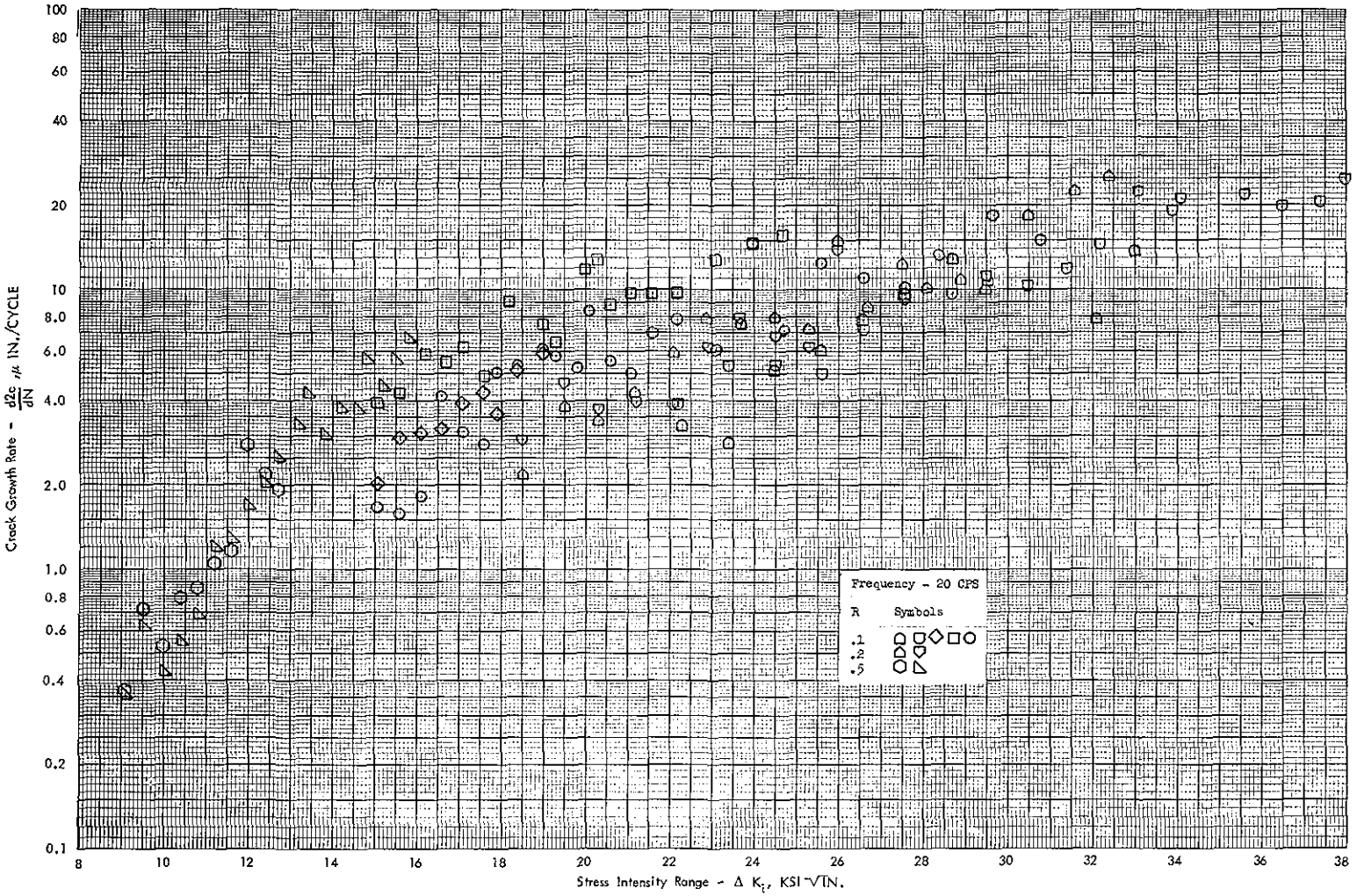

Figure 76 Cyclic Cracking Rate vs Stress Intensity Range For 1/8" Thick 300 M Steel (F_{tu} 290 KSI) Through-Crack Specimens in Moist Air Environment.

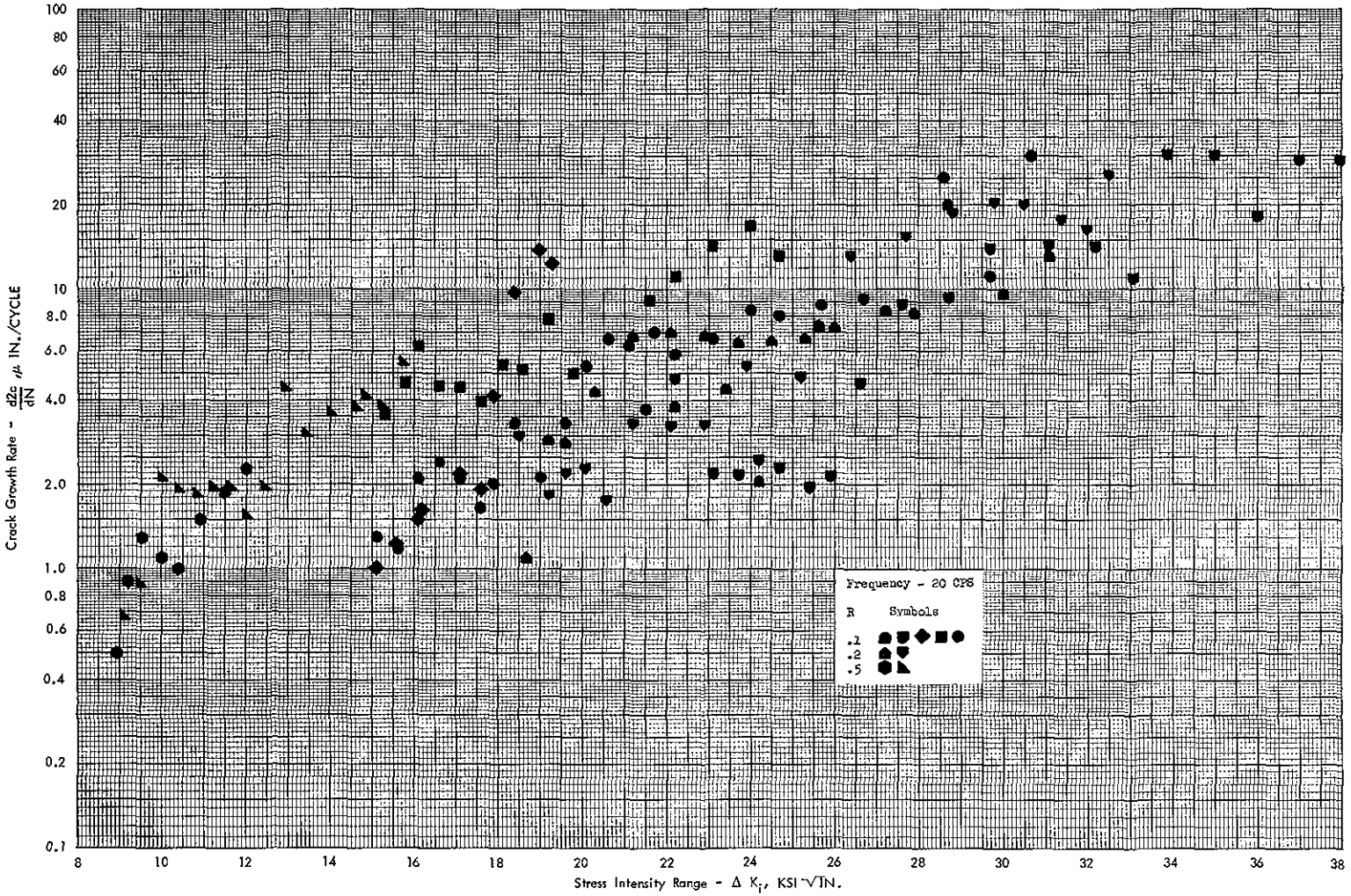

Figure 77 Cyclic Cracking Rate vs Stress Intensity Range For 1/8" Thick 300 M Steel (F_{tu} 290 KSI) Through-Crack Specimens in Salt Water Spray Environment.

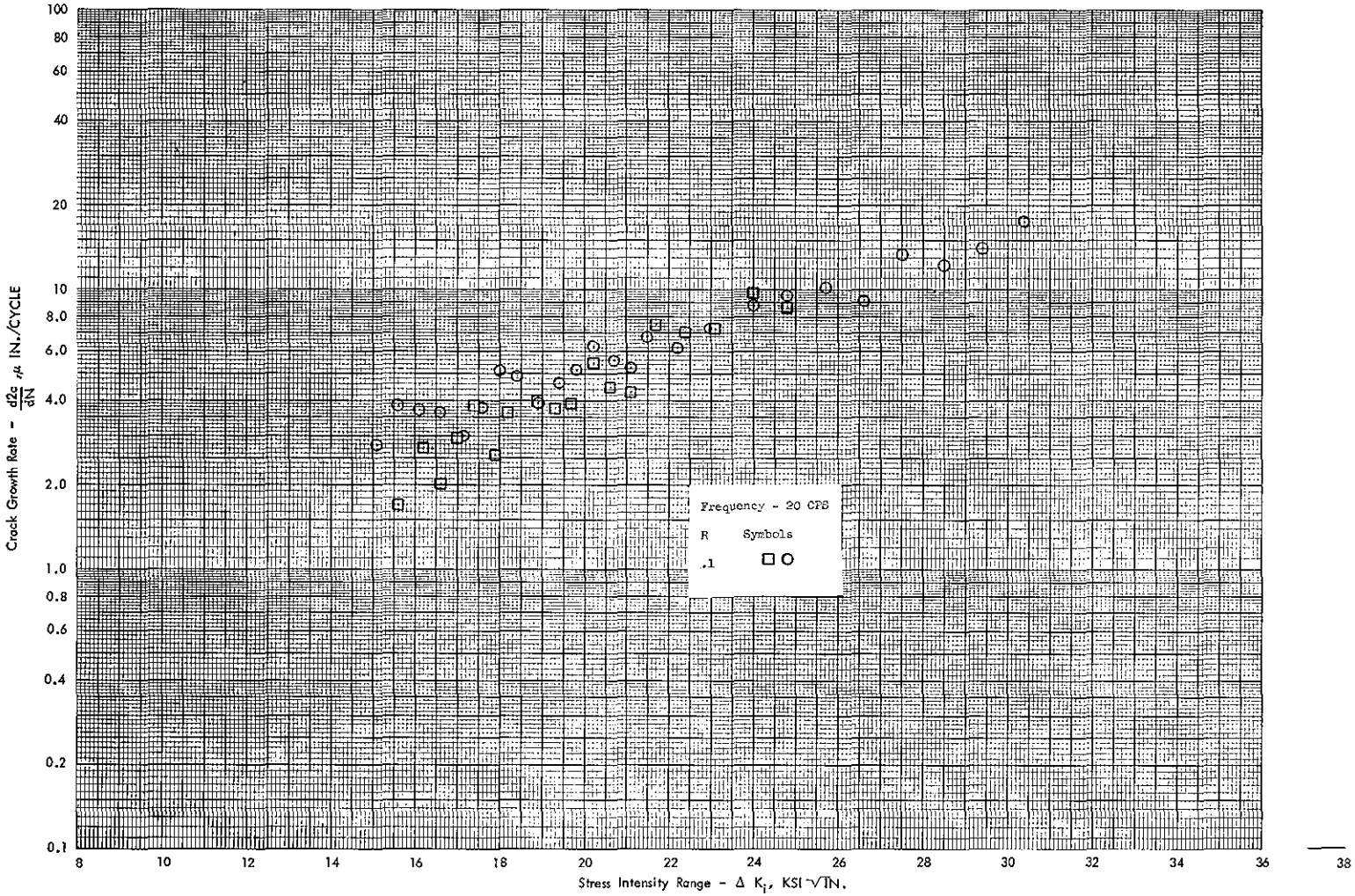

Figure 78 Cyclic Cracking Rate vs Stress Intensity Range For 3/8" Thick 300 M Steel (F_{tu} 290 KSI) Through-Crack Specimens in Moist Air Environment.

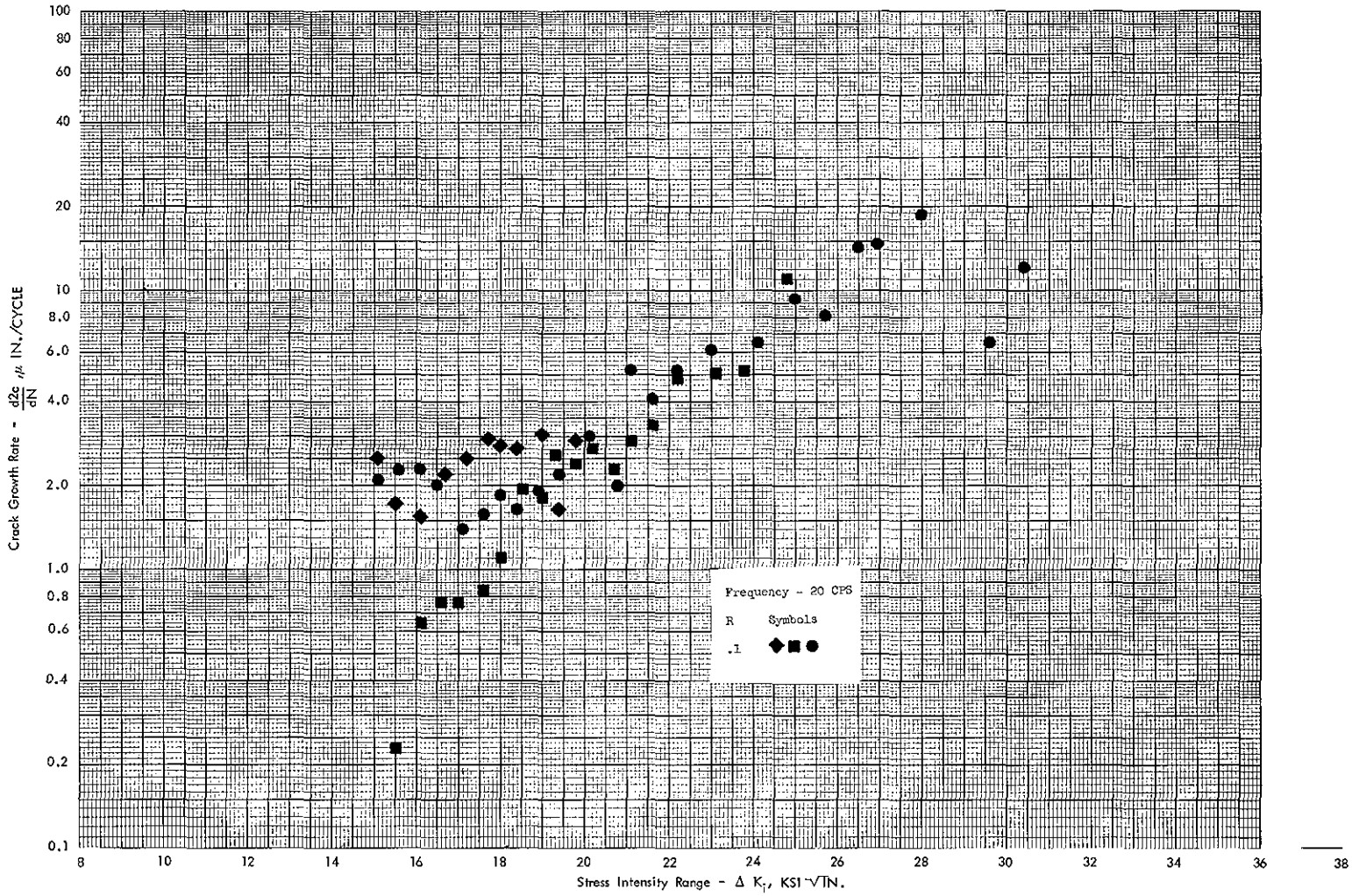

Figure 79 Cyclic Cracking Rate vs Stress Intensity Range For 3/8" Thick 300 M Steel (F_{tu} 290 KSI) Through-Crack Specimens in Salt Water Spray Environment.

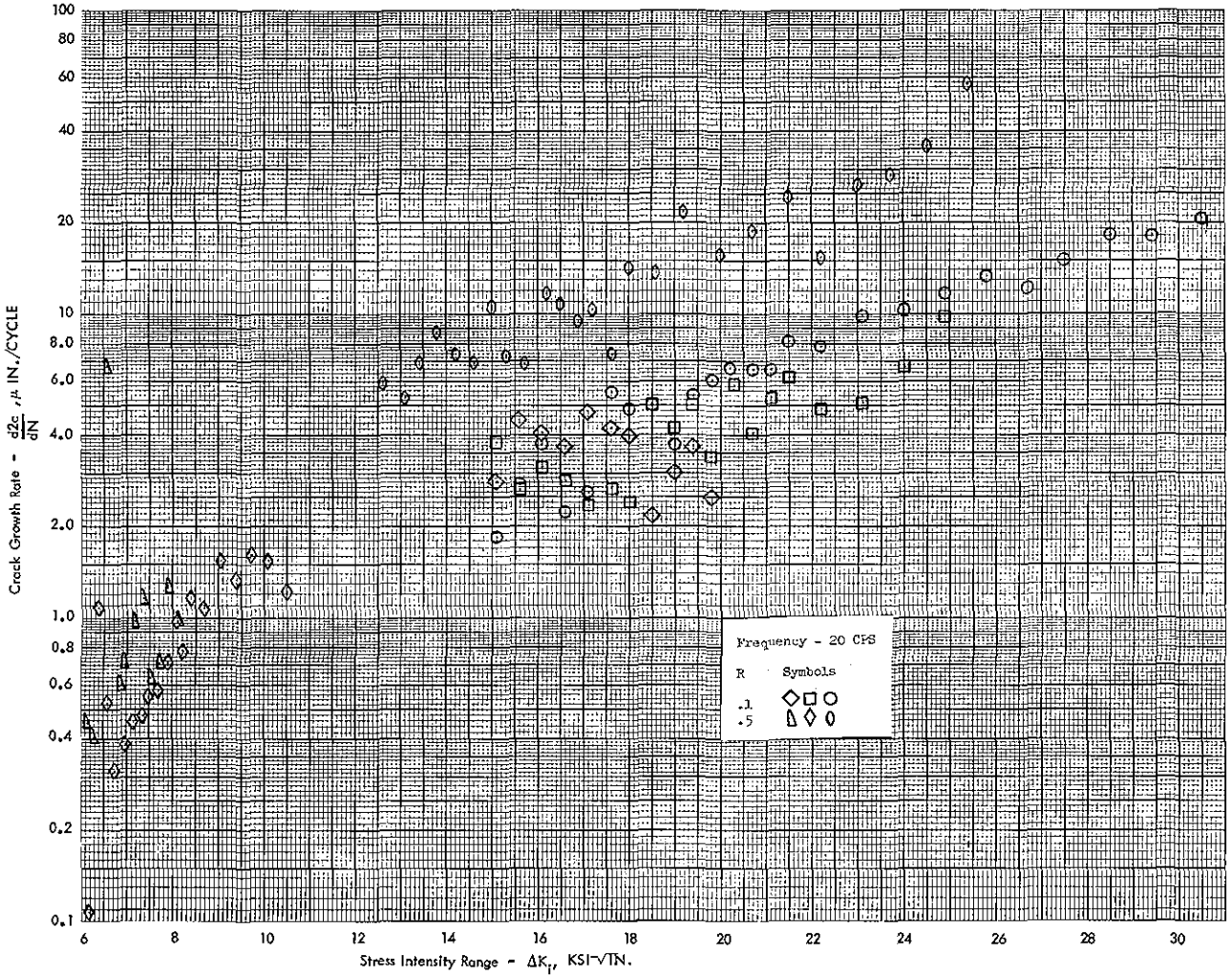

Figure 80 Cyclic Cracking Rate vs Stress Intensity Range For 3/8" Thick 300 M Steel (F_{tu} 270 KSI) Through-Crack Specimens in Moist Air Environment.

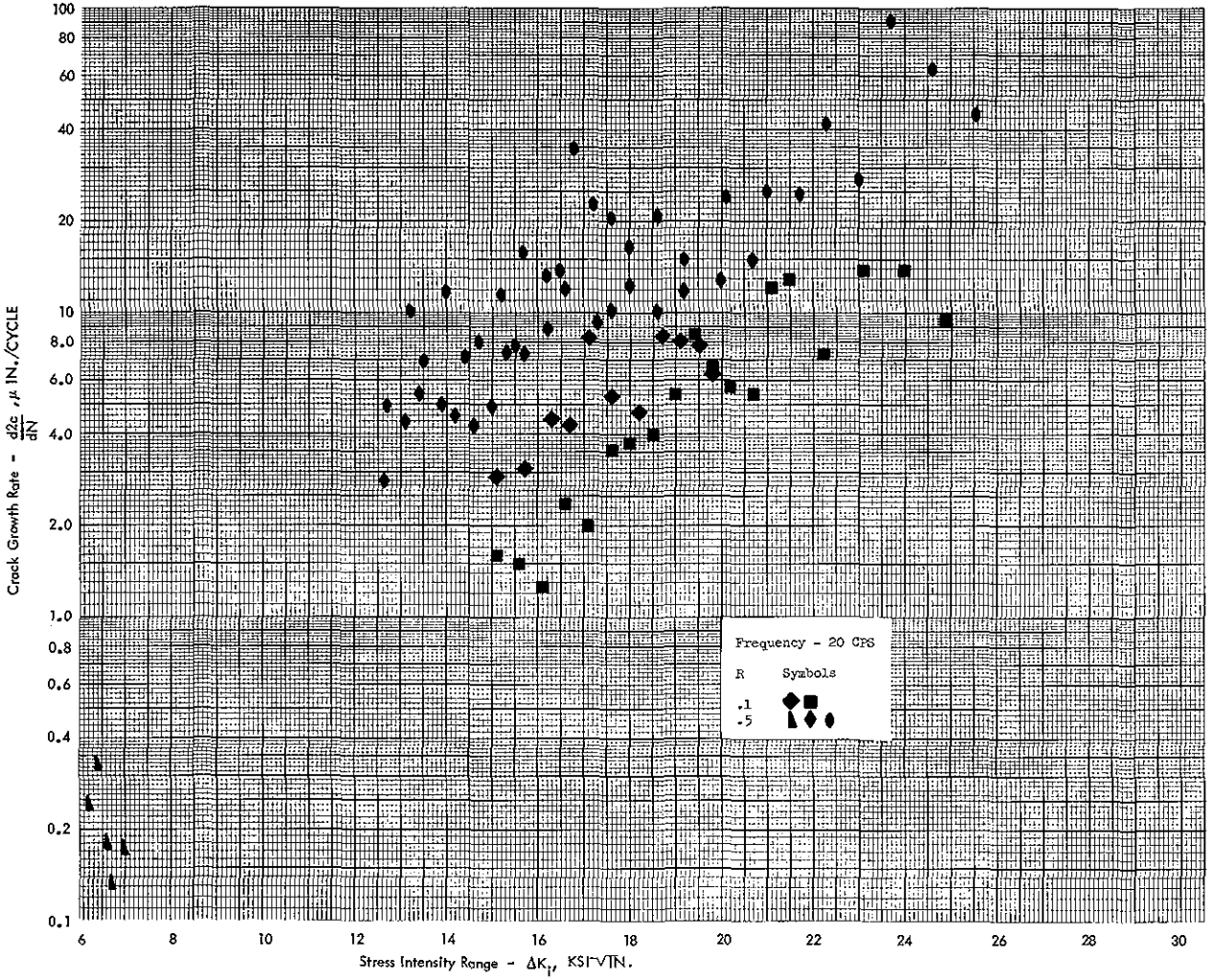

Figure 81 Cyclic Cracking Rate vs Stress Intensity Range For 3/8" Thick 300 M Steel (F_{tu} 270 KSI) Through-Crack Specimens in Salt Water Spray Environment.

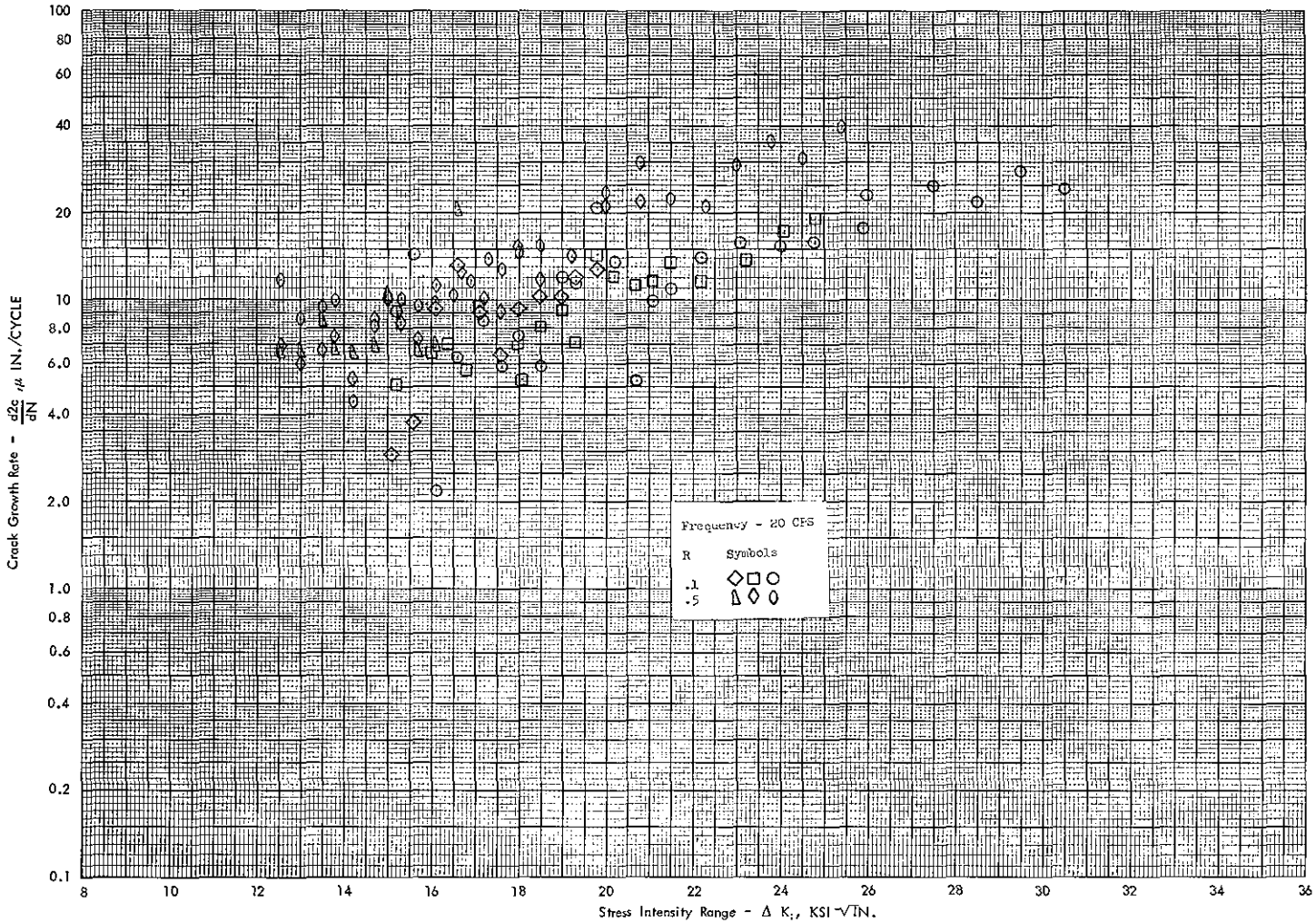

Figure 82 Cyclic Cracking Rate vs Stress Intensity Range For 3/8" Thick 300 M Steel (F_{tu} 220 KSI) Through-Crack Specimens in Moist Air Environment.

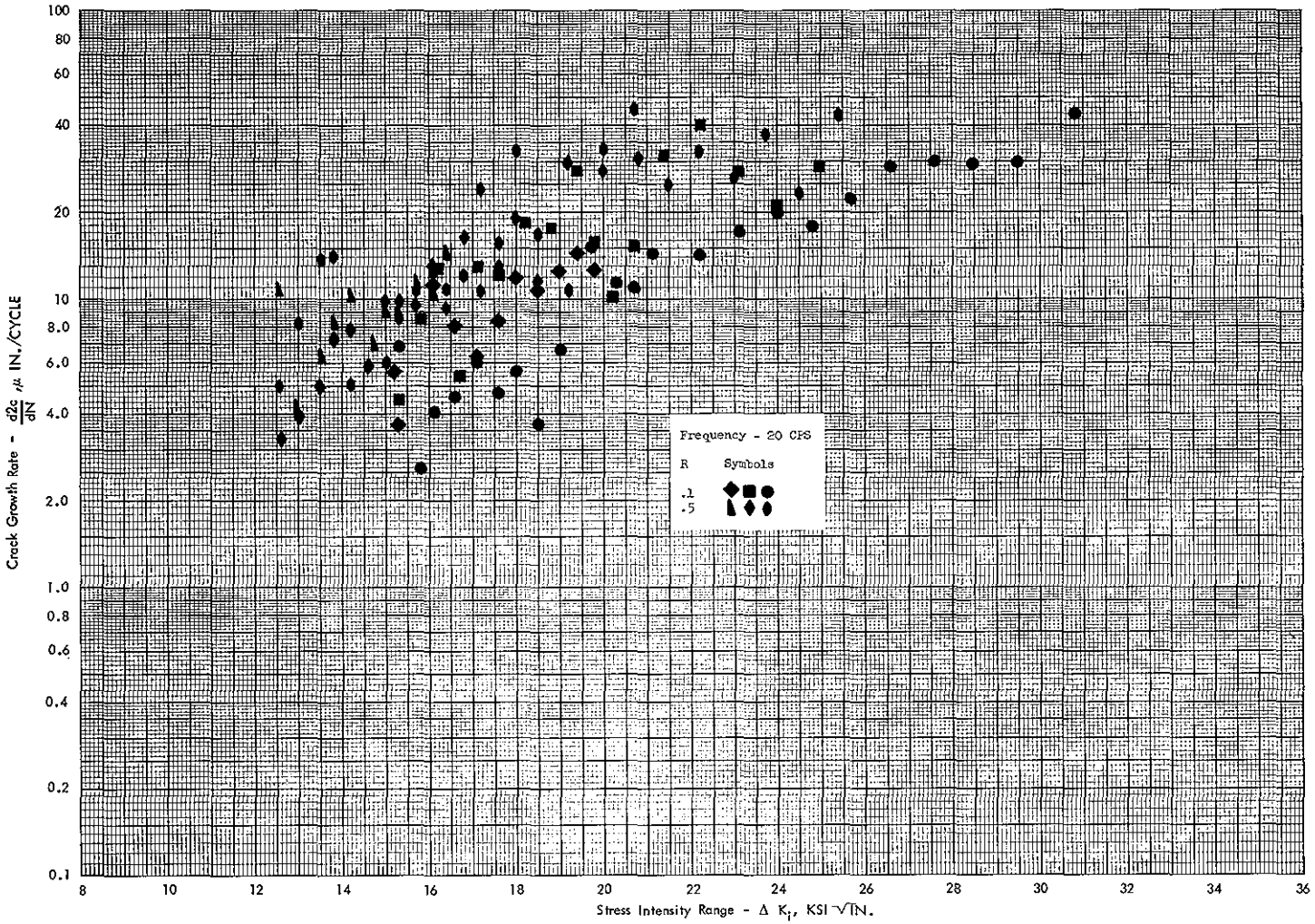

Figure 83 Cyclic Cracking Rate vs Stress Intensity Range For 3/8" Thick 300 M Steel (F_{tu} 220 KSI) Through-Crack Specimens in Salt Water Spray Environment

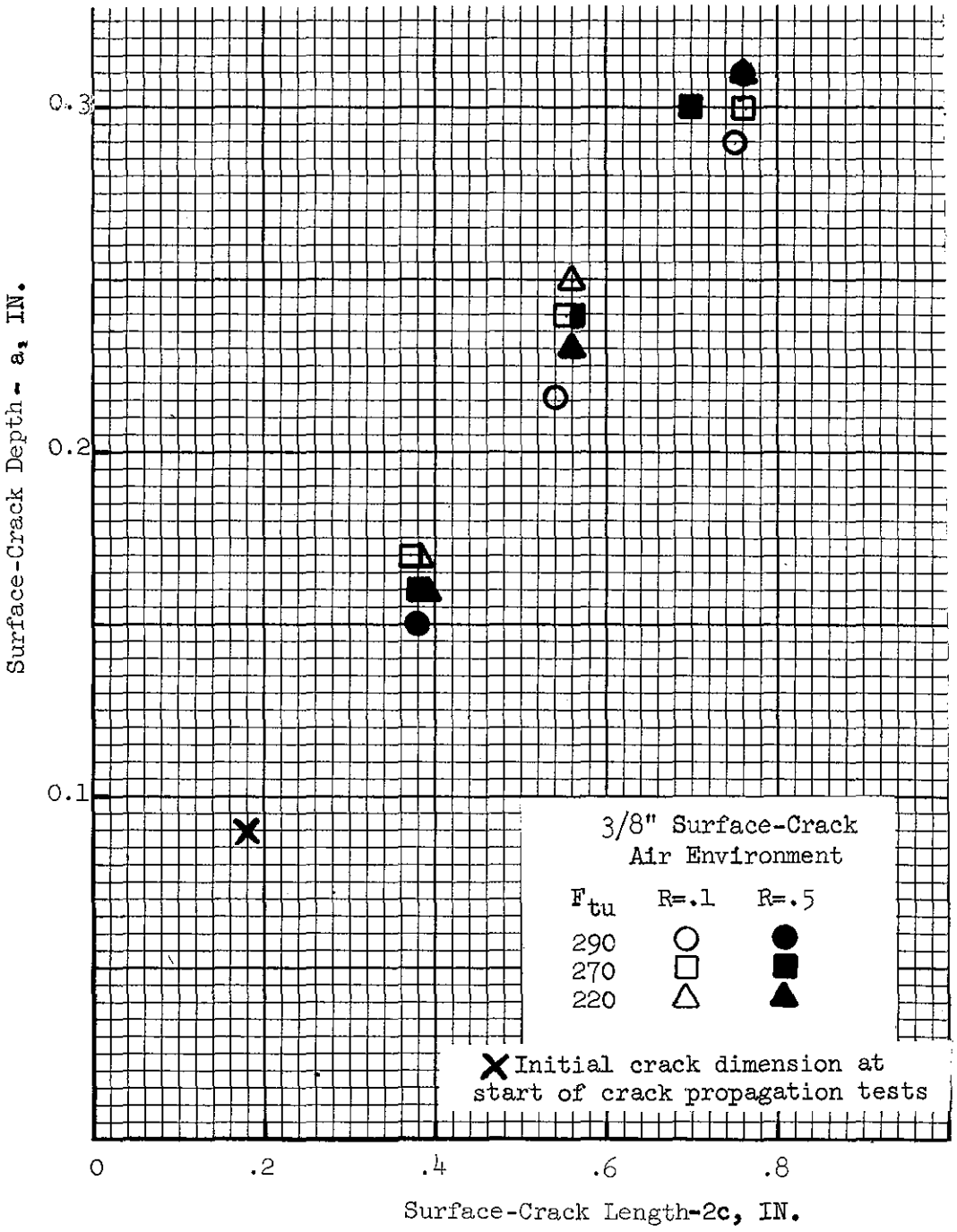

Figure 84 Surface Crack Depth (a) vs Crack Length (2c)

EVALUATION OF CRACK GROWTH RATE EQUATIONS

For the purpose of preliminary presentation of program results, equation (15) has been selected on the basis of its being the most widely used of available rate relationships, see Figures 62 through 83. These plots adequately display properties of the data such as scatter in cracking rates, stress ratio and environmental influences, differences due to thickness, strength level, part-through versus through flaws, etc. These data plots also provide a basis for evaluating possible improvements gained by using equations 18 or 21 as these later equations are modifications of equation 16.

For the purpose of evaluating equations 18 and 21, through-crack data at 270 KSI strength level, t = 3/8" has been selected. These data provide the highest values of K_{imax} for the test program as well as the greatest overlap of cracking rates for the extremes of stress ratio, R = 0.1 and R = 0.5. From a comparison of Figures 85 and 86 both equations 18 and 21 provide a means for reducing data from cracks grown at different stress ratios.

Equation 21 has been selected for use in evaluating cracking rate trends among the test data thus eliminating stress ratio as an independent variable. The influence of K_{Ic} on cracking rate is considered separately in another section.

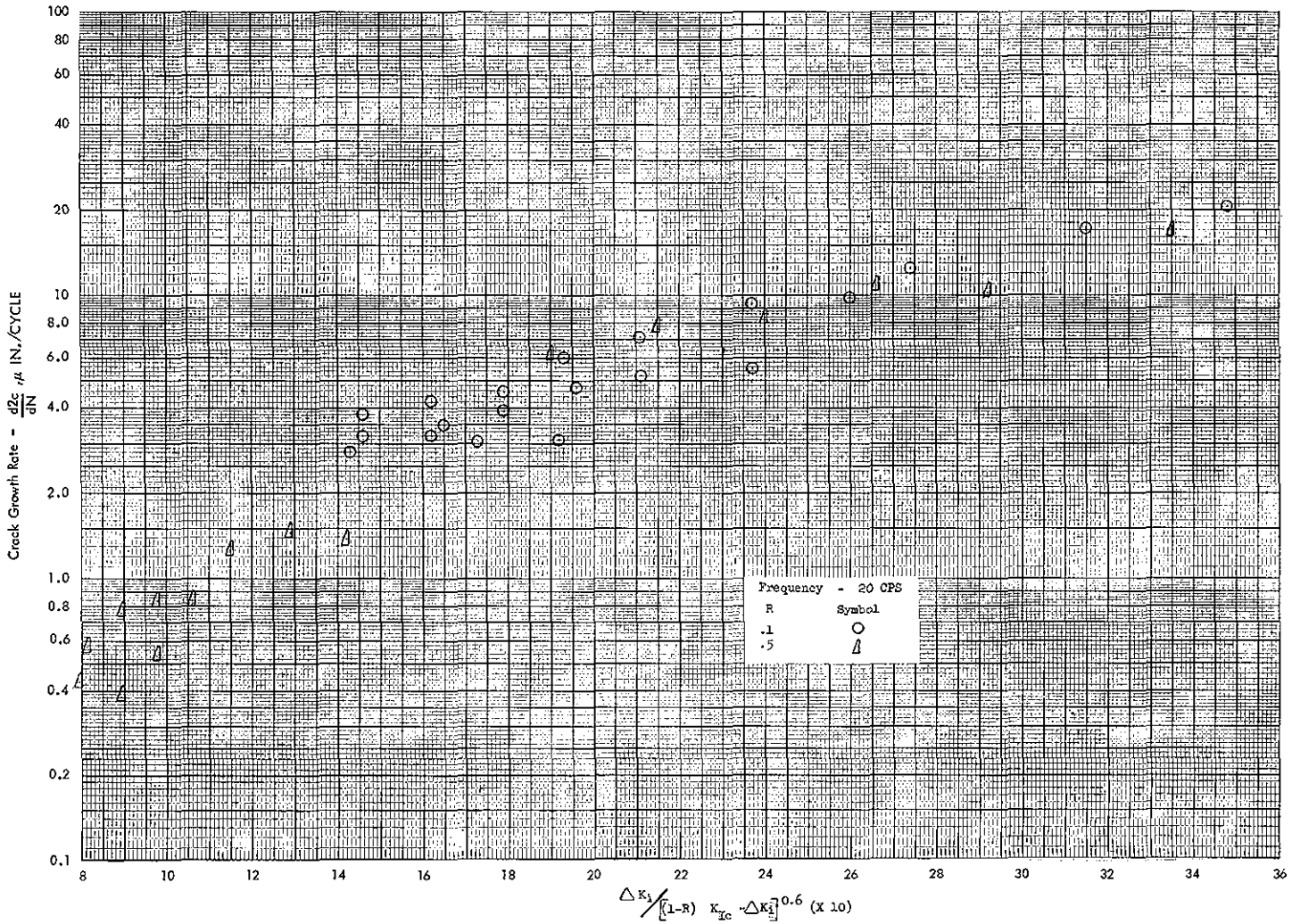

Figure 85 Relationship Between Cyclic Cracking Rate $(\frac{d2c}{dN})$ and Stress Intensity Range Parameter $\Delta K_i / [(1-R) K_{Ic} - \Delta K_i]^{0.6}$

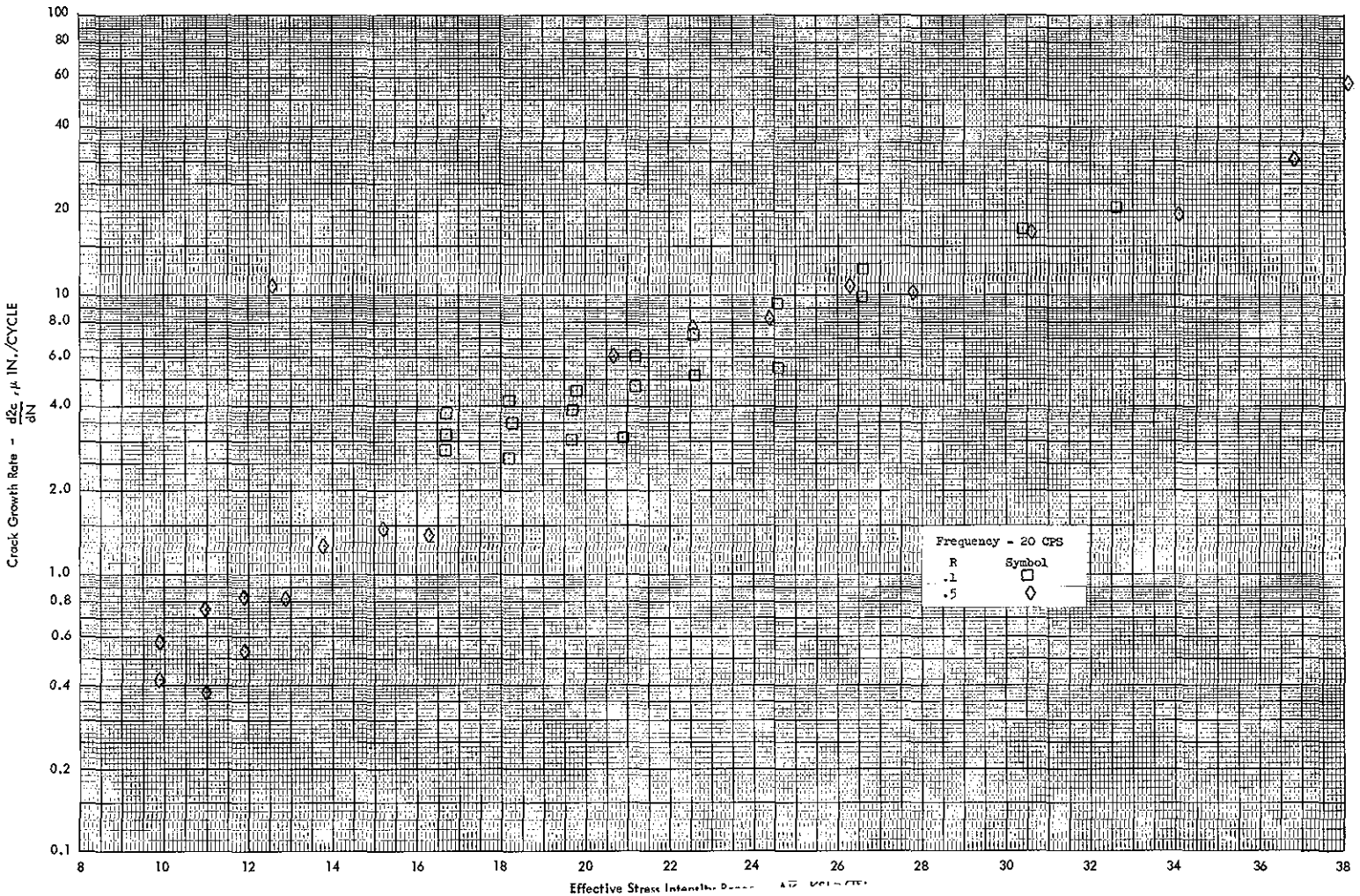

Figure 86 Relationship Between Cyclic Cracking Rate $(\frac{d2c}{dN})$ and Effective Stress Intensity Range Parameter $(\Delta\overline{K})$.

CRACK PROPAGATION CORRELATIONS

Crack growth rate behaviors for all specimens are shown on Figures 62 to 83 using ΔK_i as abscissa and d(2c)/dN as ordinate. To better illustrate trends among data, additional figures are shown in this section using selective groupings of data and eliminating stress ratio as a variable by using $\Delta\overline{K}$ (equation 21) as abscissa. The ordinate rates are based on average rates over three successive observations in order to reduce data scatter and to allow more coupons to be represented on a single figure without confusion.

In developing the data correlations, the 3/8 inch thick coupons are considered first as they represent the bulk of test data. Cracking behavior of 3/4" thick and 1/8" thick specimens are then compared to that of the 3/8" material.

Crack propagation behaviors in terms of d(2c/dN and $\Delta\overline{K}$ for 3/8 inch thick surface cracked specimens are shown on Figures 87 and 88. To aid in the comparisons, a trend curve approximating average behavior is drawn through the scatter band of data for crack propagation in air (Figure 87). This same curve is repeated on Figure 88. From Figures 87 and 88, the average behavior in salt water does not appear to be significantly different from that in air. The scatter band of cracking rates in salt water is however greater than that for air cracking. While it is not too obvious from the figures, this increase in scatter is primarily due to an increase in scatter between crack growth rate behavior in individual specimens. The scatter due to differences between sequential rate observations on an individual specimen is about the same for both air and salt water cracking.

On both Figures 87 and 88, the 220 KSI strength level data is at the top of the scatter band at higher stress intensities ($\Delta\overline{K}$) (above the knee of the trend curve). At the lower stress intensities ($\Delta\overline{K}$), the cracking rate behavior of the 220 KSI strength level is indistinguishable from that of the 270 KSI and 290 KSI strength level. The 270 KSI and 290 KSI strength level data show the same cracking rates for the entire range of stress intensities ($\Delta\overline{K}$). (Based on measured static ultimate strengths, the 270 KSI and 290 KSI nominal strength level data should probably be considered here as a single strength level see section III).

Figure 89 and 90 show crack growth rates for through the thickness cracks in air and in salt water for 3/8" thick material in a manner similar to that used for surface-cracks (Figures 87, 88). It is obvious that the computed stress intensities for a given cracking rate d(2c)/dN are greater for through-cracks than for surface-cracks. However, the behavior trends discussed above for surface-cracks appear to apply equally well to through the thickness cracks.

The cracking rates for the 220 KSI strength level data for both surface and through-cracks in 3/8" thick material are shown on Figure 91. Trend curves are shown for comparison. It is probable that the cracking rate increase as

shown by the rate data above the trend curves at higher values of $\Delta \overline{K}$, is associated with the decrease in strength level and K_{I_C}. However, the particular specimens demonstrating this increased cracking rate behavior are also from the heat of material having the highest carbon content. Specimens at 270 KSI strength level, also from this higher carbon heat of material do not however show a corresponding increase in cracking rate.

In addition to the 220 KSI strength level data, cracking data from a single stress ratio R = 0.5 specimen is shown to crack at an excessive rate, while companion R = 0.5 specimens fall well within the scatter band of data for the same cracking rates. A few other isolated specimens also show differences from their companion specimens Figures (92) through (97). The reasons for these increased cracking rates for individual specimens are not entirely clear. In some cases, observations were made which might explain these differences in behavior.

For example, 3/4 inch plate surface-crack specimen X-14239-31 was subjected to a momentary excessive cyclic rate because the resonant fatigue machine approached its natural resonant frequency. This condition was immediately eliminated by adding additional mass to the system which lowered the natural resonant frequency well below the normal operating frequency used in the test program. Also, testing of some of the 3/8 inch thick specimens was temporarily interrupted for minor repairs of the hydraulic loading system. This type of interruption occurred for specimens which exhibited normal cracking behavior as well as a few which exhibited somewhat faster cracking rates than companion specimens tested under nearly identical conditions, nevertheless, the interruptions may have affected cracking rate in some manner.

Figures 92 and 93 show data for surface-cracks in air and in salt water for 3/4 inch thick plate and forging. The trend curve for 3/8 inch surface-cracks behavior is repeated for use in comparison. The cracking rates in 3/4 inch thick material are generally slower than in 3/8 inch thick material for both air and salt water. Other than this, the data trends are similar to those of the 3/8 inch thick material. The 220 KSI strength level forging data and a single R = 0.5 specimen show higher cracking rates than the rest of the specimens. The cracking rates for plate and forgings are approximately the same. No significant trend of cracking rate with carbon content can be seen. All of the forging material and portions of the plate data are from heats having relatively high carbon content (Section III). The increase in scatter with salt water cracking that was seen in the 3/8" thick material is not as apparent in the 3/4" thick material.

Figures 94 and 95 show data for surface cracking in air and salt water for 1/8 inch thick material. Because of the thickness limitation, most of the cracks started as surface-cracks propagated through the thickness and are reported along with the cracks initiated as through the thickness cracks on Figures 96 and 97.

When compared to the 3/8" surface-crack trend curve, the 1/8 inch surface-cracks appear to exhibit slightly faster cracking than that of the 3/8 inch

thickness. Taken in context with the 3/8 and 3/4 inch crack growth rate behaviors, computed value of $\Delta\overline{K}$, a general decrease in cracking rate with increasing thickness is proba le.

Figures 96 and 97 show data for through the thickness crackin, in air and in salt water for 1/8 inch thick material. Those cracks initiated as through-cracks show cracking behavior similar to that of through-cracks in 3/8 inch material. The cracks initiated as surface-cracks which have grown through the thickness are also shown. These data were plotted as through-cracks on this figure when $2c \times 0.4 \approx a = t$. Back surface cracking was not measured due to its inaccessibility in the test fixture. Stress intensities $\Delta\overline{K}$ were computed using the surface crack measurements on the side from which the crack was initiated as shown below. Computed in this manner, the stress intensities at a given cracking rate appear to be higher than those for through-cracks in which the crack length can be assumed nearly equal on both surfaces. If the average of both surface measurements had been used these cracks growing through the thickness would probably plot within the scatter of the crack measurements taken on initially through the thickness cracks. For instance; had a surface flaw reached the rear surface at 25 KSI its average crack length would be approximately 1/2 the recorded surface-crack measurement 2c and the computed stress intensity would be less by a factor of $\sqrt{2}$ giving an adjusted stress intensity of $25/\sqrt{2} = 17.7$ KSI $\sqrt{\text{IN.}}$ This later value of 17.7 KSI $\sqrt{\text{IN.}}$ would be in the low stress intensity range of the initially through-cracked data. The real correction is probably somewhat less than $\sqrt{2}$. This approach of using the average crack length of both surfaces is further supported by the convergence of data from the two types of starter cracks at larger stress intensities (longer surface crack lengths).

The differences between $\Delta\overline{K}$ versus $d(2c)/dN$ plots of surface flaw data and through the thickness data requires consideration. The first and most obvious source of inconsistency (at least mathematically) is that the quantity da/dN or $d(a/Q)/dN$ are more closely associated with the stress intensity calculations used as the abscissa for surface flaw data. The stress intensity for surface flaws is presumably that at the extreme depth of the crack (at the end of the minor radius a) where the stress intensity is normally assumed to be a maximum. A check on the affect of plotting surface flaw data in terms of da/dN or $d(a/Q)/dN$ where a/2c is approximately 0.4 and Q is approximately two shows that

$$da/dN \approx 0.4 \times d(2c)/dN$$

$$d(a/Q)/dN \approx 0.2 \times d2c/dN$$

As illustrated on Figure 98, showing data for the 3/8 inch thickness, the difference in cracking rate is approximately a factor of 1/10 so that some additional correction would still be necessary, this most likely should be added to the free surface corrections of the surface flaw stress intensity $(\Delta\overline{K})$.

The characteristic shapes of the trend curves for surface and though the thickness cracks are very similar. Therefore, with additional refinements to the stress intensity relationships, the collapse of surface and through the thickness flaw growth data is probable.

The relationship shown on Figure 98 between d2c/dN and $\overline{\Delta K}$ for surface and through-cracks, is approximately that given by parallel straight lines on a log-log plot of $\overline{\Delta K}$ versus d(2c)/dN (Figure 99) where the slope is shown to be approximately 1/5. Had either a or (a/Q) been selected rather than 2c in computing cracking rates, the result would have been non-parallel straight lines on Figure 99. Log-log plots will be discussed further in Section 5.

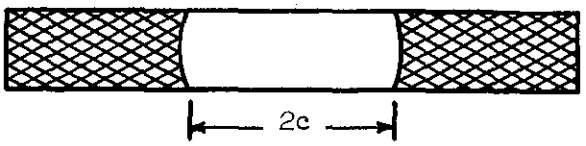

Typical geometry of crack grown from a through the thickness EDM slot.

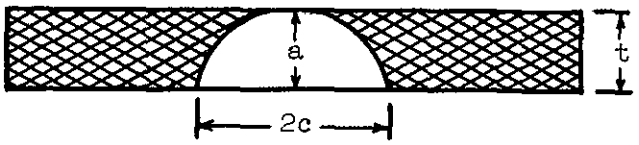

Typical geometry of crack grown through the thickness from a surface EDM cut at a≃t.

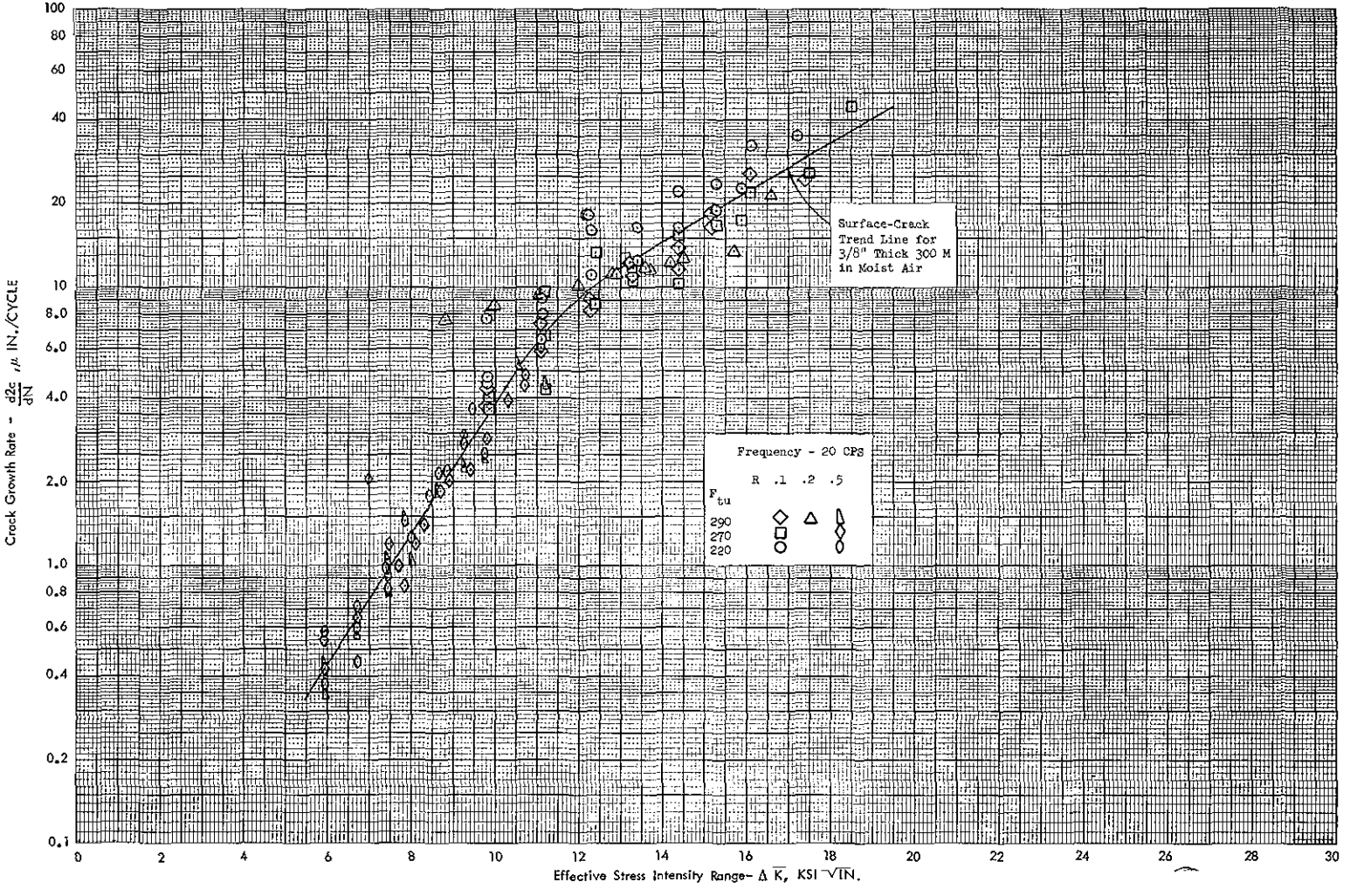

Figure 87 Cyclic Cracking Rate vs Effective Stress Intensity Range for 3/8" Thick 300 M Steel (F_{tu} 290, 270, 220 KSI) Surface-Crack Specimens in Moist Air Environment.

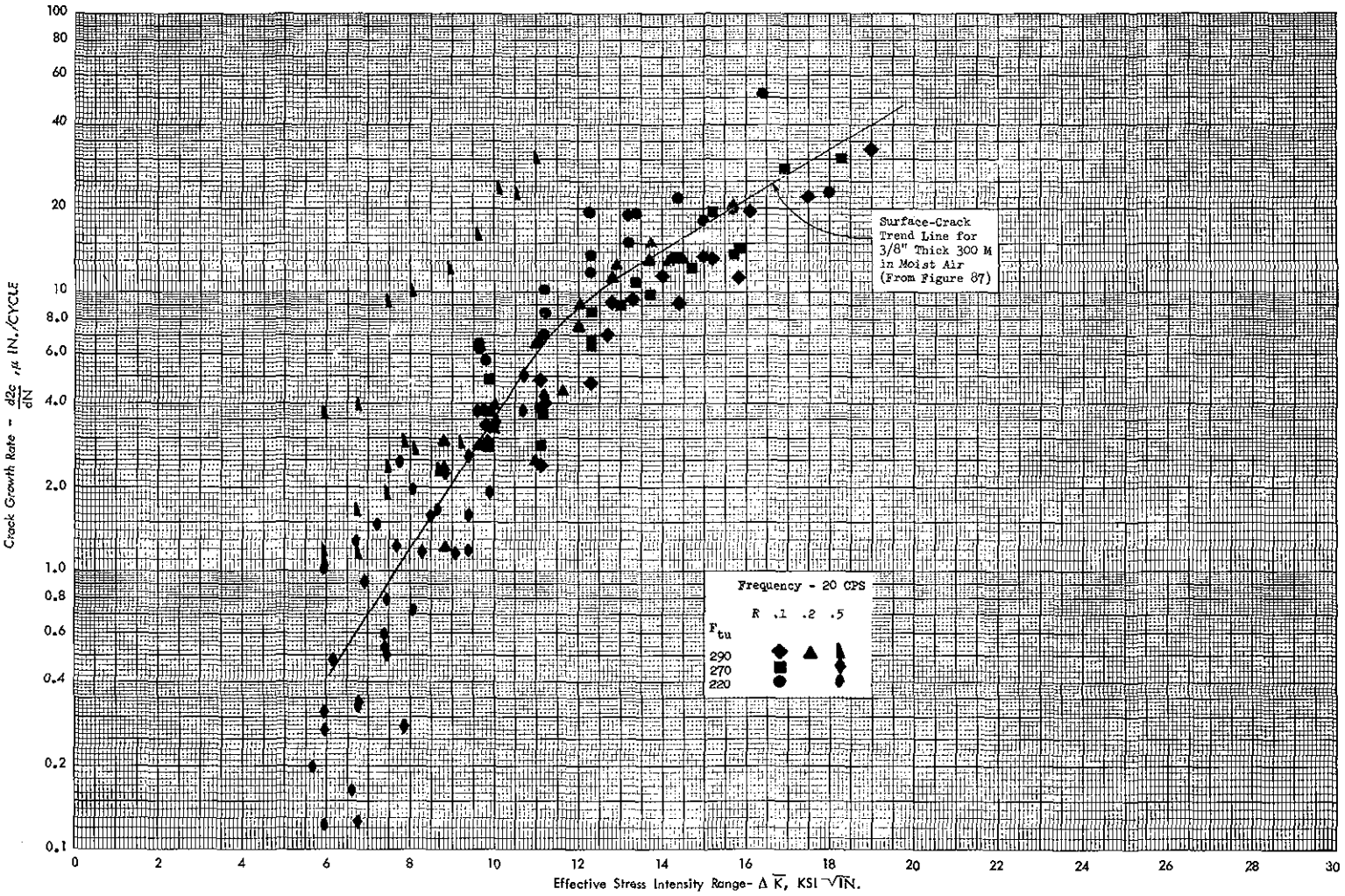

Figure 88 Cyclic Cracking Rate vs Effective Stress Intensity Range for 3/8" Thick 300 M Steel (F_{tu} 290, 270, 220 KSI) Surface-Crack Specimens in Salt Water Spray Environment.

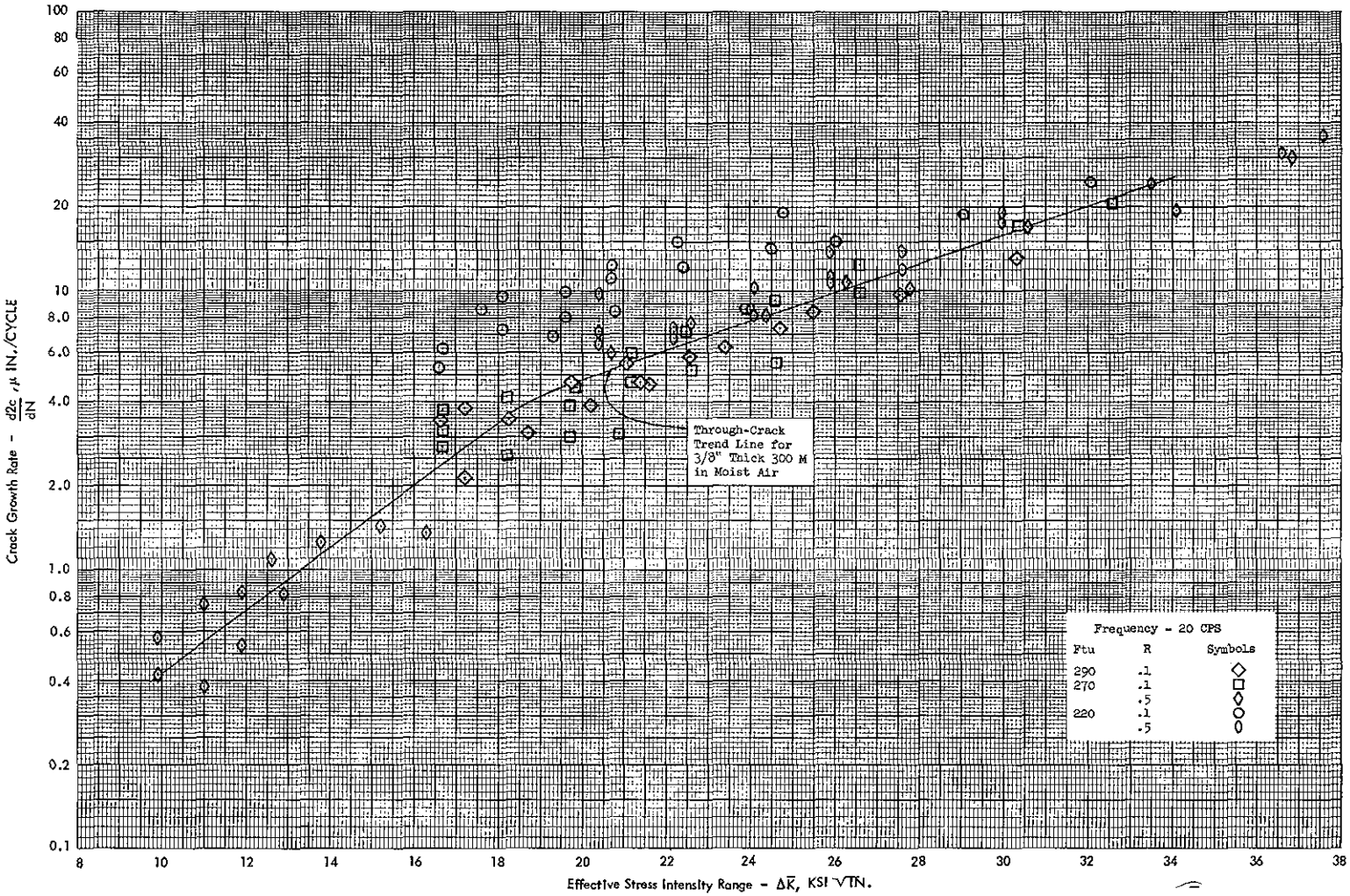

Figure 89 Cyclic Cracking Rate vs Effective Stress Intensity Range for 3/8" Thick 300 M Steel (F_{tu} 290, 270, 220 KSI) Through-Crack Specimens in Moist Air Environments.

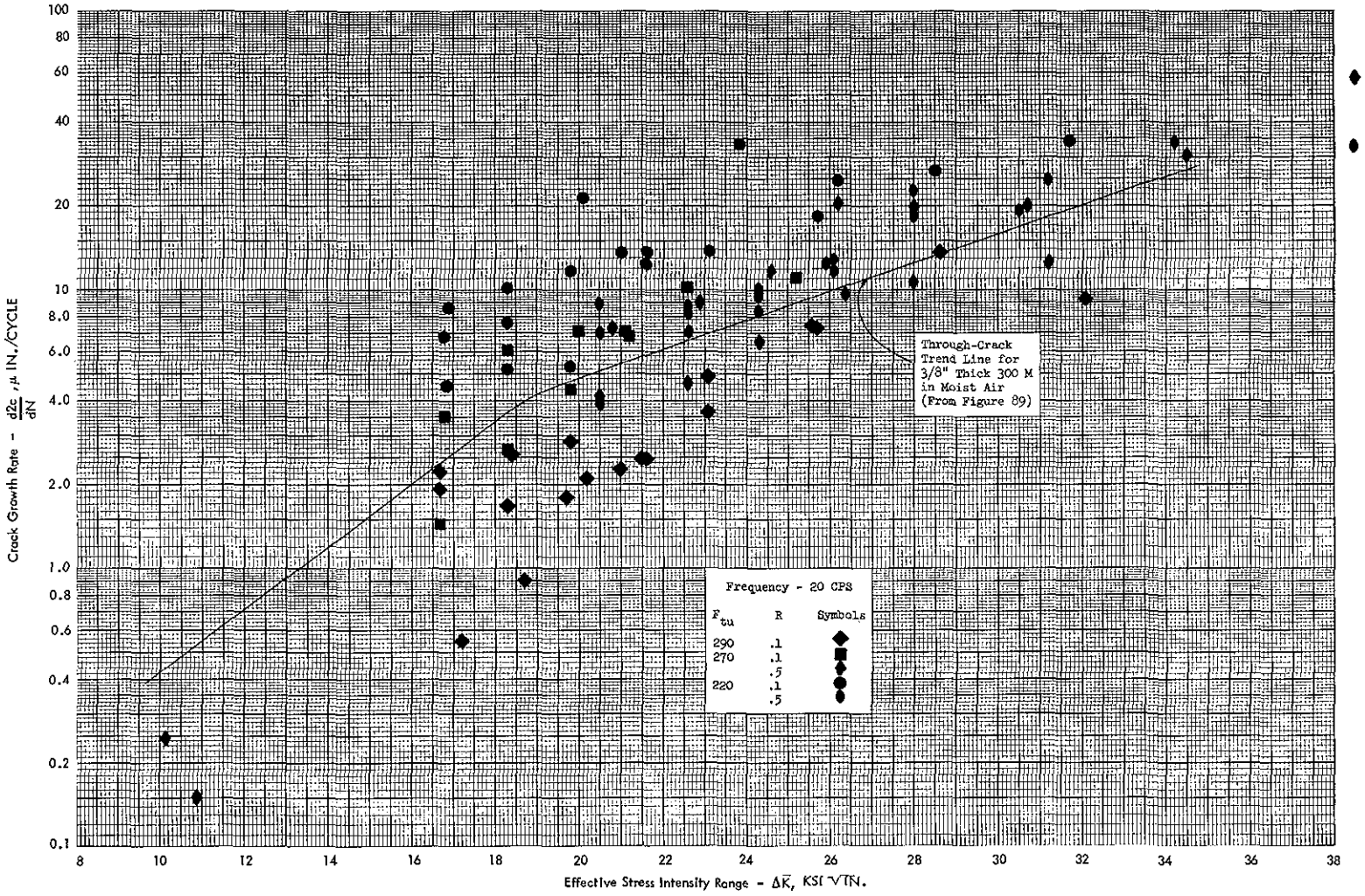

Figure 90 Cyclic Cracking Rate vs Effective Stress Intensity Range for 3/8" Thick 300 M Steel (F_{tu} 290, 270, 220 KSI) Through-Crack Specimens in Salt Water Spray Environment.

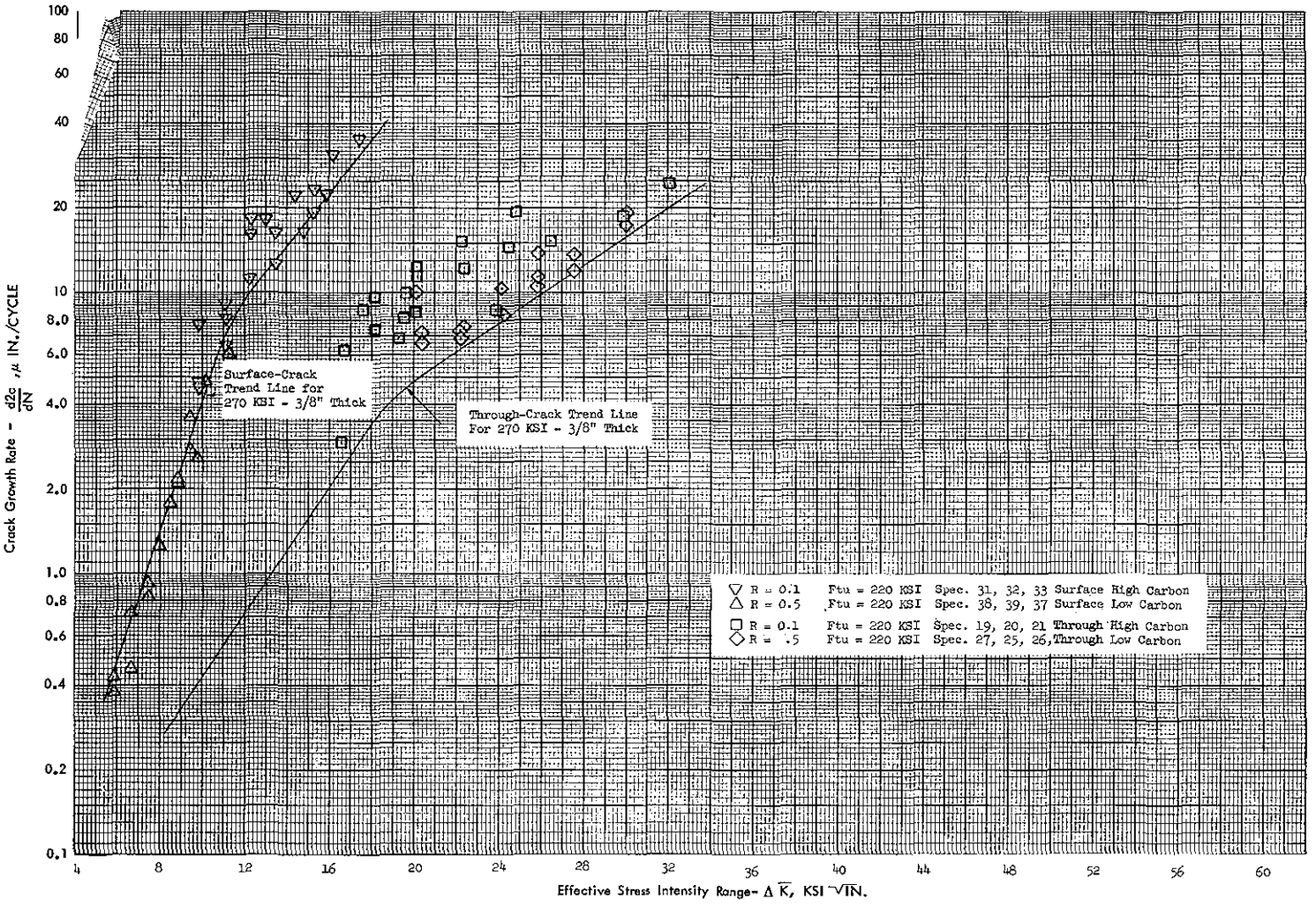

Figure 91 Cyclic Cracking Rate vs Effective Stress Intensity Range for 3/8" Thick 300 M Steel (F_{tu} 220 KSI) Surface-Crack and Through Crack Specimens in Moist Air Environment.

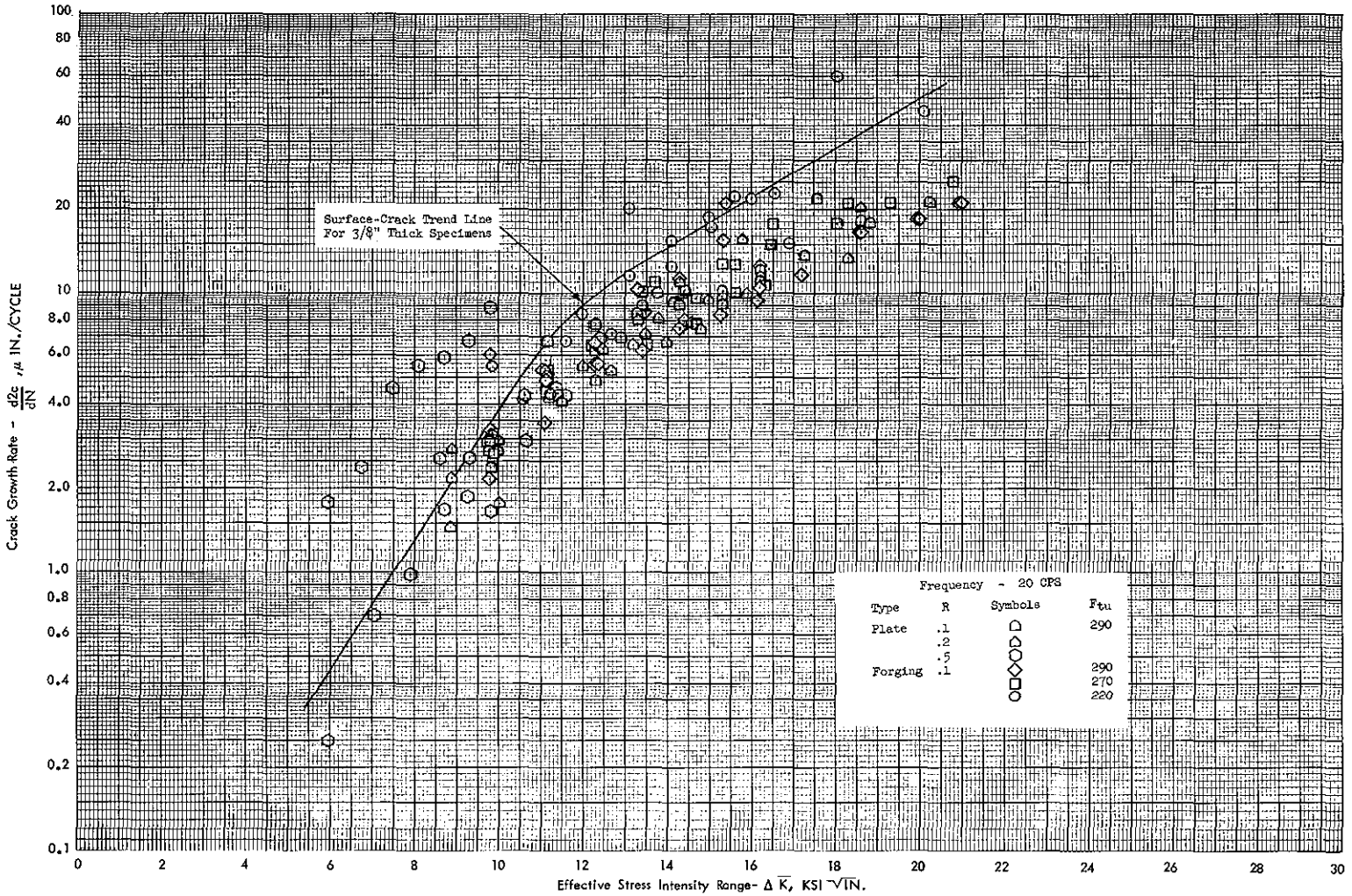

Figure 92 Cyclic Cracking Rate vs Effective Stress Intensity Range for 3/4" Thick 300 M Steel Plate (F_{tu} 290 KSI) and Forging (F_{tu} 290, 270, 220 KSI) Surface-Crack Specimens in Moist Air Environment.

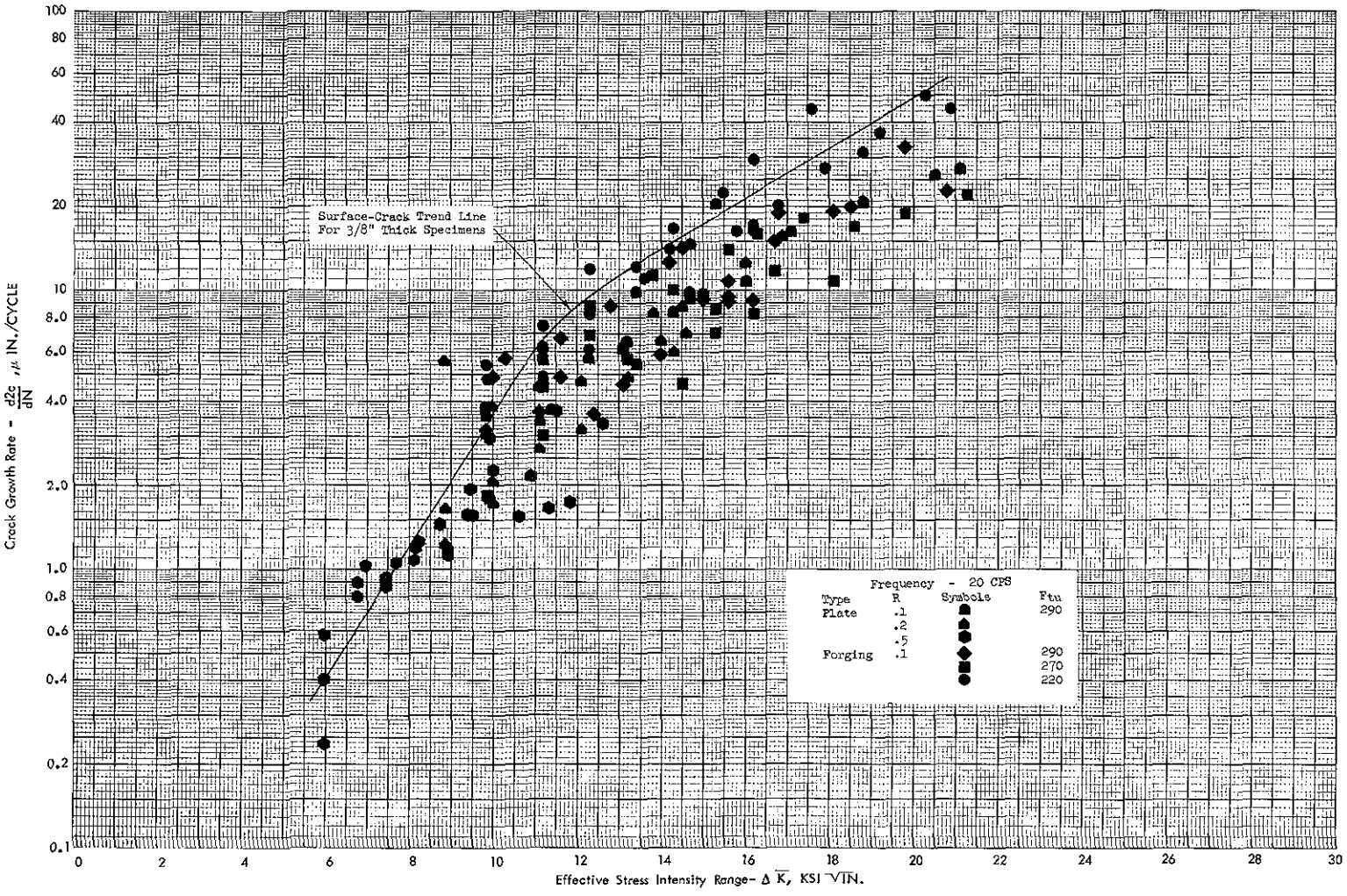

Figure 93 Cyclic Cracking Rate vs Effective Stress Intensity Range for 3/4" Thick 300 M Steel Plate (F_{tu} 290 KSI) and Forging (F_{tu} 290, 270, 220 KSI) Surface-Crack Specimens in Salt Water Spray Environment.

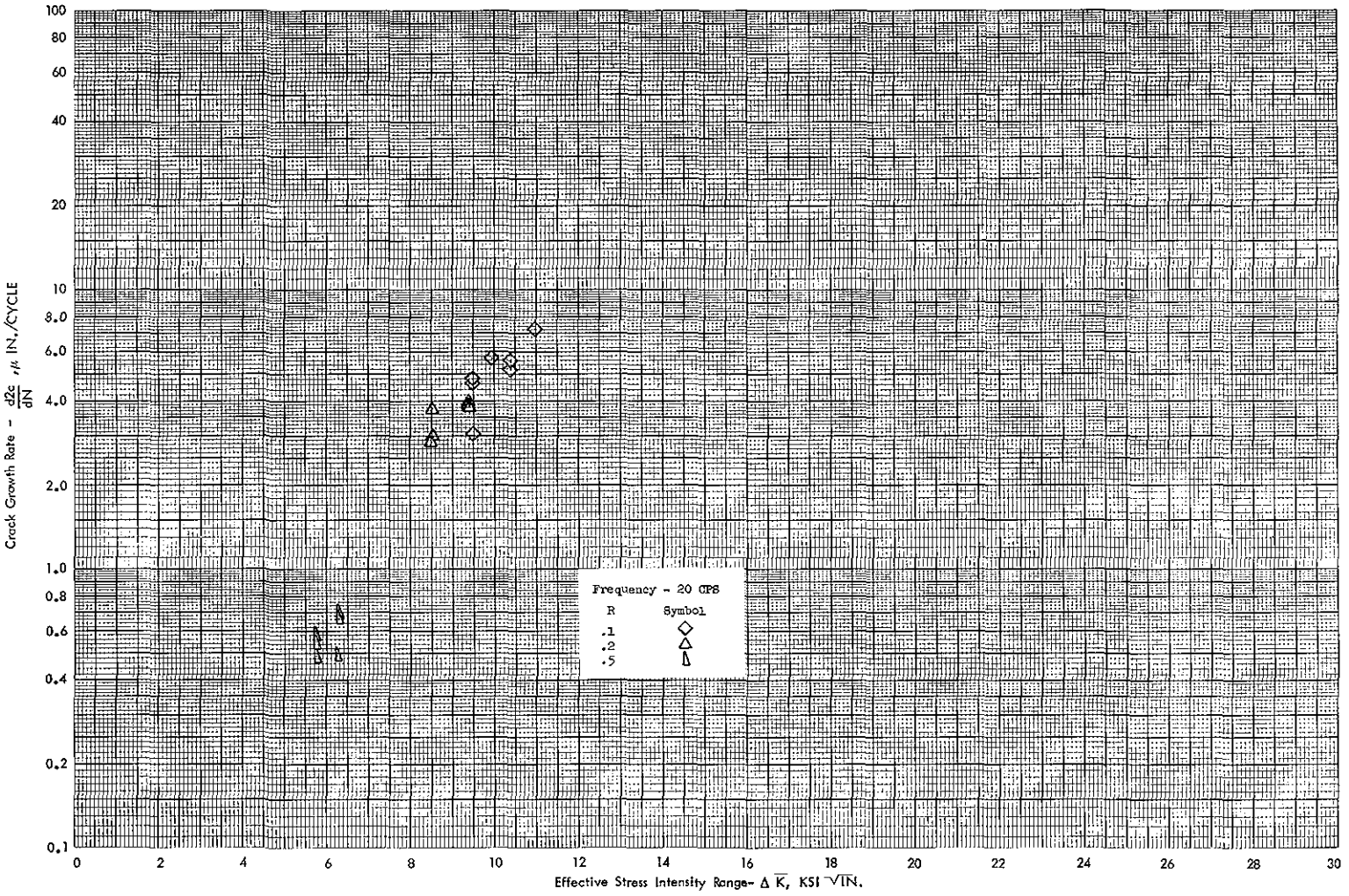

Figure 94 Cyclic Cracking Rate vs Effective Stress Intensity Range for 1/8" Thick 300 M Steel (F_{tu} 290 KSI) Surface-Crack Specimens in Moist Air Environments.

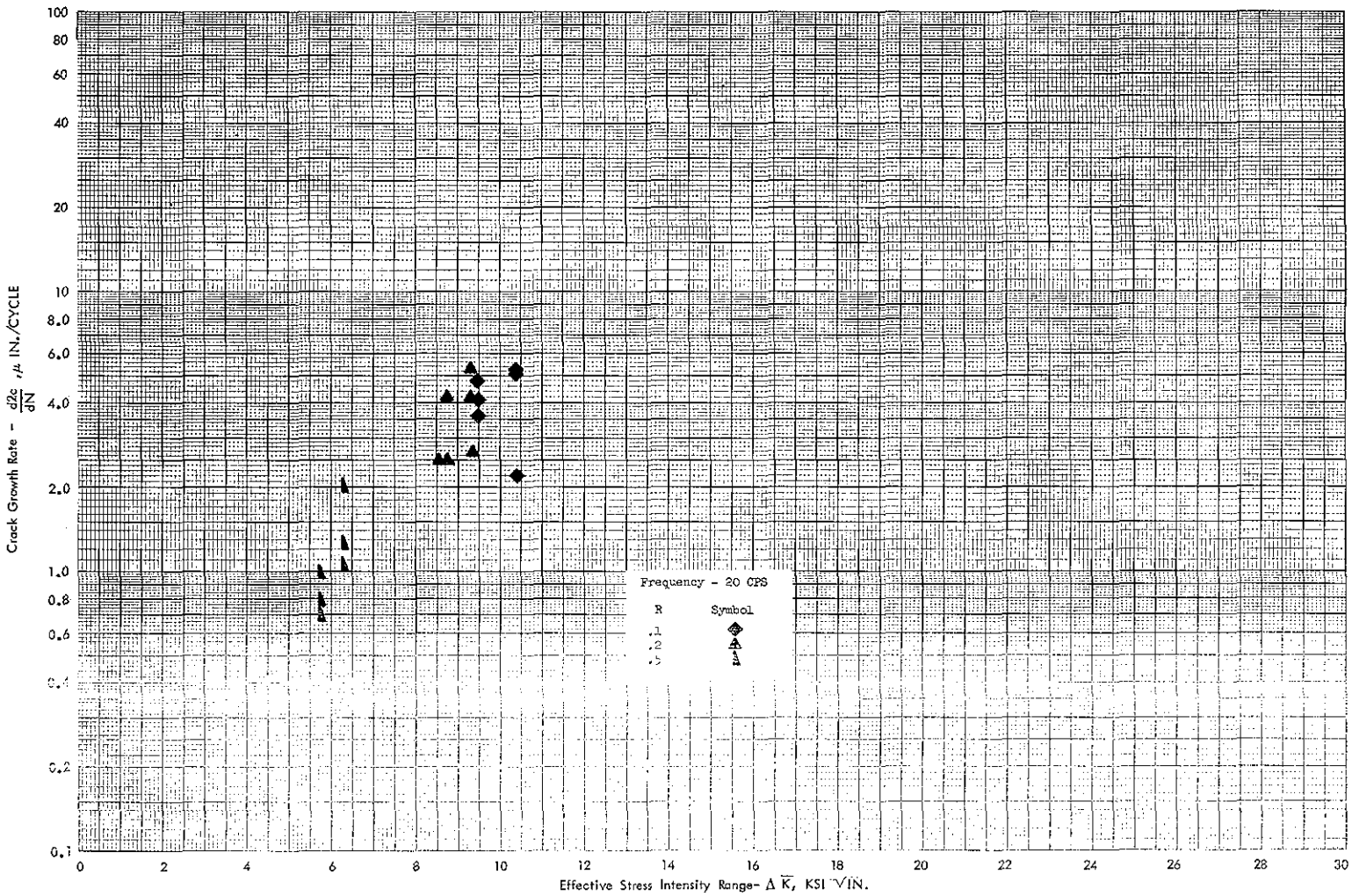

Figure 95 Cyclic Cracking Rate vs Effective Stress Intensity Range for 1/8" Thick 300 M Steel (F_{tu} 290 KSI) Surface-Crack Specimens in Salt Water Spray.

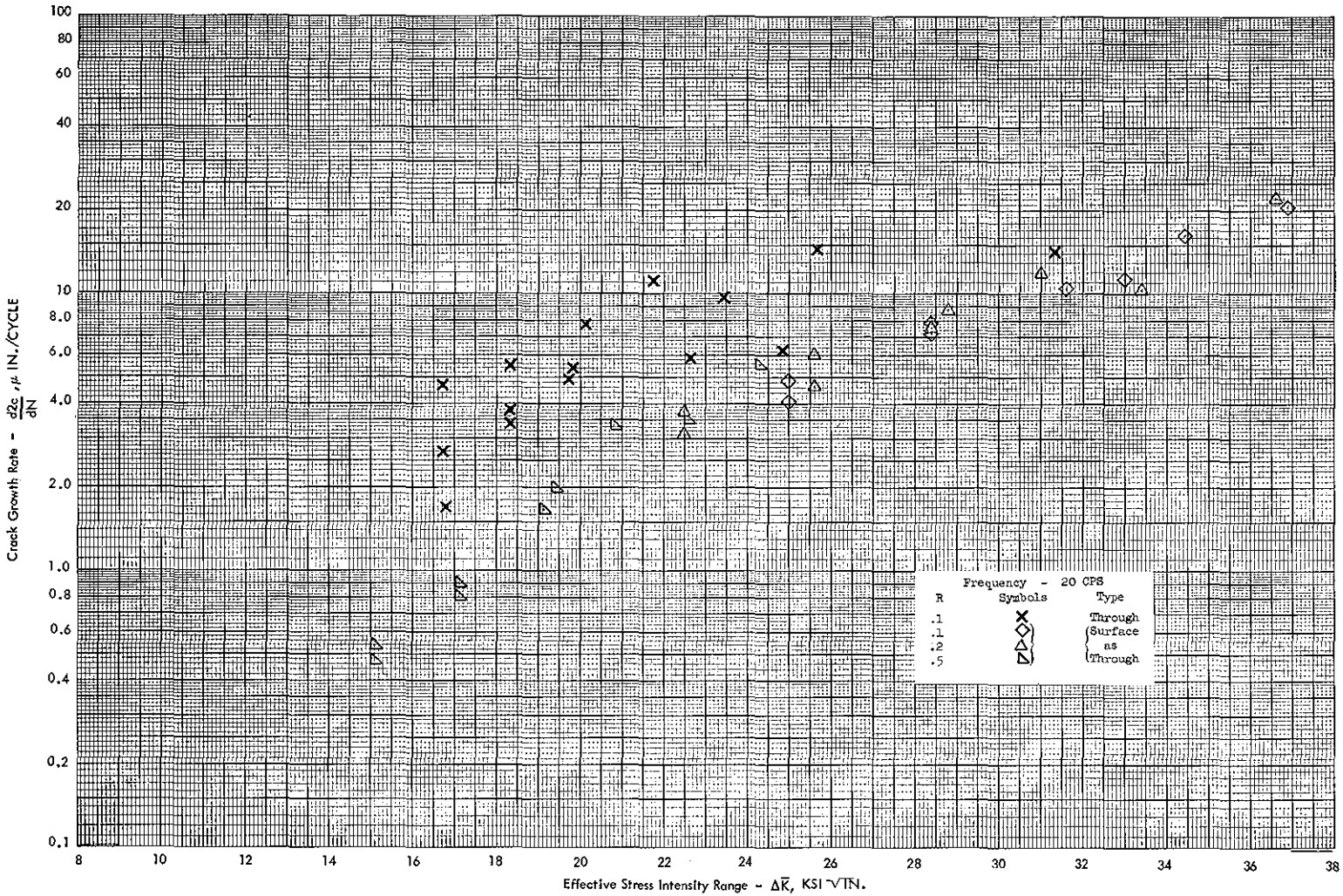

Figure 96 Cyclic Cracking Rate vs Effective Stress Intensity Range for 1/8" Thick 300 M Steel (F_{tu} 290 KSI) Through Crack Specimens in Moist Air Environment.

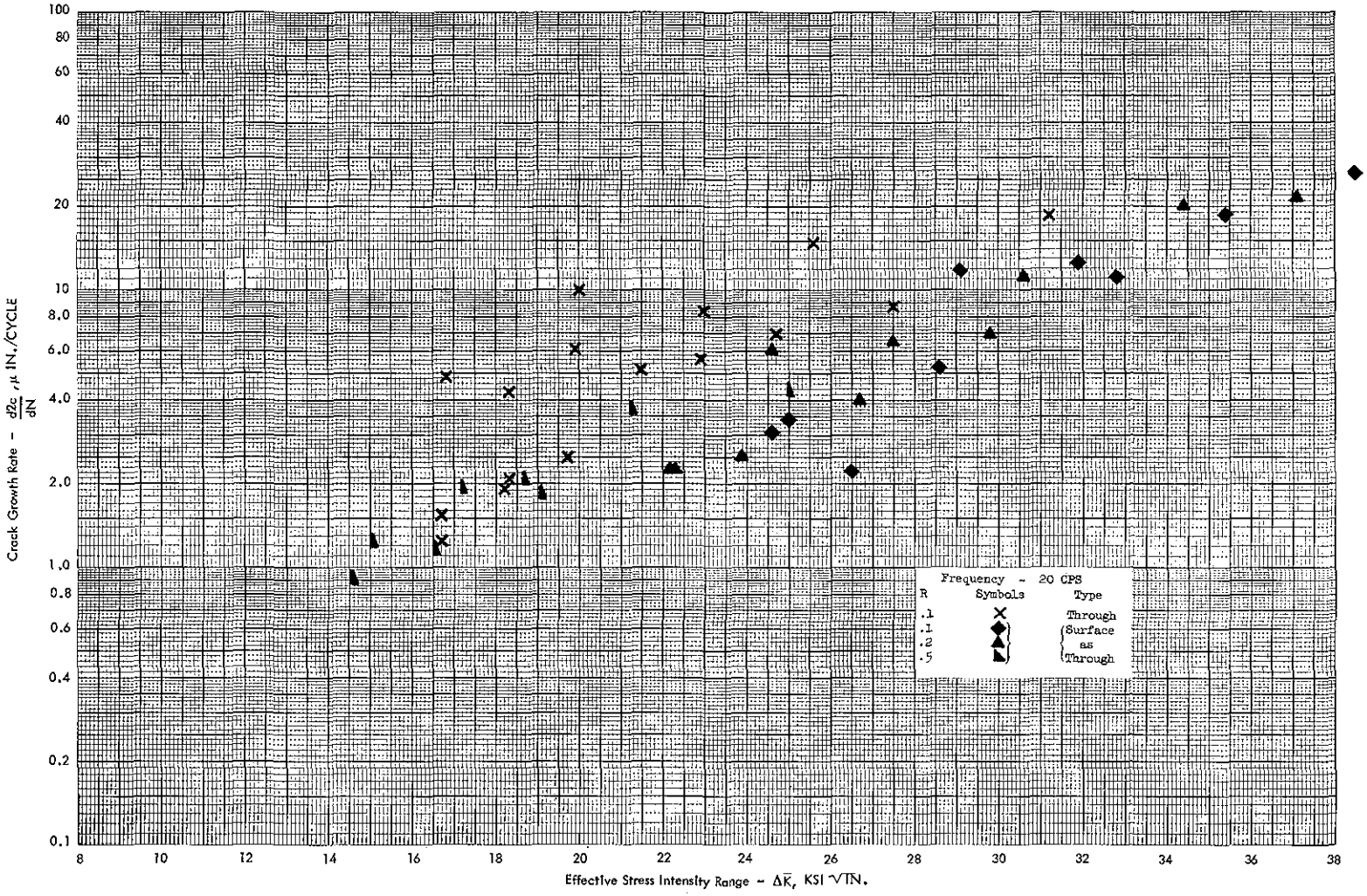

Figure 97 Cyclic Cracking Rate vs Effective Stress Intensity Range for 1/8" Thick 300 M Steel (F_{tu} 290 KSI) Through-Crack Specimens in Salt Water Spray Environment.

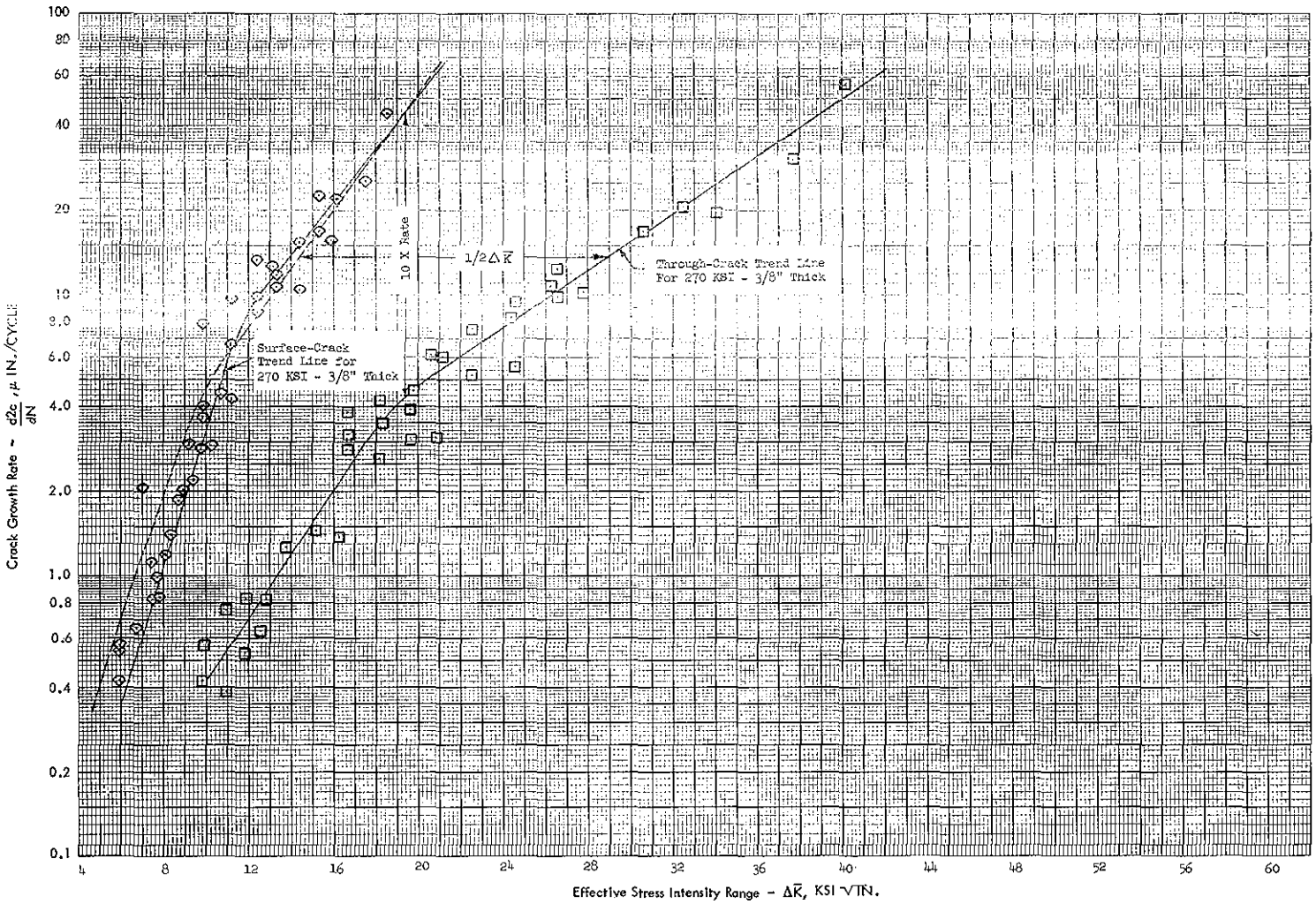

Figure 98 Cyclic Cracking Rate vs Effective Stress Intensity Range for 3/8" Thick 300 M Steel (Ftu 270 KSI) Surface-Crack and Through-Crack Specimens in Moist Air Environment.

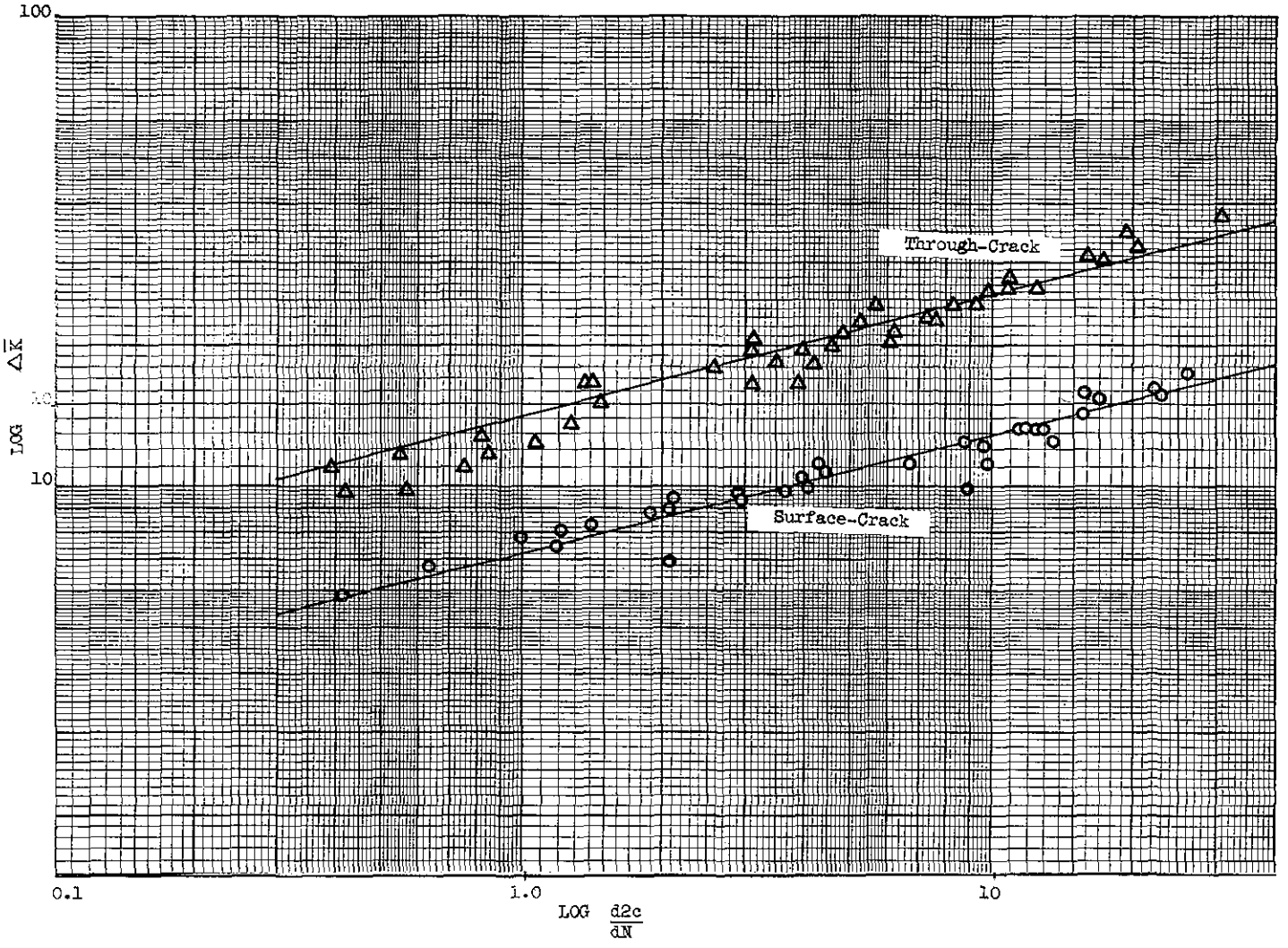

Figure 99 Relationship Between $\frac{d2c}{dN}$ and $\Delta\overline{K}$ for Surface-Crack and Through-Crack Specimens.

FRACTURE TOUGHNESS CORRELATIONS

The basic fracture toughness test results for surface-crack and through-crack specimens tested in this program are tabulated in Tables 26 through 37 in Section III. Apparent critical stress intensity values (K_{Ic}) were calculated using Equation (13), for the surface-crack specimens and Equation (7), for the through-crack specimens.

Primary correlations of apparent K_{Ic} with product, heat treatment, and test variables are made for test results from the 3/8 inch thick surface-crack and through-crack specimens. These specimen tests include all variable combinations. Specific correlations made from test results on the 1/8 and 3/4 inch thick specimens are compared with those of the 3/8 inch specimens.

By plotting gross fracture strength against crack size (a/Q) for 3/8 inch surface-crack specimen tests (Figure 100), it is apparent that gross fracture strength varies considerably from one heat of material to another. The amount of scatter due to heat variation appears significantly greater than that due to other variables. This makes it more difficult to evaluate other variables with respect to fracture toughness properties. Correlations of K_{Ic} with strength level and test variables must be evaluated within a single heat of material. Using this approach, the effect of strength level can be obtained from Figure 100. For HT 3932021, the 290 KSI strength level exhibited higher residual strength than the 220 KSI material for a/Q values higher than .12. For HT 3922452, the 270 KSI strength level material has higher residual strength than the 220 KSI strength level, etc. The data indicate that residual strength (A measure of toughness) tends to increase with ultimate strength. This trend is even more evident from a similar plot for 3/8 inch through-crack specimens (Figure 101). For HT 3932021, the 290 KSI strength level material had the highest residual strength followed by the 270 KSI material with the 220 KSI strength material the lowest. Figure 102 shows the same relationship between residual strength and strength level for 3/4 inch surface-crack specimens from forged material. The consistency of higher residual strengths with higher strength levels indicates a real effect in 300 M steel for the strength ranges investigated. This behavior is opposite from the usual behavior wherein residual strength is inversely proportional to ultimate strength level. Figures 103 and 104 present plots of gross fracture strength vs surface-crack size (a/Q) for 3/4 inch plate specimens and fracture strength vs through-crack length for 1/8 inch sheet specimens. These specimens are all at 290 KSI strength level for these two products. Figure 103 again illustrates the variation in results with different heats of 3/4 inch plate.

Figure 105 presents a plot of fracture strength vs crack length for both surface-crack and through-crack specimens for 3/8 inch specimens at 290, 270, and 220 KSI strength levels and 1/8 inch specimens at 290 KSI strength levels. It is interesting to note that a continuous smooth scatter band can encompass both the surface-crack and through-crack data using crack length as the crack size parameter.

Normally, the crack size a/Q, where a is crack depth and Q is crack shape parameter, is used for evaluating surface type flaws in high strength metals. For practical service considerations, it is difficult and in most cases impossible to determine crack depth and shape non-destructively by in service inspection techniques. The only measurable crack dimension in service inspection is usually crack length. By rationalizing that preexisting surface type flaws in aircraft components will tend to propagate in service to a fairly constant surface-crack shape with a crack depth to crack length ratio (a/2c) of approximately .4 to .5, then the a/Q crack size would be nearly proportional to crack length (2c). This would permit predictions of fracture toughness behavior from crack length measurements obtained from service inspections. For aircraft components that are essentially in axial tension, this rationalization has merit but, if bending type loading is experienced, the propagating surface-crack would tend to have a smaller and constantly changing a/2c ratio which would invalidate any proportionality of a/Q with crack length.

The effect of specimen thickness on apparent K_{Ic} for both surface-crack and through-crack specimens at 290 KSI strength level is shown in Figure 106. A constant band or K_{Ic} values was obtained for 1/8, 3/8, and 3/4 inch thick surface-crack specimens from similar heats of material. For through-crack specimens, the apparent K_{Ic} values for 1/8 inch specimens were considerably higher than for surface-crack specimens, but at 3/8 inch thickness the through-crack K_{Ic} values approached the scatter band for surface-crack specimens.

Three different crack sizes were evaluated for each test condition resulting in different crack depth to specimen thickness ratios (a/t) for the surface-crack specimens. Two of the three crack sizes exceed an a/t ratio of 0.5 which is an arbitrarily recommended limit for fracture mechanics considerations due to elastic equation restrictions and limitations of the plastic zone corrections. The effects of a/t ratios on K_{Ic} and K_{Ic}* (Equation 14) are shown in Figures 107 through 109 inclusive for 3/8 inch surface-crack specimens. A general tendency for K_{Ic} to decrease as a/t ratio increases is evident. When K_{Ic} is corrected for a/t ratio using Equation 14 (K_{Ic}*), the data shows a reverse trend of K_{Ic}* increasing with a/t ratio. This trend is also more pronounced than the K_{Ic} trend indicating that the a/t correction over corrected the a/t effect for the specimen geometries and a/t range investigated. The data obtained in this program may supply investigators with information required to derive more adequate K_{Ic} corrections. The effects of a/t on K_{Ic} values for 3/4 inch forging and plate surface-crack specimens are shown in Figure 110. The same general tendency for K_{Ic} to decrease as a/t increases is evident.

In this report, the critical stress intensity parameter, K_{Ic}, is used for all fracture toughness test results even when the a/t ratio exceeds 0.5. No attempt is made to determine the limit values of a/t ratio where the K_{Ic} parameter should or should not be used. The ASTM E-24 Committee recommends a 0.5 limit for a/t for K_{Ic} designation. This limit was arbitrarily selected on a tentative basis because very limited available test data exists for specimens containing large cracks. At this time, there is not sufficient data available to definitely establish limits for a/t ratio with the surface-crack type tensile specimen. As more test data become available, the influence of a wide

range of a/t ratio on K_{Ic} values for different materials and strength levels will be more clearly understood and the establishment of definite a/t ratio limits may be possible.

The effect of ultimate strength level on K_{Ic} at constant a/t ratios for 3/8 and 3/4 inch surface-crack specimens is shown in Figure 111. From this graph, it is not as clearly evident that K_{Ic} increases with ultimate strength level as was shown previously in the residual strength vs crack size plots. (Figures 100 and 102).

The effects of cyclic crack propagation stress ratio (R) on K_{Ic} values for 3/8, 1/8, and 3/4 inch plate surface-crack specimens at constant a/t ratios are presented in Figures 112 and 113. A definite effect is not clearly evident although a tendency for K_{Ic} to increase slightly with an increase in stress ratio is shown for 3/8 and 3/4 inch plate specimens. The increasing stress ratio can also be interpreted as a decreasing pre-cracking rate for a majority of the specimens.

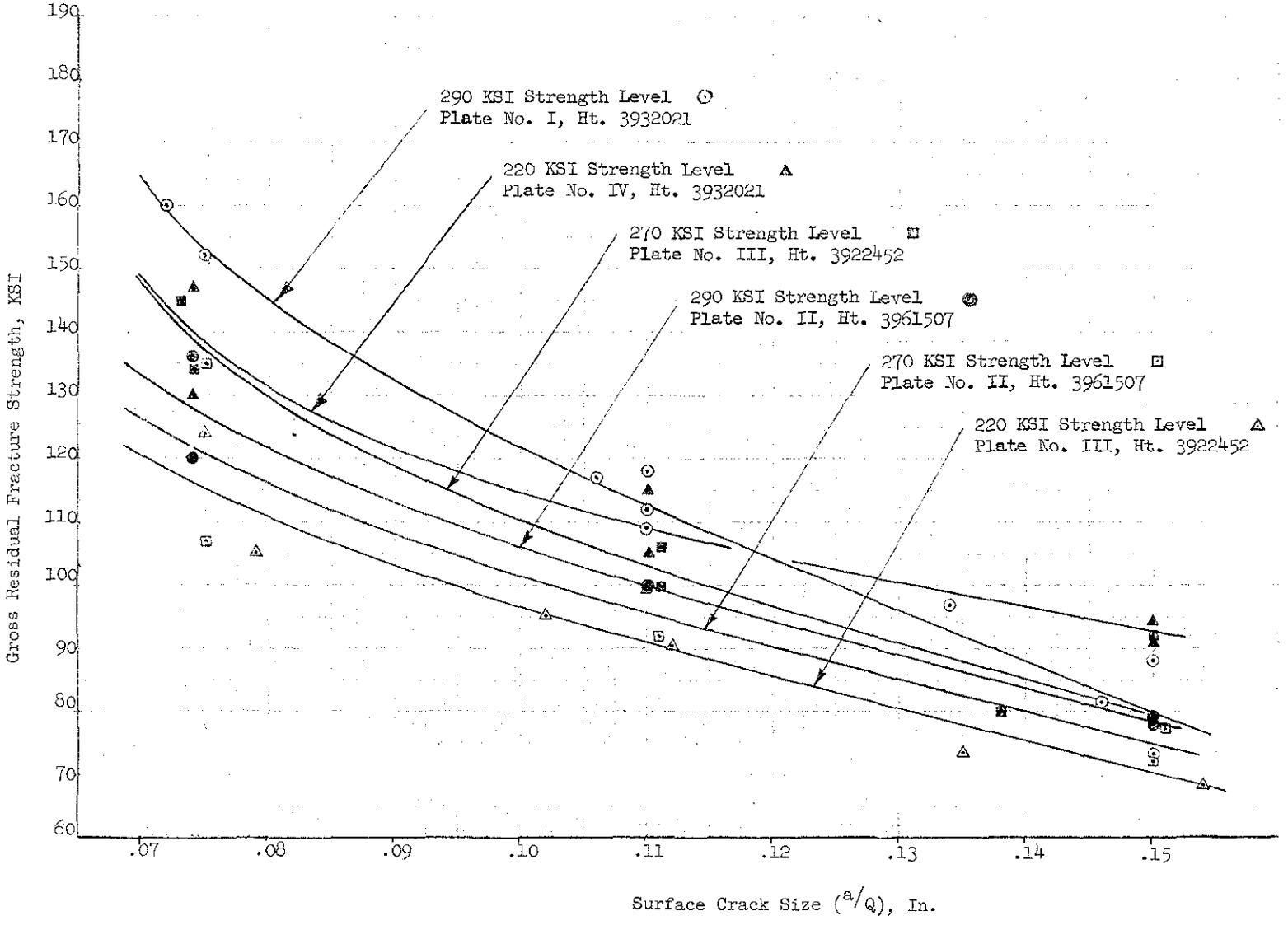

Figure 100 Effect of Surface-Crack Size on Residual Fracture Strength of 3/8 inch 300 M Steel Plate

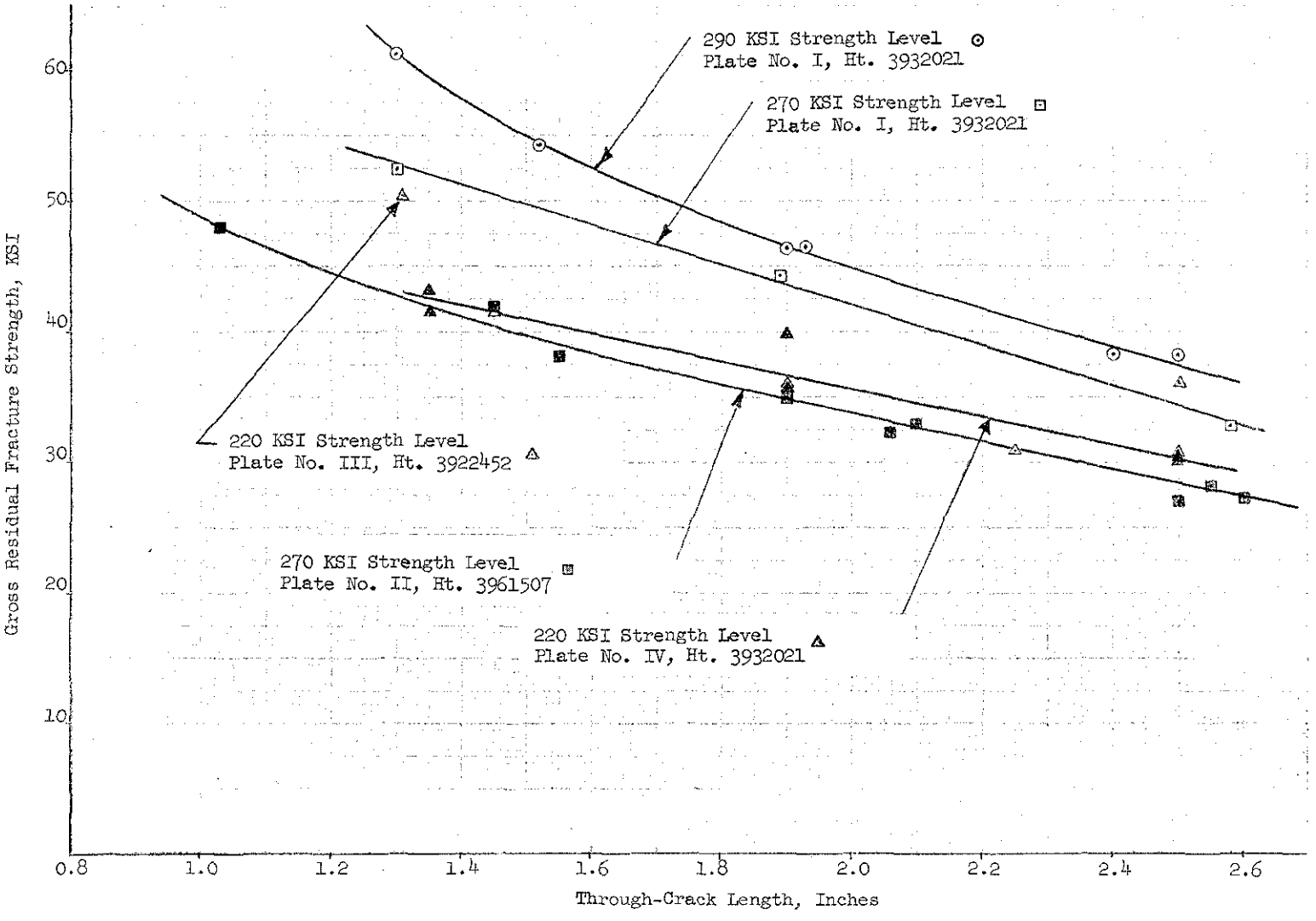

Figure 101 Effect of Through-Crack Length on Residual Fracture Strength of 3/8 Inch 300 M Steel Plate.

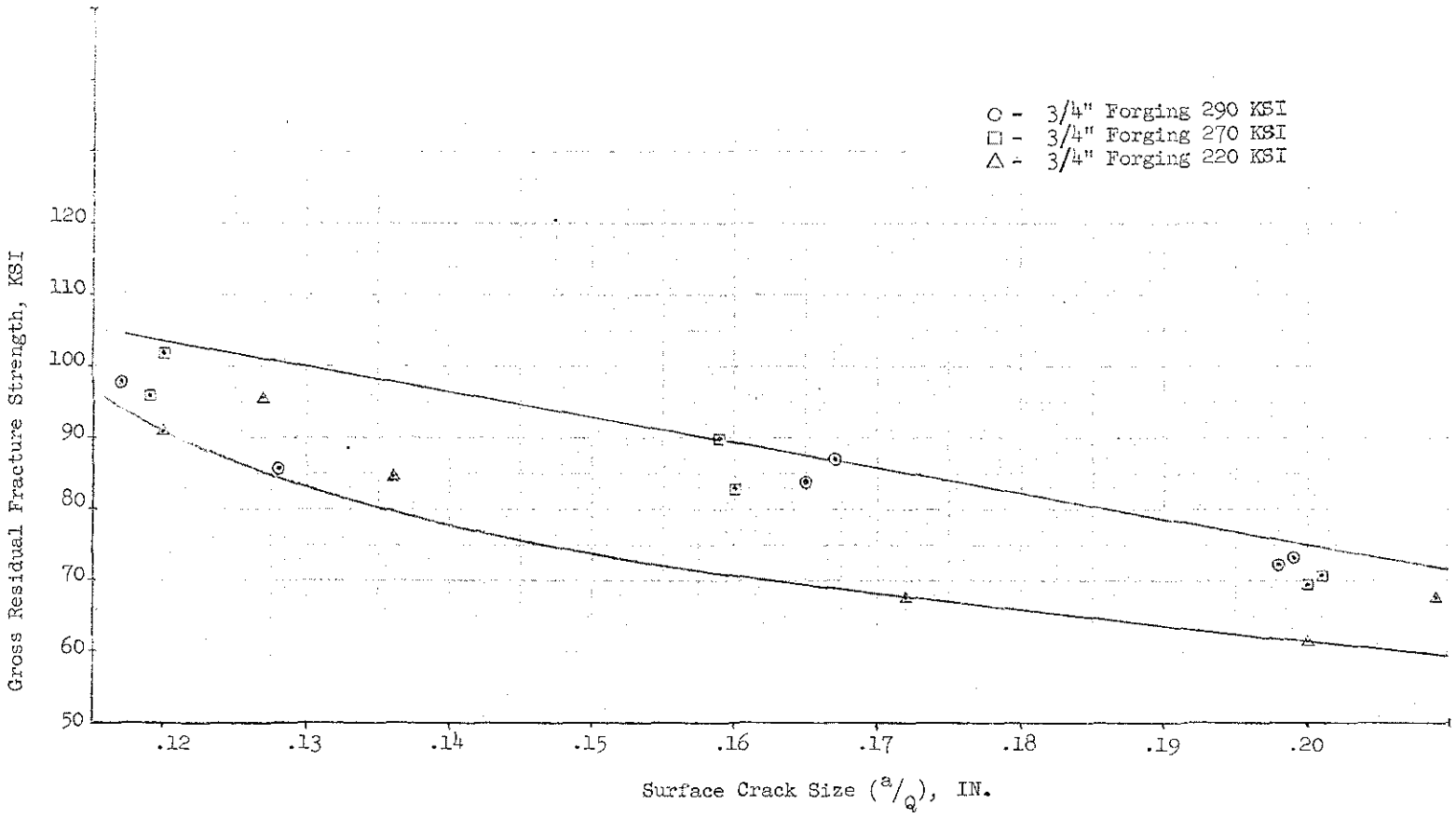

Figure 102 Effect of Surface-Crack Size on Residual Fracture Strength of 3/4 Inch 300 M Steel Forgings

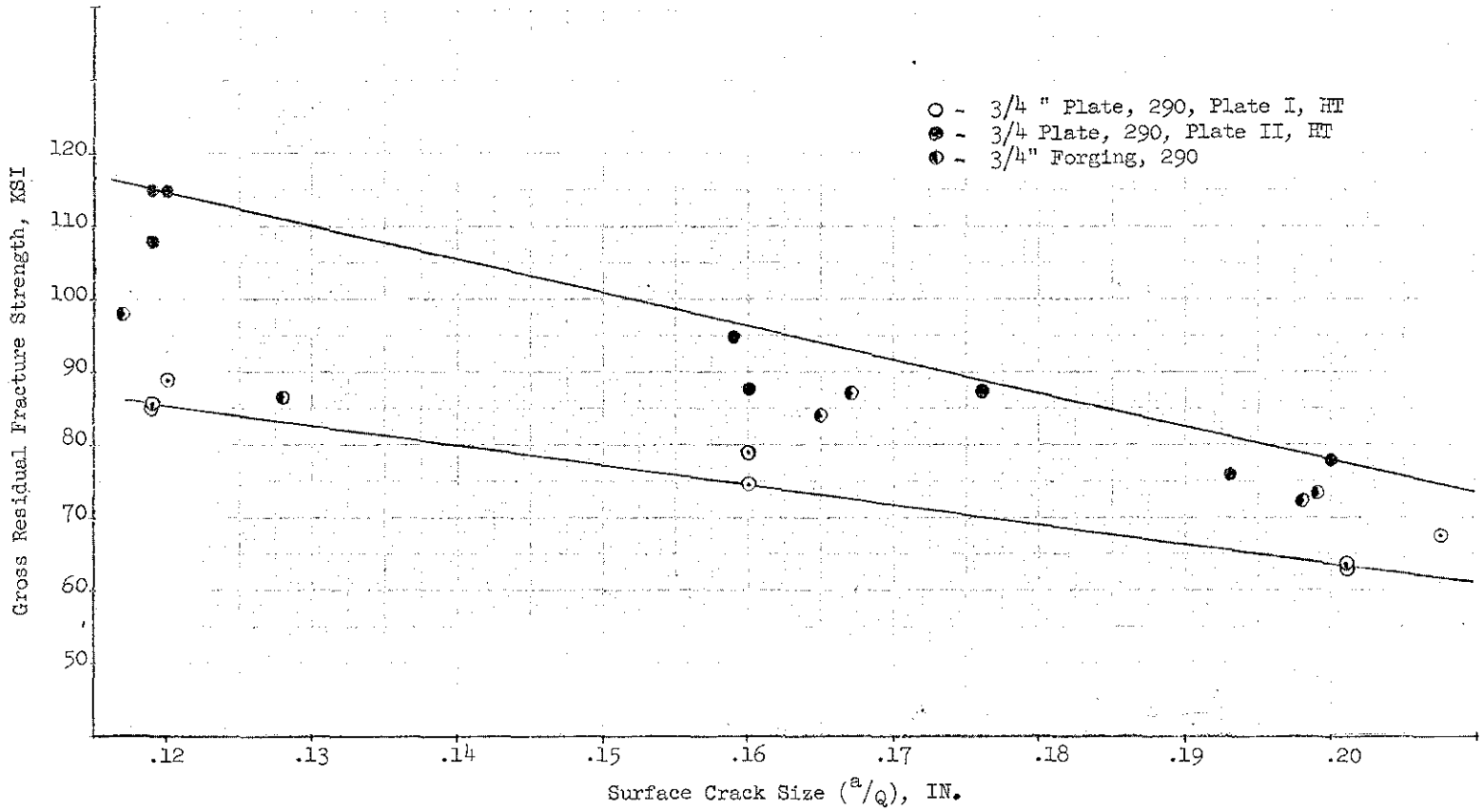

Figure 103 Effect of Surface-Crack Size on Residual Fracture Strength of 3/4 Inch 300 M Steel Plate

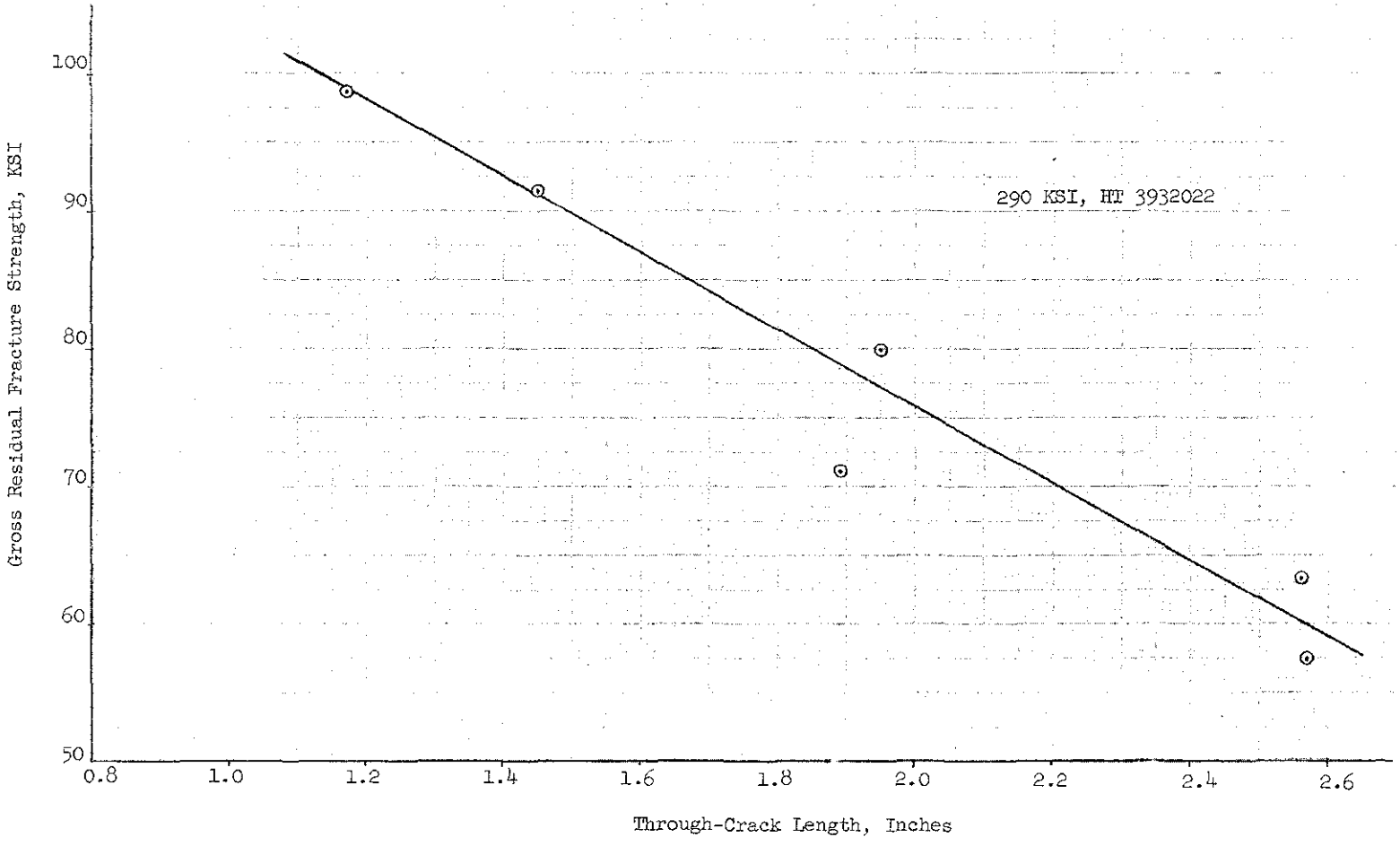

Figure 104 Effect of Through-Crack Length on Residual Fracture Strength of 1/8 Inch 300 M Steel Sheet

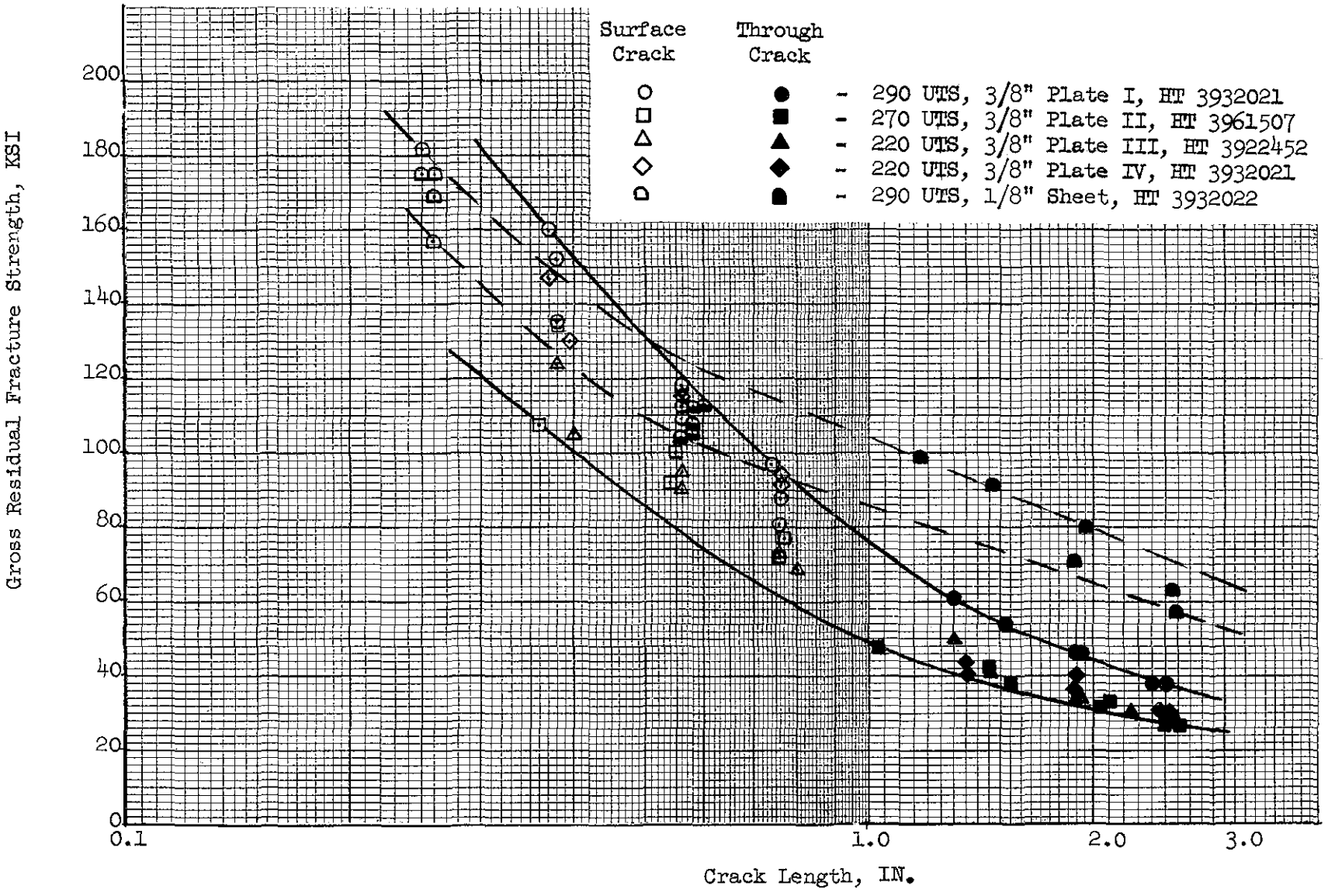

Figure 105 Effect of Surface-Crack and Through-Crack Length on Residual Fracture Strength of 300 M Steel Specimens.

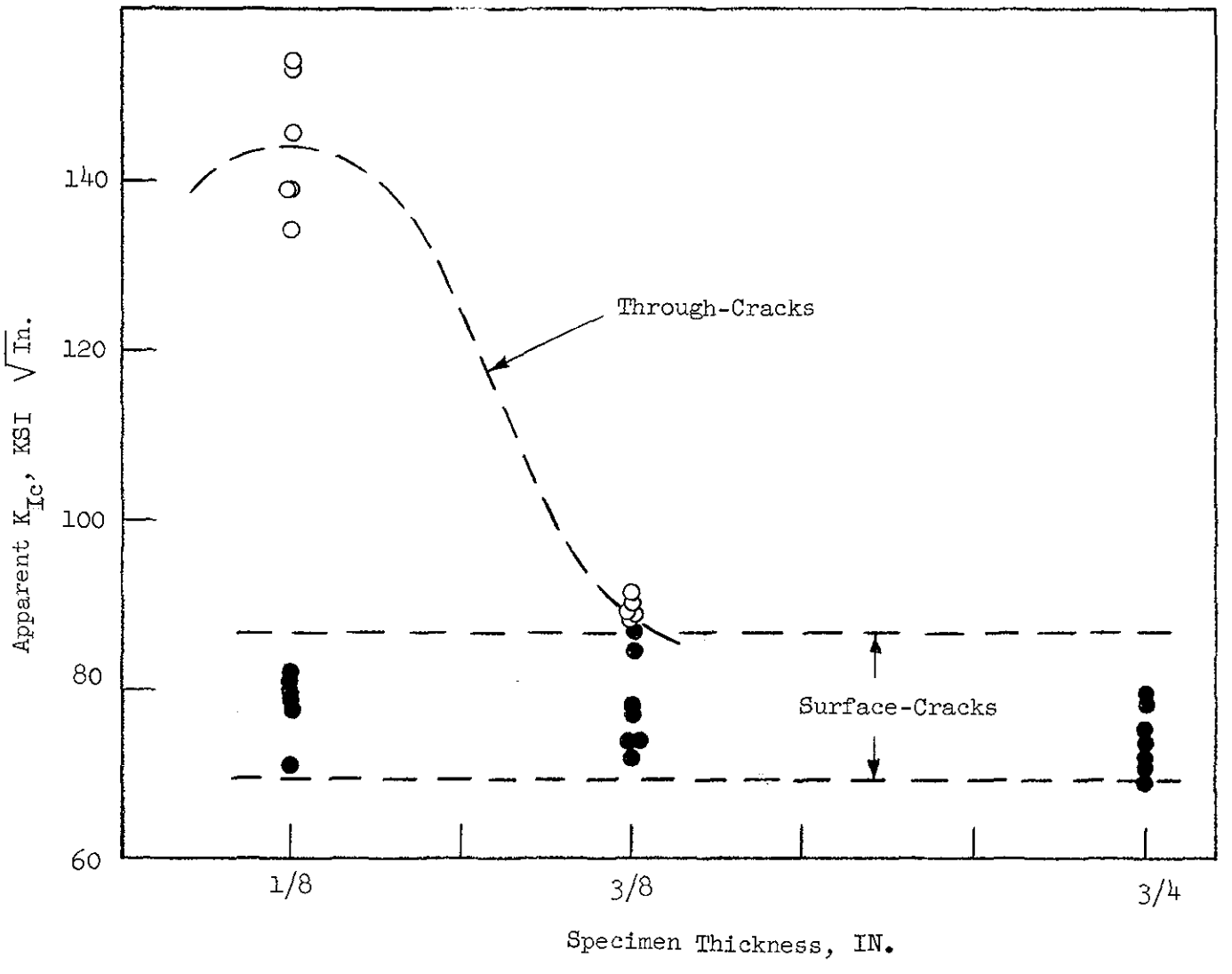

Figure 106 Effect of Specimen Thickness on Apparent K_{Ic} for 300 M Steel Surface-Crack and Through-Crack Specimens at F_{tu} 290 KSI

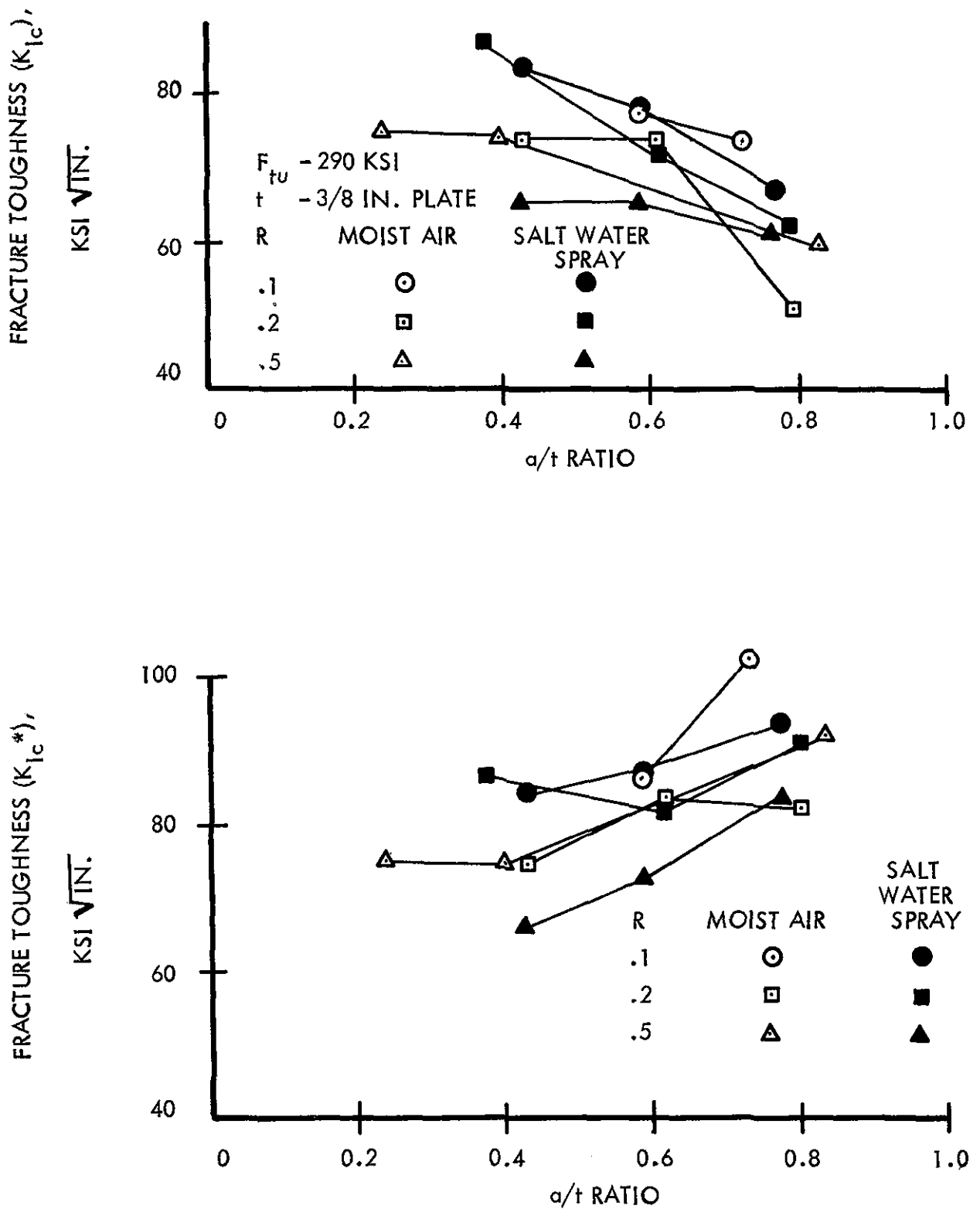

Figure 107 Effect of Crack Depth to Specimen Thickness Ratio on K_{Ic} and K_{Ic}* for 300 Steel Surface-Crack Specimens (290 KSI)

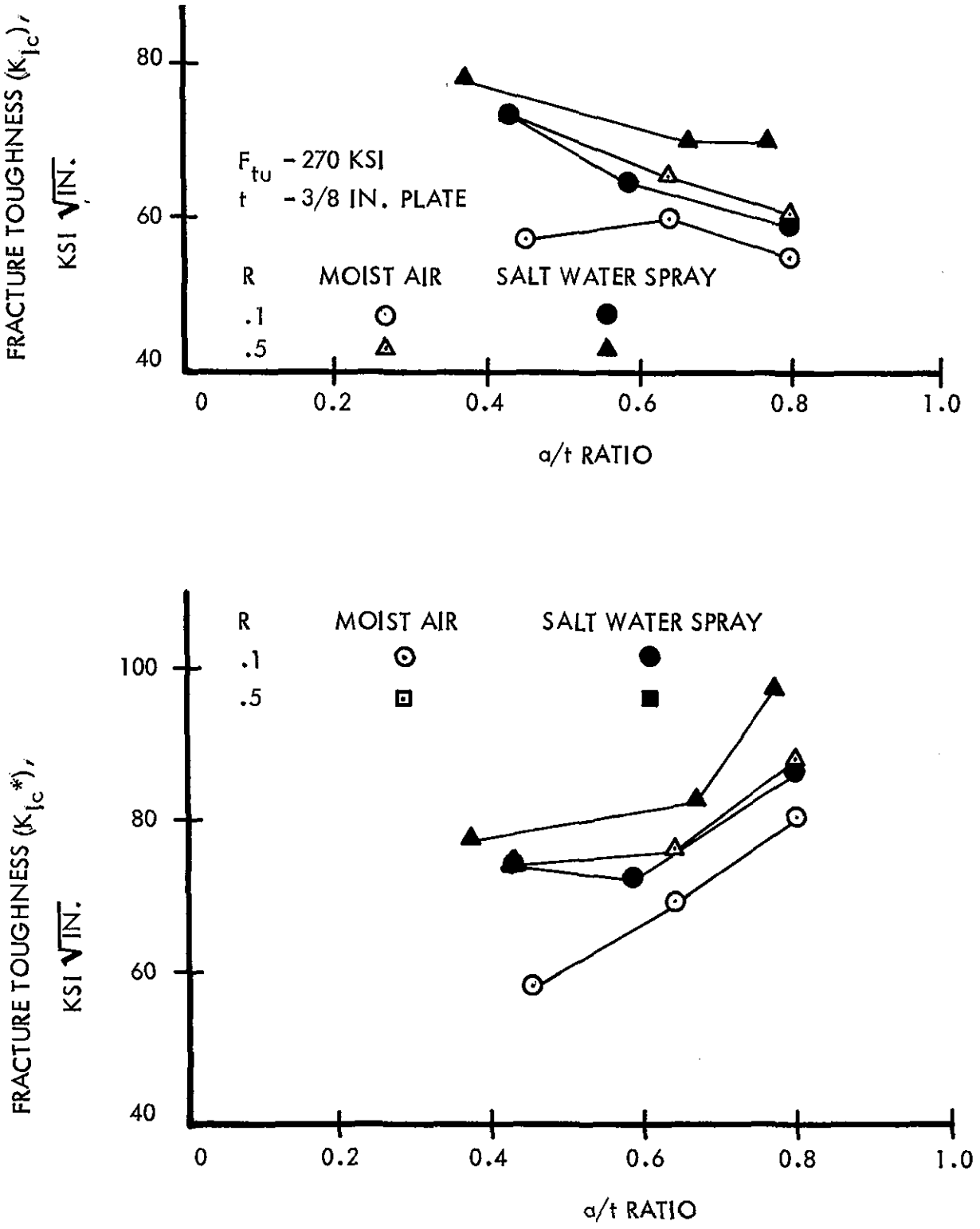

Figure 108 Effect of Crack Depth to Specimen Thickness Ratio on K_{Ic} and K_{Ic}* for 300 M Steel Surface-Crack Specimens (270 KSI)

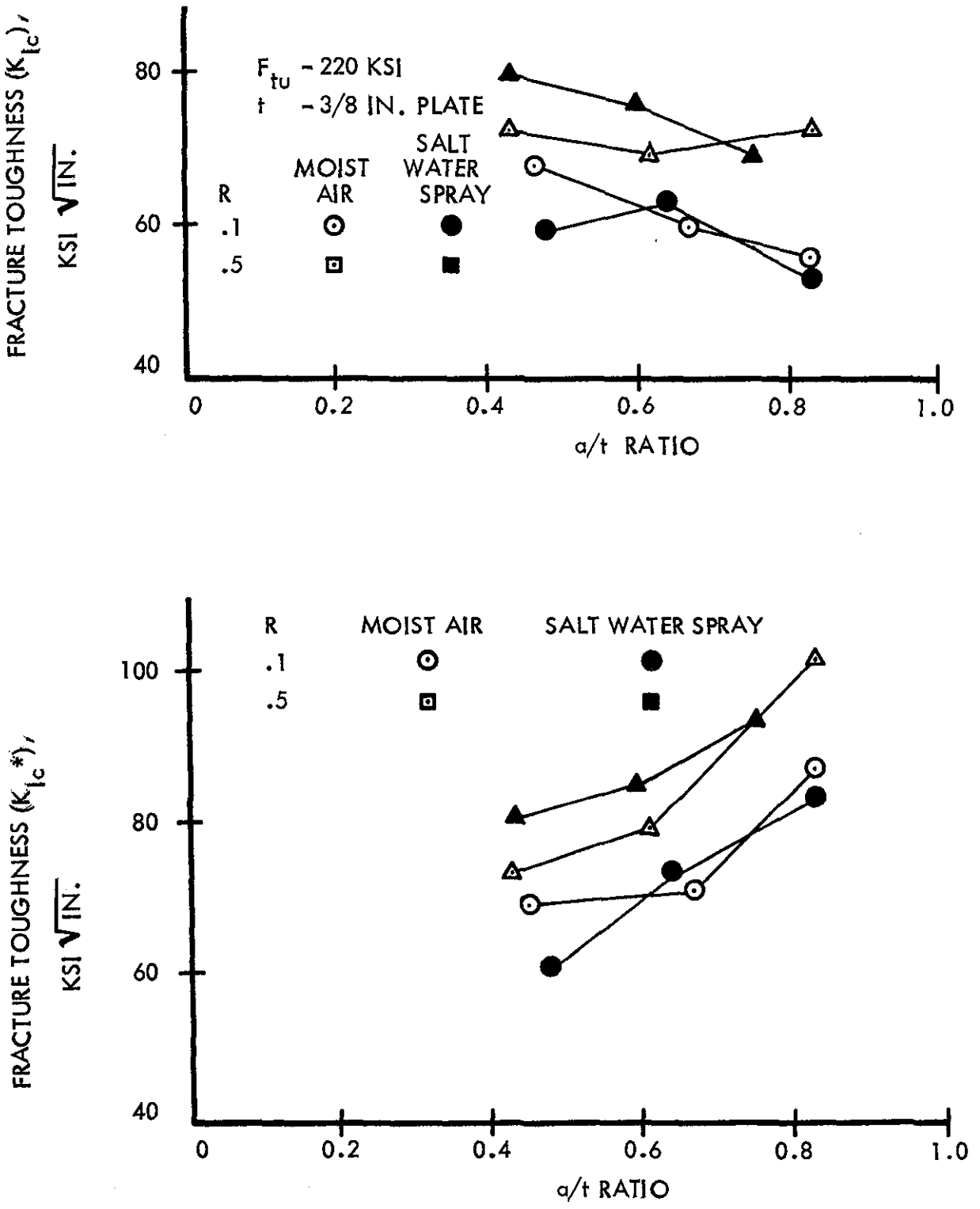

Figure 109 Effect of Crack Depth to Specimen Thickness Ratio on K_{Ic} and K_{Ic}* for 300 M Steel Surface-Crack Specimens (220 KSI)

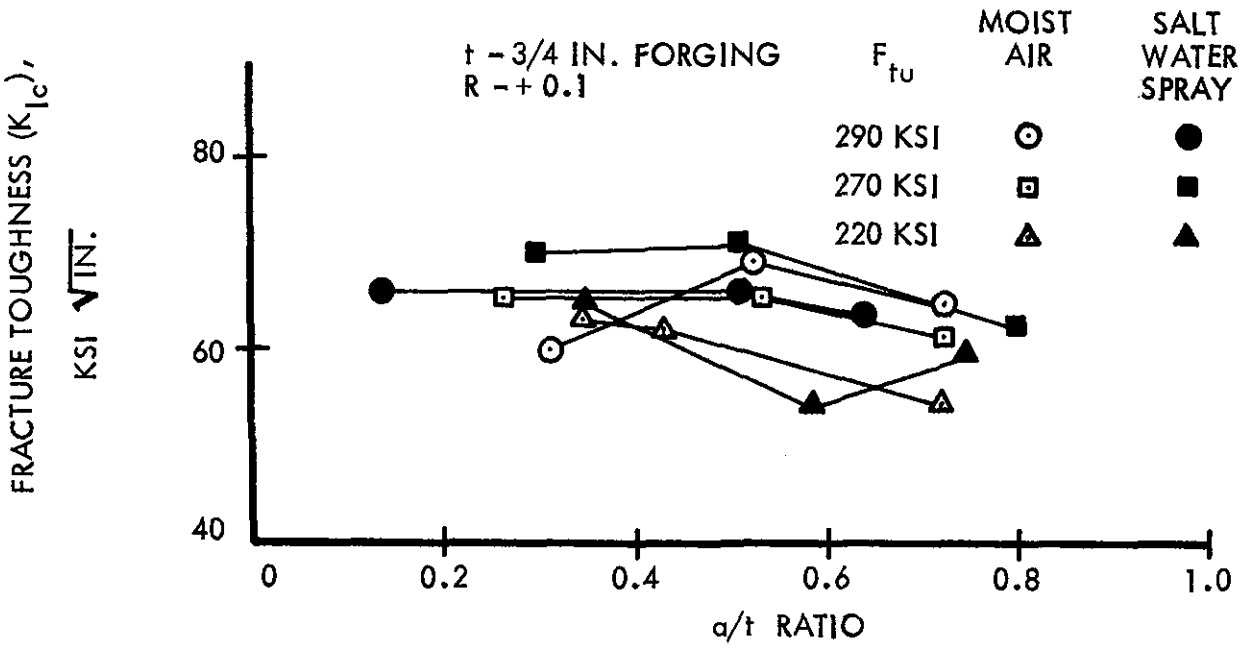

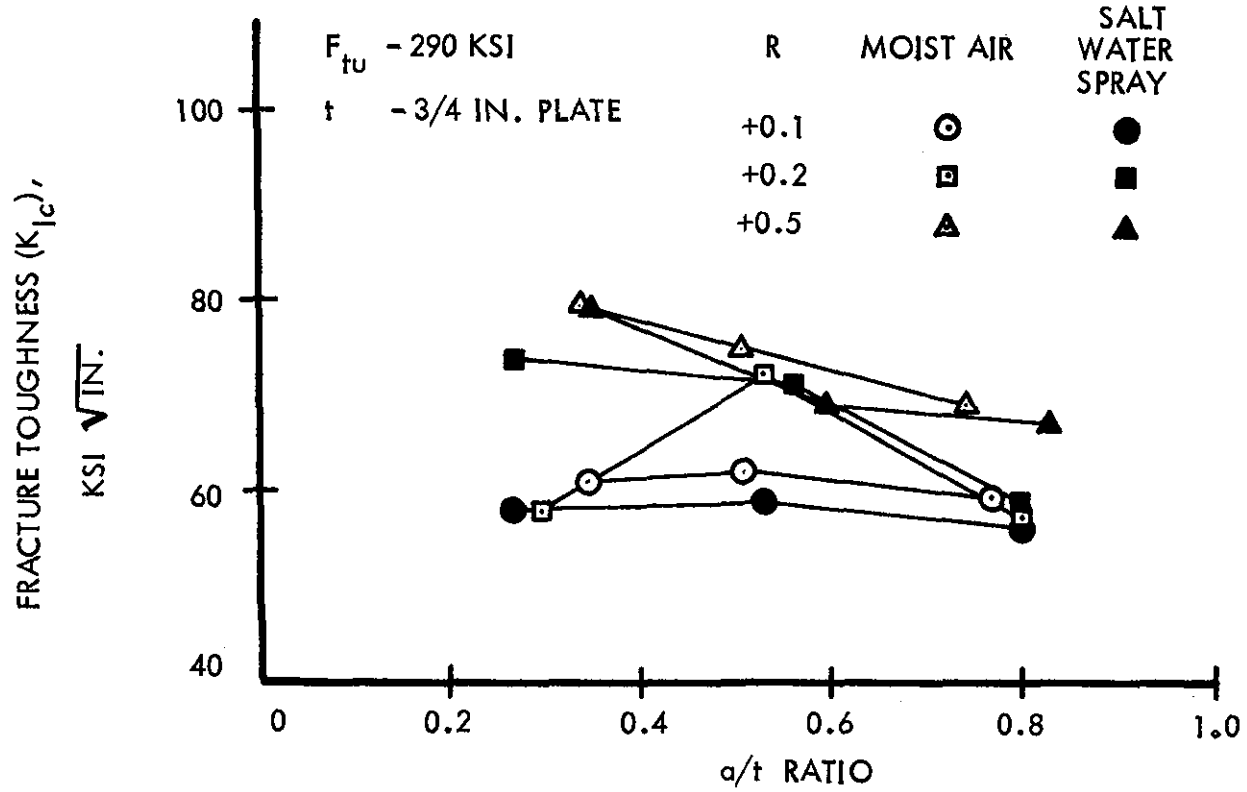

Figure 110 Effect of Crack Depth to Specimen Thickness Ratio on K_{Ic} for 300 M Steel Surface-Crack Specimens (3/4" Thickness)

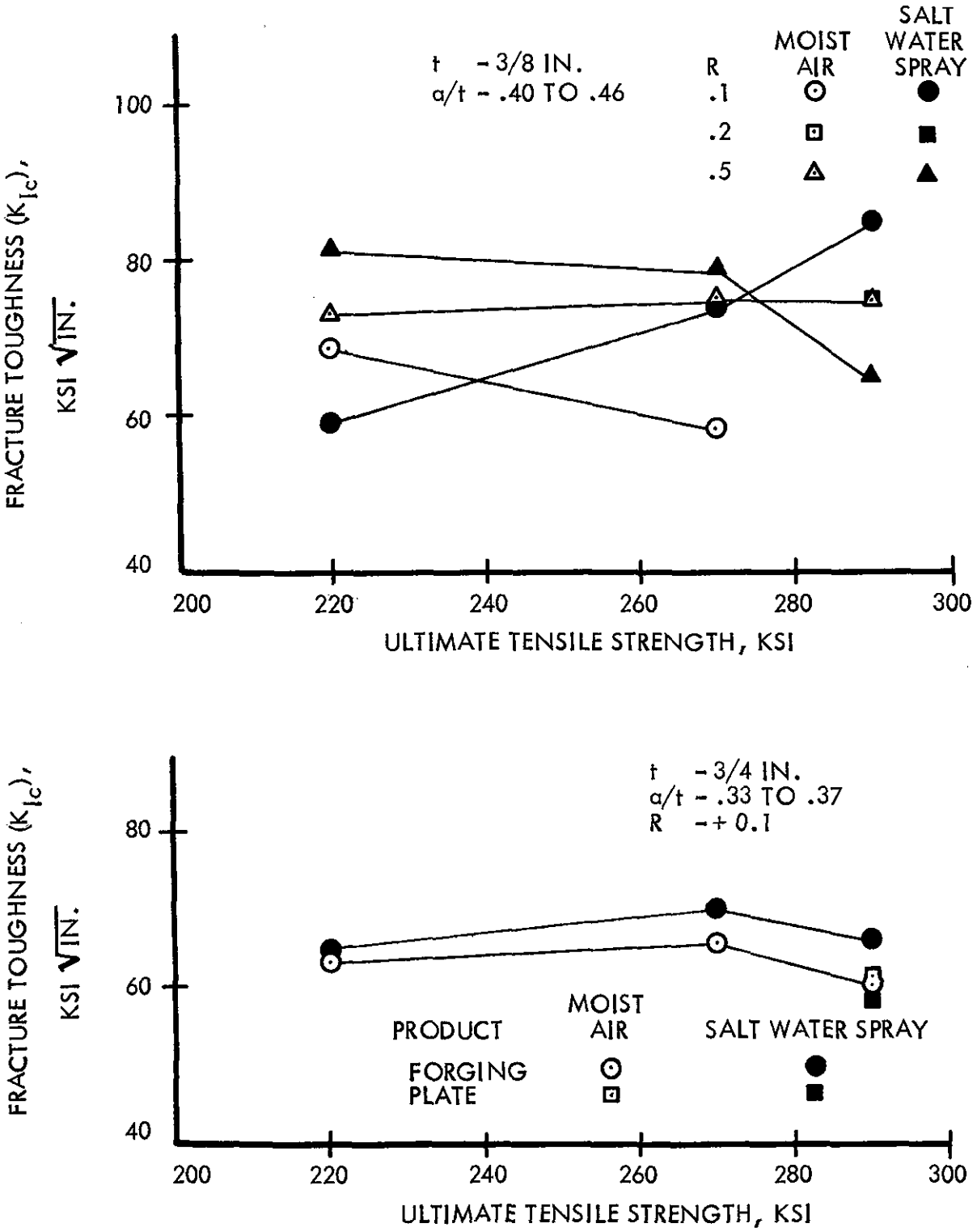

Figure 111 Effect of Ultimate Tensile Strength on K_{Ic} for 300 M Steel Surface-Crack Specimens. (3/8" and 3/4" Thickness)

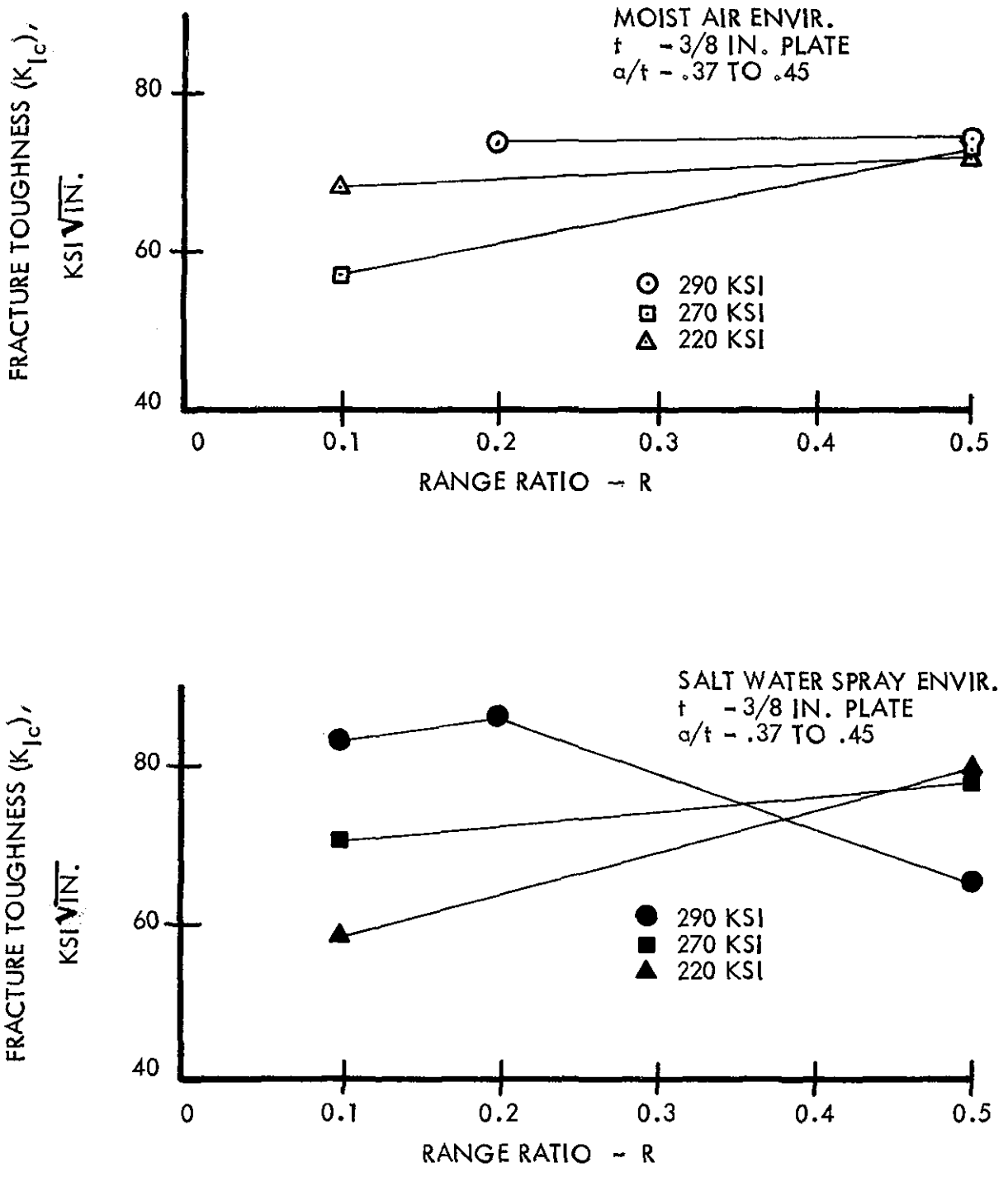

Figure 112 Effect of Range Ratio on K_{Ic} for 300 M Steel Surface-Crack Specimens (3/8" Thickness)

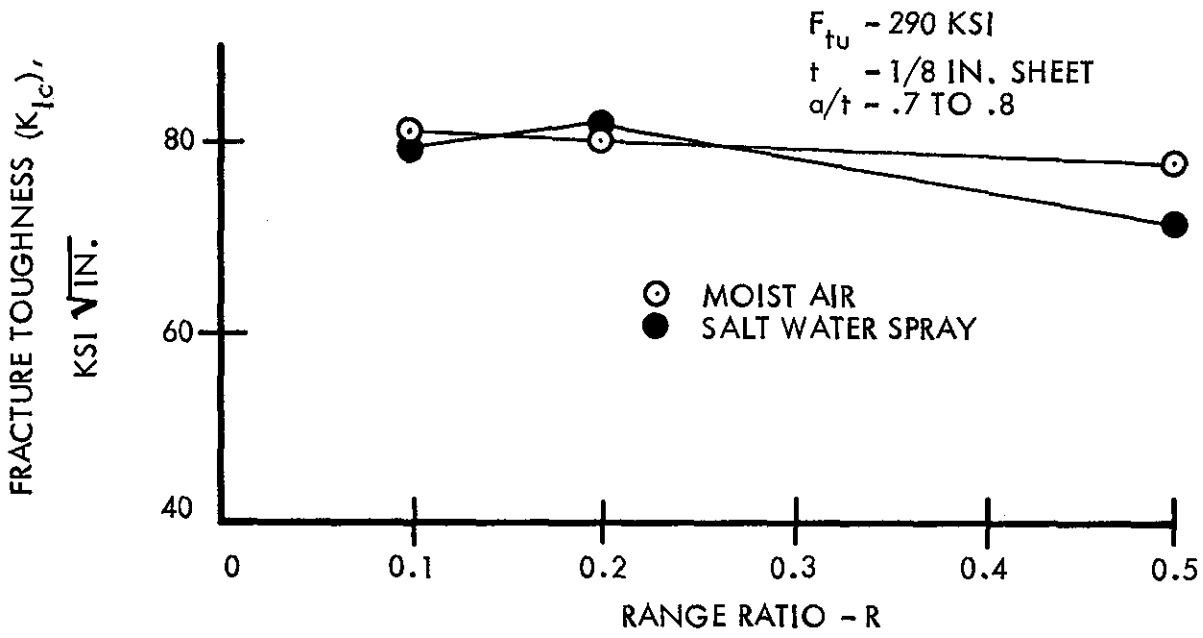

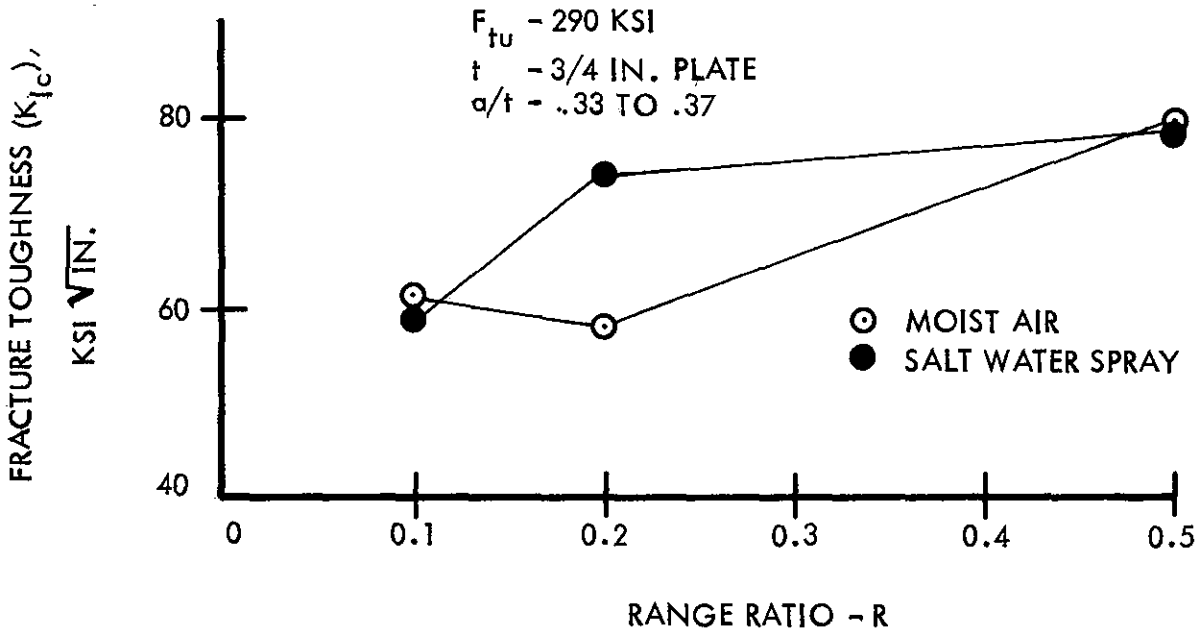

Figure 113 Effect of Range Ratio on K_{Ic} for 300 M Steel Surface-Crack Specimens (1/8" and 3/4" Thickness)

INTERRELATIONSHIP BETWEEN FRACTURE TOUGHNESS AND CRACK GROWTH RATES

In Section IV it was shown that the 220 KSI strength level material has the lowest fracture toughness. In Section IV the cracking rates for the 220 KSI strength level were shown to be highest for large values of $\Delta\overline{K}$. At lower values of $\Delta\overline{K}$, the cracking rates of the 220 KSI strength level were approximately the same as those of the other strength levels. The above would suggest that equation (18) which includes K_{Ic} might provide better data correlation than $\Delta\overline{K}$ equation(21). To check this point the extremes in toughness, 220 KSI and 290 KSI data, are compared for through-cracks at R = 0.1 (Figure 114). These data provide the highest ΔK_i values and this will show the greatest extent of convergence of the 220 KSI crack growth data with that of 290 KSI. While the data plotted on Figure 114 shows less spread between the 220 KSI and 290 KSI data than that using $\Delta\overline{K}$ (Figure 89), the trend to higher cracking rates for the 220 KSI data is still apparent.

Another possible way to include the influence of K_{Ic} would be to plot K/K_{Ic} as abscissa rather than $\Delta\overline{K}$. This later approach would not improve the overall correlation as it would tend to separate the 220 KSI data from the 270 and 290 KSI data at the lower cracking rates.

Based on the above, it appears that there is a general trend to higher cracking rates in 300 M steel with decreasing K_{Ic} in the 290 to 220 KSI range and that the mathematical relationships between K_{Ic} and rate are not adequately defined by available crack growth rate equations. This viewpoint is supported by reference 15 which evaluated the dependence of fatigue crack growth rate d(2c)/dN on fracture toughness for 4340, H-11, and on 18-Ni maraging steel. In this study the cracking rate d(2c)/dN was found to be approximately 300 μ inches/cycle when ΔK_i was approximately equal to K_{Ic}. An inverse relationship between n of equation 15 and K_{Ic} was suggested, although none of the available equations provided a satisfactory mathematical relationship between the two. This later observation, that n varies inversely with K_{Ic}, is consistent with the observed cracking behavior of the 220 KSI data. Had these and other data been plotted on log-log paper as suggested by equation 15, the slope (n) associated with the 220 KSI data would have been greater. It is important to note that the observation of higher cracking rate of 300 M at the 220 KSI strength level compared to the 270-290 KSI can not be assumed to be representative of cracking behavior in other low alloy steels. Tempering of the 300 M to the 220 KSI strength level did not produce an increase in K_{Ic} over that of the 290 KSI strength level. However further tempering of 300 M to reduce the strength below 200 KSI would be expected to raise K_{Ic} values. It is also known that certain low alloys steels such as 4330 exhibit higher K_{Ic} values at 220 KSI ultimate tensile strength than at higher strength levels.

The observation that a finite cracking rate occurred at K_{Ic} for several high strength steels (reference 15) also deserves comment with respect to the proper K_{cr} value to use in equation 18. In developing the comparison Figures 89 and 114, K_{cr} was assumed to be K_{Ic}. It has been

shown that high pre-cracking stress levels (very close to K_{Ic}) can result in an increase in measured fracture toughness, for some high strength steels (reference 16). This behavior is rationally acceptable inasmuch as cyclic strain softening near the notch tip most likely occurs in many high strength materials. For some high strength materials it is therefore possible that $Kcr > K_{Ic}$. The use of a value of $Kcr > K_{Ic}$ in equation 18 and thus for developing Figure 114 would tend to increase the data spread between the 220 KSI and 290 KSI data.

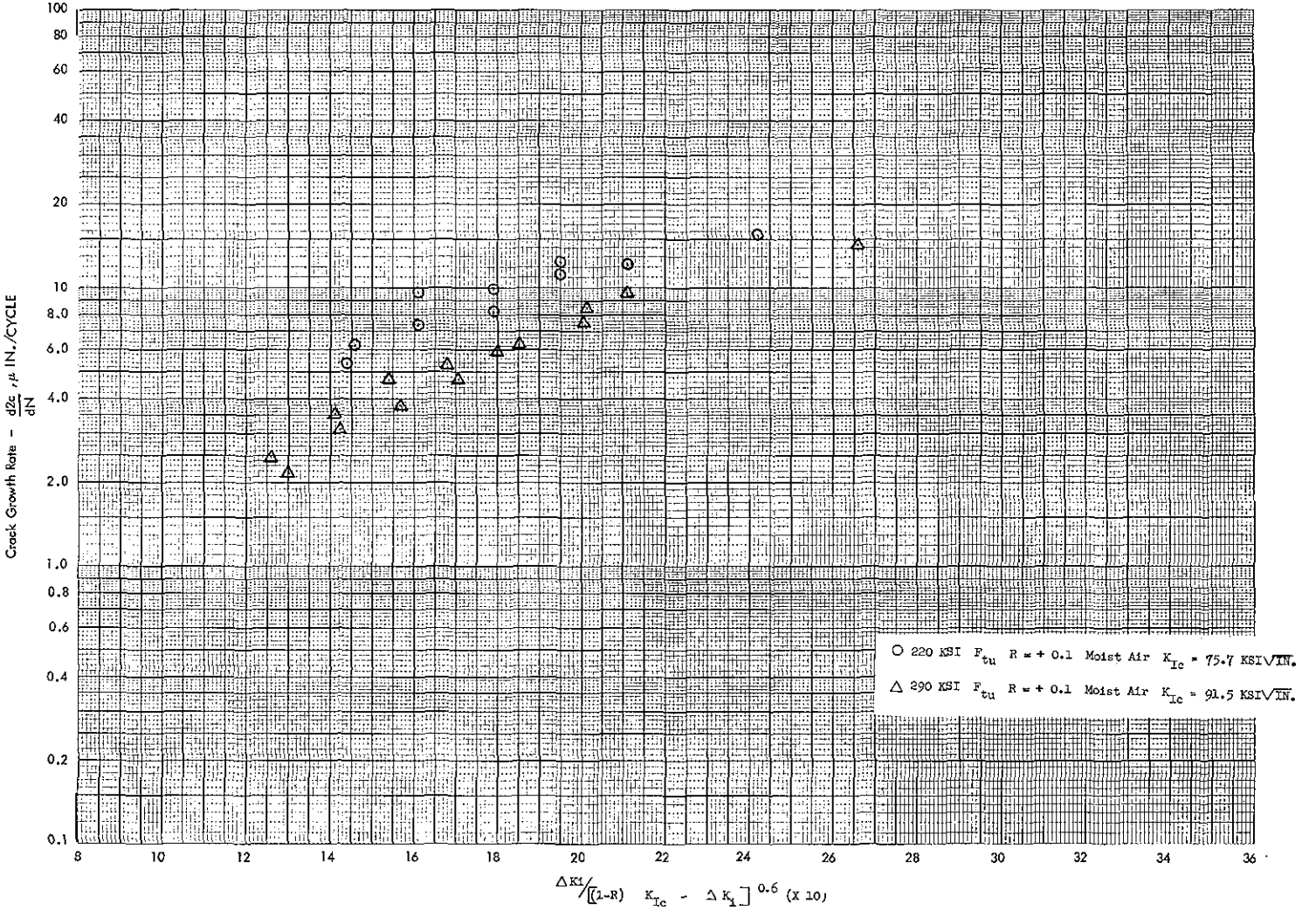

Figure 114 Relationship Between K_{Ic} and Cyclic Cracking Rate For Through-Crack Specimens

Section V

DATA PRESENTATION METHODS

The state of art of fracture mechanics has not yet resolved to a single method of relating information on material fracture toughness and cracking rates to design goals of toughness and slow crack propagation. For high strength materials, fracture mechanics based methods appear most applicable, and K_{Ic} values will soon be included in MIL HDBK 5 (Reference 18). Methods of presentation for crack growth rate behavior now need to be considered. In view of the diverse approaches concerning design requirements, applications, procedures, and even theoretical aspects of the problem, it is not appropriate to restrict considerations to a single method of data presentation at this time. Therefore, several approaches to presenting crack growth data will be discussed.

CRACK GROWTH INDEX

For the requirements for material selection or screening, it would be convenient to have a single index of cracking rate.

Though such an index may not be suitable for quantitative analysis, it could aid in initial material evaluations. The cracking rate (μ inches/cycle) for a standard stress intensity level is suggested for this purpose. This standard stress intensity could be either a selected absolute value for a class of materials, or a percentage of K_{Ic} or F_{tu}. If the stress intensity selected is consistent with pre-cracking requirements for K_{Ic}, the index could be economically obtained during the pre-cracking which precedes K_{Ic} measurement. These indices could then be tabulated with K_{Ic} values for the material.

STRESS INTENSITY-RATE PLOT (log-log)

The cracking rate index approach to data presentation has serious shortcomings in providing information for quantitative design. The simplest method of data presentation which provides useful quantitative design information is the rate vs stress intensity plot. The rate vs intensity plot can be either log-log or log-linear. Of the two, the log-log plot is less complex. While it is the least desirable as a form of presentation for analyzing differences between data, it has considerable merit for final data presentation. For the straight line log-log fit, two quantities must be specified; intercept and slope. The intercept of the straight line fit on a log-log plot at $d2c/dN = 1$ would provide a convenient index and can be considered as an alternate to the index discussed in the preceding paragraphs. As shown on Figure 99, the observation that through the thickness and surface flaws can have parallel straight lines on a log-log fit of data may be significant as the slope (n) properly defined may well be a material constant. However, the sensitivity of the slope (n) to methods of measuring crack length and/or computing stress intensity as pointed out in Section IV should be carefully considered.

It would appear from the program results and as supported by data in Reference (14)that the influence of stress ratio R for positive minimum stresses could be accounted for by using a modified stress intensity parameter $\Delta\overline{K}$ (Equation 21). While Section IV discusses an alternate method of accounting for stress ratio involving K_{Ic}, the latter is not recommended at this time as it did not adequately account for variance in cracking rate with K_{Ic} (Section IV for the 220 KSI strength level data of this program. It is probably better to treat the stress ratio problem separately from variance in rate with K_{Ic} until the relationship between rate and K_{Ic} is more clearly established.

Summing up these observations on the log-log plot of $\Delta\overline{K}$ vs. log rate, Figure 115 illustrates a suggested figure for log-log data presentation.

STRESS INTENSITY-RATE PLOT (log-linear)

The log rate vs. $\Delta\overline{K}$ on a linear scale provides additional freedom in data fitting. In studying large amounts of crack growth data (Reference 19 agreement was found between the break in slope on a log-linear plot and the rotation of through the thickness cracks from the tensile to shear mode cracking. For approximately the same cracking rates for part through cracks, References 20, 21 observed changes in cracking mechanisms. Based on these and similar observations, the knee which appears on the log-linear plot of rate vs. $\Delta\overline{K}$ may have real physical significance. If this is confirmed by further study, the semi-log plot would be preferred to the log-log plot as the latter tends to suppress the break in slope. A careful study of log-log figures such as presented in Reference 8 will show a deviation from the straight line log-log fit near where this knee is observed on a semi-log plot (Reference 20). There is thus evidence to support preference of a semi-log plot as the most physically meaningful form of data presentation. Figure 116 illustrates a suggested form of data presentation of this type.

CRACK GROWTH RATE-STRESS-CRACK LENGTH PLOTS

From a study of program results for 3/8 inch thick material, the fracture toughness varies with a/t ratio (Section IV). Also, for a given cracking rate, computed stress intensities vary for through the thickness and part through flaws. For thorough definition of crack growth fracture behavior for this or other thicknesses where crack growth from surface cracks to through the thickness cracks are probable, geometric parameters need be considered. A simple way of accomplishing this is shown in Figure 117. Using stress as ordinate and crack length (2c) as abscissa, values of rate are plotted as points. Curves of constant rate are drawn through the data. In this manner, no relationship between stress intensity and rate need be assumed. A curve of critical fracture toughness may be established in the same manner. Using this procedure, a single diagram could define the cracking behavior of a single thickness of material.

DIAGRAMS SHOWING STRESS RATIO INFLUENCE

The results of this program include only cyclic stresses in which the minimum cyclic stress is positive. It is thus known whether $\Delta\overline{K}$ determined using m=1/3 for 300 M steel should also apply to cases where minimum cyclic stresses are compressive. A simple method of data presentation including the stress ratio variable would be a modification of the Goodman Diagram (Figure 118). Its range of application would include cases where the influence of thickness need not be considered so that cracking rates could be interpreted in terms of stress intensity parameters.

OTHER VARIABLES

In the above discussions the cracking rate for surface cracks has been presented in terms of $\frac{d(2c)}{dN}$. The experience gained in this program indicates that a and a/Q will have a nearly constant relationship to 2c. Should this not prove to be an acceptable approximation for all cases of interest, the discussion here will apply equally well to data presentation in terms of a or a/Q. As long as there is a near constant relationship however. There is considerable practical advantage in using 2c measurements as these are the observable lengths from a standpoint of inspection for cracks in service parts or in laboratory tests.

The program results show that for 300 M steel cracking rates and K_{Ic} are not overly sensitive to material variables or strength level. Standard K_{Ic} and rate data are thus practical for handbook use.

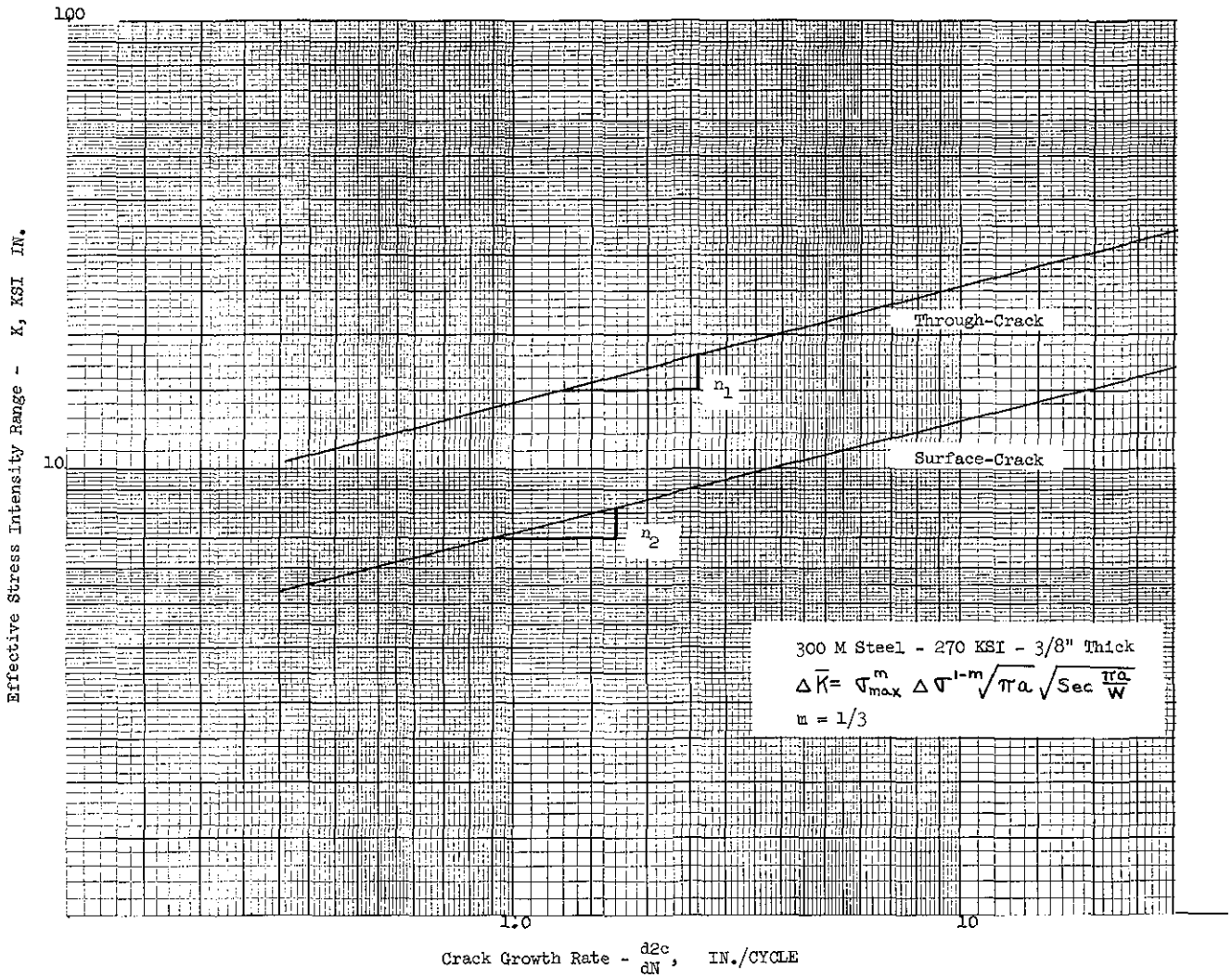

Figure 115 Stress Intensity - Rate Plot (Log-Log)

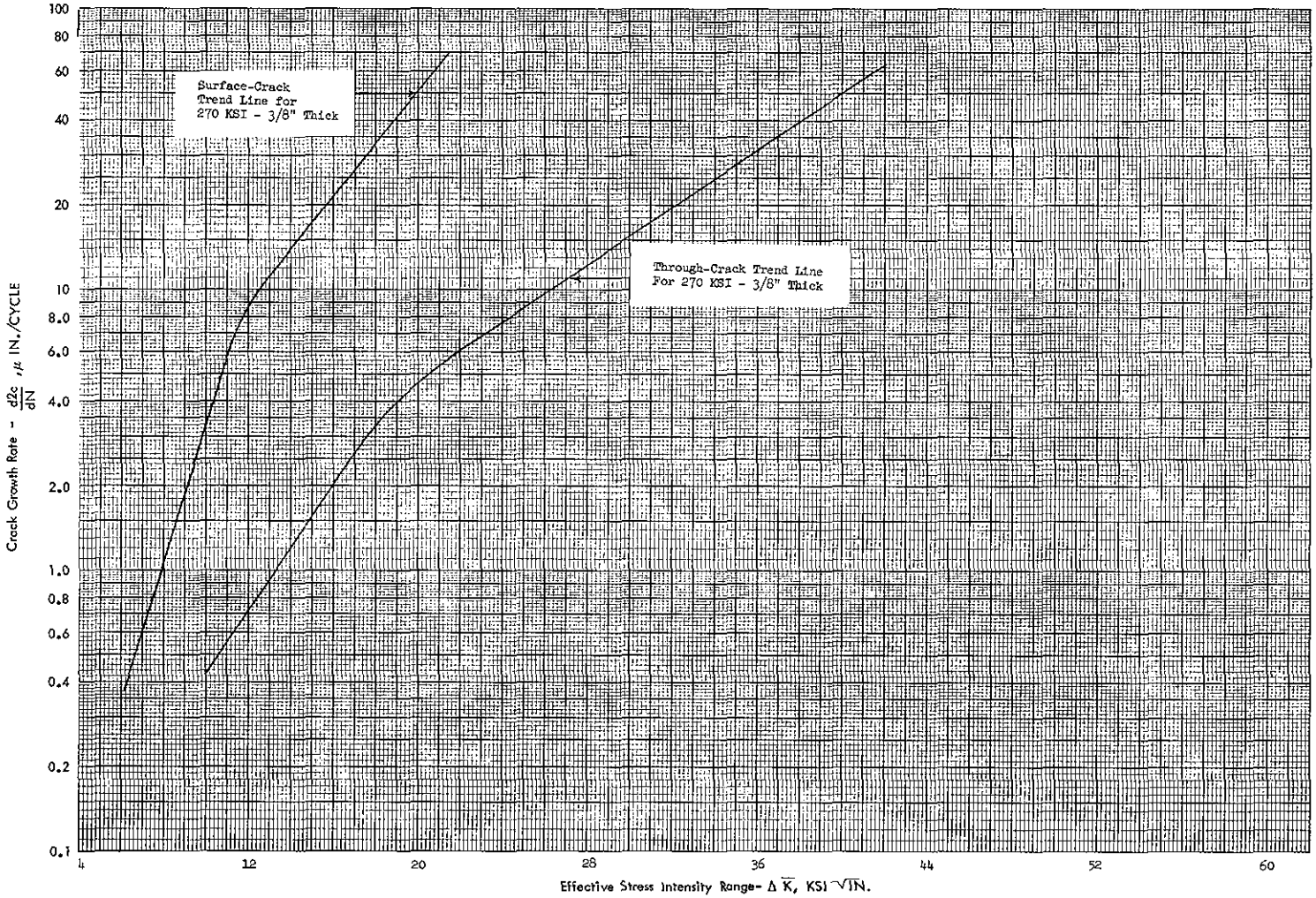

Figure 116 Stress Intensity - Rate Plot (Log - Linear)

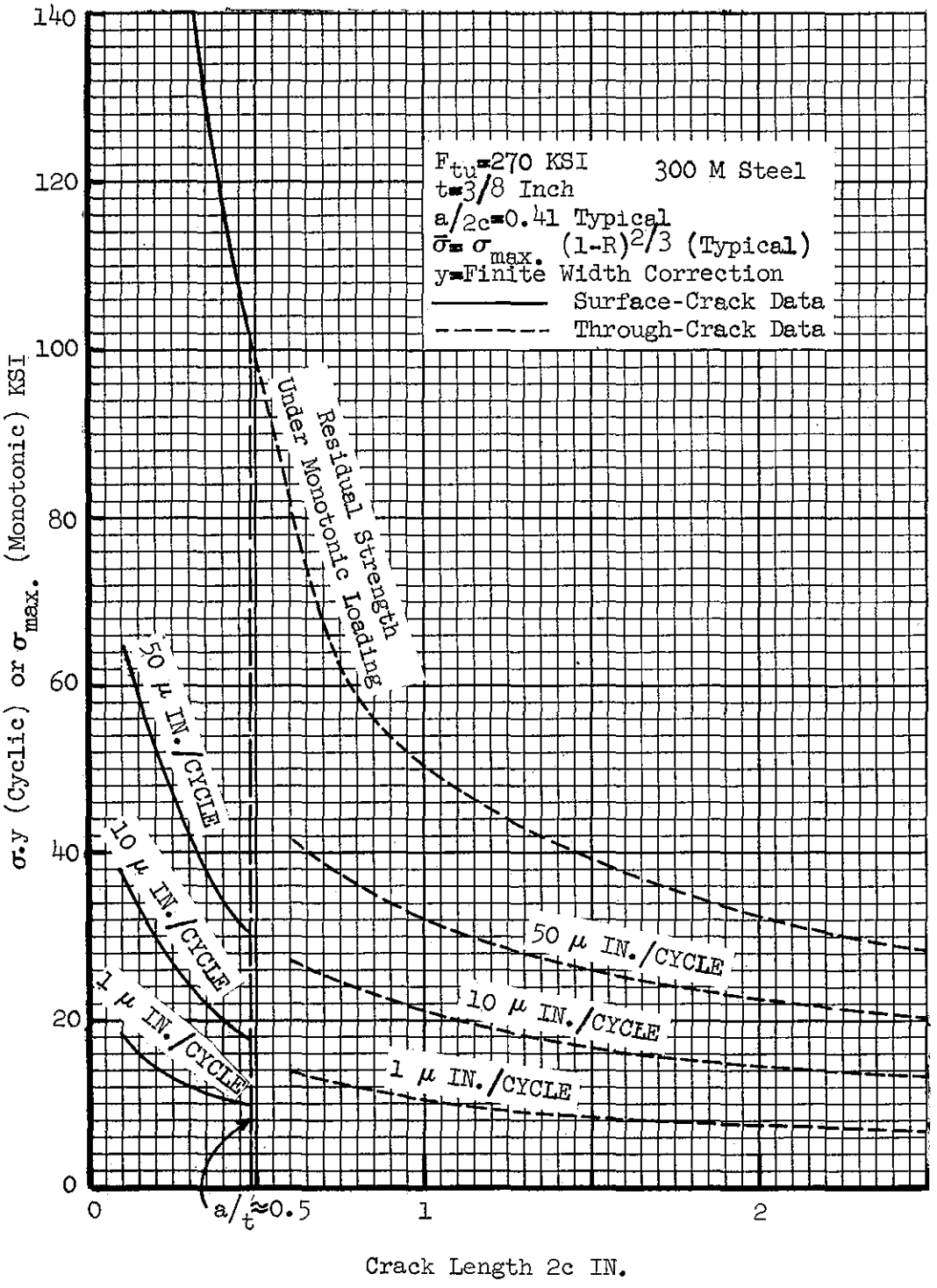

Figure 117 Crack Growth Rate-Stress-Crack Length Plot

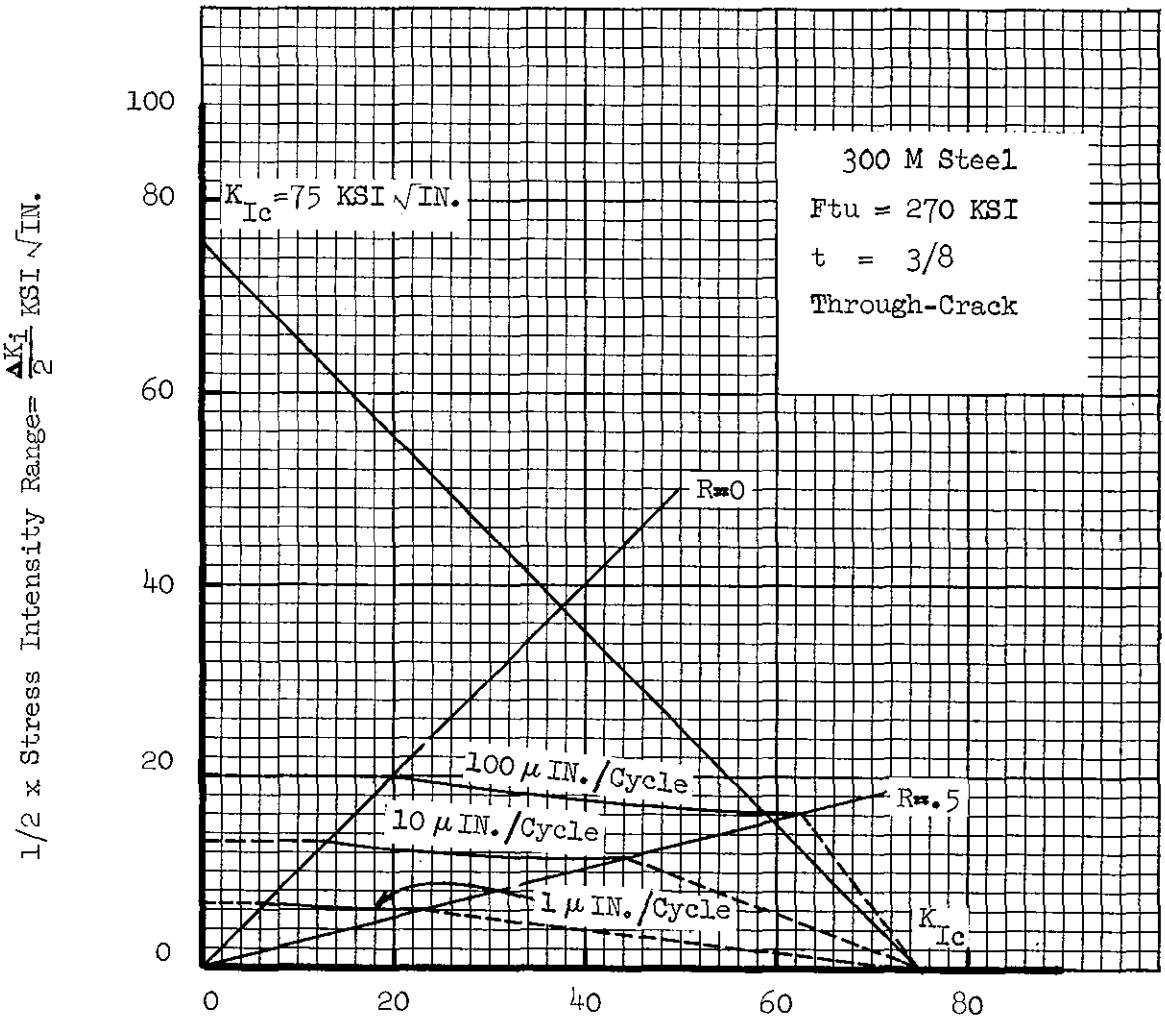

Figure 118 Modified Goodman Plot

CONCLUSIONS

It is concluded that:

1. Stress intensity methods show promise for fracture toughness and cyclic crack propagation data correlations for 300 M steel at high strength levels. Additional theoretical work needs to be accomplished for surface-cracks having a/t ratios greater than 0.5.

2. Methods suitable for handbook presentation are available. Final selection of presentation methods should be coordinated with intended use.

3. Plane-strain fracture toughness of 300 M steel was higher for 290 and 270 KSI ultimate strength levels than for 220 KSI ultimate strength level.

4. Variation of plane-strain fracture toughness was considerable for different heats of 300 M steel plate.

5. Plane-strain fracture toughness (K_{Ic}) values obtained from surface-crack specimens were similar for 1/8, 3/8, and 3/4 inch thick specimens.

6. Plane-strain fracture toughness (K_{Ic}) values obtained from through-crack specimens were considerably higher for 1/8 inch thick specimens than for 3/8 inch thick specimens. The K_{Ic} values for 3/8 inch thick specimens approached the values obtained from surface-crack specimens.

7. Plane-strain fracture toughness was essentially the same for 300 M steel sheet, plate, and forging products.

8. Plane-strain fracture toughness (K_{Ic}) values generally decreased as crack depth-to-specimen thickness ratio (a/t) increased from 0.3 to 0.8.

9. Cyclic propagating surface-cracks at a minimum-to-maximum stress ratio (R) of +0.5 generally resulted in slightly higher K_{Ic} values than at R ratios of +0.1 or +0.2.

10. The relationship between residual fracture strength and crack length was a single, continuous scatter band for both surface-crack and through-crack specimens.

11. Crack depth-to-crack length ratio (a/2c) remained essentially constant at approximately 0.4 during cyclic propagation of surface-cracks in all surface-crack specimens except when the surface-crack propagated through the specimen thickness in the 1/8 inch thick specimens.

12. Cyclic cracking rate (d2c/dN) was the same for 290 and 270 KSI strength 300 M steel. The 220 KSI strength material had a higher cracking rate at high stress intensities.

13. Variations in heats of material had no significant effect on cyclic cracking rates.

14. Surface-crack specimens exhibited larger computed $\Delta\overline{K}$ values than through-crack specimens at equal cracking rates (d2c/dN). The slope (n) of log d2c/dN vs log $\Delta\overline{K}$ was approximately equal to 1/5 and the same for both surface-crack and through-crack specimens. The slope (n) is sensitive to geometric variables and should not be considered as entirely a material constant.

15. For equal cracking rate (d2c/dN), computed stress intensities were higher for 3/4 inch thick surface-crack specimens than for 3/8 inch thick specimens. The 1/8 and 3/8 inch thick surface-crack and through-crack specimens exhibited similar cracking rate-stress intensity relationships.

16. Cyclic cracking rate (d2c/dN) decreased as minimum-to-maximum stress ratio (R) increased when evaluated with respect to $\Delta\overline{K}$. The influence of R in the range of +0.5 to +0.1 can be expressed in the form $(K_{i\ max})^m\ (\Delta K_i)^{1-m}$.

17. Cyclic cracking rate (d2c/dN) increased as K_{Ic} decreased. Available cracking rate equations do not quantitatively account for this trend.

18. Salt water spray cracking environment increased scatter in average cracking rate among individual specimens but the nominal cracking rate was the same as for moist air cracking environment.

RECOMMENDATIONS

1. Real time cyclic loading and environmental conditions are considerably different than those usually considered practical for crack propagation testing. Quantitative data to determine the importance of such environmental factors as cyclic frequency or environmental simulation technique are lacking for most materials. The influence of cyclic frequency on crack propagation rates for 300 M steel should be studied for both salt spray and salt solution cracking. Possible relationship to stress corrosion cracking test K_{Iscc} and to stress corrosion rates should be studied. Time compression test techniques should be evaluated and analytical methods accounting for cyclic frequency effects explored.

2. Analytical studies are required for improved stress intensity calculations to relate surface and through the thickness cracking to a single rate curve. Related studies are required to develop methods of computing stress intensities for crack of intermediate size (a/t 70.5 and $2c$ measured on opposing surfaces unequal). To accomplish these studies, a supporting test program will be required in which cracks are initiated as surface cracks and propagate through the thickness to proportions similar to through cracks. Several thicknesses of materials and strength levels should be included.

3. Further studies are desirable to evaluate interrelationships between material static strength and fatigue properties fracture toughness, cyclic strain characteristics and metallurgical variables. These studies would provide guidelines for developing materials with improved cracking resistance as well as providing improved means of material selection for design use. These studies should include both air and saline environments.

4. A survey of service experience with steels of the 4340 and 300 M type should be conducted to provide the basis for proposing fracture toughness and cracking rate requirements for these materials. Design philosophies for using these materials should be reviewed in view of the survey results. Improvements in design procedures should be proposed as guidance to the MIL-HDBK-5 Committee in selecting cracking rate data presentation methods.

ACKNOWLEDGEMENTS

J. J. Pengra of the Lockheed-California Company is acknowledged for his major contribution to the program in performing most of the calculations and plotting required for data analysis, and T. R. Brussat of the Lockheed-California Company is acknowledged for his assistance in data analysis and computer programing.

REFERENCES

1. Srawley, J. E. and Brown, W. F. Jr., "Fracture Toughness Testing Methods," NASA TN D-2599, Jan. 1965.

2. Irwin, G. R., "Crack Extension Force for a Part-Through Crack in a Plate," Journal of Applied Mechanics (Trans. A.S.M.E.), Dec. 1962, pp 651-654.

3. American Society for Testing and Materials, Fracture Toughness Testing and its Applications, ASTM STP 381, Apr. 1965.

4. Randall, P. N., "Severity of Natural Flaws as Fracture Origins and a Study of the Surface-Cracked Specimen," Air Force Materials Laboratory Technical Report AFML-TR-66-204, August, 1966.

5. ASTM Special Committee on Fracture Testing of High-Strength Metallic Materials, "Fracture Testing of High-Strength Sheet Materials," ASTM Bulletin, Jan. 1960, pp 29-40 and Feb. 1960, pp 18-28.

6. Irwin, G. R., "Fracture," Encyclopedia of Physics V. 6, Springer, Berlin, 1958, pp 551-590.

7. Federson, W. "Fracture Toughness Data," Agenda Item 64-16, 32nd Coordinating Meeting of MIL-HDBK 5, Philadelphia, Oct. 4-6, 1966, (especially p. 6).

8. Paris, P. C. and Erdogan, F., "A Critical Analysis of Crack Propagation Laws," Jl of Basic Engineering (Trans. ASME), Dec. 1963, pp 528-534.

9. Donaldson, D. R. and Anderson, W. E., "Crack Propagation Behavior of Some Airframe Materials," Proceedings of the Crack Propagation Symposium, Cranfield, 1961, V. II, pp 375-441.

10. Barrois, W., "Critical Study on Fatigue Crack Propagation," NATO Advisory Group for Aeronautical Research and Development, Report 412, June 1962.

11. Broek, D. and Schijve, J., "The Influence of the Mean Stress on the Propagation of Fatigue Cracks in Aluminum Alloy Sheet," National Aero- and Astronautical Research Institute Report NLR-TR M. 2111, Amsterdam, Jan. 1963.

12. Forman, R. G., Kearney, and Engle, "Numerical Analysis of Crack Propagation in Cyclic-Loaded Structures," ASME Paper 66-WA/Met-4, 1966.

13. Erdogan, F., "Crack-Propagation Theories," NASA CR-901, Oct. 1967

14. Walker, E. K,. "The Influence of Maximum and Alternating Stresses on Crack Propagation Rates and Low Cycle Fatigue Life for 2024T3 and 7075T6

Aluminum Alloys" - Paper to be presented at the 1968 fall meeting of ASTM, Atlanta,Georgia, Sept 29, 1968.

15. Miller, G. A., "The Dependence of Fatigue-Crack Growth on Stress Intensity Factor and the Mechanical Properties of some High-Strength Steels, Homer Research Laboratories, Bethlehem Steel Corporation, Bethlehem, Penn. Paper presented to ASTM committee E-24, March 1968.

16. Walker, E. F., Mar, M. J., A note on the effect of fatigue pre-cracking stress on the plane strain fracture toughness of several martensitic steels BISRA - The Inter-Group Laboratories of the British Steel Corporation, Metallurgy Division, Sheffield, Jan. 1968.

17. Federal Aviation Agency, Federal Aviation Regulations Part 25 Airworthiness Standards: Transport Category Airplanes.

18. MIL HDBK-V Item 64-16, 34th Meeting Agenda

19. Wilhem, D. P., Investigation of Cyclic Crack Growth Transition Behavior ASTM Fatigue Crack Propagation Symposium, Atlantic City, N. J. June 30, July 1, 1966.

20. Meyn, D. A., Observations on Micromechanisms of Fatigue Crack Propagation in 2024 Aluminum, Transactions, American Society for Metals Volume 61, March 1968.

21. Meyn, D. A., The Nature of Fatigue-Crack Propagation in Air and Vacuum for 2024 Aluminum, Transactions, American Society for Metals Volume 61, March 1968.

APPENDIX

SUPPLIER TEST REPORT DATA

Supplier test report data on 300 M forgings and plate material are presented in this appendix.

TABLE A-1 MATERIAL DETAILS

	300M Forgings	300M Plate
Melt History:	CEVM, Cameron Iron Works	CEVM, Republic Steel
Heat Number:	51782	See Table A-2
Billet Size:	8" x 15" x 16'	
Supplier:	Shultz Steel	Pacific Metals
Finished Size:	1" x 13" x 34"	3/16, 1/2, and 7/8 Plate
Condition:	Normalized and Tempered to RC 33 Max.	Normalized and Tempered to RC 33 Max.
Specification:	MIL-S-8844B Class 2	AMS6438 Except Chemistry to MIL-S-8844B Class 2

TABLE A-2 CHEMICAL ANALYSIS

Material	Heat Number	C	Mn.	Phos.	Sul.	Sil.	Ni.	Cr.	Mo.	V
Plate										
3/16	3932022	.40	.72	.008	.006	1.73	1.76	.87	.40	.09
1/2 & 7/8	3932021	.39	.87	.009	.005	1.73	1.76	.87	.39	.08
1/2	3961507	.40	.83	.007	.006	1.60	1.82	.83	.41	.09
7/8	3922452	.42	.90	.007	.005	1.59	1.85	.85	.40	.08
Forgings	51782	.43	.74	.009	.005	1.63	1.80	.81	.39	.08
Spec. Range MIL-S-8844B Class 2		.38-.43	.65-.90	.015 Max.	.015 Max.	1.45 1.80	1.65 2.00	.70-.95	.35-.45	.05 Min.

TABLE A-3 PLATE TENSILE PROPERTIES TRANSVERSE GRAIN DIRECTION(1)

Plate Thickness-Inches	Heat Number Airmelt	Heat Number CEVM	Tensile Ultimate KSI	Tensile Yield KSI	% Elong.	% R.A.
3/16	3323188 Electrode 13	3932022	282	233	8	25
1/2	3323188 Electrode 10	3932021	288	251	10	40
1/2	3312997 Electrode 2	3961507	289	246	11	43
7/8	3323188 Electrode 10	3932021	288	245	10	42
7/8	3352605 Electrode 3	3922452	297	253	10	42

(1) Normalize: 1700°F - 1 hr. AC, Austenitize: 1600°F - 1 hr. OQ.
Double Temper: 575°F - 2+2 hrs. AC.

TABLE A-4 BILLET TENSILE PROPERTIES TRANSVERSE GRAIN DIRECTION(1)

Specimen Location(2)	Tensile Ultimate KSI	Tensile Yield KSI	% Elong.	% R.A.
T-5 Mid-Rad	287.1	234.6	11.0	33.7
T-5 Center	289.6	234.6	9.0	29.3
T-5 Center	287.5	231.4	10.0	31.7
T-5 Mid-Rad	291.2	237.0	8.0	27.5
B-5 Mid-Rad	280.7	228.6	10.0	32.9
B-5 Center	282.7	232.6	10.0	34.5
B-5 Center	284.3	233.8	10.0	31.7
B-5 Mid-Rad	283.9	229.4	11.0	36.9

(1) Normalize: 1700°F - 1 hr. AC, Austenitize: 1600°F - 1 hr. OQ.
Double Temper: 575°F - 2+2 hrs. AC.

TABLE A-5 V-NOTCH CHARPY IMPACT RESULTS (Ft.-Lbs.)[1][2]

Heat No.	Location	Test Number 1	2	3
3932021	Top	14.0	13.0	13.5
	Bottom	13.3	15.0	17
3961507	Top	15.5	17	
	Bottom	16.5	16.8	
51782	Top	15.5	16.0	16.0
	Bottom	15.5	16.0	16.0

(1) Normalize: 1700°F - 1 hr. AC, Austenitize: 1600°F - 1 hr. OQ
Temper: 575°F - 4 hrs. AC

(2) Req'd MIL-S-8844B Class 2 - 13 Ft.-Lbs.

TABLE A-6 J K RATING - PLATE MATERIAL

Location(1)	A	B	C	D
Heat 3323188				
Top	.5	0	0	1.0
	0	0	0	.5
Bottom	0	0	0	1.0
	.5	0	0	.5
Top	0	0	0	1.0
	.5	0	0	0
Bottom	.5	0	0	1.0
	0	0	0	0
Top	1.0	1.0	0	1.0
	.5	0	0	0
Bottom	0	0	0	.5
	.5	0	0	.5
Heat 3312997				
Top	1.0	.5	0	.5
	.5	0	0	0
Bottom	.5	.5	0	.5
	.5	0	0	0
Top	.5	.5	0	.5
	0	0	0	.5
Bottom	0	0	0	.5
	0	0	0	.5

(1) Tests for several electrodes

TABLE A-7 INCLUSION CONTENT - FORGINGS - ASTM-E-45

Specimen Location	A		B		C		D	
	Thin	Heavy	Thin	Heavy	Thin	Heavy	Thin	Heavy
T-5 B-5								
Req'd MIL-S-8844B Class 2	1.5	1.0	1.5	1.0	1.0	1.0	1.5	1.0

MagnaFlux (All Products)

Frequency 00 Severity 00

APPENDIX B

ADDITIONAL DATA ON FRACTURE TOUGHNESS AND CRACK PROPAGATION - HIGH STRENGTH STEELS

A summary of some test results obtained from a previous Lockheed funded test program on fracture toughness and cyclic crack propagation of 9Ni-4Co, 300M, D6Ac, and 4340 steel forged billets are presented in this appendix. Table B-1 summarizes the test materials and conditions.

TEST MATERIALS AND SPECIMENS

The materials evaluated in this investigation were vacuum melted 9Ni-4Co, 300M, D6Ac, and 4340 steels. The materials were obtained in the form of forged billets with about a 9 in. by 9 in. cross section. Two billets of 300M steel were evaluated. One had high carbon content (.45C) and one had low carbon (.39C). The 9Ni-4Co steel was evaluated with both martensitic and bainitic structures. Vendor reported chemical analyses for the test materials are presented in Table B-2.

Round, one inch gage length, tensile specimens and surface-crack type tensile specimens (Figure B-1) were machined from the steel billets in the longitudinal grain direction. Specimen locations within the billets are shown in Figure B-2. All specimens were machined oversize by .025 inch per surface to allow for final machining after heat treatment to remove any possible decarburization. The test specimens were heat treated to 270-290 ksi strength level according to the following schedules and then finish machined to the final specimen dimensions.

Heat Treat Schedule

9Ni-4Co Steel (martensitic)

1. Normalize - 1600° F, 1 hour, air cool
2. Austenitize - 1450° F, 1 hour, air cool
3. Refrigerate - -100° F, 2 hours
4. Within one hour after refrigeration cycle, double temper - 475° F, 2 hours, air cool (two times).

9Ni-4Co Steel (bainitic)

1. Normalize - 1600° F, 1 hour, air cool
2. Austenitize - 1450° F, 1 hour and immediately transfer to furnace at 460° F for 8 hours, air cool.
3. Double temper - 425° F, 2 hours, air cool (two times)

300M Steel

1. Normalize - 1700° F, 1 hour, air cool
2. Austenitize - 1600° F, 1 hour, oil quench
3. Double temper - 575° F, 2 hours, air cool (two times)

D6Ac Steel

1. Normalize - 1650° F, 1 hour, air cool
2. Austenitize - 1550° F, 1 hour, oil quench
3. Double temper - 600° F, 2 hours, air cool (two times)

4340 Steel

1. Normalize - 1650° F, 1 hour, air cool
2. Austenitize - 1500° F, 1 hour, oil quench
3. Temper - 450° F, 4 hours, air cool

TEST PROCEDURE

Tensile Tests

Tensile tests were conducted for all steel alloys and heat treatments to insure satisfactory heat treat responses. The tests were conducted at room temperature at a load rate equivalent to an elastic strain rate of 0.005 inch per inch per minute according to ASTM Specification E-8.

Fracture Toughness Tests

Various sized semi-elliptically shaped fatigue cracks were generated at the center of one side of the surface-crack tensile specimens by repeated constant-moment bending in a hydraulically operated fatigue machine (Figure B-3). A small electric-discharge machined notch was used to accurately locate and initiate the fatigue crack. The fatigue crack was observed and measured on the specimen surface until the desired crack length was attained.

After the specimens were fatigue cracked, they were statically loaded in tension to failure at a load-rate equivalent to an elastic strain-rate of 0.005 inch per inch per minute in Universal hydraulic test machines (Figure B-4). An autographic load-extension curve to failure was obtained with a Model PD-1M deflectometer. The fatigue crack length and depth were measured from the fractured surface of each specimen.

Crack Propagation Tests

Semi-elliptically shaped fatigue cracks were generated in specimens identical to those used in the fracture toughness tests using the procedures previously described except that the cracks were propagated to the same size for each specimen. This condition constituted the initial pre-crack condition for starting the axial tension-tension fatigue crack propagation tests.

Specimens of each steel alloy and heat treatment were then axial tension-tension fatigue tested at a maximum gross area stress of 45 ksi and a minimum-to-maximum stress ratio (R) of +0.1 with the crack exposed to an air, distilled water, or 3 1/2 percent NaCl salt water environment. The water solutions were maintained over the crack with an "O" ring placed on the specimen surface around the crack. The tests were conducted in a hydraulically operated fatigue machine at a cyclic frequency of 20 cps. Figure B-5 shows the fatigue machine with specimen installed for salt water environment testing. A plastic scale was placed on the specimen surface adjacent to the crack for crack length measurements (Figure B-6). In order to measure the crack length during the test, the fatigue machine was stopped with the mean load remaining on the specimen until the measurement was completed. Fatigue crack length and corresponding number of cycles were recorded at crack length increments of 0.04 inch.

TEST RESULTS

Tensile Tests

The tensile test results are presented in Table B-3. 300M steel (.45C) exhibited the highest ultimate strength (291 ksi) and 4340 steel the lowest (274 ksi). D6Ac steel had the highest 0.2 percent yield stress (244 ksi) and 4340 steel the lowest (227 ksi). The percent elongation in a 1 in. gage length and percent reduction in area ranged from 9 to 12 and 31 to 54 respectively for all alloys and heat treatments tested.

Fracture Toughness Tests

The results of the fracture toughness tests for martensitic 9Ni-4Co, bainitic 9Ni-4Co, 300M (.45C), 300M (.39C), D6Ac, and 4340 are presented in Table B-4. Plane-strain fracture toughness (K_{Ic}) values were calculated using Equation (13) of this report. The effects of crack size (a/Q) on gross fracture strength are shown in Figure B-7.

Bainitic 9Ni-4Co, 4340, and 300M (.39C) steels exhibited the highest gross fracture strengths and K_{Ic} values followed in decreasing order by martensitic 9Ni-4Co, D6Ac, and 300M (.45C) steels. A comparison of fracture toughness results for the two heats of 300M steel indicate that variations in carbon content significantly influence the toughness properties of this alloy. The low carbon heat (.39C) exhibited considerably higher fracture strengths and K_{Ic} values than the .45 carbon heat at approximately the same ultimate strength level.

The effects of crack size (a/Q) on calculated K_{Ic} values for all alloys and heat treatments evaluated are shown in Figures B-8 to B-13. These results indicate general tendencies for K_{Ic} to increase with increasing crack size for the tougher alloys (bainitic 9Ni-4Co, 4340, and low carbon 300M steels) and for K_{Ic} to decrease with increasing crack size for the less tough alloys (martensitic 9Ni-4Co, D6Ac, and high carbon 300M steels).

Crack Propagation Tests

Tabulated crack propagation test results for martensitic 9Ni-4Co, bainitic 9Ni-4Co, 300M (.45C), 300M (.39C), D6Ac, and 4340 steels in air, salt water, and distilled water environments are presented in Tables B-5, B-6, and B-7. The initial crack lengths at the start of the axial tension-tension fatigue crack propagation tests were from 0.16 to 0.18 inch. These initial crack lengths were generated by constant-moment bending as described previously. In order to evaluate crack propagation behavior without influences from initial crack size variations and pre-crack stressing conditions, the crack propagation data is reported from a constant crack length of 0.20 inch which occurred after the initial crack had started propagating under the stress and environment conditions used for the crack propagation tests. There are no test data reported in Table B-5 for 4340 steel tested in the air environment because the initial crack did not propagate under the axial crack propagation test stress conditions after 10^6 cycles at which time the tests were discontinued.

Figures B-14, B-15, and B-16 present graphical plots of crack length vs. number of fatigue cycles for the crack propagation tests in air, salt water, and distilled water environments. These graphs indicate that the slowest cyclic crack propagation under the stress conditions tested was exhibited by 4340 steel in air environment, 300M (.39C) steel in salt water environment, and martensitic 9Ni-4Co steel in distilled water environment. Crack propagation was generally faster in salt water and distilled water environments than in air with salt water tending to be more damaging than distilled water.

Figures B-17, B-18, and B-19 present the cyclic crack propagation test results in terms of cracking rate $(\frac{d2c}{dN})$ and stress intensity range $(\triangle K_I)$ and Figures B-20, B-21, and B-22 present the data in terms of $\frac{d2c}{dN}$ and effective stress intensity range $(\triangle \bar{K})$. These are the same type data presentations as presented for 300M steel in the main body of this report. In these data presentations, the crack propagation data for all alloys and heat treatments tested fall within a reasonable single scatter band. However, within the scatter band, the same general relationships among the different alloys exist as were indicated by the crack length vs. number of cycles plots (Figures B-14, B-15, and B-16).

TABLE B-1 SUMMARY OF CYCLIC CRACK PROPAGATION TESTS

MATERIAL	ULTIMATE STRENGTH (KSI)	TEST ENVIRONMENT	MAXIMUM FATIGUE STRESS (KSI)	MIN.-TO-MAX. FATIGUE STRESS RATIO (R)
9Ni-4Co Steel (Martensitic)	280	Air	45	+0.1
		Salt Water	45	+0.1
		Distilled Water	45	+0.1
9Ni-4Co Steel (Bainitic)	275	Air	45	+0.1
		Salt Water	45	+0.1
300M Steel (.45 Carbon)	291	Air	45	+0.1
		Salt Water	45	+0.1
		Distilled Water	45	+0.1
300M Steel (.39 Carbon)	287	Air	45	+0.1
		Salt Water	45	+0.1
D6Ac Steel	279	Air	45	+0.1
		Salt Water	45	+0.1
		Distilled Water	45	+0.1
4340 Steel	274	Air	45	+0.1
		Salt Water	45	+0.1
		Distilled Water	45	+0.1

TABLE B-2 CHEMICAL COMPOSITIONS OF STEEL ALLOYS INVESTIGATED

ALLOY	VENDOR	HEAT NO.	CHEMICAL COMPOSITION										
			C	MN	P	S	SI	CR	NI	MO	V	CU	CO
9Ni-4Co Steel	Republic Steel Corp.	3931129	.44	.19	.005	.007	.01	.34	7.73	.29	.08		4.09
300M Steel	American Alloy Metals, Inc.	50604	.45	.90	.006	.004	1.49	.86	1.75	.39	.10	.15	
300M Steel	Crucible Steel Corp.	16451	.39	.86	.008	.005	1.79	.87	1.80	.41	.07		
D6Ac Steel	Republic Steel Corp.	3951333	.47	.67	.010	.004	.22	1.07	.54	1.00	.08		
4340 Steel	Republic Steel Corp.	3961320	.39	.72	.007	.004	.23	.81	1.77	.26			

TABLE B-3 TENSILE TEST RESULTS

MATERIAL	SPEC. NO.	GRAIN DIR.	F_{tu} (KSI)	F_{ty} (KSI)	% EL. 1" GAGE	% R.A.
9Ni-4Co Steel (martensitic)	C1	Long.	279	239	11	48
	C2	Long.	281	241	12	51
	C3	Long.	279	241	12	49
	Avg.	Long.	280	240	12	49
9Ni-4Co Steel (bainitic)	N1	Long.	273	231	11	54
	N2	Long.	275	236	11	53
	N3	Long.	276	238	11	53
	N4	Long.	275	236	11	54
	Avg.	Long.	275	235	11	54
300M Steel (.45C)	0M-10	Long.	293	241	8	30
	0M-11	Long.	293	241	10	31
	0M-12	Long.	289	236	10	32
	0M-13	Long.	289	237	9	31
	0M-14	Long.	291	240	9	31
	0M-15	Long.	291	242	8	32
	Avg.	Long.	291	240	9	31
300M Steel (.39C)	2M-1	Long.	284	237	10	44
	2M-2	Long.	290	243	10	40
	2M-3	Long.	284	242	10	35
	2M-4	Long.	289	241	9	37
	Avg.	Long.	287	241	10	39
D6Ac Steel	D1	Long.	280	245	11	39
	D2	Long.	281	243	11	40
	D3	Long.	278	242	10	41
	D4	Long.	280	241	10	36
	D5	Long.	278	246	11	45
	D6	Long.	276	245	10	40
	Avg.	Long.	279	244	11	40
4340 Steel	43-1	Long.	274	226	12	53
	43-2	Long.	275	230	12	53
	43-3	Long.	272	223	12	52
	43-4	Long.	276	228	12	51
	43-5	Long.	277	229	12	51
	43-6	Long.	270	228	12	51
	Avg.	Long.	274	227	12	52

TABLE B-4 FRACTURE TOUGHNESS TEST RESULTS

MATERIAL	SPECIMEN NUMBER	CRACK DEPTH a (IN.)	CRACK LENGTH 2c (IN.)	$\frac{a}{2c}$	GROSS AREA FRACTURE STRENGTH (KSI)	0.2% OFF-SET YIELD STRESS (KSI)	$\frac{\text{FRACTURE STRENGTH}}{\text{YIELD STRESS}}$	$\frac{a}{Q}$	K_{Ic} (KSI $\sqrt{\text{IN}}$)
9Ni-4Co Steel (Martensitic)	M-2	.055	.150	.367	214	240	1.08	.331	76
	M-3	.063	.175	.360	199		.83	.379	75
	M-4	.085	.255	.334	153		.64	.515	68
	M-5	.095	.325	.293	125		.52	.630	61
	M-6	.100	.370	.250	118		.49	.725	60
	M-7	.105	.410	.256	112	240	.47	.756	59
9Ni-4Co Steel (Bainitic)	B-1	.075	.215	.349	196	235	.83	.463	82
	B-2	.075	.215	.349	198		.84	.463	83
	B-3	.100	.295	.339	168		.72	.641	81
	B-5	.095	.285	.333	178		.76	.601	85
	B-7	.067	.168	.399	206		.88	.376	77
	B-8	.084	.254	.331	173	235	.74	.532	77
300M Steel (.45C)	OM-2	.026	.057	.456	251	240	1.04	.133	56
	OM-3	.027	.058	.466	246		1.02	.135	55
	OM-4	.053	.114	.465	189		.79	.255	58
	OM-5	.041	.094	.436	196		.82	.209	54
	OM-6	.062	.144	.431	164		.68	.313	56
	OM-7	.070	.197	.355	143		.60	.402	56
	OM-8	.086	.290	.297	114		.48	.562	52
	OM-9	.105	.417	.252	89	240	.37	.752	47
300M Steel (.39C)	3M-13	.028	.075	.374	267	241	1.11	.175	68
	3M-14	.031	.070	.443	256		1.06	.163	63
	3M-15	.044	.110	.400	237		.98	.252	73
	3M-16	.080	.240	.334	182		.76	.500	76
	3M-17	.090	.308	.292	165		.69	.617	80
	3M-18	.108	.404	.268	141	241	.59	.761	75
D6Ac Steel	D-2	.028	.071	.394	242	244	.99	.163	60
	D-3	.027	.067	.403	240		.98	.153	57
	D-4	.032	.079	.405	237		.97	.182	61
	D-5	.041	.104	.394	220		.90	.233	65
	D-6	.069	.147	.470	190		.78	.329	66
	D-7	.088	.207	.425	156		.64	.440	63
	D-8	.100	.322	.311	117		.48	.633	57
	D-9	.111	.366	.303	96	244	.39	.708	49
4340 Steel	C-1	.030	.080	.375	256	227	1.13	.188	68
	C-2	.050	.110	.454	220		.97	.254	67
	C-5	.100	.290	.345	170		.75	.618	82
	C-6	.120	.390	.308	144		.64	.780	78
	C-8	.100	.270	.371	174		.77	.581	81
	C-9	.060	.140	.429	217		.96	.319	75
	C-12	.120	.400	.300	135	227	.60	.786	74

TABLE B-5 CYCLIC CRACK PROPAGATION IN AIR TEST RESULTS

AIR ENVIRONMENT									
9Ni-4Co STEEL (MARTENSITIC)		9Ni-4Co STEEL (BAINITIC)		300 M STEEL (.45C)		300 M STEEL (.39C)		D6Ac STEEL	
CRACK LENGTH (IN.)	NO. OF CYCLES (10^{-3})	CRACK LENGTH (IN.)	NO. OF CYCLES (10^{-3})	CRACK LENGTH (IN.)	NO. OF CYCLES (10^{-3})	CRACK LENGTH (IN.)	NO. OF CYCLES (10^{-3})	CRACK LENGTH (IN.)	NO. OF CYCLES (10^{-3})
.20	0	.20	0	.20	0	.20	0	.20	0
.24	8.9	.24	12.0	.24	12.0	.24	8.0	.24	8.0
.28	13.8	.28	22.0	.28	18.0	.28	12.0	.28	13.0
.32	18.5	.32	28.3	.32	22.0	.32	16.0	.32	18.0
.36	23.0	.36	33.5	.36	25.0	.36	20.0	.36	22.0
.40	26.9	.40	37.6	.40	27.0	.40	23.0	.40	25.0
.44	30.1	.44	40.5	.44	28.0	.44	26.0	.44	28.0
.48	32.2	.48	43.0	.48	29.0	.48	29.0	.48	30.5
.52	34.0	.52	45.0	.52	30.0	.52	32.0	.52	33.0
.56	35.7	.56	46.5			.56	34.5	.56	35.0
.60	37.3	.60	48.0			.60	36.5	.60	37.0
.64	38.2	.64	50.0			.64	38.0	.64	39.0
.68	39.0	.68	51.0			.68	39.0	.68	41.0
.72	39.7	.72	52.0			.72	40.0	.72	42.5
.76	40.0	.76	53.0			.76	41.0	.76	44.0
		.80	54.0			.80	41.5	.80	45.0

TABLE B-6 CYCLIC CRACK PROPAGATION IN SALT WATER TEST RESULTS

SALT WATER ENVIRONMENT											
9Ni-4Co STEEL (MARTENSITIC)		9Ni-4Co STEEL (BAINITIC)		300 M STEEL (.45C)		300 M STEEL (.39C)		D6Ac STEEL		4340 STEEL	
CRACK LENGTH (IN.)	NO. OF CYCLES (10^{-3})	CRACK LENGTH (IN.)	NO. OF CYCLES (10^{-3})	CRACK LENGTH (IN.)	NO. OF CYCLES (10^{-3})	CRACK LENGTH (IN.)	NO. OF CYCLES (10^{-3})	CRACK LENGTH (IN.)	NO. OF CYCLES (10^{-3})	CRACK LENGTH (IN.)	NO. OF CYCLES (10^{-3})
.20	0	.20	0	.20	0	.20	0	.20	0	.20	0
.24	5.8	.24	5.9	.24	5.3	.24	7.5	.24	3.1	.24	6.0
.28	9.8	.28	10.6	.28	9.0	.28	13.5	.28	5.0	.28	8.0
.32	13.0	.32	14.6	.32	12.0	.32	19.5	.32	6.5	.32	10.0
.36	15.5	.36	18.0	.36	14.0	.36	25.5	.36	8.0	.36	12.0
.40	17.6	.40	21.0	.40	15.5	.40	30.5	.40	9.0	.40	13.5
.44	19.7	.44	23.5	.44	17.0	.44	34.5	.44	10.0	.44	15.0
.48	21.5	.48	25.7	.48	18.0	.48	38.0	.48	11.0	.48	16.5
.52	23.2	.52	28.0	.52	19.0	.52	41.0	.52	12.0	.52	18.0
.56	24.5	.56	30.0	.56	19.5	.56	43.0	.56	13.0	.56	19.0
.60	25.5	.60	32.0	.60	20.0	.60	45.0	.60	14.0	.60	20.0
.64	26.5	.64	34.0	.64	20.5	.64	47.0	.64	14.7	.64	21.0
.68	27.4	.68	35.5			.68	48.0	.68	15.5	.68	22.0
.72	27.9	.72	36.5			.72	49.0	.72	16.3	.72	22.5
.76	28.6	.76	37.5			.76	50.0	.76	17.0	.76	23.0
.80	29.0					.80	51.0			.80	23.5

TABLE B-7 CYCLIC CRACK PROPAGATION IN DISTILLED WATER TEST RESULTS

DISTILLED WATER ENVIRONMENT							
9Ni-4Co STEEL (MARTENSITIC)		300 M STEEL (.45C)		D6Ac STEEL		4340 STEEL	
CRACK LENGTH (IN.)	NO. OF CYCLES (10^{-3})	CRACK LENGTH (IN.)	NO. OF CYCLES (10^{-3})	CRACK LENGTH (IN.)	NO. OF CYCLES (10^{-3})	CRACK LENGTH (IN.)	NO. OF CYCLES (10^{-3})
.20	0	.20	0	.20	0	.20	0
.24	12.4	.24	8.0	.24	5.5	.24	3.9
.28	21.2	.28	14.0	.28	9.7	.28	7.8
.32	28.2	.32	18.5	.32	13.0	.32	11.5
.36	33.7	.36	21.5	.36	16.0	.36	15.0
.40	38.0	.40	23.5	.40	18.5	.40	17.8
.44	41.5	.44	25.5	.44	21.0	.44	20.0
.48	44.5	.48	27.0	.48	23.0	.48	22.0
.52	47.0	.52	28.0	.52	25.0	.52	24.0
.56	49.5	.56	29.0	.56	26.5	.56	26.0
.60	51.5	.60	29.7	.60	28.0	.60	28.0
.64	53.5			.64	29.0	.64	29.0
.68	55.0			.68	30.0	.68	30.0
.72	56.0			.72	31.0	.72	31.0
				.76	32.0	.76	32.0
				.80	33.0	.80	33.0

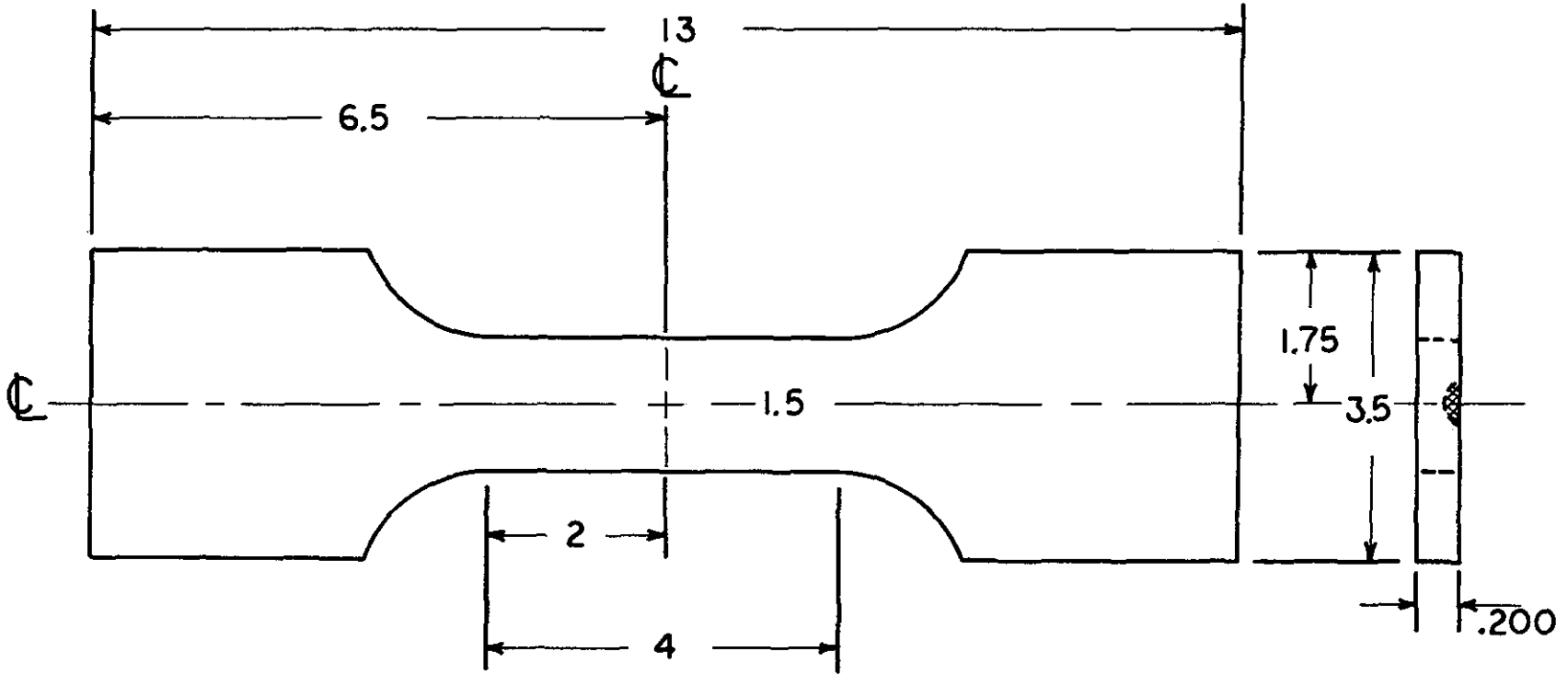

Figure B-1 Fracture Toughness and Crack Propagation Specimen

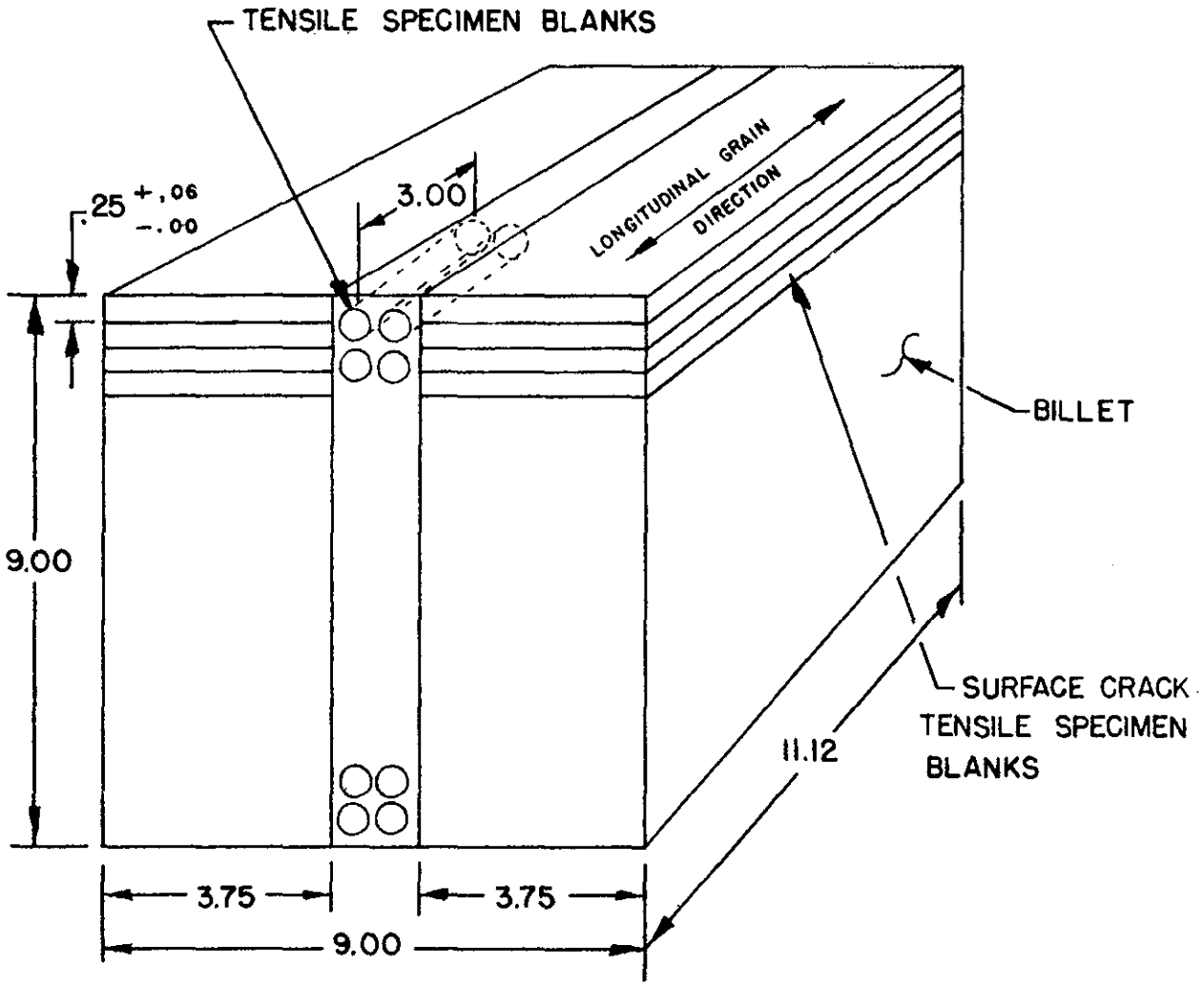

Figure B-2 Location of Specimen Blanks in Billets

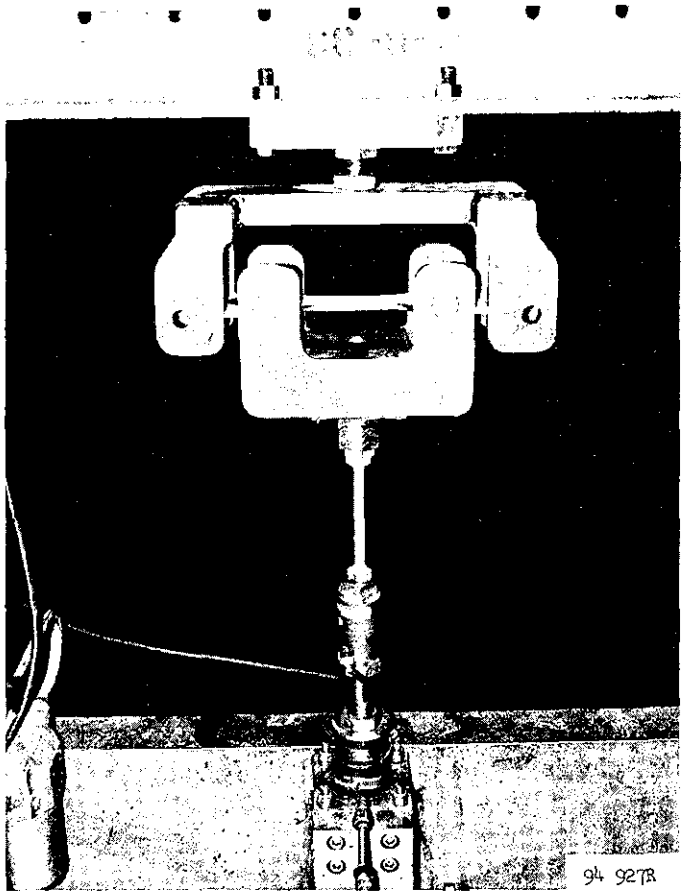

Figure B-3 Photograph of Test Set-up for Generating Semi-elliptically Shaped Fatigue Cracks in Tensile Specimens by Repeated Constant-Moment Bending

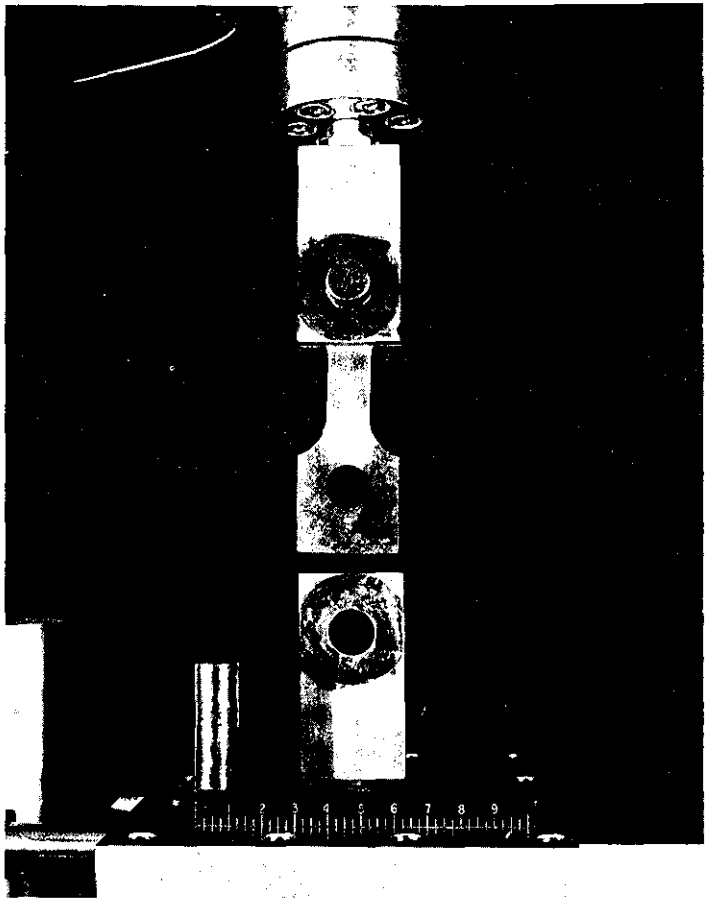

Figure B-4 Photograph of Test Set-up for Static Tensile Testing of Surface Pre-cracked Specimens in Hydraulic Test Machine

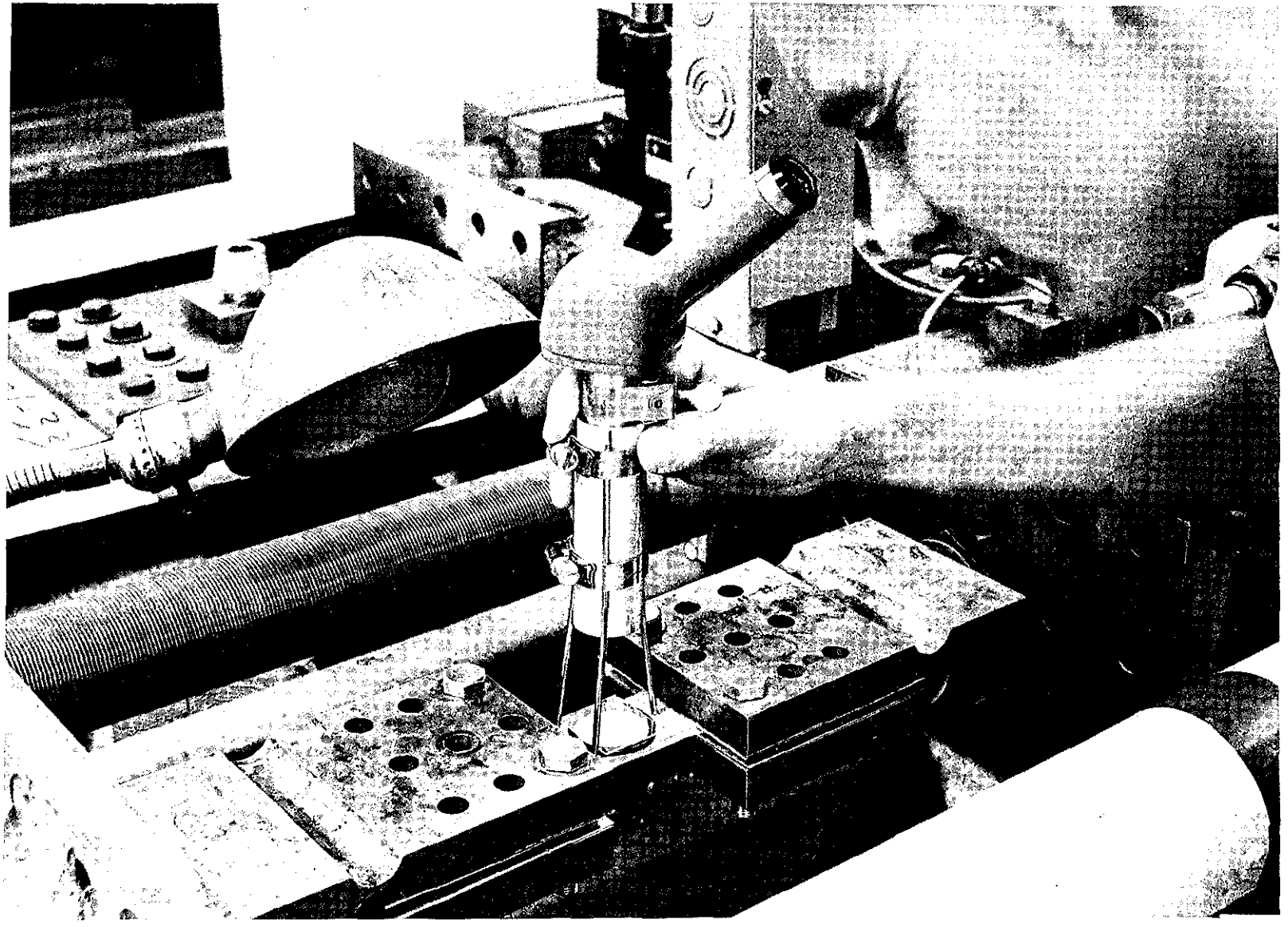

Figure B-5 Fatigue Machine with Specimen Installed

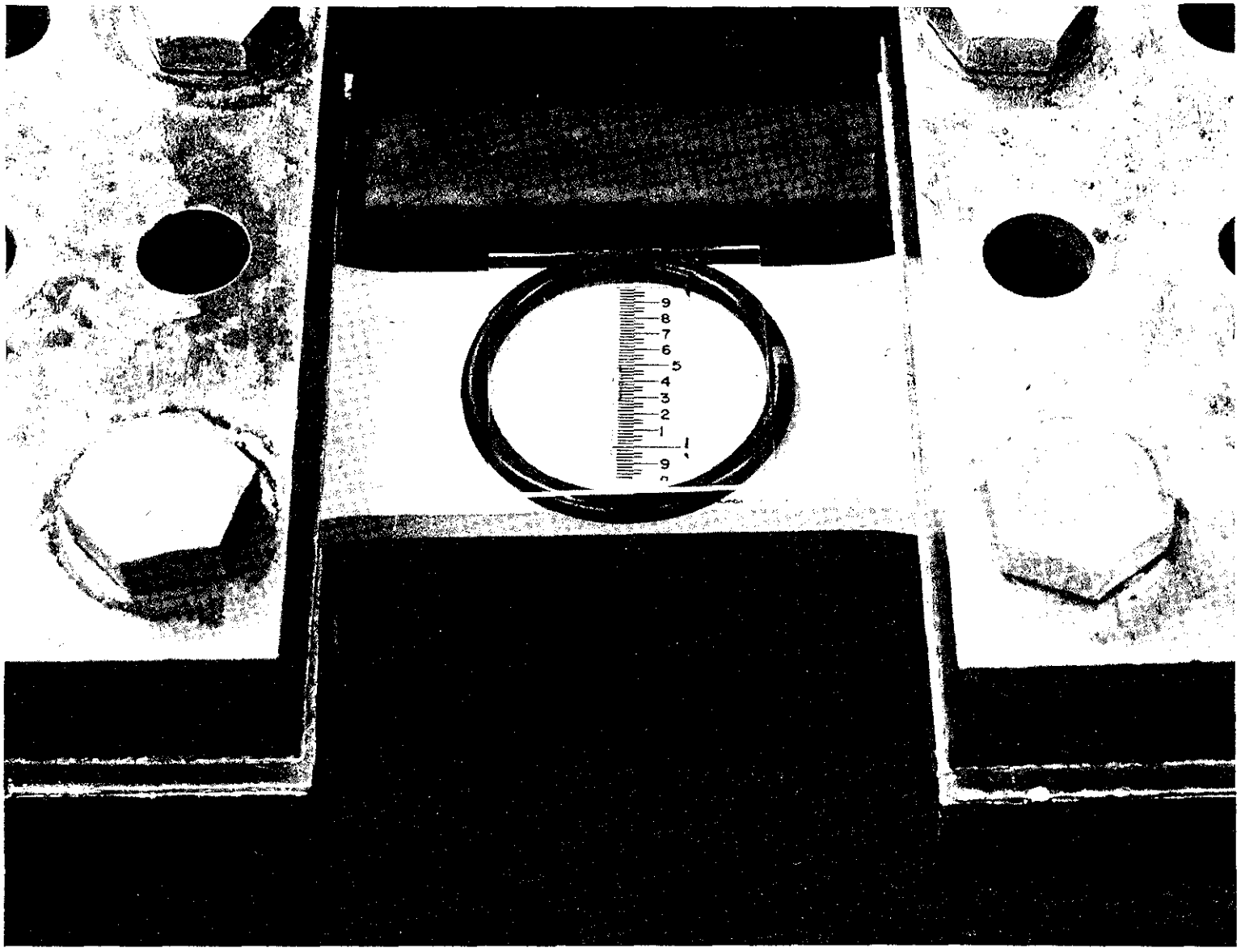

Figure B-6 Specimen with Scale and "O" Ring Water Container

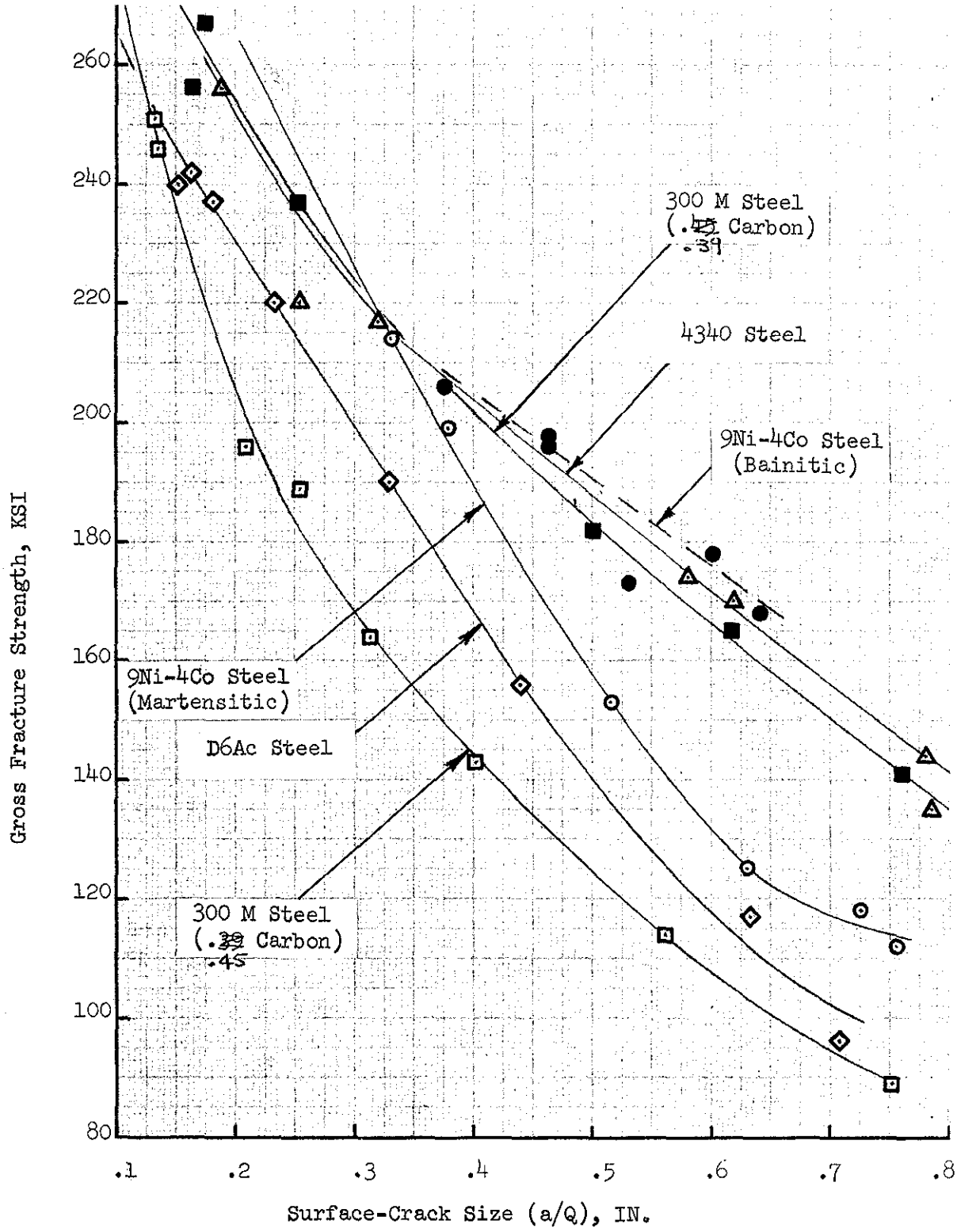

Figure B-7 Effect of Surface-Crack Size on Fracture Strength

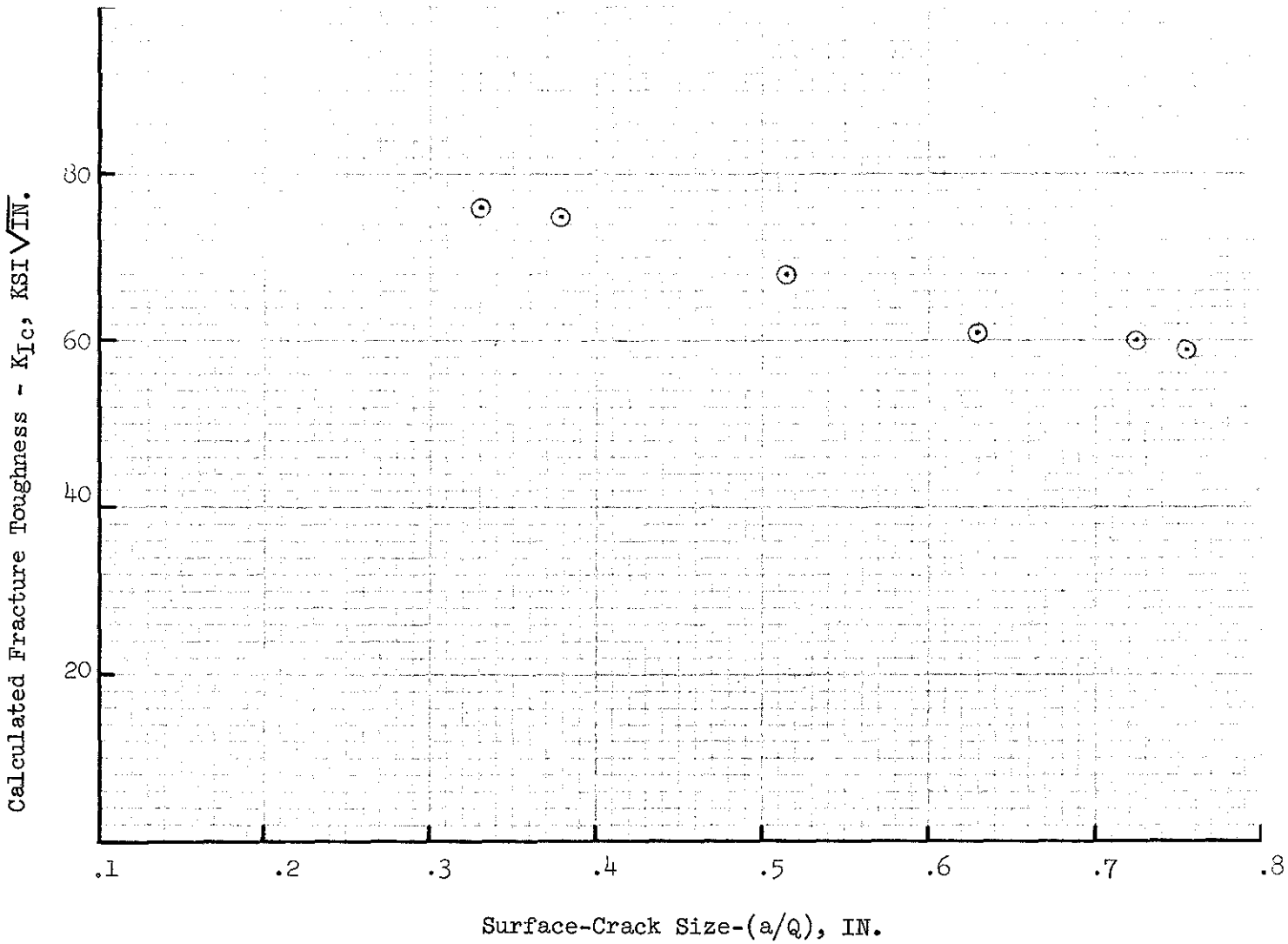

Figure B-8 Effect of Surface-Crack Size on Calculated K_{Ic} for Martensitic 9Ni-4Co Steel

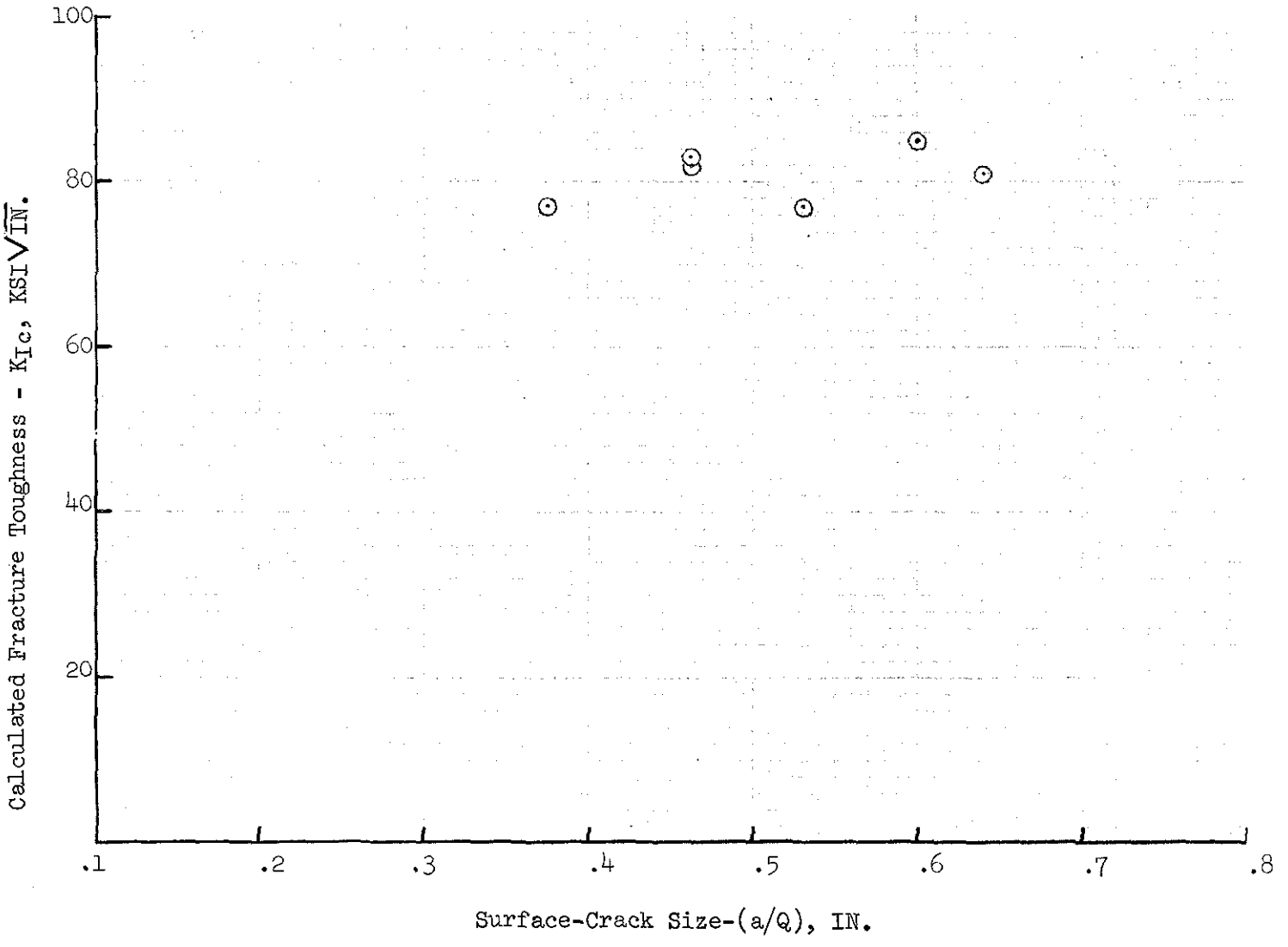

Figure B-9 Effect of Surface-Crack Size on Calculated K_{Ic} for Bainitic 9Ni-4Co Steel

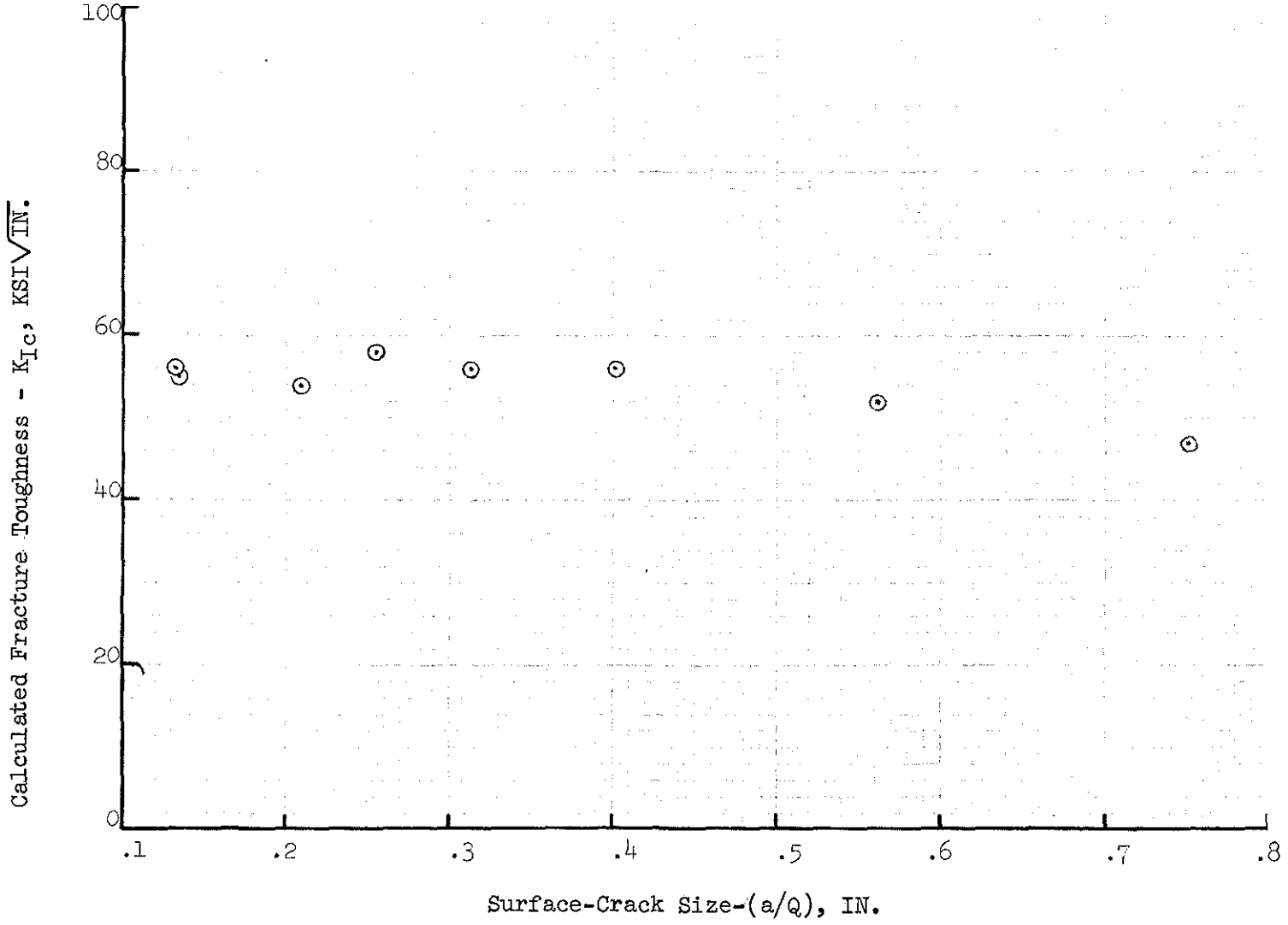

Figure B-10 Effect of Surface-Crack Size on Calculated K_{Ic} for 300 M (.45C) Steel

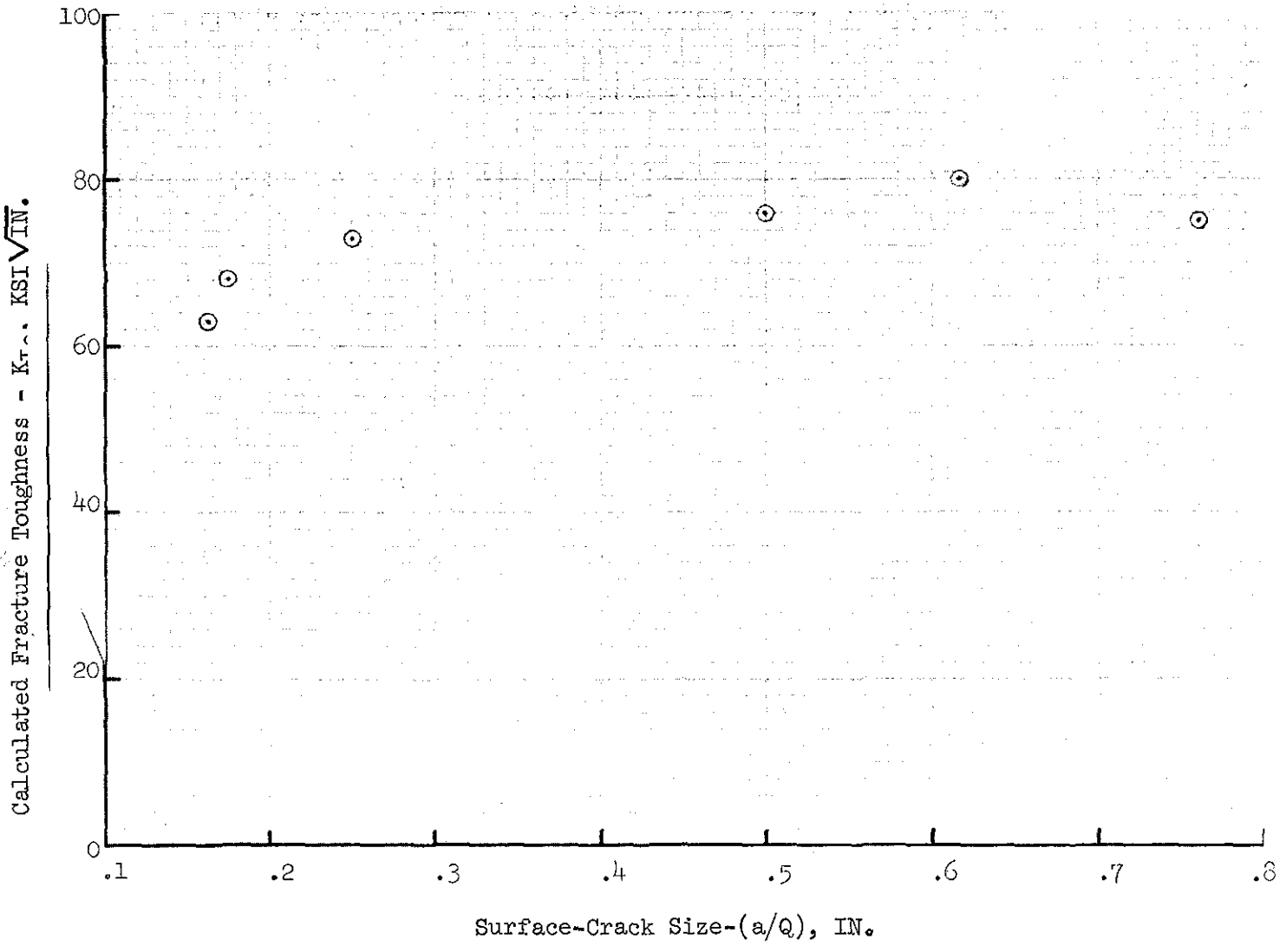

Figure B-11 Effect of Surface-Crack Size on Calculated K_{Ic} for 300 M (.39C) Steel

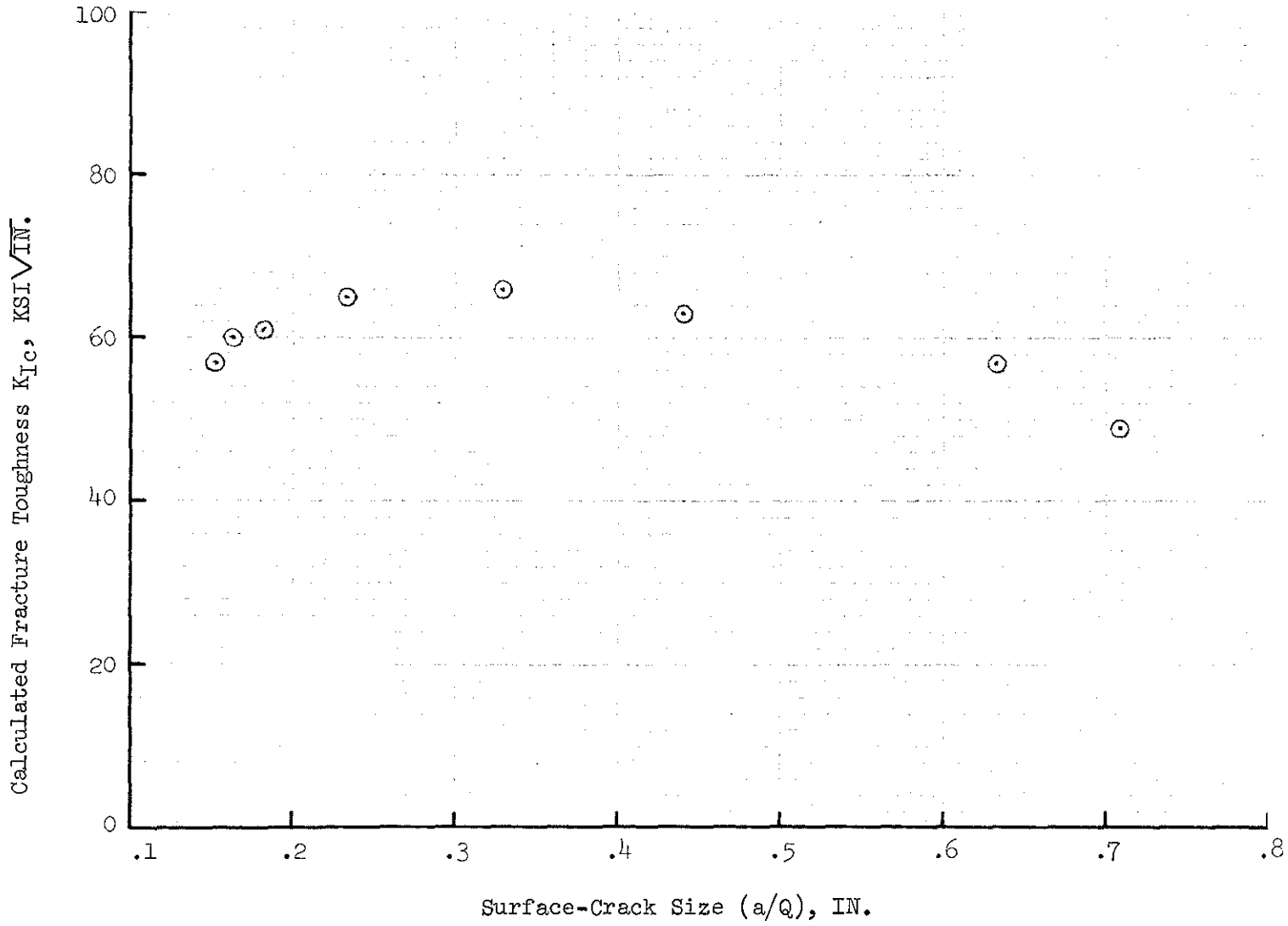

Figure B-12 Effect of Surface-Crack Size on Calculated K_{Ic} for D6Ac Steel

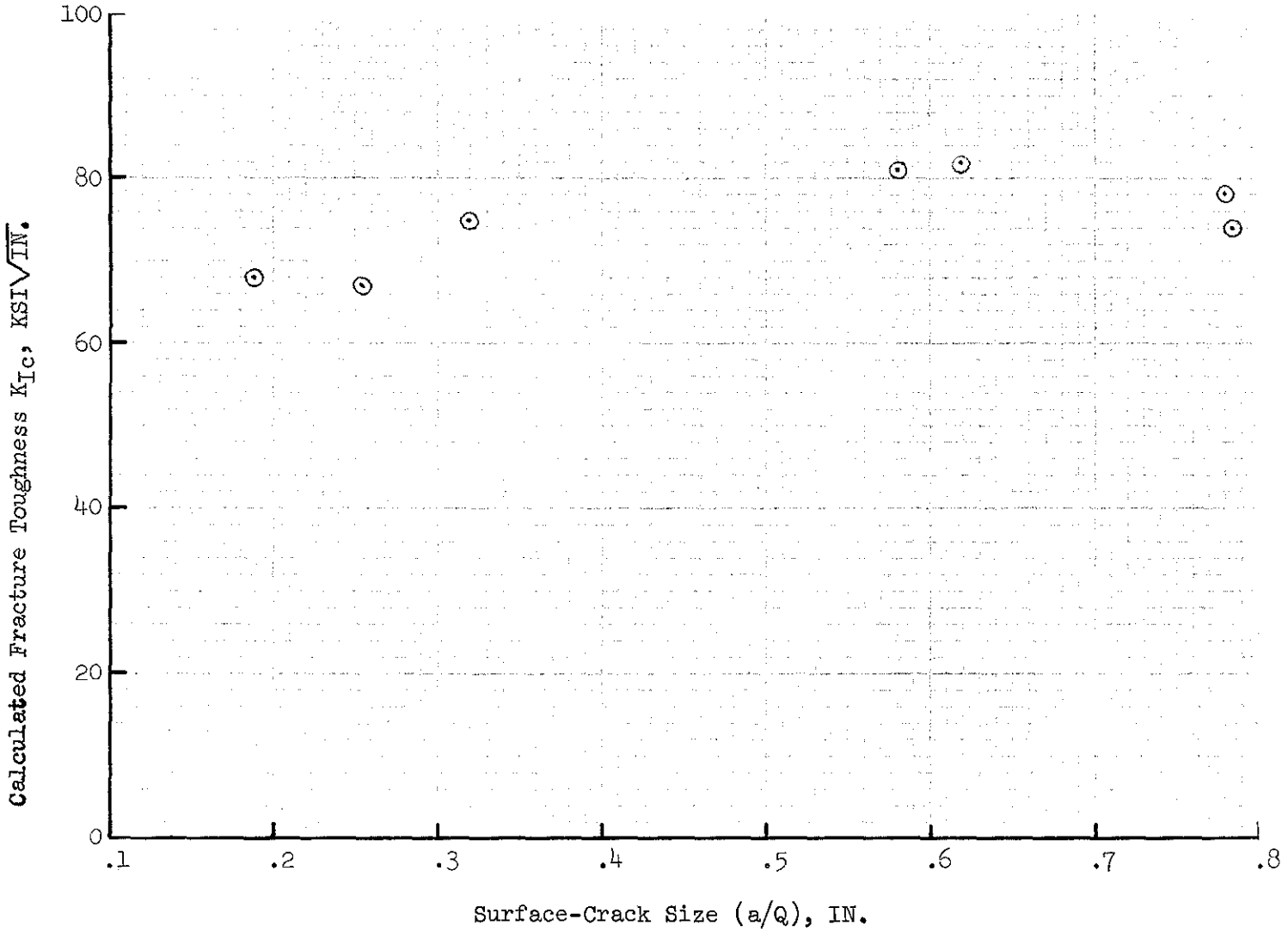

Figure B-13 Effect of Surface-Crack Size on Calculated K_{Ic} for 4340 Steel

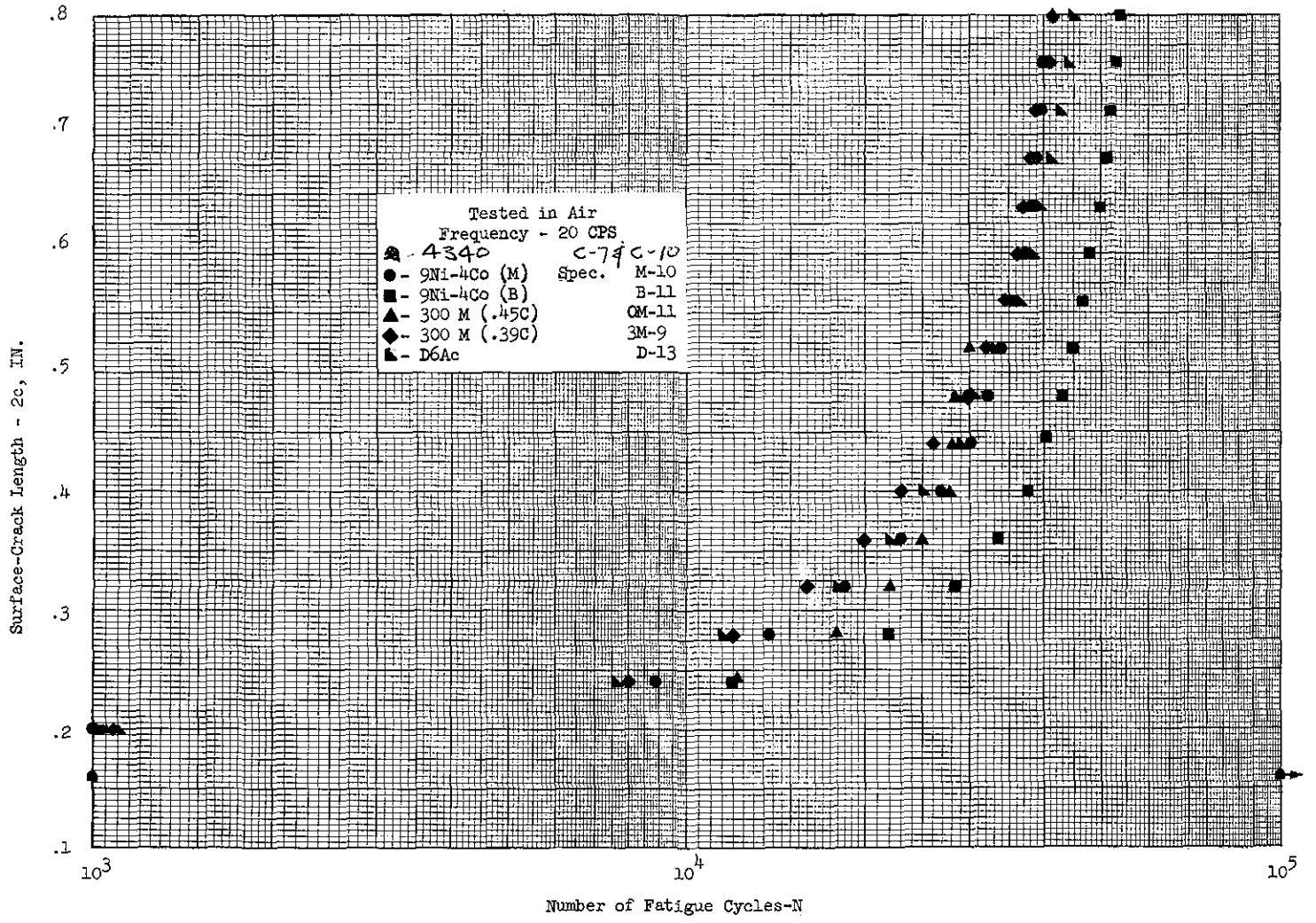

Figure B-14 Cyclic Crack Propagation of High Strength Steels in Air at 45 KSI Maximum Stress and 0.1 R Ratio

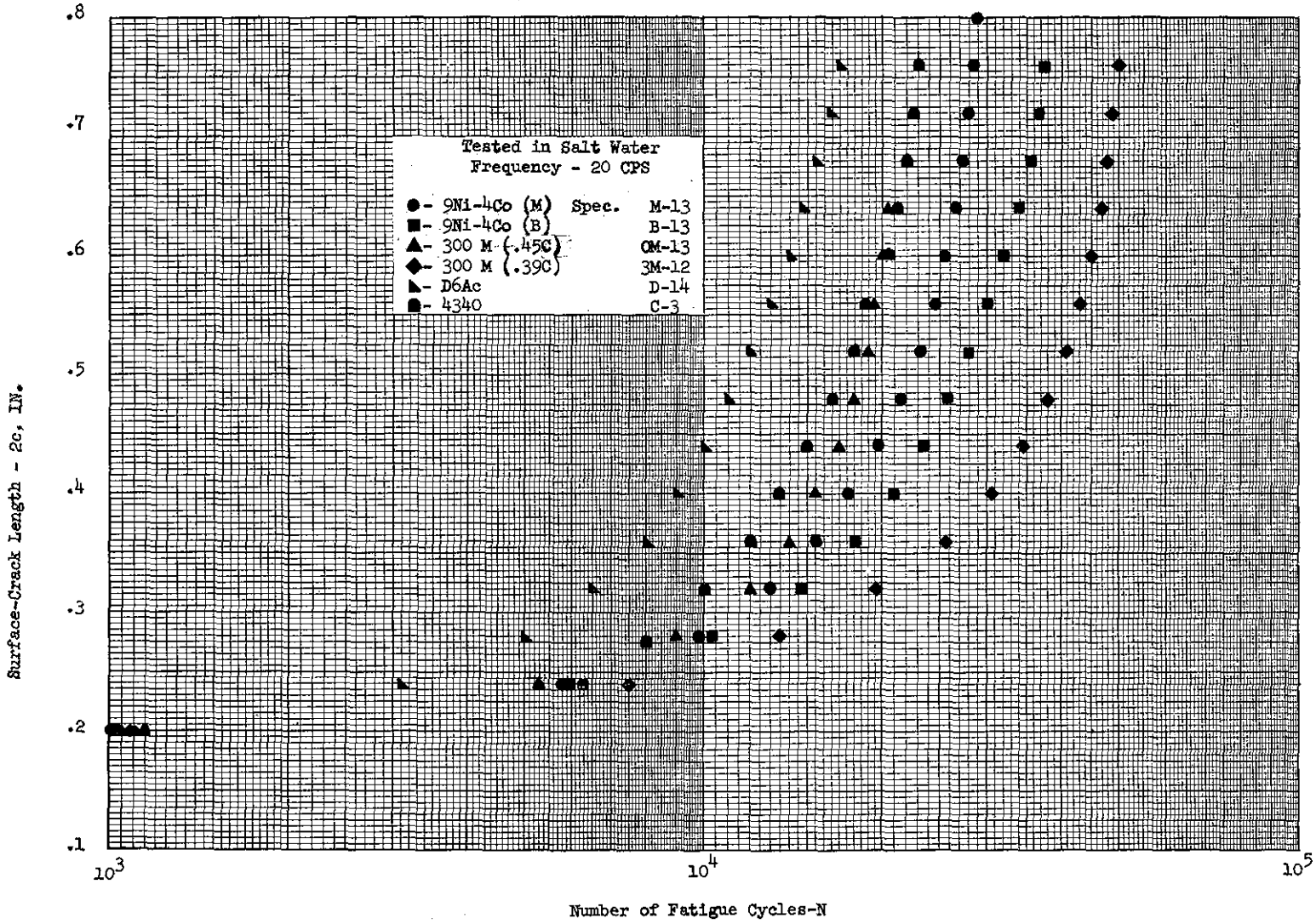

Figure B-15 Cyclic Crack Propagation of High Strength Steels in Salt Water at 45 KSI Maximum Stress and 0.1 R Ratio

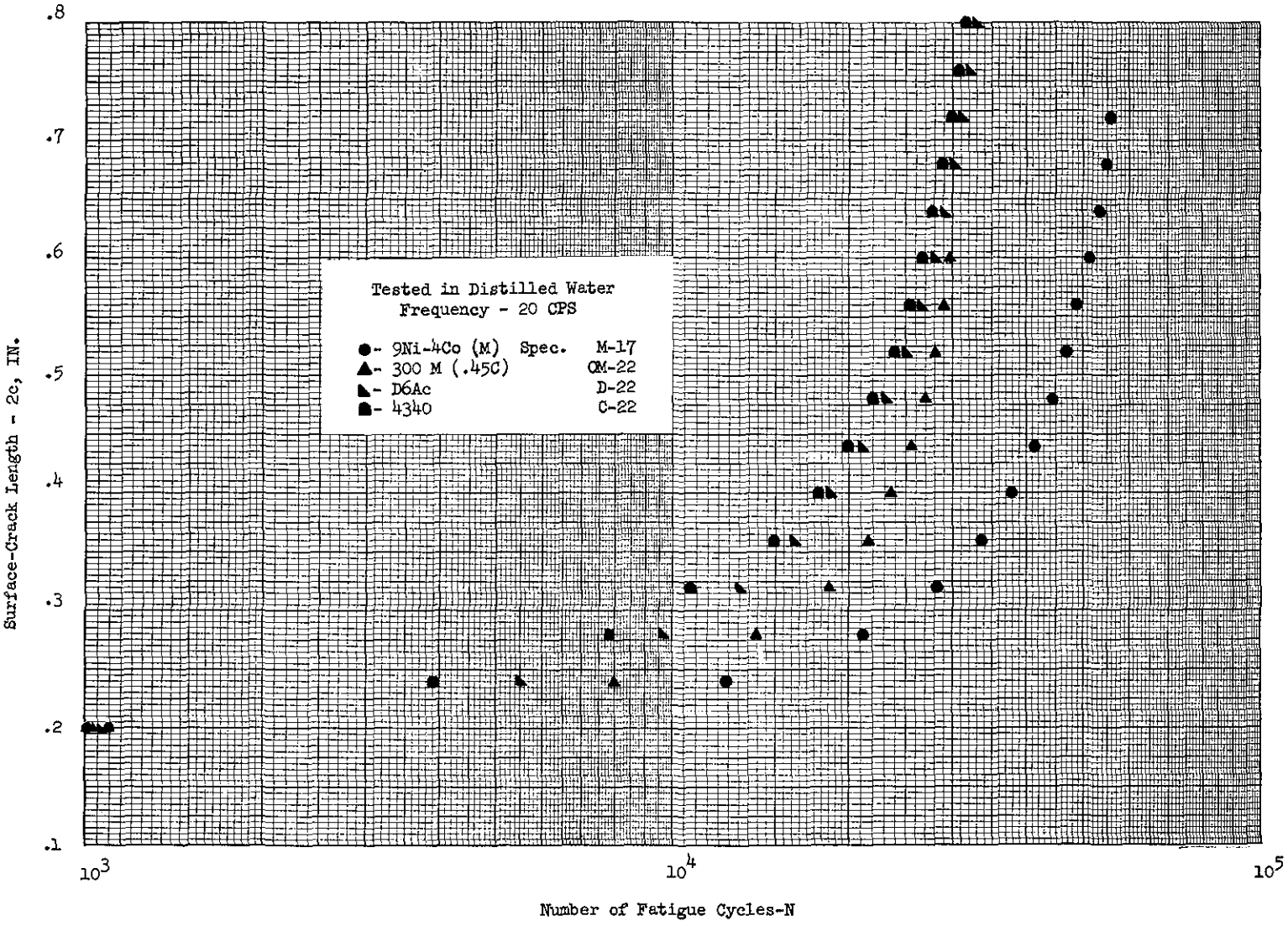

Figure B-16 Cyclic Crack Propagation of High Strength Steels in Distilled Water at 45 KSI Maximum Stress and 0.1 R Ratio

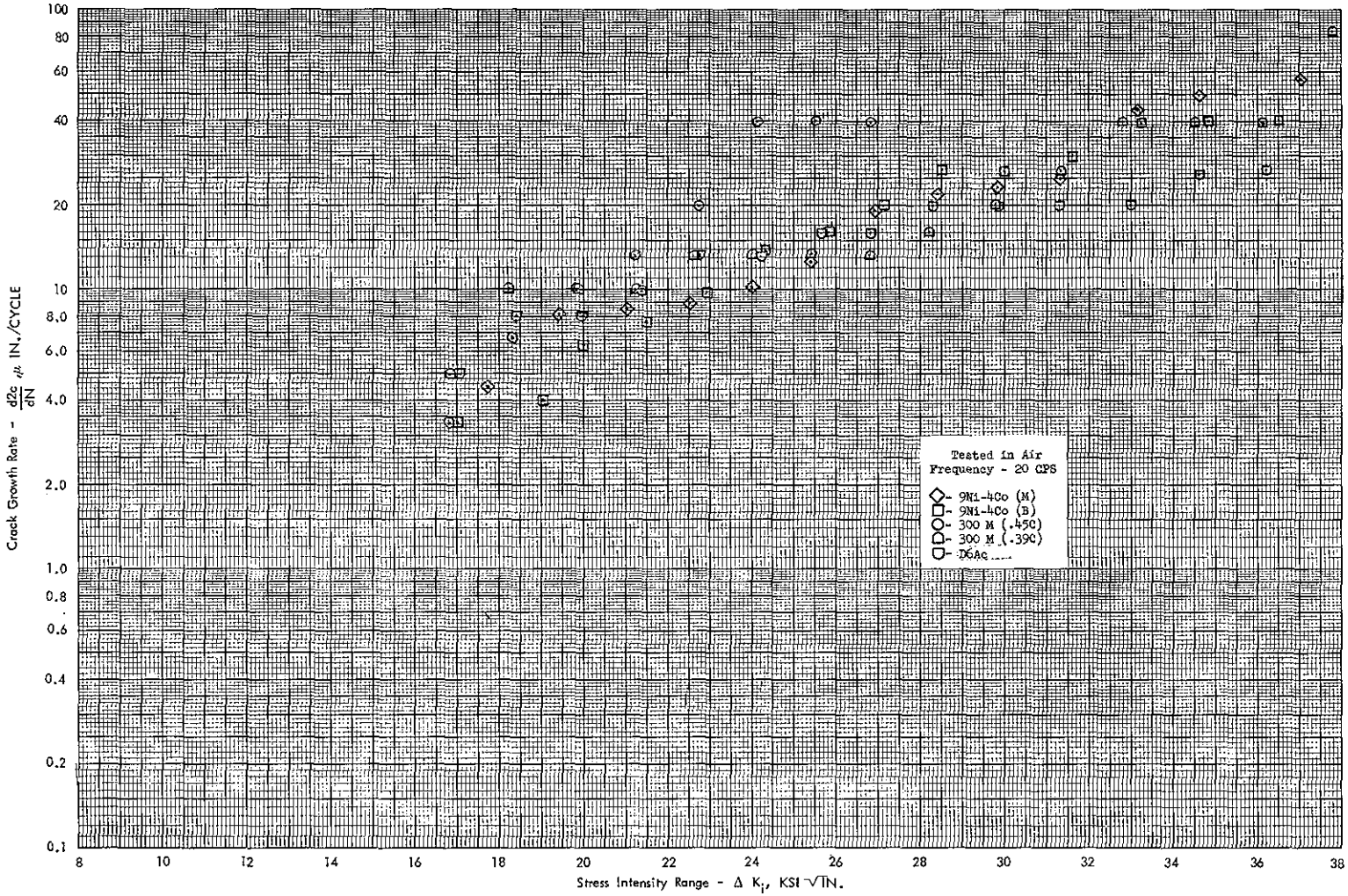

Figure B-17 Cyclic Cracking Rate vs Stress Intensity Range for Surface-Crack Specimens in Air

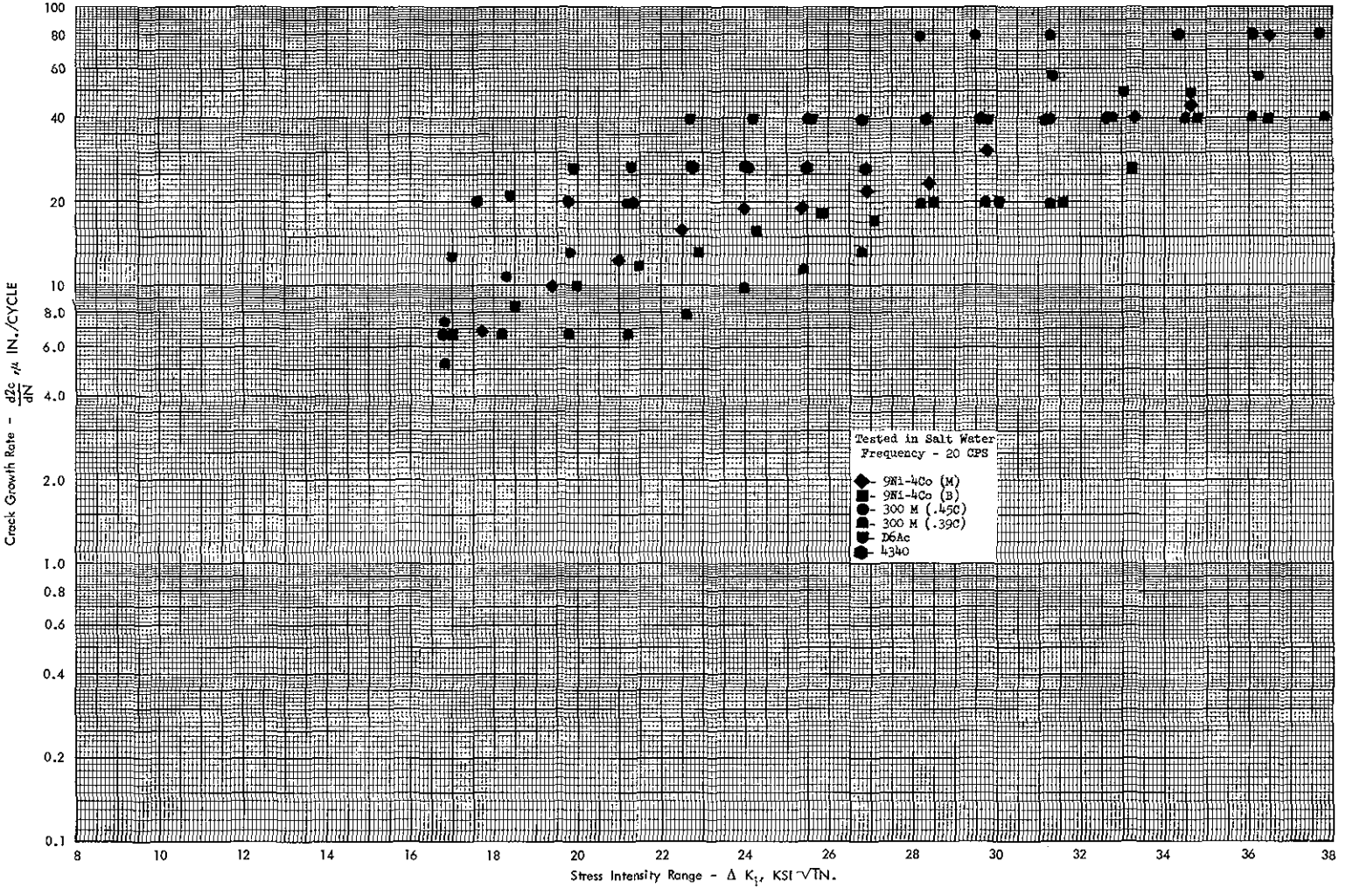

Figure B-18 Cyclic Cracking Rate vs Stress Intensity Range for Surface-Crack Specimens in Salt Water

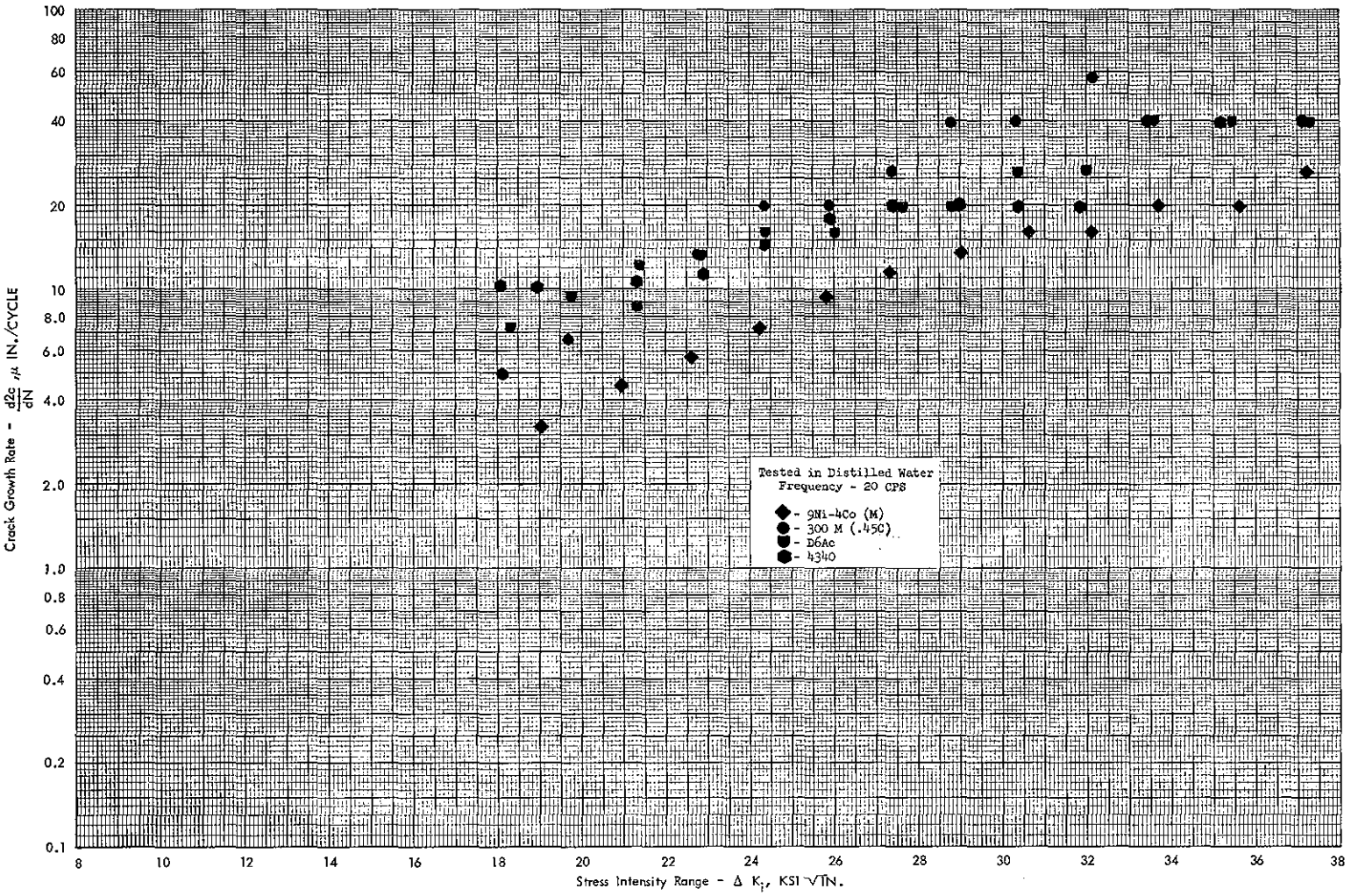

Figure B-19 Cyclic Cracking Rate vs Stress Intensity Range for Surface-Crack Specimens in Distilled Water at R = 0.1

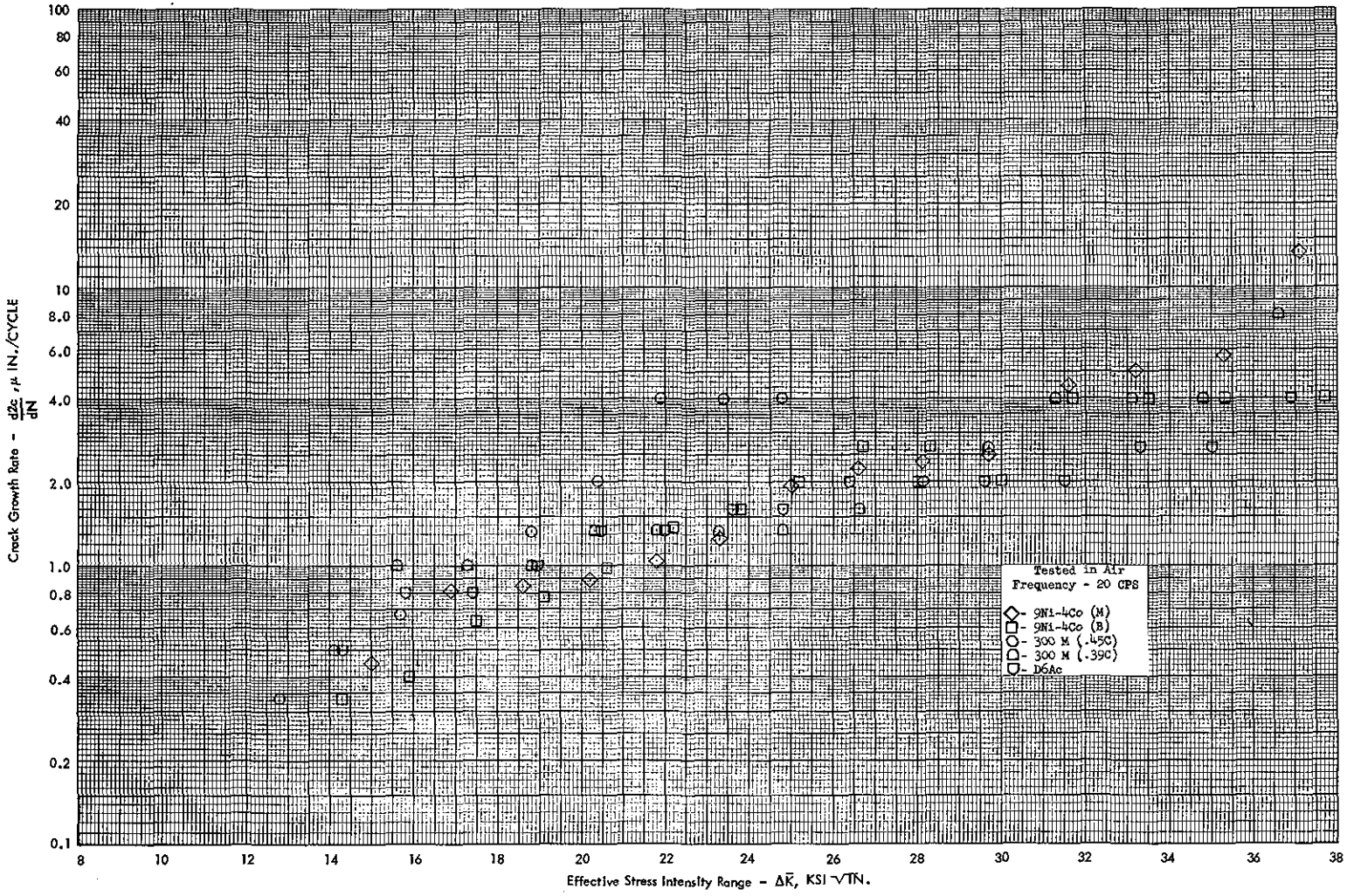

Figure B-20 Cyclic Cracking Rate vs Effective Stress Intensity Range for Surface-Crack Specimens in Air

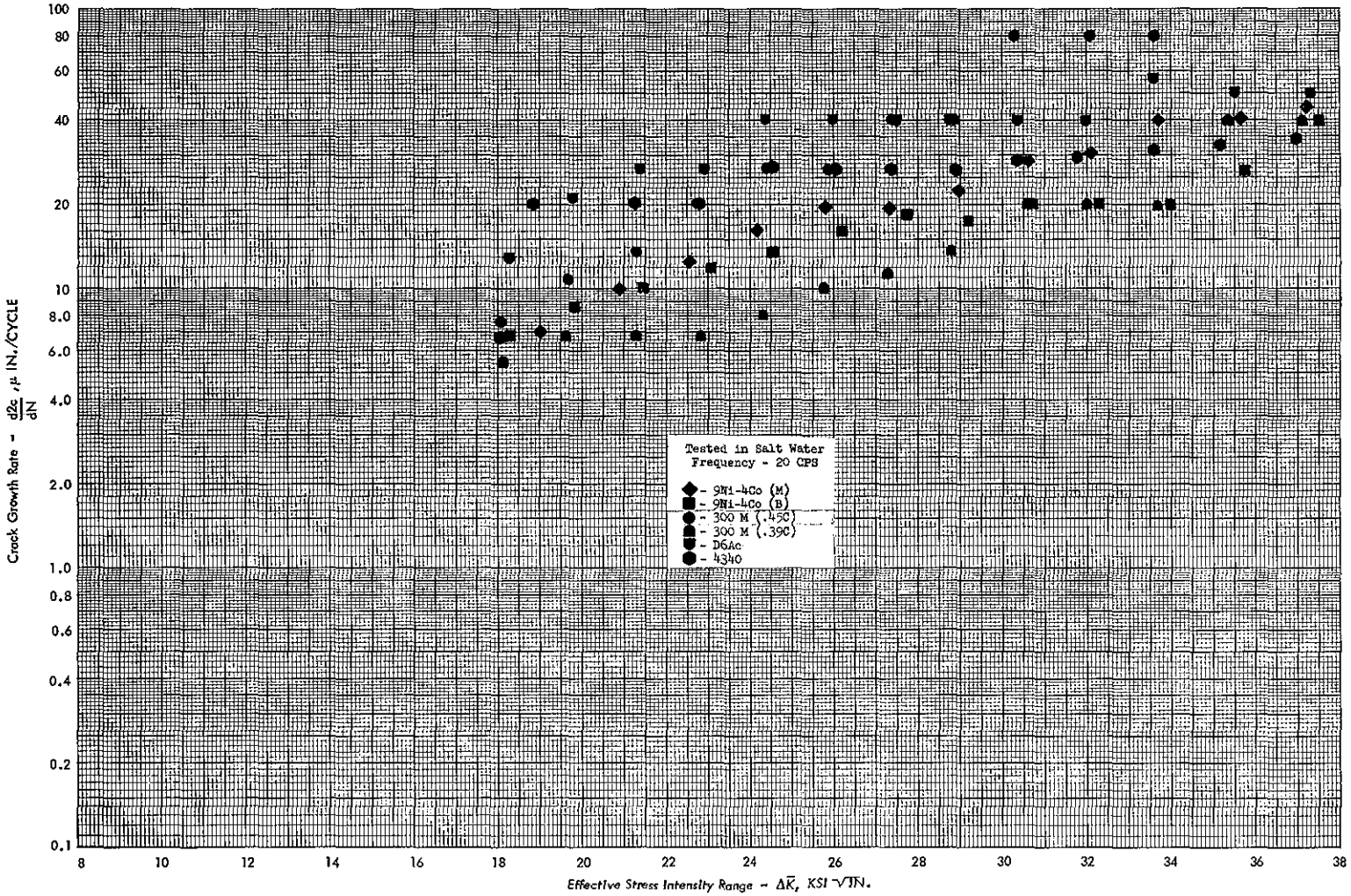

Figure B-21 Cyclic Cracking Rate vs Effective Stress Intensity Range for Surface-Crack Specimens in Salt Water

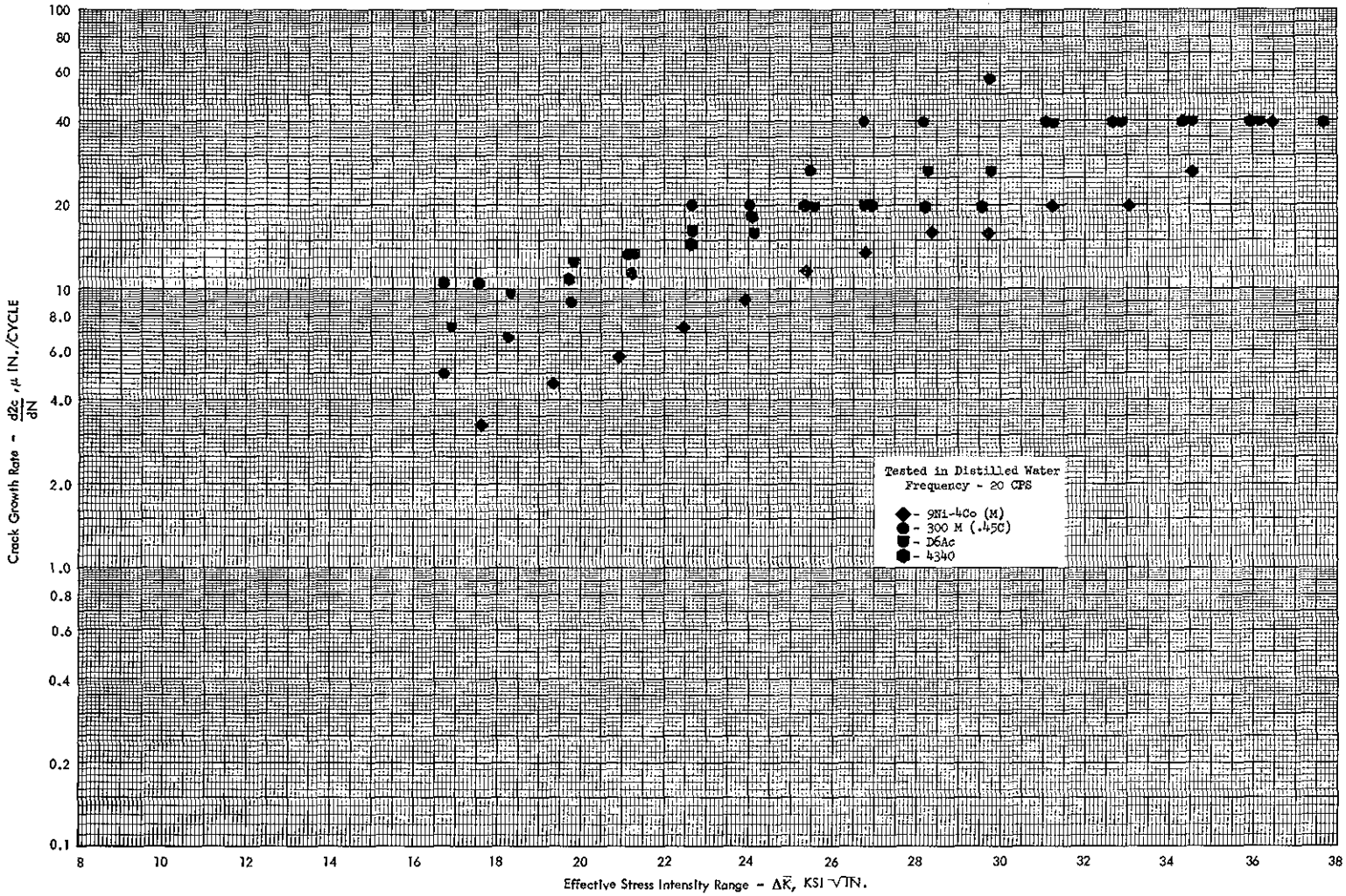

Figure B-22 Cyclic Cracking Rate vs Effective Stress Intensity Range for Surface-Crack Specimens in Distilled Water